UNIVERSITY OF KWAZULU-NATAL

A PHYTOCHEMICAL INVESTIGATION OF TWO SOUTH AFRICAN PLANTS WITH THE SCREENING OF EXTRACTIVES FOR BIOLOGICAL ACTIVITY

BY

ANDREW BRUCE GALLAGHER
B.Sc Honours (*cum laude*) (UKZN)

Submitted in fulfilment of the requirements for the degree of
Master of Science
In the School of Biological and Conservation Science
and
The School of Chemistry
University of KwaZulu-Natal, Howard College campus
Durban
South Africa

2006

ABSTRACT

Two South African medicinal plants, *Strophanthus speciosus* and *Eucomis montana*, were investigated phytochemically. From *Strophanthus speciosus* a cardenolide, neritaloside, was isolated, whilst *Eucomis montana* yielded three homoisoflavanones, 3,9-dihydroeucomin, 4'-demethyl-3,9-dihydroeucomin, and 4'-demethyl-5-O-methyl-3,9-dihydroeucomin. The structures were elucidated on the basis of spectroscopic data. The homoisoflavanones were screened for anti-inflammatory activity using a chemiluminescent luminol assay, modified for microplate usage. All of the homoisoflavanones exhibited good inhibition of chemiluminescence, with IC_{50} values for 3,9-dihydroeucomin, 4'-demethyl-3,9-dihydroeucomin, and 4'-demethyl-5-O-methyl-3,9-dihydroeucomin being 14mg/mL, 7 mg/mL, and 13mg/mL respectively. The IC_{50} value of 4'-demethyl-3,9-dihydroeucomin compared favourably with the NSAID control (meloxicam), which had an IC_{50} of 6mg/mL. Neritaloside was not screened for biological activity as the yield of 14.4mg was insufficient for the muscle-relaxant screen for which it was intended.

An assay for antioxidant/free radical scavenging activity was also performed. All the compounds had excellent antioxidant/free radical scavenging activity, with percentage inhibition of the reaction being 92%, 96%, and 94% for 3,9-dihydroeucomin, 4'-demethyl-3,9-dihydroeucomin, and 4'-demethyl-5-O-methyl-3,9-dihydroeucomin respectively at a concentration of 10mg/mL. However, the control compounds, diclofenac and meloxicam, also exhibited strong activity, with the result that the precise mode of anti-inflammatory activity could not be unequivocally determined.

The results from the biological screenings thus provided a rational scientific basis for the indigenous ethnomedicinal use of *Eucomis* species in the treatment of rheumatism, inflammation and pain.

STRUCTURES OF COMPOUNDS ISOLATED

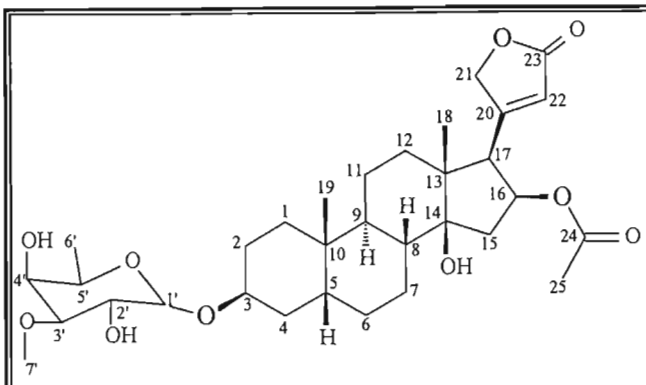

Compound **1**: Neritaloside

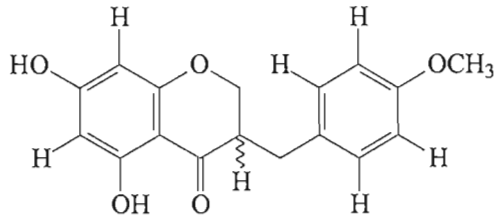

Compound **2:** 3,9-dihydroeucomin

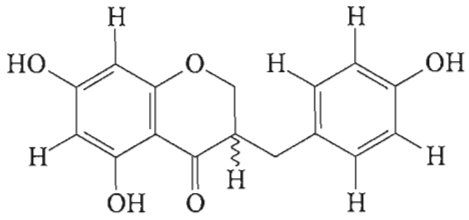

Compound **3**: 4'-demethyl-
3,9-dihydroeucomin

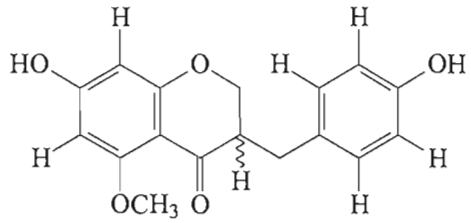

Compound **4**: 4'-demethyl-
5-O-methyl-3,9-dihydroeucomin

Compounds isolated from *Strophanthus speciosus* and *Eucomis montana*.

PREFACE

The phytochemical research described in this dissertation was carried out in the Natural Product Research Laboratory of the School of Chemistry, University of KwaZulu-Natal, Howard College campus, Durban. The biological assays were carried out in the Biochemistry Research Laboratory/Pollution Research Laboratory of the School of Biological and Conservation Sciences, University of KwaZulu-Natal, Howard College campus, Durban. This study was supervised by Professor Michael T. Smith and Doctor Neil A. Koorbanally.

This study represents original work by the author and has not been submitted in any other form to another university. Where use was made of the work of others it has been duly acknowledged in the text.

Signed:

.....

Andrew B. Gallagher

B.Sc. honours *cum laude* (UKZN)

I hereby certify that the above statement is correct.

Signed:

.....

Professor M.T. Smith

(Supervisor)

.....

Doctor N.A. Koorbanally

(Co-supervisor)

ACKNOWLEDGEMENTS

This research would not have been possible without the input of various people. I wish to sincerely thank the following people:

- Professor Michael Smith of the School of Biological and Conservation Sciences, of KwaZulu-Natal, Durban, who was my supervisor. Thank you Mike for all the work and ideas you contributed towards this dissertation. Your contributions have been invaluable for this project.

- Dr. Neil Koorbanally of the School of Chemistry, University of KwaZulu-Natal, Durban, who was my co-supervisor. Thank you Neil for all of your help and teachings throughout this project. Thank you for all the hard work you put into this dissertation, for teaching me the ins and outs of natural product chemistry, and for all the extra chemistry lessons. Without your help I would never have been able to complete this research.

- Mr. Dilip Jagjivan for the NMR spectra and for teaching me about NMR spectroscopy, and thank you to Mr. Brett Parel for the mass spectra, and for providing all the laboratory consumables.

- Dr. Neil Crouch at the National Botanical Institute, Durban, who collected all the plant material for this project and for supplying me with the photographs of the different plants.

- Dr. Nicola Giubellina, my neighbour in the laboratory. Thank you Nic for all the help and tips you gave me during this project, and for being a good mate. Your presence really made the running of columns much more enjoyable.

- Thank you to the staff and students of both the Natural Product Research Group and the Biochemistry/Pollution Research Group. A special thank you to Trisha, my vacation student, for all your help in the laboratory.

- The South African National Blood Service for supplying the buffy coat cells used in the anti-inflammatory screening.

- The National Research Foundation for financial support and the University of KwaZulu-Natal for the Graduate Scholarship I was awarded. Without the financial support given, this project would not have been possible.

- Finally, thank you to my family, friends and girlfriend for all their support throughout this study.

LIST OF ABBREVIATIONS

δ_C – Carbon-13 chemical shift

δ_H – Proton chemical shift

APT – Attached proton test

ATP – Adenosine triphosphate

BLK – Blank

^{13}C NMR – Carbon-13 nuclear magnetic resonance

CL – Chemiluminescence

CoA – Coenzyme A

COSY – Correlation spectroscopy

COX – Cyclooxygenase

d- Doublet

DBA – 10,10'-Dimethyl-9,9'-biacridium dinitrate

dd – Double doublet

dq – Double quartet

DEPT – Distortionless enhancement by polarization transfer

DMSO – Dimethyl sulfoxide

EI-MS – Electron impact mass spectrometry

FAB-MS – Fast atom bombardment mass spectrometry

GC – Gas chromatography

^1H NMR – Proton nuclear magnetic resonance

HEPEs – 4-(2-hydroxyethyl)piperazine-1-ethanesulfonic acid

HIV/AIDS – Human immunodeficiency virus/ acquired immune deficiency syndrome

HMBC – Heteronuclear multiple bond correlation

5-HPETE – 5-Hydroperoxyeicosatetraenoic acid

HSQC – Heteronuclear single quantum correlation

Hz – Hertz

IC_{50} – Concentration needed to inhibit 50% of the reaction

IL-1 – Interleukin-1

INEPT – Insensitive nuclei enhancement by polarization transfer

IR – Infrared

J - Coupling constant

LC-ESI-MS – Liquid chromatography/electrospray mass spectrometry

LOX – 5-Lipoxygenase

LT – Leukotriene

M^+ - Molecular ion

m – Multiplet

mM – Millimolar

MIC – Minimum inhibitory concentration

MPO – Myelperoxidase

MS – Mass spectrometry

m/z – Mass-to-charge ratio

NAD^+ - Nicotinamide adenine dinucleotide

NADPH – Reduced nicotinamide adenine dinucleotide phosphate

NaOAc – Sodium acetate

NIH – National Institute of Health

NMR – Nuclear magnetic resonance

NOESY – Nuclear Overhauser effect spectroscopy

NSAID- Non-steroidal anti-inflammatory drug

PAMPs – Pathogen-associated molecular pattern

PBS – Phosphate buffered saline

PG – Prostaglandin

PMA – Phorbol myristate acetate

ppm – Parts per million

RDA – *Retro*-Diels-Alder

ROS – Reactive oxygen species

rxn - reaction

TNF-α – Tumour necrosis factor-alpha

UV – Ultraviolet

LIST OF FIGURES

		PAGE
1.1.	Examples of different compounds previously isolated in Apocynaceae	11
1.2.	Examples of different types of compounds isolated in Hyacinthaceae	14
1.3.	Basic structure of cardenolide aglycone	18
2.1.	Structure of a cardenolide and bufadienolide	27
2.2.	Structure of various cardiac glycoside aglycones whose structures were determined through the use of x-ray crystallography	32
2.3.	Structures of nerizoside and neritaloside, cardenolides displaying central nervous system depressant activity	34
3.1.	Structural difference between isoflavanoids and homoisoflavanones, and the different skeletons systems of homoisoflavonoids	42
3.2.	Homoisoflavanone numbering system	43
3.3.	The three basic structural types of homoisoflavanones	43
3.4.	Structure of scillascillin, brazilin, comosin, and haematoxylin type homoisoflavanones	44
3.5.	Origins of the A and B rings of homoisoflavanones	51
4.1.	Compounds isolated from *Eucomis montana*	64
4.2.	HMBC and NOESY correlations that support attachment of methoxyl group to C-5	74
6.1.	Diagram showing the two methods of release of mediators by mast cells. (i) Release of preformed mediators present in granules. (ii) Release of mediators formed through the metabolism of arachidonic acid	87
6.2.	Generation of reactive oxygen species. E represents associated energy levels of components. Diagram does not show oxygen side products produced during the reactions	88

6.3.	Crystallographic model of ovine COX-1 and murine COX-2 regions of prostaglandin endoperoxide synthase (from Protein Data Bank, file 1PRH and COX5 respectively). Yellow = membrane binding domain; light green = dimerisation domain; red = heme. Peroxidase active site visible as cleft at top of diagram	90
6.4.	The fate of arachidonic acid in cells after the action of the lipoxygenases to form leukotrienes and HPETEs; or by cyclooxygenases to prostaglandins. Many NSAIDs block the synthesis of prostaglandin G_2	91
6.5.	The major enzymatic pathways responsible for microbial metabolism and oxygenation, and the relationship between these activities and chemiluminescence. The cytoplasmic milieu is separated from those of the phagosome-phagolysosome-extracellular milieu	95
6.6.	Diagram showing the catalysed oxidation of luminol by hydrogen peroxide in a basic solution resulting in the generation of light	97
6.7.	Biological oxidation of luminol. i) Luminol is dehydrogenated by hypochlorous acid to form diazaquinone; ii) diazaquinone is dioxygenated by hydrogen peroxide to give an excited 3-aminophthlate that liberates light upon relaxation	97
6.8.	Oxidation of luminol to 3-aminophthalate resulting in chemiluminescence by i) singlet oxygen; and ii) superoxide anions in biological systems	98
6.9.	The effect of PMA on chemiluminescence. Conditions for tests are ~20 000 leukocytes in 50μL phosphate buffered saline; 80μL luminol; 50μL PMA	99
6.10.	The effect of zymosan on chemiluminescence. Conditions for tests are ~20 000 leukocytes in 50μL phosphate buffered saline; 80μL luminol; 100μg opsonized zymosan	100
6.11.	Luminol versus DBA dioxygenation. i) Shows the general dioxygenation of luminol; ii) the reductive-dioxygenation of DBA	100

6.12. Possible pathways to DBA dioxygenation. (i) Classical pathway involving divalent reduction and dioxygenation by H_2O_2; (ii) univalent reduction resulting in a radical-radical, cation-anion annihilation reaction with superoxide anions; (iii) divalent reduction catalysed by metals or metalloproteins followed by dioxygenation by singlet oxygen 102

7.1. Graph of varying concentrations of luminol solution. Volume of blood cells and opsonized zymosan stimulant were kept constant at 400uL and 100uL respectively 110

7.2. Graph of varying volumes of luminol solution, opsonized zymosan, and blood cells. In legend: BC = blood cell solution; L = luminol solution; Z = opsonized zymosan 111

7.3. Graph illustrating the inhibition of chemiluminescence by diclofenac. 5μL of five different concentrations of diclofenac solution were added to each well and compared with an uninhibited reaction. BLK = blank 112

7.4. Graph illustrating the inhibition of chemiluminescence by diclofenac. 15μL of five different concentrations of diclofenac solution were added to each well and compared with an uninhibited reaction. BLK = blank 113

7.5. Graph illustrating the inhibition of chemiluminescence by diclofenac. 30μL of five different concentrations of diclofenac solution were added to each well and compared with an uninhibited reaction. BLK = blank 113

7.6. Graph illustrating the inhibition of chemiluminescence by diclofenac. 50μL of five different concentrations of diclofenac solution were added to each well and compared with an uninhibited reaction. BLK = blank 114

7.7. Graph illustrating the inhibition of chemiluminescence by meloxicam. 5μL of five different concentrations of diclofenac solution were added to each well and compared with an uninhibited reaction. BLK = blank 114

7.8. Graph illustrating the inhibition of chemiluminescence by meloxicam. 15μL of five different concentrations of diclofenac solution were added to each well and compared with an uninhibited reaction. BLK = blank 115

7.9. Graph illustrating the inhibition of chemiluminescence by meloxicam. 30μL of five different concentrations of diclofenac solution were added to each well and compared with an uninhibited reaction. BLK = blank 115

7.10. Graph illustrating the inhibition of chemiluminescence by meloxicam. 50μL of five different concentrations of diclofenac solution were added to each well and compared with an uninhibited reaction. BLK = blank 116

7.11. Graph of anti-inflammatory activity of 3,9-dihydroeucomin (compound **2**) in the standardised assay system. 50μL of compound **2** at varying concentrations was added to each well. BLK = blank, rxn = reaction 117

7.12. Graph of anti-inflammatory activity of 4'-demethyl-3,9-dihydroeucomin (compound **3**) in the standardised assay system. 50μL of compound **3** at varying concentrations was added to each well. BLK = blank, rxn = reaction 118

7.13. Graph of anti-inflammatory activity of 4'-demethyl-5-O-methyl-3,9-dihydroeucomin (compound **4**) in the standardised assay system. 50μL of compound **4** at varying concentrations was added to each well. BLK = blank, rxn = reaction 118

7.14. Calculation of IC_{50} for 3,9-dihydroeucomin (compound **2**) 119

7.15. Calculation of IC_{50} for 4'-demethyl-3,9-dihydroeucomin (compound **3**) 119

7.16. Calculation of IC_{50} for of 4'-demethyl-5-O-methyl-3,9-dihydroeucomin (compound **4**) 120

7.17. Calculation of IC_{50} for diclofenac 120

7.18. Calculation of IC_{50} for meloxicam 120

7.19. Results of antioxidant / free radical scavenging activity of 3,9-dihydroeucomin (compound **2**) at four concentrations using the luminol CL assay 121

7.20. Results of antioxidant / free radical scavenging activity of 4'-demethyl-3,9-dihydroeucomin (compound **3**) at four concentrations using the luminol CL assay 122

7.21. Results of antioxidant / free radical scavenging activity of 4'-demethyl-5-O-methyl-3,9-dihydroeucomin (compound **4**) at four concentrations using the luminol CL assay 122

7.22. Results of antioxidant / free radical scavenging activity of meloxicam at four concentrations using the luminol CL assay 123

7.23. Results of antioxidant / free radical scavenging activity of diclofenac at four concentrations using the luminol CL assay 123

7.24. Structures of phenol, catechol and quercetin, a flavanoid with good antioxidant activity 128

7.25. Structures of two important biological antioxidants, tocopherol and ascorbic acid, and 7-hydroxy-3[3',4',5'-trihydroxyphenyl) methylene]-4-chromanone, a homoisoflavanone with high antioxidant activity 130

LIST OF SCHEMES **PAGE**

2.1. Formation of pregnenolone from cholesterol 35

2.2. Formation of progesterone from pregnenolone 36

2.3. Formation of 3β,14β,21-trihydroxy-5β-pregnan-20-one 377

2.4. Formation of the lactone ring in cardenolide biosynthesis 38

3.1. Mass spectrum fragmentation scheme for eucomol 46

3.2. Formation of the chalcone from L-phenylalanine 52

3.3. Mechanism illustrating the NIH shift 52

3.4. The proposed biosynthetic pathway for the conversion of chalcones to homoisoflavanones 54

3.5. Proposed biosynthetic pathway for the formation of scillascillin 55

3.6. Proposed biosynthetic pathway for the formation of brazilin 55

4.1. Proposed fragmentation pattern for neritaloside (compound **1**) 62

4.2. Mass spectrum fragmentation pattern for 3,9-dihydroeucomin (compound **2**) 66

4.3. Mass spectrum fragmentation pattern for 4'-demethyl-3,9-dihydroeucomin (compound **3**) 70

4.4. Mass spectrum fragmentation pattern for 4'-demethyl-5-O-3,9-dihydroeucomin (compound **4**) 73

LIST OF TABLES **PAGE**

1.1. Selected phytochemical agents employed in modern medicines 8

1.2. Selected cardenolides previously isolated from the *Strophanthus* genus (only aglycone named-variations in alternate name due to different sugar moieties) 18

2.1. Variations in ^{13}C chemical shifts for ten cardenolides (δ_C in ppm downfield from TMS)(Tori *et al.*, 1973), compared with ^{13}C chemical shifts for stigmasterol (De-Eknamkul and Potduang, 2003) and sitosterol (Saxena and Albert, 2005), two common plant phytosterols 31

3.1. Characteristic ^{13}C NMR chemical shifts for the three main classes of homoisoflavanones 48

4.1. ^{1}H, ^{13}C, HMBC, COSY and NOESY data for compound **1**($CDCl_3$) 63

4.2. ^{1}H, ^{13}C, HMBC, COSY and NOESY data for compound **2** and ^{13}C literature values ($CDCl_3$) 68

4.3. ^{1}H, ^{13}C, HMBC, COSY and NOESY data for compound **3** ($CDCl_3$) 71

4.4. ^{1}H, ^{13}C, HMBC, COSY and NOESY data for compound **4** ($CDCl_3$) 75

4.5. Comparison of ^{1}H NMR data for compound **4** with 4'-demethyl-5-O-methyl-3,9-dihydroeucomin 75

6.1. Inflammatory mediators released by mast cells 87

7.1. Comparison of percentage inhibition of luminescence of the various compounds and controls in the anti-inflammatory assay 125

7.2. Comparison of percentage inhibition of luminescence of the various compounds and controls in the antioxidant/ H_2O_2 scavenging assay 127

LIST OF STRUCTURES

	PAGE
1.1. Structures of morphine, codeine, papaverine and noscarpine	3
1.2. Structure of pilocarpine	4
1.3. Structures ofvinblastine, vincristine and vincamine	4
1.4. Structure of physostigmine	5
1.5. Structures of digitoxin and digoxin	5
1.6. Structures of emetine and cephaeline	6
1.7. Structure of quinine	7
1.8. Structure of reserpine	7
2.1. Structure of strogogenin	28
2.2. Structure of stigmasterol and sitosterol	31
3.1. Structure of 3-benzyl-4-chromanone type homoisoflavanone	46
3.2. Structure of 3-benzyl-3-hydroxyl-4-chromanone type homoisoflavanone	47
3.3. Structure of E and Z configurations of 3-benzylidene-4-chromanone type homoisoflavanones	47
3.4. Structure of intricatin and intricatinol	49
3.5. Structure of 3-(4'-hydroxybenzyl)-5-hydroxyl-6,7,8-trimethyloxy chroman-4-one	50
3.6. Structure of 3-(4'-methoxybenyl)-7,8-methlenedioxy-chroman-4-one and 7-(1'-hydroxyethyl)-2-(2"-hydroxyethyl)-3,4-dihydrobenzopyran)	50
4.1. Structure of neritaloside	59
4.2. Structure of 3,9-dihydroeucomin	65
4.3. Structure of 4'-demethyl-3,9-dihydroeucomin	69
4.4. Structure of 4'-demethyl-5-O-dihydroeucomin	72
6.1. Structure of arachidonic acid	89
6.2. Structure of aspirin or acetyl salicylic acid	92
6.3. Structure of ibuprofen	92
6.4. Structure of diclofenac and indomethacin	93
6.5. Structure of celecoxib, rofecoxib and meloxicam	93

TABLE OF CONTENTS

	PAGE
Abstract	i
Structures of compounds isolated	ii
Preface	iii
Acknowledgements	iv
List of abbreviations	vi
List of figures	viii
List of schemes	xiii
List of tables	xiv
List of structures	xv
Table of contents	xvi
CHAPTER 1: INTRODUCTION	1
1.1. General	1
1.2. The Apocynaceae and Hyacinthaceae families	9
1.2.1. Introduction to Apocynaceae	9
1.2.2. Introduction to Hyacinthaceae	12
1.3. Species investigated	15
1.3.1. *Strophanthus speciosus* (Apocynaceae)	15
1.3.2. *Eucomis montana* (Hyacinthaceae)	19
1.4. Aims and objectives	23
1.5. References	24
CHAPTER 2: THE CLASSIFICATION, BIOLOGICAL ACTIVITY AND BIOSYNTHESIS OF CARDENOLIDES	27
2.1. Occurrence and classification of cardenolides	27

2.2. Biological activity of cardenolides 33

35

2.3. Biosynthesis of cardenolides

39

2.4. References

CHAPTER 3: THE CLASSIFICATION, BIOLOGICAL ACTIVITY AND BIOSYNTHESIS OF HOMOISOFLAVANONES 42

3.1. Occurrence and classification of homoisoflavanones 42

3.2. Biological activity of homoisoflavanones 49

3.3. Biosynthesis of homoisoflavanones 51

3.4. References 56

CHAPTER 4: STRUCTURAL ELUCIDATION OF EXTRACTED COMPOUNDS 58

4.1. Extractives from *Strophanthus speciosus* 58

4.1.1. Introduction 58

4.1.2. Structure elucidation of compound 1: Neritaloside 59

4.2. Extractives from *Eucomis montana* 64

4.2.1. Introduction 64

4.2.2. Structure elucidation of compound 2: 3,9-dihydroeucomin 65

4.2.3. Structure elucidation of compound 3: 4'-demethyl-3,9-dihydroeucomin 69

4.2.4. Structure elucidation of compound 4: 4'demethyl-5-O-methyl-3,9-dihydroeucomin 72

4.3. References 76

CHAPTER 5: EXPERIMENTAL 78

5.1. Foreword to experimental 78
5.1.1. Nuclear magnetic resonance spectroscopy (NMR spectroscopy) 78
5.1.2. Infrared spectroscopy (IR spectroscopy)
5.1.3. Ultraviolet absorption spectroscopy (IR spectroscopy) 78
5.1.4. Optical rotations 78
5.1.5. Melting points 78
5.1.6. Mass spectrometry 79
5.1.7. General chromatography 79

5.2. Isolation of compounds 1-4 79

5.3. Physical data 81
5.3.1. Compound 1 81
5.3.2. Compound 2 81
5.3.3. Compound 3 82
5.3.4. Compound 4 82

5.3. References 83

CHAPTER 6: ANTI-INFLAMMATORY BIOASSAY BACKGROUND 84

6.1. Introduction 84

6.2. The inflammation pathway 84
6.2.1. Acute inflammation reaction 85
6.2.2. Reactive oxygen species 88

6.2.3. Prostaglandins and leukotrienes 89
6.2.4. Non-steroidal anti-inflammatory drugs 92

6.3. The chemiluminescent assay 95

6.4. References 103

CHAPTER 7: SCREENING OF COMPOUNDS FOR BIOLOGICAL ACTIVITY 106

7.1. Reagents 106
7.1.1. Dextran solution 106
7.1.2. HEPES buffer 106
7.1.3. Lysis buffer 106
7.1.4. Luminol solution 106
7.1.5. Opsonized zymosan 107
7.1.6. Antioxidant/ free radical scavenging assay reaction medium 107

7.2. Methodology 108
7.2.1. Leukocyte separation and preparation 108
7.2.2. Anti-inflammatory chemiluminescent screening 108
7.2.3. Antioxidant/ free radical scavenging screening 109

7.3. Anti-inflammatory assay optimisation 110
7.3.1. Optimisation of luminol concentration 110
7.3.2. Optimisation of luminol, opsonized zymosan, and leukocyte solution volumes 111
7.3.3. Commercial anti-inflammatory controls 112

7.4. Anti-inflammatory activity of isolated homoisoflavanones 117

7.4.1. Calculation of IC_{50} 119

7.5. Antioxidant/ free radical scavenging activity of isolated homoisoflavanones 121

7.6. Discussion of results 124

7.7. References 131

CHAPTER 8: SUMMARY AND CONCLUSIONS 133

APPENDICES 135

CHAPTER 1: INTRODUCTION

1.1. GENERAL

When humankind was in its infancy, treating ailments was a 'magical' process. Few plants were utilised, and those used were usually psychoactive ones. As time passed, an empirical system replaced this approach, whereby plants were used for the treatment of various afflictions (Naranjo, 1995). The usage of plants in medicine can be traced back over five millennia, with written documentation coming from China, India and the Middle East (Chadha and Singh, 1991; Hamburger and Hostettmann, 1991). The herbalist-shaman approach was replaced by one more rational, based on medicinal principles, and when scientific medicine arose, and with the birth of chemistry, artificial pharmaceuticals were first synthesized (Chadha and Singh, 1991; Naranjo, 1995).

In spite of all the advances in synthetic chemistry, and science in general, there is still a need for the search of novel drugs. It has been estimated that in developing countries within Asia, Africa, Latin America and many Pacific Ocean islands, approximately twenty percent of the population benefit from modern drugs, with the rest of the population relying on traditional remedies (Bojor, 1991; Alcorn, 1995; Cordell and Colvard, 2005). Traditional medicines however have a number of benefits, particularly that of low cost. Traditional medicines also may have fewer harmful side effects than synthetic drugs that are often potent and may have strong, and possibly dangerous, side effects. Between three to five percent of hospital admissions are attributed to adverse reactions to synthetic pharmaceuticals and this has led to the World Health Organisation (WHO) advocating the study of traditional medicines in 1977 in a bid to reach its goal of 'health for everyone in the year 2000' (Naranjo, 1995).

Over the last 15 years there has been a dramatic increase in interest in developing pharmaceuticals of plant origins. In Western Europe, the consumption of medicinal plants has almost doubled during this period, and it is thought that the reason for this increase is due especially to an increased demand for non-classical therapies (Hamburger and Hostettmann, 1991). A report by the World Health Organisation showed that:

- Over 50% of the population in industrialized regions in Europe and North America has used complementary, or alternative medicines
- 70% of the Canadian population has used alternative medicines at least once
- 90% of Germans have used alternatives medicines
- Up to 75% of people from San Francisco, London and South Africa living with HIV/AIDS use traditional medicines
- USD (United States Dollars) 17 billion was spent on traditional medicines in 2000 in the USA, and USD 230 million is spent annually in the United Kingdom on traditional remedies
- The global expenditure on traditional medicines is estimated at USD 60 billion (WHO Fact Sheet No. 134).

Between thirty five and fifty percent of modern medications have their origins in traditional medicines (Holmstedt and Bruhn, 1995; Patwardhan, 2005), and almost every class of drug has a model structure equivalent found in plant natural products that exhibits the same pharmacological effect. Some well-known examples of plant-derived natural products with medicinal uses are morphine, pilocarpine, vincristine, emetine, physostigmine, digitoxin, quinine, and reserpine (Holmstedt and Bruhn, 1995).

One of the first reported plants to be used medicinally was *Papaver somniferum*, commonly known as the opium poppy. Opium is the air-dried latex from the unripe capsules of the opium poppy, and was first used more than 4000 years ago as an analgesic, sleep-inducer, and in the treatment of coughs. In modern medicine, many purified opium alkaloids and their derivatives are used. Morphine (**Structure 1.1**) is a powerful narcotic analgesic and remains one of the most important drugs for the relief of severe pain. The most widely used opium alkaloid is codeine, which is the 3-O-methyl ether of morphine. Codeine (**Structure 1.1**) is an analgesic, but unlike morphine, it does not have the same addictive properties. Codeine is also a useful anti-tussive, capable of relieving or suppressing coughing. Other useful opium alkaloids are papaverine

(**Structure 1.1**), which acts as an antispasmodic and vasodilator; and noscapine (**Structure 1.1**), an anti-tussive (Dewick, 2001; Gilani and Atta-ur-Rahman, 2005).

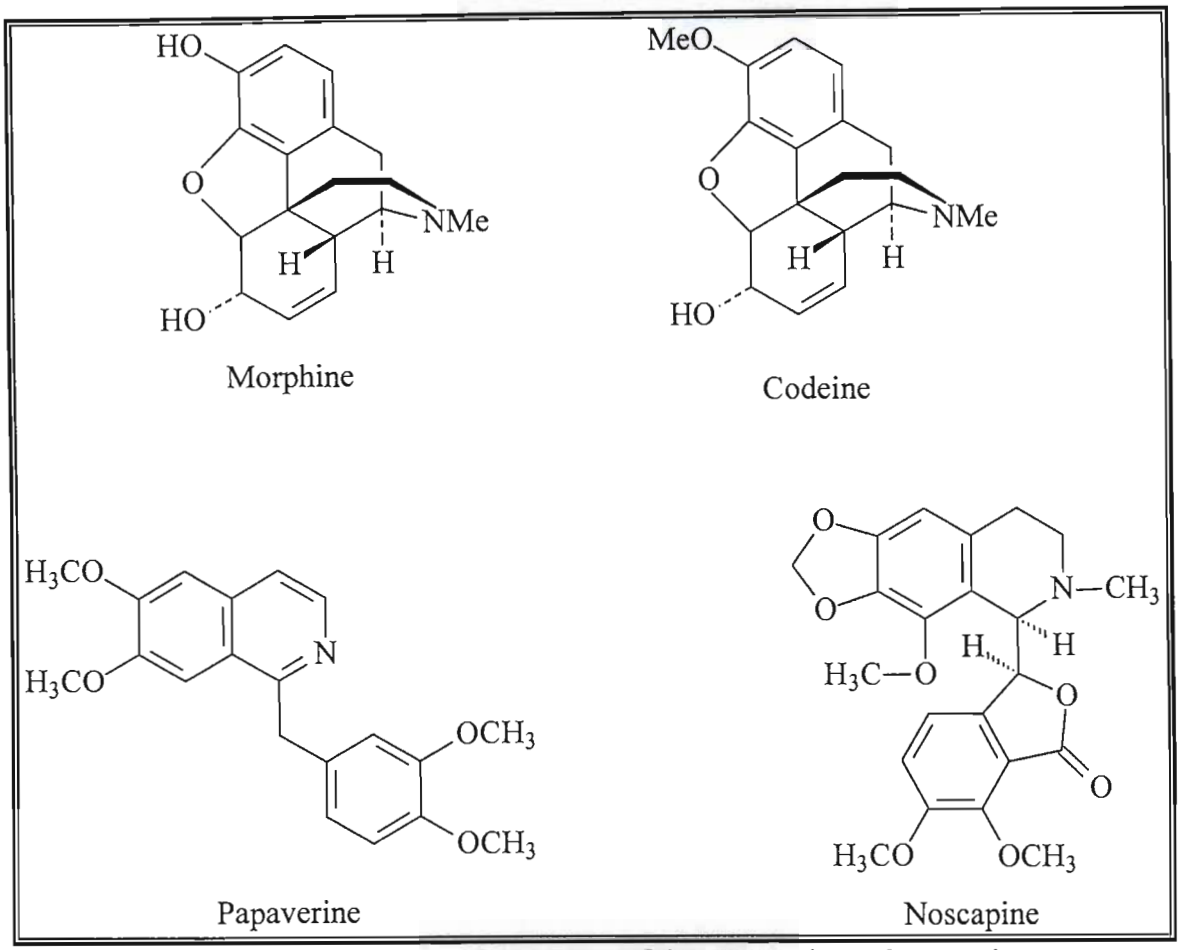

Structure 1.1: Structures of morphine, codeine, papaverine and noscarpine

Pilocarpine (**Structure 1.2**) is an important ophthalmic pharmaceutical found in *Pilocarpus jaborandi*. It was first isolated in the 19th century by scientists studying the plant due to its traditional medicinal uses, where it was used as a diuretic, and to treat baldness. It is used in modern medicine as an antiglaucoma agent due to its diaphoretic/miotic effect (Packer and Brandt, 1992). Pilocarpine acts as a cholinergic agent, and by activating the muscarinic receptors in the eye, it causes the pupil to constrict, resulting in the enhancement of outflow of the aqueous humour. This gives relief to both narrow-angle and wide-angle glaucoma. Pilocarpine has also been used to treat the dryness of mouth associated with cancer patients undergoing radiation therapy for mouth and throat cancer. Due to muscarinic agonist effects, it is being investigated in the potential treatment of Alzheimer's disease (Dewick, 2001).

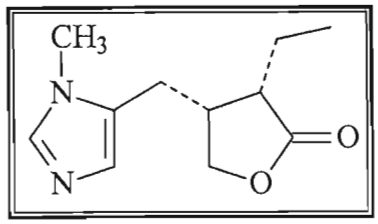

Structure 1.2: Structure of pilocarpine

In the Apocynaceae family, the genus *Catharanthus* (formerly *Vinca)* contains a number of medicinally valuable terpenoid indole alkaloids. Vincristine and vinblastine (**Structure 1.3**) are powerful anti-tumour agents (anti-neoplastic) and are two of the most effective anti-cancer agents in use. Vinblastine is used mainly in the treatment of Hodgkin's disease; cancer affecting the lymph glands, spleen and liver. Vincristine is a more powerful anti-tumour agent, but is also more neurotoxic. It is used predominantly in the treatment of childhood leukaemia where it has a high remission rate, but is also successfully used in the treatment of some lymphomas, small cell lung cancer, and cervical and breast cancer. Another medicinally important alkaloid from the species of *Catharanthus* is vincamine (**Structure 1.3**). It is used clinically as a vasodilator to increase the blood flow in cases of senility (Dewick, 2001).

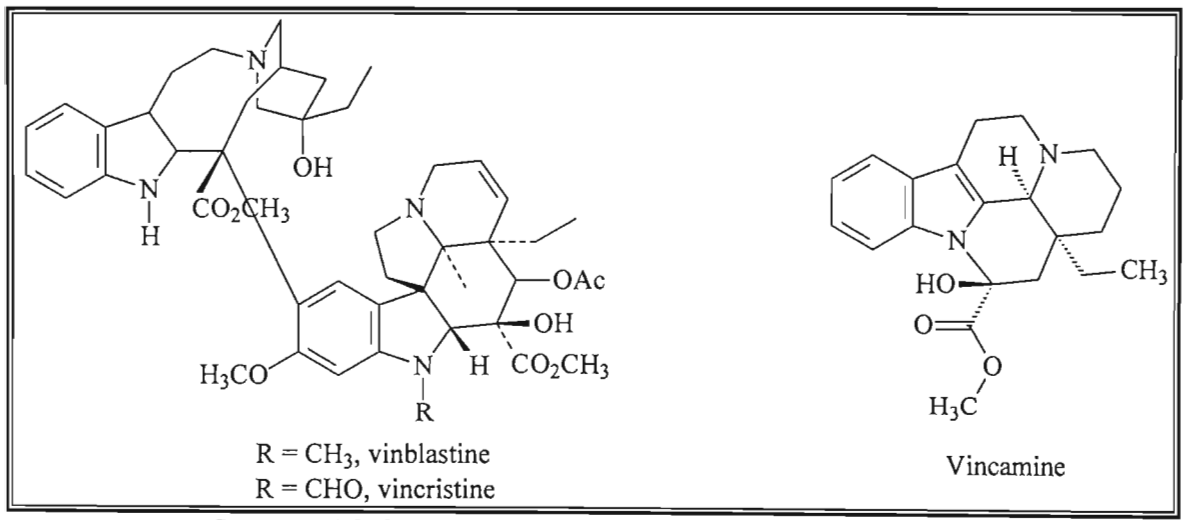

Structure 1.3: Stuctures of vinblastine, vincristine and vincamine

Physostigmine (**Structure 1.4**) is a pyrroloindole alkaloid found in the seeds of the vine *Physostigma venenosum.* It is a reversible cholinesterase inhibitor, preventing the destruction of acetylcholine, and has been shown to improve long-term memory (Davis *et al.*, 1978; Dewick, 2001) and aid memory in people suffering with Alzheimer's disease. It is also extensively used as a miotic to counteract the effects of mydriatics such as

atropine. Its miotic effect has also been utilized in the treatment of glaucoma, as it enhances the outflow of the aqueous humour (Dewick, 2001).

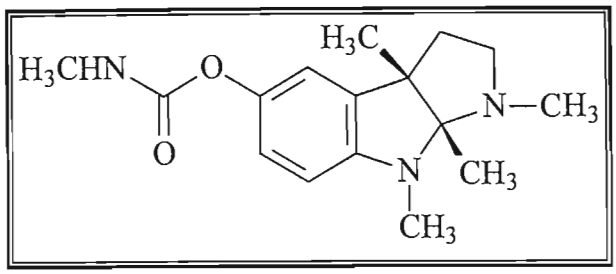

Structure 1.4: Structure of physostigmine

The red foxglove, *Digitalis purpurea,* is a biennial herb found in Europe and North America. The dried leaves were used as a cardiac medicine called digitalis. The medicinal effect is due to the cardiac glycosides contained in the leaves, but in modern times the powdered leaves have been replaced by the pure glycosides. Digitoxin (**Structure 1.5**) is one of the glycosides contained in the leaves of *Digitalis purpurea*, and is routinely used as a drug for the treatment of congestive heart failure, cardiac arrhythmias and atrial fibrillation. Digoxin (**Structure 1.5**) from *Digitalis lanata* is also widely used in the treatment of congestive heart failure, arrhythmias and atrial fibrillation, and has a more rapid action and quicker elimination time than digitoxin (Dewick, 2001; Gilani and Atta-ur-Rahman, 2005).

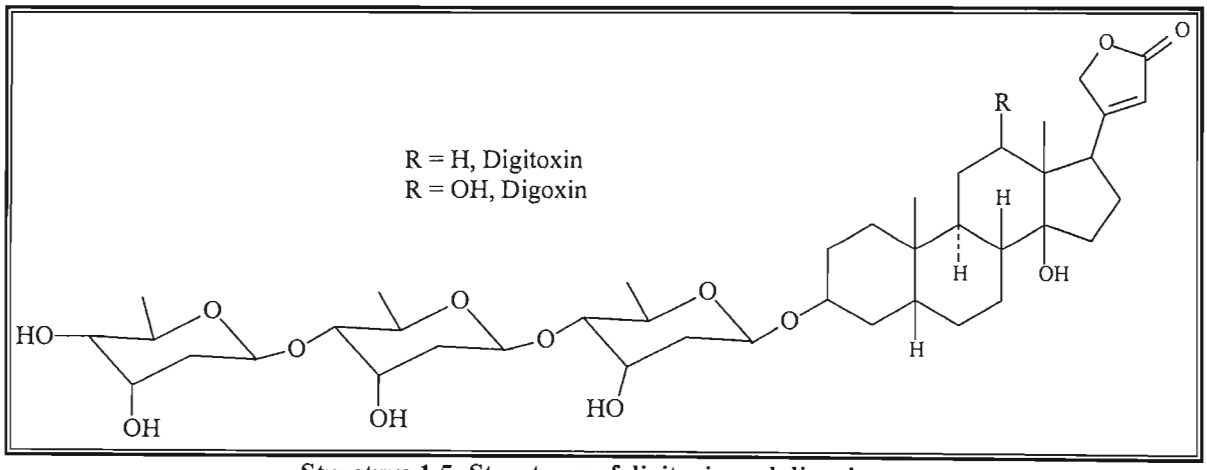

Structure 1.5: Structures of digitoxin and digoxin

Cephaelis ipecacuanha is a low straggling shrub found in South America. South American Indians used the dried rhizomes and roots of the plant for the treatment of dysentery. Phytochemical investigation of the rhizomes and roots found two medicinally

important terpenoid tetrahydroisoquinoline alkaloids, emetine and cephaeline (**Structure 1.6**). Emetine has been used as an anti-amoebic in the treatment of amoebic dysentery, but had a side effect of severe nausea. Although it is no longer used for treatment of dysentery, the emetic action of the alkaloid has made it an important drug for the treatment of poisoning overdoses. Emetine and cephaeline are also both potent inhibitors of protein synthesis, as well as displaying anti-tumour and anti-viral properties.

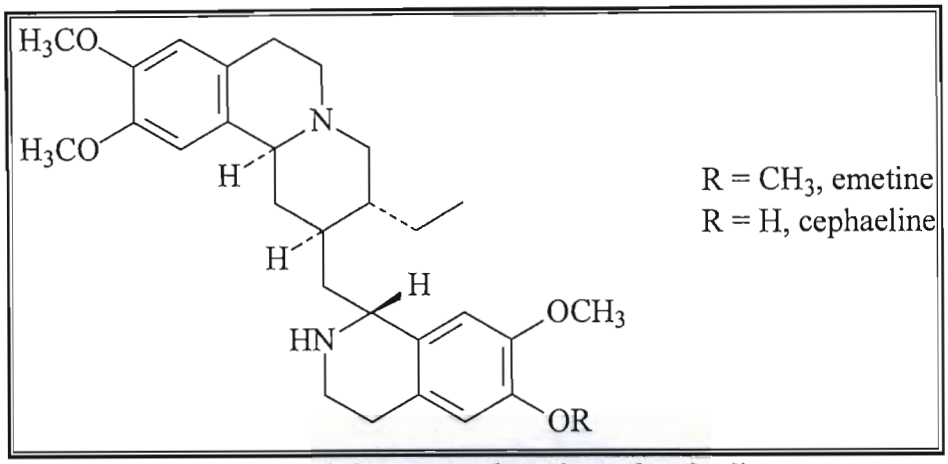

Structure 1.6: Structures of emetine and cephaeline

In the early 1630s Jesuit missionaries in South America discovered the medicinal value of the dried bark from the species *Chinchona*. The bark contains the quinoline alkaloid quinine (**Structure 1.7**), which is used in the treatment of malaria. It is believed that quinine prevents the polymerization of toxic haemoglobin breakdown products formed by the parasite *Plasmodium falciparum*, which is responsible for the malarial disease. Many anti-malarials are now based on the quinine structure, including chloroquine, primaquine, and mefloquine. These synthetic antimalarials replaced quinine as the main antimalarials in use, but due to resistant strains of *Plasmodium falciparum* (from wide spread use of the prophylactic chloroquine), quinine has been reintroduced (Dewick, 2001).

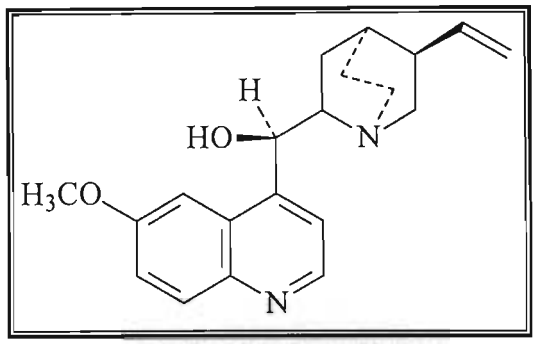

Structure 1.7: Structure of quinine

Another terpenoid indole alkaloid that has found widespread medicinal use is reserpine (**Structure 1.8**). It is found in the plant species *Rauvolfia* and its usage dates back for at least 3000 years in India, as well as being used for hundreds of years in Africa, where it was used to treat stomach pains, fever, vomiting, headaches and insanity. In 1949 it was brought to the attention of the Western world by Vakil who described its use in hypertension, but only in 1958 was the active ingredient reserpine was isolated and synthesized (Gilani and Atta-ur-Rahman, 2005). Reserpine is widely used in modern medicine as an anti-hypertensive and mild tranquilizer. The mode of action is through interference with catecholamine storage, resulting in a depletion of available neurotransmitters (Dewick, 2001).

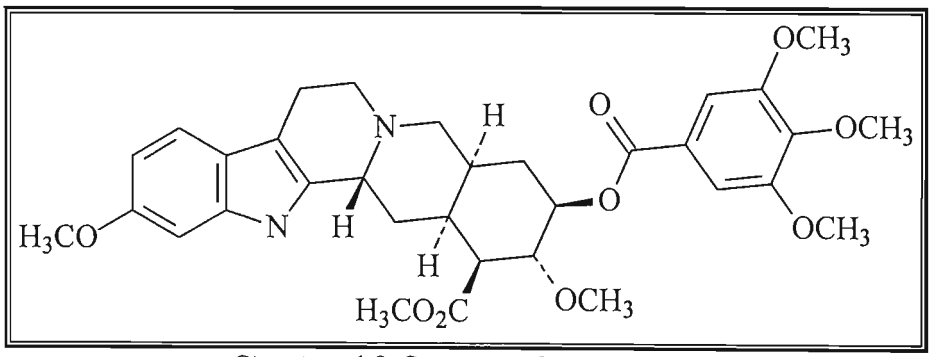

Structure 1.8: Structure of reserpine

Table 1.1: Selected phytochemical agents employed in modern medicines (Wijesekera, 1991)

COMPOUND	PLANT SPECIES	COMPOUND	PLANT SPECIES
Acetyldigoxin	*Digitalis lantana*	Khellin	*Amni visnaga*
Adoniside	*Adonis vernalis*	Lanatosides	*Catharanthus roseus*
Aescin	*Aesculus hippocastamum*	Linoleic acid (GLA)	*Nonnea macrosperma*
Ajmaline	*Rauvolfia vomitoria*	α-lobeline	*Lobelia spp.*
Aloin	*Aloe barbadenis*	Menthol	*Mentha spp.*
Anisodamine	*Anisodus barbadensis*	Morphine	*Papaver spp.*
Anisodine	*Scopolia tanguticus*	Papain	*Carica papaya*
Arecoline	*Areca catechu*	Palmatine	*Berbis spp.*
Belladonna (extract of)	*Atropa belladonna*	Physostigmine	*Physostigma venenosum*
Brucine	*Brucea spp.*	Pilocarpine	*Pilocarpus jaborandi*
Caffeine	*Camelia sinensis* *Theobroma cacao*	Procillaridin A	*Urginea spp.*, *U. maritima, U. Indica*
Camphor	*Cinnamomum camphora*	Protoveratrines A & B	*Veratrum album*
Cocaine	*Erythroxylon coca*	Quinine	*Cinchona spp.*
Codeine	*Papaver spp.*	Quinidine	*Cinchona spp.*
Colchicine	*Colchicum autumnale*	Rescinnamine	*Rauvolfia serpentina*
Curcumin	*Cucuma longa*	Reserpine	*Rauvolfia canescens*
Deserpidine	*Rauvolfia spp.*	Ruscogenins	*Ruscus aculeatus*
Digitoxin	*Digitalis lantana*	Rutin	*Cassia spp.*
Digoxin, digitoxigenin	*Digitalis lantana*	Santonin	*Cassia spp.*
L-Dopa	*Mucuna pruiens*	Scillarins A & B	*Urginea spp.*
Emetine	*Cephaclis ipecacuanha*	Scopolamine	*Scopolia tangutica*
Ephedrine	*Ephedra spp.*	Strychnine	*Strychnos nux-vomica*
Eugenol	*Eugenia caryophyllata*	Tetrahydrocannabinol	*Cannabis spp.*
Glycyrrhizin	*Glycyrrhiza glabra*	Theobromine	*Theobroma cacao*
Hyoscine	*Duboisia spp.*	Theophylline	*Theobroma cacao*
Hesperidin	*Citrus spp.*	Vincamine	*Vinca minor*
Hyoscyamine	*Datura spp.; Hyoscymus muticus*	Vincaleucoblastine (vinblastine)	*Catharanthus roseus*
Kawain, dihydrokawain	*Piper methysticum*	Vincristine (leurocristine)	*Catharanthus roseus*

It is estimated that there are between a quarter, to half a million different plant species, but only a very small percentage have been explored phytochemically, and even fewer have been tested for biological or pharmaceutical activity (Hamburger and Hostettmann, 1991). There is a wealth of potential medicinal compounds contained in the pool of secondary plant metabolites. Currently seventy-five percent of prescription medicines are synthetic, and most of the remaining twenty-five percent are semi-synthetic natural products. It is predicted in the year 2030 that the world population will be between 8-9 billion people. With this increased population, there may not be sufficient raw materials to supply 8-9 billion people with cost effective synthetic and semi-synthetic medication. This population growth however is going to generally be restricted to the developing world and so the need for rationalization and exploration of alternative medications is critical (Cordell and Colvard, 2005).

1.2. The Apocynaceae and Hyacinthaceae families.

1.2.1. Introduction to Apocynaceae

The Apocynaceae is a large family, divided into two subfamilies, and five tribes. Altogether it is composed of 180 genera and 1500 species. They are tropical plants, generally being found in tropical regions of both hemispheres. Seventeen genera and forty species are indigenous, or naturalised in Southern Africa.

Apocynaceaes are usually twining shrubs or woody climbers, which rarely stand erect, and are often tropical lianas. The leaves are simple, generally opposite but sometimes are whorled, and usually have close parallel veins. The inflorescence can be a panicle, cyme, raceme or solitary flower, and bracts and bracteoles are present. The flowers vary in size from small-to-large, and are often showy and fragrant (Codd, 1963; Hickey and King, 1981).

Apocynaceae have been used commercially in the past as a source of inferior rubber from the latex of the plant, they have been used as showy ornamentals, and as sources for several medications and alkaloids. *Acokanthera, Adenium, Catharanthus, Gonioma, Holarrhena, Nerium, Rauvolfia*, and *Strophanthus* have previously been investigated for

medicinal properties, with *Catharanthus* and *Rauvolfia* the most significant as they contain vinblastine, vincristine (*Catharanthus*) and reserpine (*Rauvolfia*) (Codd, 1963; Watson and Dallwitz, 1992).

Compounds previously isolated from Apocynaceae are varied, but the majority contains indole alkaloids, including tryptophan, steroidal and harman-type alkaloids. Flavonols have been found in some species, with the most common flavonols being kaempferol and quercetin. The family produces iridoid compounds and various cardiotonic glycosides, i.e. bufadienolides and cardenolides; some members are cyanogenic; and saponins are occasionally present (Hutchings, 1996; **Figure 1.1**).

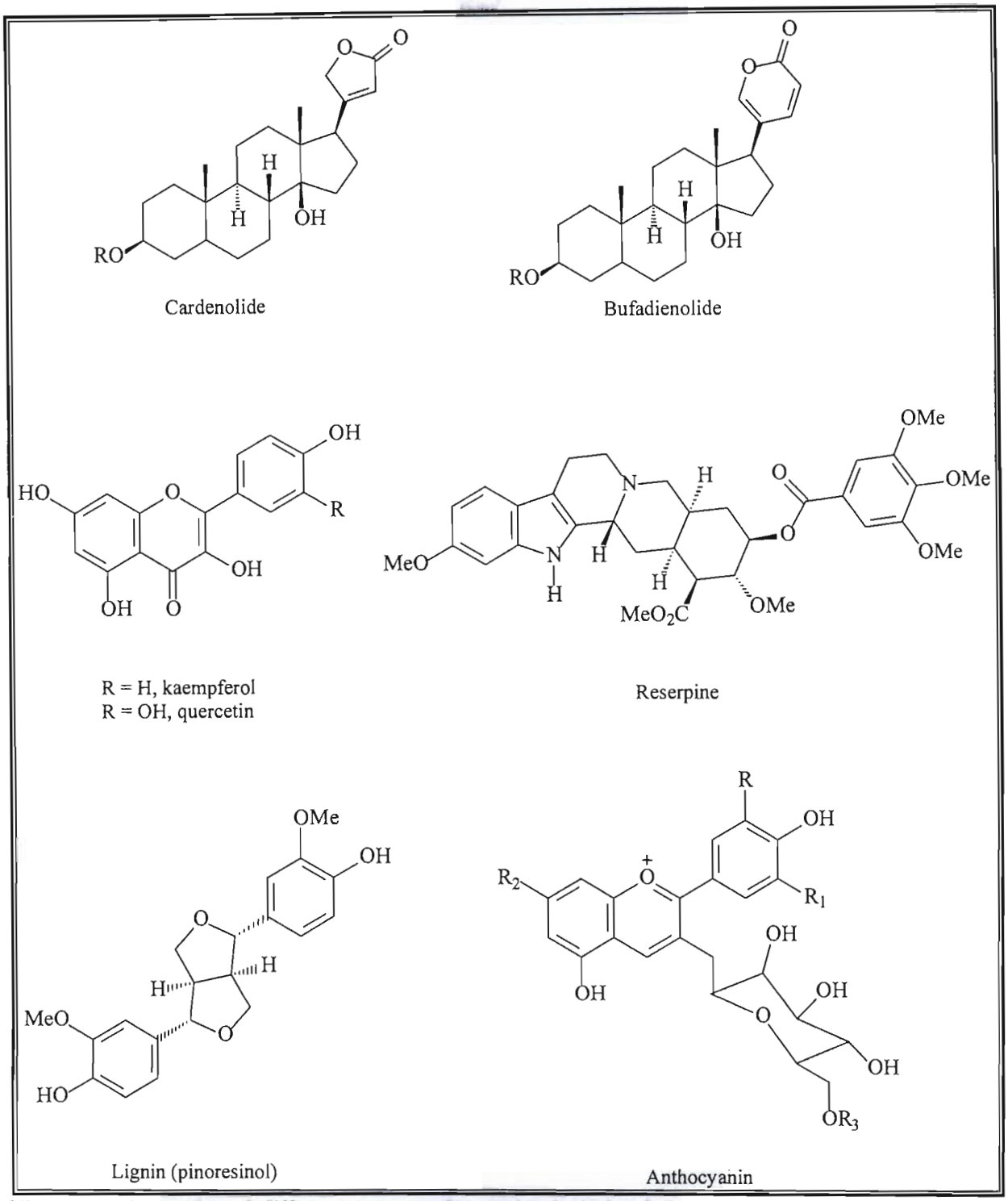

Figure 1.1: Examples of different compounds previously isolated in Apocynaceae (Codd, 1963; Watson and Dallwitz, 1992; Hutchings, 1996; Dewick, 2001)

1.2.2. INTRODUCTION TO HYACINTHACEAE

In ancient Greek times, the family Hyacinthaceae was divided into three genera; *Hyacinthus, Ornithogalum* and *Scilla*. These genera were based purely on flower characteristics, and as a consequence, distributing species amongst only three genera represented a highly unnatural classification. The three genera have now been "split" into several homogeneous genera reflecting phylogenetic relationships. The family Hyacinthaceae now consists of approximately 70 genera and 1000 species world wide, with 27 genera and 368 species found in South Africa (Pohl *et al.*, 2000; Pfosser and Speta, 2001). The family is divided into five subfamilies: Chlorogaloideae; Oziroeoideae; Urgineoideae; Ornithogaloideae; and Hyacinthoideae, of which the last three are found in South Africa (Speta, 1998).

Hyacinthaceae are monocotyledonous, bulbous plants, with subterraneous or epigeal bulbs. They are widely distributed across the world, where they prefer open sunny habitats with hot, dry vegetation periods (Speta, 1998).

The compounds isolated from the Hyacinthaceae can be grouped into three main chemical classes: homoisoflavanones, cardiac glycosides, and steroidal-type compounds. Miscellaneous compounds, not falling into the above categories, have also been isolated. A large number of homoisoflavanones have been isolated in many genera of the Hyacinthaceae. Homoisoflavanones are naturally occurring oxygen heterocycles with a skeleton consisting of sixteen carbon atoms (Pohl *et al.*, 2000).

Two types of steroidal compounds have been previously isolated from members of the Hyacinthaceae: spirocyclic nortriterpenes; and cholestane glycosides/steroidal saponins. Spirocyclic nortriterpenes have a basic lanosterol triterpenoid skeleton, and eucosterol is a commonly isolated example found in various *Eucomis* species. Variability in the compounds isolated is normally due to differing degrees of oxygenation in the aglycone, and differing combinations of sugars. Cholestane glycosides have previously only been isolated in the species *Ornithogalum*. A basic cholestane triterpenoid skeleton is the characteristic feature of these compounds, and the degree of oxygenation in the aglycone

and side chains, and the position of the glycoside varies extensively between members of this group (Pohl *et al.*, 2000).

Bufadienolides and cardenolides are two types of cardiac glycosides isolated in the Hyacinthaceae. Both are characterised by a steroidal aglycone with either a five or six membered lactone ring. Cardenolides have a β-substituted unsaturated, five membered lactone ring; whilst bufadienolides have a β-substituted, doubly saturated six membered lactone ring (Pohl *et al.*, 2000).

The miscellaneous compounds isolated include chromones, stilbenes, chalcones, acids, pyrones, phenolic compounds and alkaloids (Pohl *et al.*, 2000).

Many members of the Hyacinthaceae have varied economic uses as well. Many are utilised medicinally, with some usages dating back to 1554 B.C., where *Charybdis maritima*, the sea onion, was used for the treatment of dropsy, and bufadienolides from this species are used in the production of cardio-active substances. Occasionally the bulbs are eaten; in Greece, bulbs of *Muscari comosum* are eaten pickled; the inflorescences of *Loncomelos pyrenaicus* are consumed as a vegetable in France; and the San people in Africa consume the bulbs of some *Ledebouria* species. The most important economic uses however, are as ornamentals and as cut flowers. Numerous species are cultivated as ornamentals, and are grown and sold for their flowers (Speta, 1998).

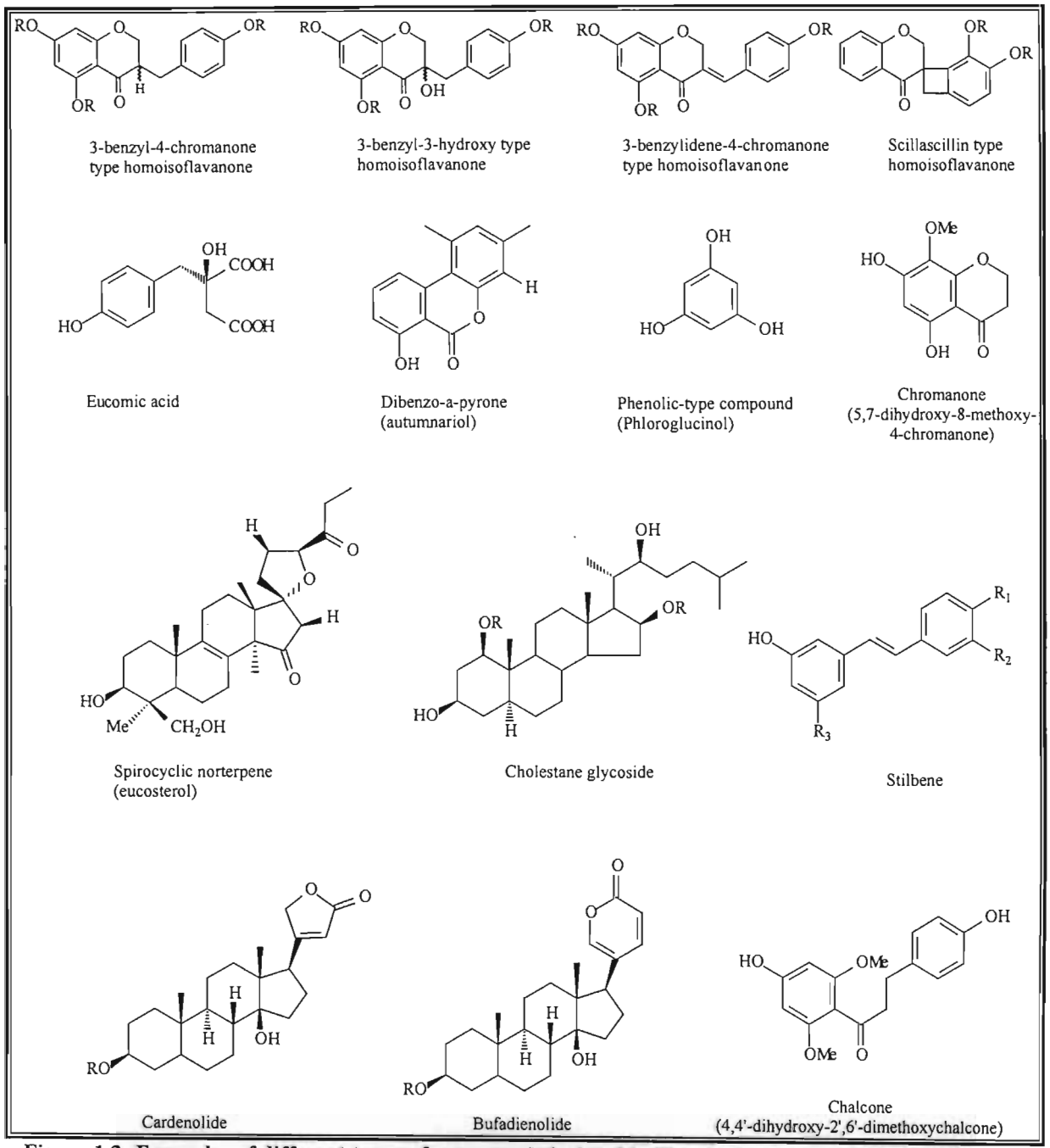

Figure 1.2: Examples of different types of compounds isolated in Hyacinthaceae (Pohl, 2000 *et al.*)

1.3. SPECIES INVESTIGATED

1.3.1. *STROPHANTHUS SPECIOSUS* (APOCYNACEAE)

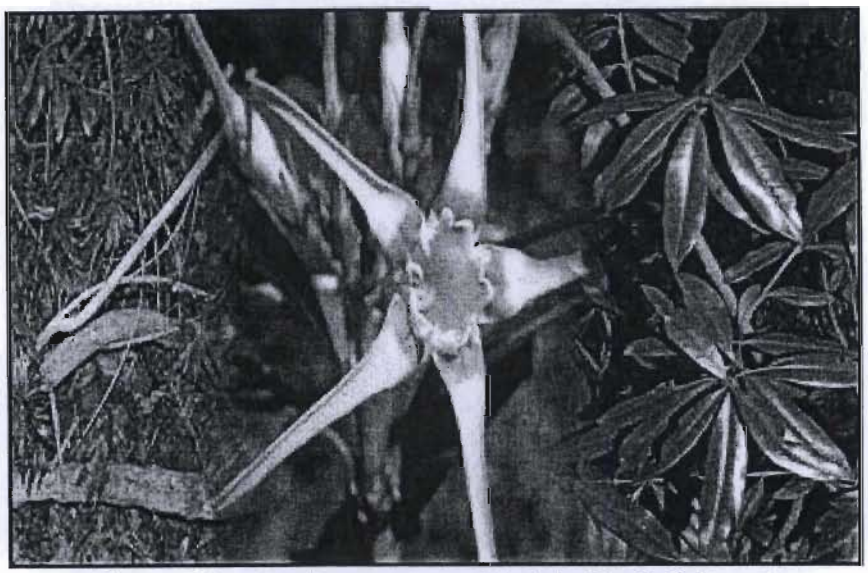

Photo of Strophanthus speciosus (photo by Dr. Neil Crouch)

Strophanthus speciosus has many common and Zulu names: bobbejaantou, gewone giftou, monkey ropes, osdoring, poison ropes, amasebele, indodabindenye, isihlungu, ubuhlungubendlovu, and umshayimamba (Hutchings, 1996), often referring to its poisonous and liana nature. It is a many-branched woody climber, which can grow to heights of up to 10m. The leaves occur in whorls of three, with short petioles, and are narrowly elliptical to oblanceolate in shape. They are between 3-10cm in length and between 0.8-2.5cm wide, and are glabrous with a glossy upper surface. The flowers of *Strophanthus speciosus* are yellow with a dull red mark at the base of each corolla lobe, and occur as a corymbose inflorescence containing up to sixteen flowers (Codd, 1963).

In South Africa, *Strophanthus speciosus* is found in forest margins and scrub forests in the Eastern Cape, KwaZulu Natal midlands, Swaziland and Mpumulanga. There is some variation in leaf length and breadth dependent on location: Eastern Cape varieties have smaller leaves; whilst towards KwaZulu-Natal the leaves become longer. There is not sufficient variation to separate the species into separate varieties (Codd, 1963).

The most abundant chemical compounds isolated in the *Strophanthus* are cardiac glycosides, with sixty different glycosides being recorded (Hutchings, 1996). The seeds

contain the majority of the glycosides reported, which are collectively named the strophanthins. Pharmacologically, the two most potent species of *Strophanthus* are *Strophanthus kombe* and *Strophanthus gratus*, with both species yielding very potent glycosides (Iwu, 1993).

Strophanthus kombe contains a mixture of glycosides collectively called strophanthin K, with the principle glycosides being K-strophanthoside, K-strophanthin-B, and cymarin, with the aglycone being strophanthidin. *Strophanthus gratus* contains one glycoside, g-strophanthin or ouabain, with the aglycone attached to a rhamnose moiety. Ouabain is active at very low concentrations, is soluble in water, and has several pharmacokinetic advantages over digitalis glycosides for patients who require rapid digitalization (administration of digitalis with a rapid onset of therapeutic effect) (Iwu, 1993).

Other species of *Strophanthus* containing glycosides are: *Strophanthus hispidus* that contains K-strophanthoside-a, cymaroside, saponosides and H-strophanthin; *Strophanthus sarmentosu*, which contains sarvogenin, and glycosides based on sarmentogenin; and *Strophanthus gracilis* that contains strophanthidin, strophanthidol, emicymarin, odoroside H and G, and graciloside (Iwu, 1993).

Strophanthus glycosides have essentially the same pharmacological activities as the digitalis glycosides, but they cannot match the activity of digitalis. They do however have an extremely rapid response when injected intravenously, having an observable effect on the pulse, and easing dyspnea within minutes of being administered (Iwu, 1993). In the early 1900's tinctures of *Strophanthus* were administered as a premedication before chloroform anaesthesia to prevent pre-anaesthetic excitement. The compounds are also useful in coronary insufficiency and angina, and from 1910-1935 many intravenous injections of strophanthin were administered for the treatment of cardiac failure. In the mid 1950s, the glycoside ouabain was used with good results to treat myocardial depression in cases of cardiogenic shock. It was also used in the mid-1950s to improve the circulatory state of patients under anaesthesia (McKenzie, 2002).

The *Strophanthus* glycosides however are very potent, toxic drugs, active in very low doses, and so there is the potential for fatalities due to overdose (Iwu, 1993).

Traditional Zulu healers have used *Strophanthus speciosus* in a variety of ways. Powdered roasted roots are taken as a snuff and are also used to treat snakebite, sometimes with roasted snakeheads included in the medication. Cattle are also treated for snakebite using similar formulations. It has also been used to treat hysteria, as an arrow poison, and as a homicidal agent (Hutchings, 1996).

Compounds previously isolated in *Strophanthus speciosus* are the cardiac glycosides strospeside (0.15%) and christyoside (0.3%) (Chen *et al.*, 1951; Schindler and Reichstein, 1952; Hutchings, 1996).

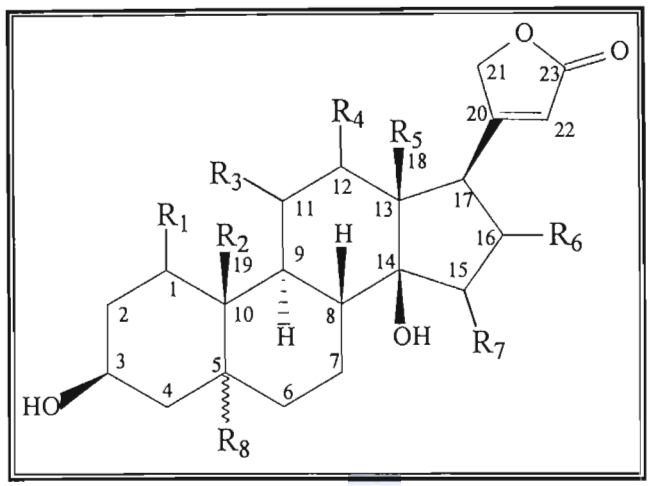

Figure 1.3: Basic structure of cardenolide aglycone (Pohl *et al.*, 2000)

Table 1.2: Selected cardenolides previously isolated from the *Strophanthus* genus (only aglycone named. Variations in alternate name due to different sugar moieties) (Chen *et al.*, 1951; Schindler and Reichstein, 1952).

Systematic name	Alternate name	R_1	R_2	R_3	R_4	R_5	R_6	R_7	R_8
3β,5β,14β-trihydroxy-19-oxo-card-20(22)-enolide	Strophanthidine K-strophanthidin	H	CHO	H	H	CH_3	H	H	OH
3β,11α,14β-trihydroxy-5β-card-20(22)-enolide	Sarmentogenin	H	CH_3	OH	H	CH_3	H	H	H
3β,14β,16β-trihydroxy-19-oxo-card-20(22)-enolide	Glaucorigenin	H	CHO	H	H	CH_3	OH	H	H
3β,14β-dihydoxy-19-oxo-5α-card-20(22)-enolide	Corotoxigenin Gofruside	H	CHO	H	H	CH_3	H	H	H
3β,14β-dihydroxy-5β-card-20(22)-enolide	Evomonoside Honghelin Honghеloside G Somalin Odoroside A Odorosid B Odoroside H Cheiroside A	H	CH_3	H	H	CH_3	H	H	H
16β-(acetyloxy)-3β,14β-dihydroxy-5β-card-20(22)-enolide	Honghеloside	H	CH_3	H	H	CH_3	OAc	H	H
3β,14β,15β-trihydroxy-19-oxo-5α-card-20(22)-enolide	Allo-glaucotoxigenin	H	CHO	H	H	CH_3	H	OH	H
1β,3β,14β-trihydroxy-5β-card-20(22)-enolide	Acovenoside A Acovenoside C	OH	CH3	H	H	CH_3	H	H	H
1-(acetyloxy),3β,14β-dihydroxy-card-20(22)-enolide	Acovenoside B	OAc	CH3	H	H	CH_3	H	H	H
3β,14β,16β-trihydroxy-5β-card-20(22)-enolide	Digitalin Strospeside	H	CH3	H	H	CH_3	OH	H	H

1.3.2. *EUCOMIS MONTANA* (HYACINTHACEAE)

Eucomis montana is one of ten species of the genus *Eucomis* and is found throughout Southern Africa. It occurs as a deciduous, bulbous geophyte, with several basal leaves, which are lorate to obovate in shape. The inflorescence occurs as a raceme of many flowers on a stout scape, and is topped by leafy bracts, with the flowers being white, pale green or yellow in colour (Speta, 1998; Leistner, 2000). They are predominantly found in rocky areas of the high grasslands of KwaZulu-Natal, Mpumulanga and Swaziland (Koorbanally *et al.*, 2006)

There have been no reported traditional medicinal uses for *Eucomis montana*, but other species in the genus are used by traditional healers. *E. autumnalis* has been used to treat urinary disease, is used as an emetic, to treat fevers, and as an infusion to help facilitate delivery of babies during pregnancy. The Tswana people have used decoctions of the bulbs and roots for the treatment of colic, flatulence, and abdominal distension. Decoctions of the bulbs are also used to treat hangovers and syphilis. The subspecies *Eucomis autumnalis clavata* has also been used to treat coughs and other respiratory ailments, venereal disease, and to prevent premature child birth (Hutchings, 1996).

Other *Eucomis* species that are used as traditional medicines are *Eucomis bicolor*, whose bulbs are used as purgatives, and *Eucomis comosa* which is used as an anti-rheumatic, and to help teething babies (Hutchings, 1996). *Eucomis* species are also widely used in different parts of South Africa for the treatment of pain and inflammation (Hutchings and Terblanche, 1989).

In a previous study (Koorbanally *et al.*, 2006), one eucosterol-type nortriterpenoid, and eleven homoisoflavanones were found in the bulbs of *Eucomis montana*. Four different classes of homoisoflavanones were represented: 3-benzyl-4-chromanone; 3-benzyl-3-hydroxy-4-chromanone; 3-benzylidenyl-4-chromanone; and the scillascillin type.

1.3.2.1.Eucosterol-type nortriterpenoid:

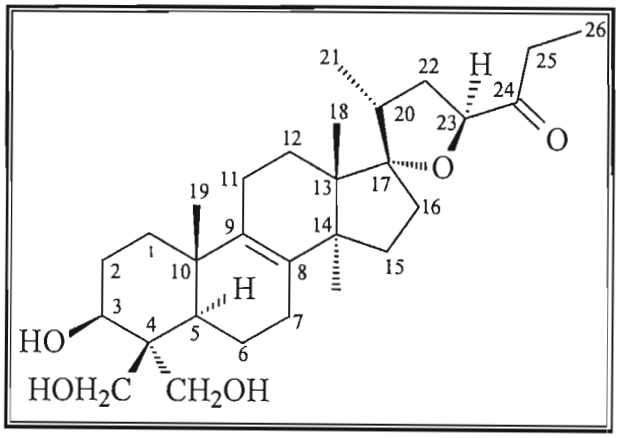

Name
(23S)-17α,23-epoxy-3β,28,29-trihydroxy-27-norlanost-8-en-24-one

1.3.2.2. 3-benzyl-4-chromanone type homoisoflavanones

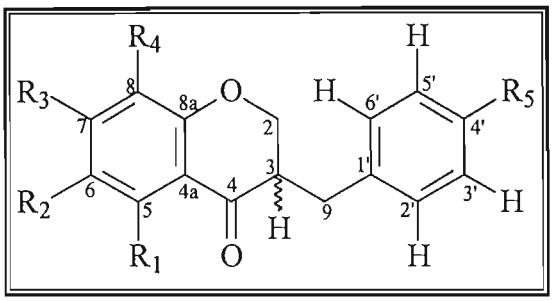

Name	R_1	R_2	R_3	R_4	R_5
4'-demethyl-3,9-dihydroeucomin	OH	H	OH	H	OH
3,9-dihydroeucomin	OH	H	OH	H	OCH_3
4'-demethyl-5-O-methyl-3,9-dihydroeucomin	OCH_3	H	OH	H	OH
8-O-demethyl-7-O-methyl-3,9-dihydropunctatin	OH	H	OCH_3	OH	OH
7-O-methyl-3,9-dihydropunctatin	OH	H	OCH_3	OCH_3	OH
7-hydroxy-3-(4'-hydroxybenzyl)-5,6-dimethoxy-4-chromanone	OCH_3	OCH_3	OH	H	OH

1.3.2.9. 3-benzyl-3hydroxy-4-chromanone type homoisoflavanones

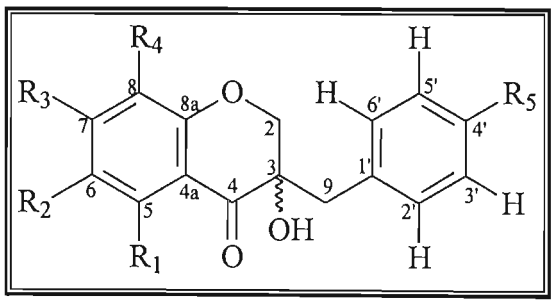

Name	R_1	R_2	R_3	R_4	R_5
3,5,7-trihydroxy-3-(4'-hydroxybenzyl)-4-chromanone	OH	H	OH	H	OH
Eucomol	OH	H	OH	H	OCH_3
7-O-methyleucomol	OH	H	OCH_3	H	OCH_3

1.3.2.3. 3-benzylidenyl-4-chromanone type homoisoflavanone

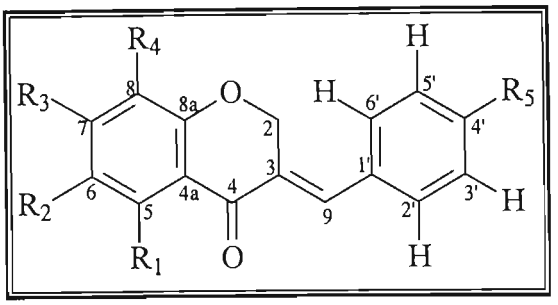

Name	R_1	R_2	R_3	R_4	R_5
(E)-eucomin	OH	H	OH	H	OCH_3

1.3.2.5. Scillascillan type homoisoflavanones

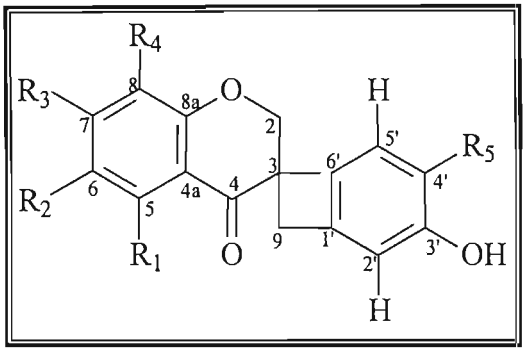

Name	R_1	R_2	R_3	R_4	R_5
3',5,7-trihydroxy-4'-methoxyspiro[2H-1-benzopyran-3(4H),7'-bicyclo[4.2.0]octa[1.3.5]-triene]-4-one	OH	H	OH	H	OCH_3

Other species of *Eucomis* have yielded lanosterol oligosaccharides, acids, dibenzo-α-pyrones, and chromanones (Sidwell et al., 1971; Heller and Tamm, 1978; Ziegler and Tamm, 1976; Pillay, 2003).

1.4. AIMS AND OBJECTIVES:

The research presented in this study has two main aims: firstly to phytochemically examine two South African plants, *Strophanthus speciosus* and *Eucomis montana*, for potential medicinal compounds; and secondly to test the compounds isolated for biological activity, and in doing so rationalize their traditional medicinal usages. It is intended that *Strophanthus speciosus* will be screened for muscle relaxant activity as part of a collaboration with the University of Sienna, and *Eucomis montana* for anti-inflammatory and antioxidant activity, as these are the traditional usages of the plants. Both the anti-inflammatory and antioxidant assays will utilize the oxidative burst of human leukocytes, that occurs during the inflammatory response, to form quantifiable screens.

1.5. REFERENCES:

Alcorn J.B, 1995. The scope and aims of ethnobotany in a developing world. From: *Ethnobotany: evolution of a discipline*. Eds: Schultes, R. and von Reis, S. Dioscorides Press, Portland, Oregon, pp 23-39.

Bojor O, 1991. Methodology of economic mapping of medicinal plants in the spontaneous flora. From: *Medicinal plant industry*. Ed: Wijesekera R.O.B. CRC Press, Boca Raton, USA, pp 18.

Chadha Y and Singh G, 1991. Information on medicinal plants. From: *Medicinal plant industry*. Ed: Wijesekera R. CRC Press, Boca Raton, USA, pp 237-239.

Chen K.K, Henderson F.G, and Anderson R.C, 1951. Comparison of forty-two cardiac glycosides and aglycones. *Journal of Pharmacology and Experimental Therapeutics,* **103**, 420-430.

Codd L, 1963. Apocynaceae. From: *Flora of Southern Africa: The republic of South Africa, Basutoland, Swaziland and South West Africa, Vol 26*. Eds: Dyer R, Codd L, and Rycroft H. Government Printer, Republic of South Africa, pp 244-295.

Cordell G.A and Colvard M.D, 2005. Some thoughts on the future of ethnopharmacology. *Journal of Ethnopharmacology,* **100**, 5-14.

Davis K.L, Mohs R.C, Tinklenberg J.R, Pfefferbaum A, Hollister L.E, and Kopell B.S, 1978. Physostigmine: Improvement of Long-Term Memory Processes in Normal Humans. *Science,* **201**, 272-274.

Dewick P.M, 2001. *Medicinal natural products: a biosynthetic approach, 2nd edition.* John Wiley & Sons, Chichester, pp 246-380.

Gilani A.H and Atta-ur-Rahman, 2005. Trends in ethnopharmacology. *Journal of ethnopharmacology,* **100,** 43-49.

Hamburger M and Hostettmann K, 1991. Bioactivity in plants: the link between phytochemistry and medicine. *Phytochemistry,* **30**, 3864-3874.

Heller W and Tamm C, 1978. 5,7-Dihydroxy-8-methoxychroman-4-one aus dem zwiebelwachs von Eucomis comosa. *Helvetica Chimica Acta,* **61**, 1257-1261.

Hickey M and King C.J, 1981. *100 Families of flowering plants*. Cambridge University Press, England, pp 314-315.

Holmstedt B.R and Bruhn J.G, 1995. Ethnopharmacology- A challenge. From: *Ethnobotany: Evolution of a discipline*. Eds: Schultes, R. and von Reis, S. Dioscorides Press, Portland, Oregon, pp 338-342.

Hutchings A and Terblanche S.E, 1989. Observations on the use of some known and suspected toxic Liliflorae in Zulu and Xhosa medicine. *South African Medical Journal*, **75**, 62-69.

Hutchings A, 1996. *Zulu medicinal plants: an inventory*. University of Natal Press, Pietermarizburg, South Africa, pp 242.

Iwu M.W, 1993. *Handbook of African medicinal plants*. CRC Press, Boca Raton, USA, pp 242-244.

Koorbanally N.A, Crouch N.R, Harilal A, Pillay B, and Mulholland D.A, 2006. Coincident isolation of a novel homoisoflavanoid from *Resnova humifusa* and *Eucomis Montana* (Hyacinthoideae: Hyacinthaceae). *Biochemical Systematics and Ecology,* **34**, 1-5.

Leistner O, (ed.) 2000. *Seed plants of southern Africa: families and genera. Strelitzia 10*. National botanical institute, Pretoria, pp 613.

McKenzie A.G, 2002. The rise and fall of strophanthin. *Internal Congress Series,* **1242**, 95-100.

Naranjo P, 1995. The urgent need for the study of medicinal plants. From: *Ethnobotany: Evolution of a discipline*. Eds: Schultes, R. and von Reis, S. Dioscorides Press, Portland, Oregon, 362-368.

Packer M and Brandt J.D, 1992. Ophthalmology's botanical heritage. *Survey of Ophthalmology,* **36**, 357-375.

Patwardhan B, 2005. Ethnopharmacology and drug discovery. *Journal of Ethnopharmacology,* **100**, 50-52.

Pfosser M and Speta F, 2001. Hyacinthaceae: *Hyacinthus*, *Ornithogalum*, *Scilla* and their relatives. From: http://tolweb.org/tree?group=Hyacinthaceae&contgroup=Asparagales. Accessed: February 2006.

Pillay B, 2003. Extractives from *Eucomis montana* and *Agapanthus inapertus*. M.Sc. dissertation, University of KwaZulu-Natal Press, South Africa.

Pohl T.S, Crouch N.R, and Mulholland D.A, 2000. Southern African Hyacinthaceae: chemistry, bioactivity and ethnobotany. *Current Organic Chemistry,* **4,** 1287-1324.

Schindler O, and Reichstein T, 1952. Identification of substance no. 763 from *Strophanthus speciosus* and *S. boivinii* as stropeside (desglucodigitalinum verum). *Helvetica Chimica Acta,* **35**, 442-446.

Sidwell W, Fritz H, and Tamm C, 1971. Autumnariol and autumnariniol. Two new dibenzo-α-pyrones from *Eucomis autumnalis*. Detection of long-range coupling over six bonds in the NMR spectra. *Helvetica Chimica Acta*, **54**, 207-215.

Speta F, 1998. Hyacinthaceae. From: *The families and genera of vascular plants*. Ed: Kubitzki K. Springer-Verlag, Berlin, Germany, pp 261-277.

Watson L, and Dallwitz M.. 1992. *The families of flowering plants: descriptions, illustrations, identification, and information retrieval*. http://delta-intkey.com. Version: 23rd October 2005.

Wijesekera R.O.B, 1991. Plant derived medicines and their role in global health. From: *Medicinal plant industry*. Ed: Wijesekera R.O.B. CRC Press, Boca Raton, USA, 1-18.

World Health Organisation Fact sheet No. 134: Tradition medicines. Taken from: http://www.who.int/mediacentre/factsheets/fs134/en/print.html. Accessed: February 2006.

Ziegler R and Tamm C, 1976. Isolation and structure of eucosterol and 16β-hydroxyeucosterol. Two novel spirocyclic nortriterpenoids and of a new 24-nor-5α-chola-8,16-diene-23-oic acid from bulbs of several *Eucomis* species. *Helvetica Chimica Acta*, **59**, 1997-2010.

CHAPTER 2: AN INTRODUCTION TO CARDENOLIDES

2.1. OCCURRENCE AND CLASSIFICATION

Many plants contain a class of compounds collectively referred to as cardioactive glycosides, which have been used as arrow poisons and also as heart drugs (Singh and Rastogi, 1970; Cabrera *et al.*, 1993; Langford and Boor, 1996; Dewick, 2001; Dinan *et al.*, 2001; Grosa *et al.*, 2005). They are composed of three distinct regions, a steroid backbone, an attached lactone ring, and a carbohydrate or sugar moiety with a glycosidic link to the steroid backbone. The steroid backbone together with the lactone ring is referred to as the genin or aglycone. The sugar moiety is attached at C-3 of the aglycone via an oxygen atom. There are two major classes of cardiac glycosides: bufadienolides, which were first isolated in the skin glands of toads; and cardenolides, which naturally occur in plant tissues. The differentiation is made depending on the nature of the lactone ring at C-17 (Singh and Rastogi, 1970; Langford and Boor, 1996).

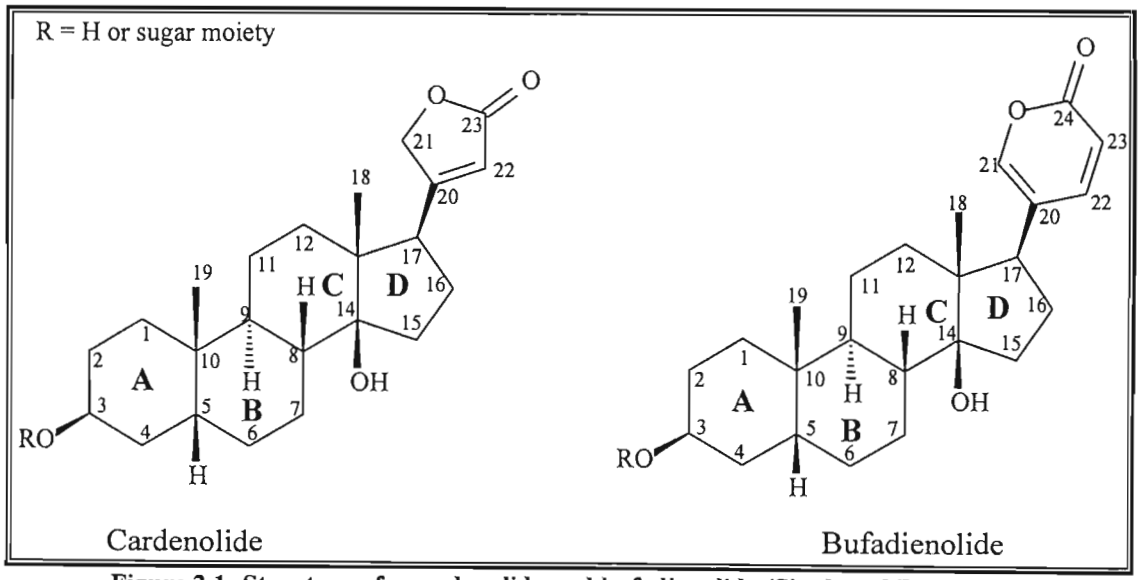

Figure 2.1: Structure of a cardenolide and bufadienolide (Singh and Rastogi, 1970)

Bufadienolides are typically polyhydroxy C-24, cardioactive steroidal compounds, with the main characteristic feature being a doubly saturated, six-membered lactone ring (α-pyrone or hexadienolide) attached to C-17 in the β-position. They are further characterized by the junction between the B- and C-rings being *trans* in nature, whilst that between the C- and D-rings is *cis*. Bufadienolides do not occur widely in nature being most commonly found in Bufonidae (toads), with the venom from about ten species

of *Bufo* containing bufadienolides and their esters (Krenn and Kopp, 1998; Dinan *et al.*, 2001). In the plant kingdom, their occurrence is restricted six angiosperm families: Crassulaceae, Hyacinthaceae, Iridaceae, Melianthaceae, Ranunculaceae and Santalaceae (Krenn and Kopp, 1998; Dinan *et al.*, 2001; Meng *et al.*, 2001; Pohl *et al.*, 2001).

Cardenolides are C-23 plant steroids that occur naturally as glycosides. Structurally they are very closely related to bufadienolides, but attached at C-17 is a five-membered α,β unsaturated γ-lactone (butenolide) ring. Variations between cardenolides usually involve: different substitutions at C-3 and C-5, where, different sugars can attach at C-3; the level of saturation of the lactone ring can vary; and there may be the presence or absence of oxygen functions attached to the skeleton (Singh and Rastogi, 1970; Paryzek and Blaszczyk, 1999; Dinan *et al.*, 2001). Variation can also occur through different functional group attachment at C-10 and/or C-13 (Langford and Boor, 1996).

Variation at C-5 occurs as the attached substituent can be in either α or β configuration. Digitalis-strophanthus type cardenolides predominate with β-substitution at C-5, and variants include aglycones with 3α-hydroxy substitution; acetoxy substitution; and rarer variants with a 16-O-isovaleryl group attached. Other variants encountered are C7-8, C8-14 and C11-12 epoxides; and aglycones with unsaturated A and/or B rings. The compound strogogenin (**Structure 2.1**) was the first cardiac aglycone isolated that had an additional lactone ring (Singh and Rastogi, 1970).

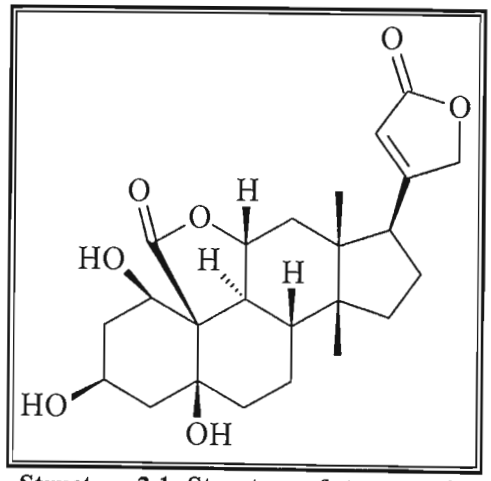

Structure 2.1: Structure of strogogenin

Although the majority of cardenolides have C-17β lactone rings, some compounds have been isolated with a C-17α attached lactone ring. It has been shown that plants containing these aglycones contain enzymes that are responsible for this configurational inversion (Singh and Rastogi, 1970).

Cardenolides predominate as cardenolide-3-O-glycosides, but cardenolide-2,3-O-diglycolsides and 3-O-sulfate esters have also been isolated (Dinan *et al.*, 2001). The sugars attached are usually either normal sugars or 2-deoxy sugars. There are usually between one to four sugar units present (Singh and Rastogi, 1970; Langford and Boor, 1996). Unbranched aldohexoses (generally 6-deoxy type) predominate, but 2-O-methyl and 2-O-acetyl sugars are also found. Both D- and L- configurations occur, but interestingly, in *Strophanthus*, the D-configuration is only found in African varieties, whilst the L-configuration is restricted to the Asian varieties (Singh and Rastogi, 1970).

The sugar units of cardenolides are specific for each compound, and the unique sugar unit imparts considerable variation with respect to biological functioning and solubility on the cardenolide. As a result, the structure-activity relationships for cardenolides are strongly affected by the particular sugar attached and, to a lesser extent, by the functional group substitution at C-10 and C-13 on the aglycones (Langford and Boor, 1996).

Cardenolides are fairly widely distributed throughout the plant kingdom, but are particularly associated with Asclepiadaceae (*Periploca* and *Calotropis*), Apocynaceae (*Nerium* and *Strophanthus*), Scrophulariaceae (*Digitalis*), Ranunculaceae (*Adonis*), and Convallariaceae (*Convallaria* and *Speirantha*) (Singh and Rastogi, 1970; Begum *et al.*, 1999; Eisenbeib *et al.*, 1999; Elgamal *et al.*, 1999; Chee Chang *et al.*, 2000; Dinan *et al.*, 2001; Kamel *et al.*, 2001). Due to their poor stability towards acids and bases, their thermal lability, and their low concentrations in plants, detection and characterization is often difficult. NMR, UV, IR, and MS techniques are needed in order to make structural determinations and assignments (Singh and Rastogi, 1970; Grosa *et al.*, 2005).

NMR spectroscopy is an invaluable tool when determining the structure of cardiac glycosides. Both ^{1}H NMR and ^{13}C NMR spectroscopy are extremely useful when making structural assignments, and the application of modern pulse techniques such as DEPT (Distortionless Enhancement by Polarization Transfer); J-modulation, INEPT (Insensitive Nuclei Enhanced by Polarization Transfer), and APT (Attached Proton Test); as well as two-dimensional techniques such as COSY (Correlation Spectroscopy), NOESY (Nuclear Overhauser Effect Spectroscopy), HMBC (Heteronuclear Multiple Bond Correlation) and HSQC (Heteronuclear Single Quantum Correlation) allow for unambiguous characterization of both the aglycones as well as the sugar moiety (Tori *et al.*, 1973; Steyn *et al.*, 1986; Krenn and Kopp, 1998).

An examination of the ^{13}C NMR spectra of cardenolides shows that C-7, C-8, C-9, C-13, C-14, C-15 and C-16 chemical shifts are generally deshielded when compared with the values for A/B-*cis* C/D-*trans* steroids. The upfield shifts for C-7 and C-9 resonances are due to steric interactions between the axial hydrogens at these positions and the C(14)-C(15) bond. In other steroids the high field methine group is assigned to C-8, but due to the equatorial β-effect of the C-14β hydroxyl this does not occur in cardenolides (Tori *et al.*, 1973).

Table 2.1: Variations in ^{13}C chemical shifts for ten cardenolides (δ_C in ppm downfield from TMS) (Tori *et al.*, 1973), compared with ^{13}C chemical shifts for stigmasterol (Structure 2.2) (De-Eknamkul and Potduang, 2003) and sitosterol (Structure 2.2) (Saxena and Albert, 2005), two common plant phytosterols.

	δ_C Cardenolide	δ_C Stigmasterol	δ_C Sitosterol		δ_C Cardenolide	δ_C Stigmasterol	δ_C Sitosterol
C-1	30-31	37	37	**C-13**	50-56	42	42
C-2	25-28.	-	30	**C-14**	84-146	57	57
C-3	67- 71	72	80	**C-15**	31-108	24	24
C-4	31-34	42	39	**C-16**	25-136	29	28
C-5	37-40	141	140	**C-17**	46-158	56	56
C-6	26.5-27	122	122	**C-18**	10-20	-	12
C-7	20-24	32	32	**C-19**	23.5-24	-	19
C-8	36.7-41.9	32	32	**C-20**	173-177	-	-
C-9	33 -45	50	51	**C-21**	73-77	-	-
C-10	35-36	36	37	**C-22**	112-121	-	-
C-11	21-30	21	21	**C-23**	175-177	-	-
C-12	31-75	40	40				

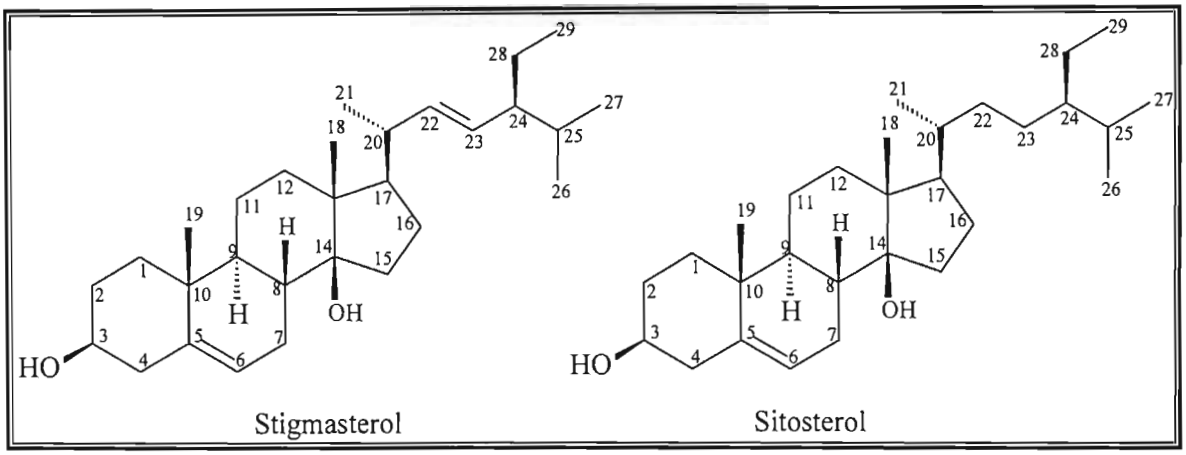

Structure 2.2: Structures of stigmasterol and sitosterol

Mass spectrometry is another valuable tool in determining the structure of cardiac glycosides. Fast atom bombardment-mass spectrometry (FAB-MS) and electron impact-mass spectrometry (EI-MS) allows for additional information to be obtained pertaining to the position of the sugars in the sugar moiety, the structure of both algycone and sugar moiety, and the molecular weight of the compound to be determined; whilst gas chromatography-mass spectrometry (GC-MS) allows one to determine the composition of the sugar moiety and their specific linkages (Cabrera *et al.*, 1993; Krenn and Kopp,

1998). In thermally labile cardenolides EI-MS is not suitable and soft-ionisation techniques, such as in FAB-MS and liquid chromatography/electrospray mass spectrometry (LC-ESI-MS) is necessary for characterization of compounds (Grosa *et al.*, 2005).

Crystallography has also been used to determine stereochemistry of cardiac glycosides. Gamabufotalin, proscillaridin and arenobufagin were all investigated using this method, and the structures of bryophyllin A and daigremontianin were confirmed through single-crystal X-ray analysis (Krenn and Kopp, 1996; **Figure 2.2**).

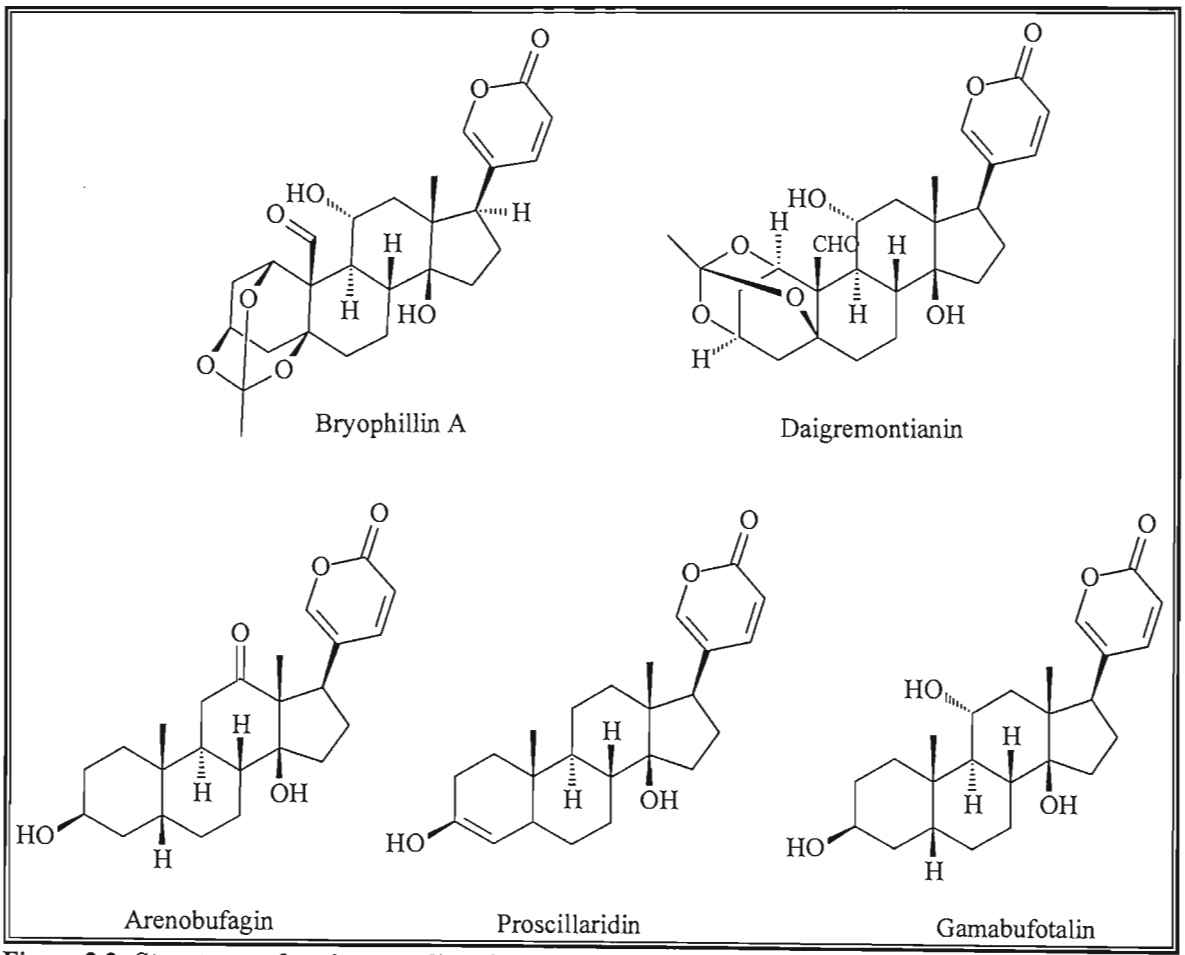

Figure 2.2: Structures of various cardiac glycoside aglycones whose structures were determined through the use of x-ray crystallography

2.2. BIOLOGICAL ACTIVITY

Cardenolides have a number of biological effects. They have been used traditionally in Africa, South America and Southeast Asia as arrow poisons (Singh and Rastogi, 1970; Dinan *et al.*, 2001; Mitaine-Offer *et al.*, 2001); in medicine/pharmacology as cardiac drugs (Singh and Rastogi, 1970; Cabrera *et al.*, 1993; Langford and Boor, 1996; Siddiqui *et al.*, 1997; Zotzmann *et al.*, 2000; Dinan *et al.*, 2001), central nervous system depressants (Siddiqui *et al.*, 1997), and anti-cancer/cytotoxic compounds (Singh and Rastogi, 1970; Begum *et al.*, 1999; Chee Chang *et al.*, 2000; Laphookhieo *et al.*, 2004); and commercially as insecticides (Dinan *et al.*, 2001; Supratman *et al.*, 2001).

The most important application of cardenolides is the therapeutic use of digitoxin and its derivatives as Na^+/K^+-ATPase inhibitors, which regulate heart contractions. The physiological action is attributed to the binding of the cardenolide to this enzyme (Singh and Rastogi, 1970; Langford and Boor, 1996; Zotzmann *et al.*, 2000; Dinan *et al.*, 2001). Na^+/K^+-ATPase is a transmembrane enzyme found in almost all animal cells, and functions in coupling ATP hydrolysis with Na^+ and K^+ transport. This establishes an ion gradient across the membrane that drives other transport systems, such as intake of glucose, amino acids and Ca^{2+}. It also underlies almost all of the electrical activity in the central nervous system, cardiac and skeletal muscles. In addition, Na^+/K^+-ATPase is also the receptor for cardioactive steroids. The binding of a cardioactive cardenolide to Na^+/K^+-ATPase inhibits the Na^+ pumping activity of the enzyme, resulting in a decrease in the Na^+ gradient across the membrane of cardiac myocytes (cardiac muscle cells). This results in less energy being available for Ca^{2+} transport out of the cell via Na^+/Ca^{2+} exchange, resulting in raised Ca^{2+} levels within the cell. These elevated Ca^{2+} levels ultimately results in the positive ionotropic effect caused by cardenolides. The lactone ring of the cardenolides appears to be the main group responsible for interaction between Na^+/K^+-ATPase and the cardenolide (Singh and Rastogi, 1970; Langford and Boor, 1996; Zotzmann *et al.*, 2000). Although the pharmacological activity resides in the aglycone, the sugar/s attached has fundamental importance as well, as they increase water solubility and affect the binding of the cardenolide in the myocyte membrane (Dewick, 2001).

The cardenolides nerizoside and neritaloside (**Figure 2.3**) have been shown to have central nervous system depressant activity. It was found that at a concentration of 25mg compound per kilogram of mouse they decreased locomotive activity, and at 50mg per kilogram mouse, there was a decrease in motor activity, touch response, gait, and respiration in the mice (Siddiqui *et al.*, 1997; Begum *et al.*, 1999).

Cardenolides have been previously shown to be cytotoxic, and this has applications in cancer research (Singh and Rastogi, 1970; Hoffmann and Cole, 1977; Begum *et al.*, 1999; Chee Chang *et al.*, 2000; Laphookhieo *et al.*, 2004). Several cardenolides have been shown to exhibit antiproliferative and anti-estrogenic activities against human colon cancer cell lines, and Ishikawa cancer cell lines. It is thought that the presence of a C-11/C-12 epoxide group may lead to increased biological activity against these cell lines (Chee Chang *et al.*, 2000). Some cardenolides have also been shown to inhibit the growth of oral human epidermoid carcinoma (Hoffmann and Cole, 1977; Laphookhieo *et al.*, 2004), human breast cancer cells, and human small cell lung cancer (Laphookhieo *et al.*, 2004).

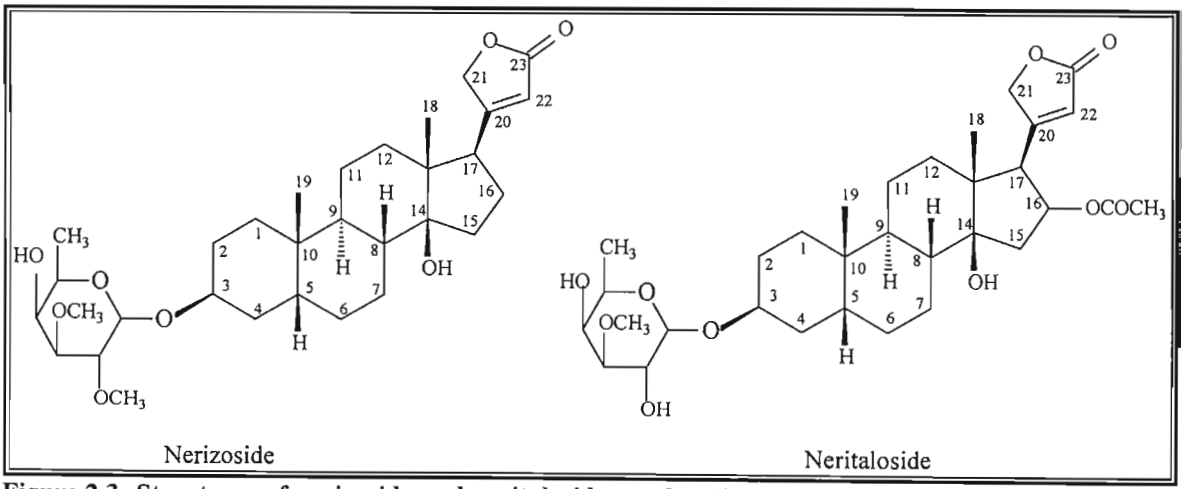

Figure 2.3: Structures of nerizoside and neritaloside, cardenolides displaying central nervous system depressant activity

2.3. BIOSYNTHESIS

The biosynthetic origin of cardenolides occurs via the metabolism of cholesterol, whereby the cholesterol side chain is cleaved forming an acetyl group, followed by the subsequent addition of three carbons to complete the lactone ring (Dewick, 2001). This process follows the following pathway: cholesterol → pregnenolone → progesterone → digitoxigenin (cardenolide) (Bennett *et al.*, 1968; Caspi and Lewis, 1968; Sauer *et al.*, 1968; Singh and Rastogi, 1970; Aberhart *et al.*, 1973; Anastasia and Ronchetti, 1977; Dewick, 2001).

The first stage in the formation of cardenolides is the conversion of cholesterol into pregnenolone (**Scheme 2.1**). The cholesterol side chain is shortened through stepwise oxidation reactions at C-22 and C-20, requiring oxygen and NADPH, followed by the oxidative cleavage between the hydroxyls of C-20 and C-22 resulting in pregnenolone (Dewick, 2001).

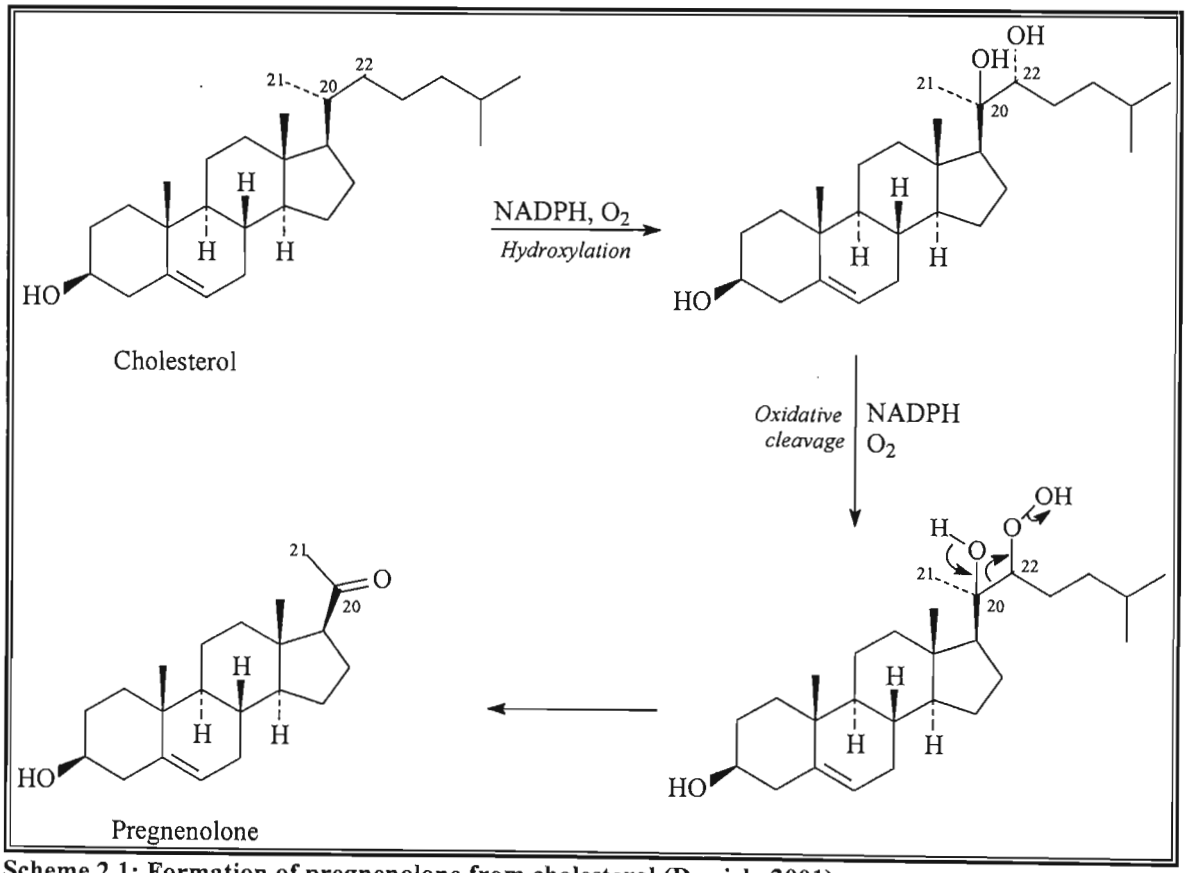

Scheme 2.1: Formation of pregnenolone from cholesterol (Dewick, 2001)

In an NAD^+ dependent reaction, pregnenolone is then oxidized at C-3, and this is followed by keto-enol tautomerism to form progesterone (Bennett *et al.*, 1968; Dewick, 2001; **Scheme 2.2**).

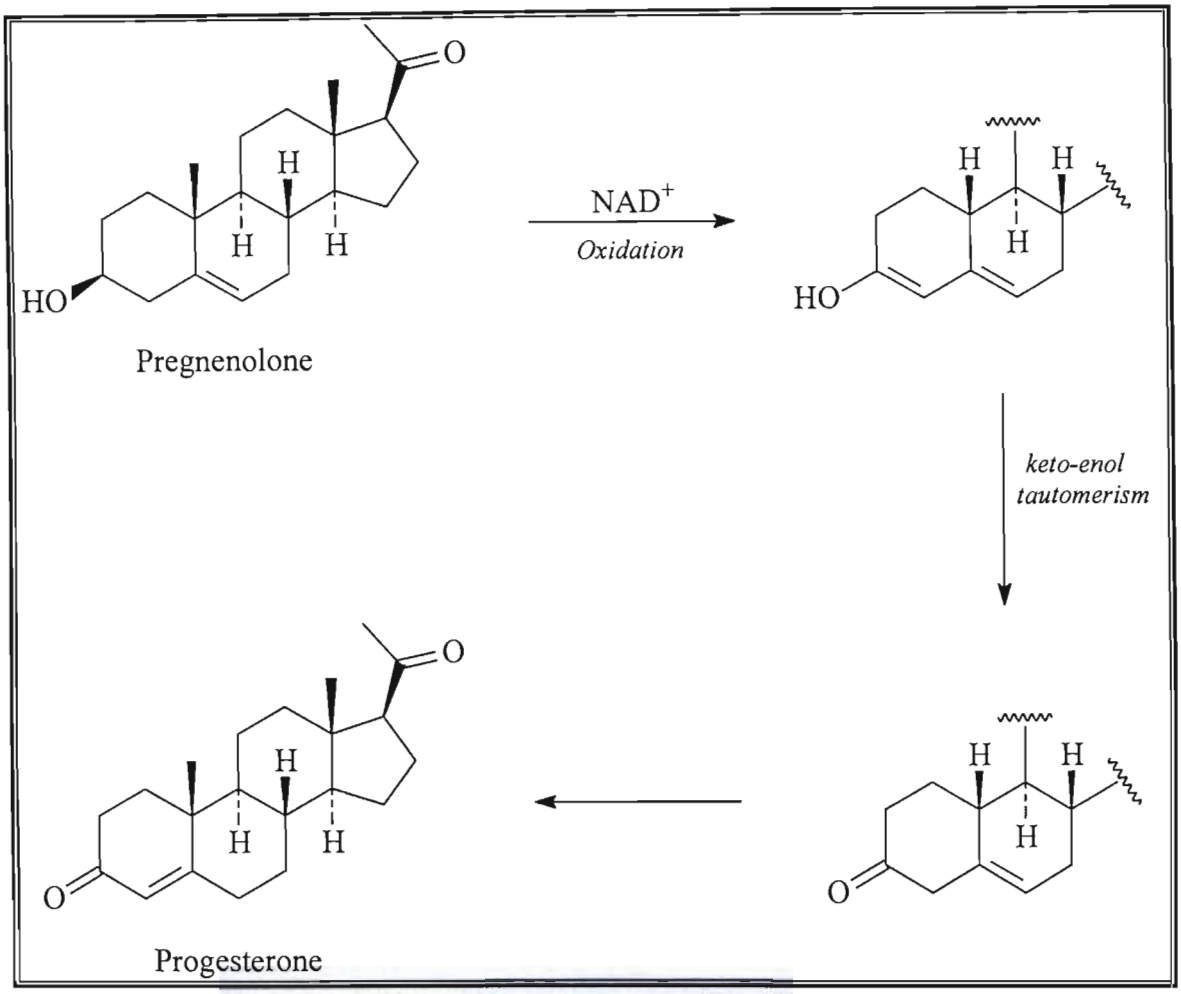

Scheme 2.2: Formation of progesterone from pregnenolone (Dewick, 2001)

In an NADPH dependent reduction, the C-4/5 double bond in progesterone is reduced, giving rise to *cis*-fused A/B rings. The ketone group at C-3 is subsequently reduced to a 3β-hydroxyl group to form 3β-hydroxy-5β-pregnan-20-one. This is the substrate that undergoes 14β-hydroxylation, i.e. the inversion of stereochemistry around this centre (Maier *et al.*, 1986; Dewick, 2001). Although the mechanism involved is not known, the inversion suggests an S_N2 type mechanism. If the reaction occurred via known biological mechanisms however, a 14α-hydroxyl product would form (Caspi and Lewis, 1968; Anastasia and Ronchetti, 1977). This reaction is catalysed by mono-oxygenases, but inversion is atypical for hydroxylation by mono-oxygenases. This hydroxylation is

followed by an oxidation of the acyl methyl group at C-21, forming 3β,14β,21-trihydroxy-5β-pregnan-20-one, which is the starting point for the formation of the lactone ring (Maier *et al.*, 1986; Dewick, 2001; **Scheme 2.3**).

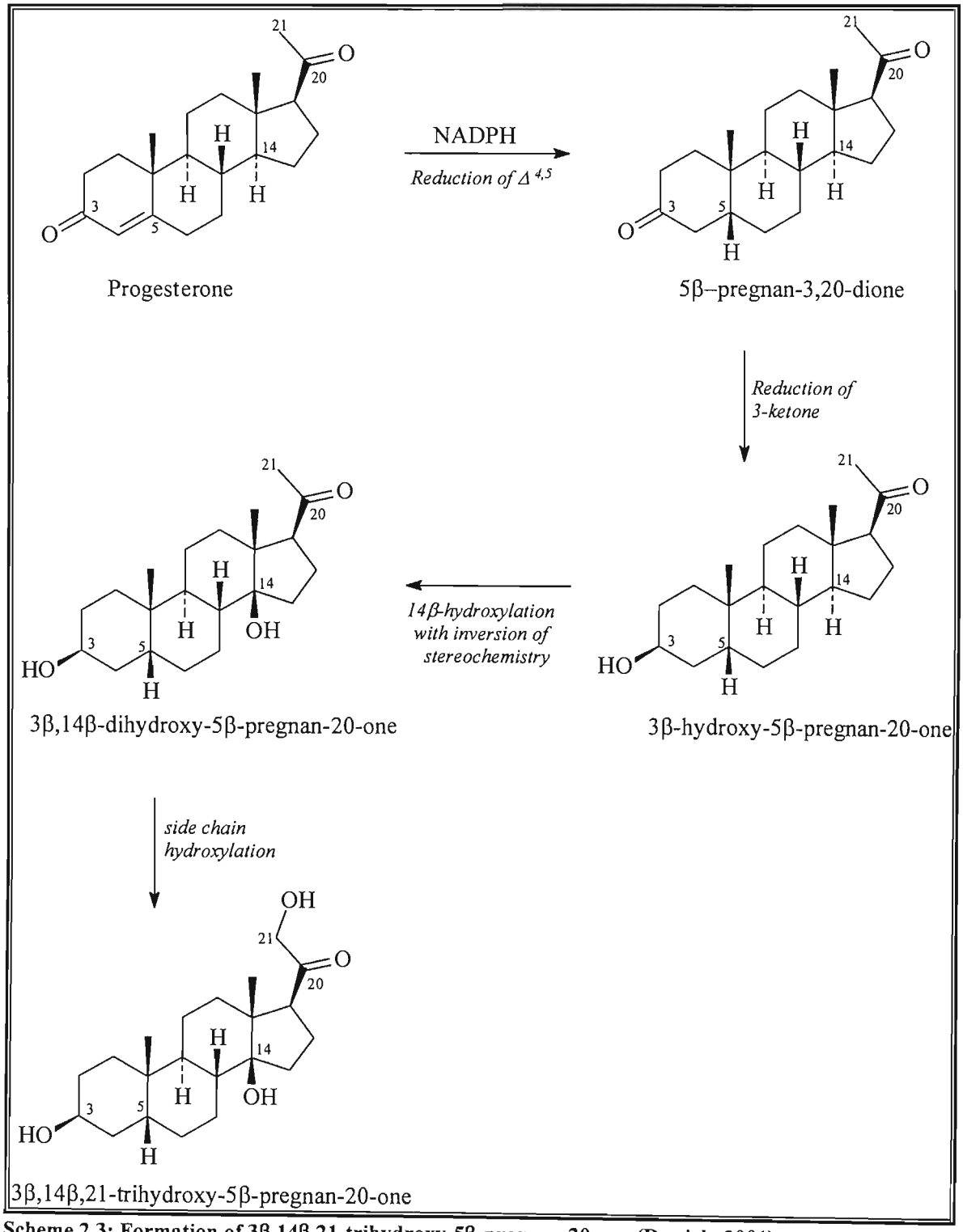

Scheme 2.3: Formation of 3β,14β,21-trihydroxy-5β-pregnan-20-one (Dewick, 2001)

The lactone or butenolide ring is formed through the addition of malonyl-CoA at C-21. The initial reaction forms a malonate ester, followed by a suspected aldol addition reaction that occurs with a concomitant decarboxylation. Dehydration in the ring produces the cardenolide digitoxigenin (**Scheme 2.4**). Further reactions including hydroxylations, acetylations, and others are responsible for the formation of different aglycones (Maier, 1986; Dewick, 2001).

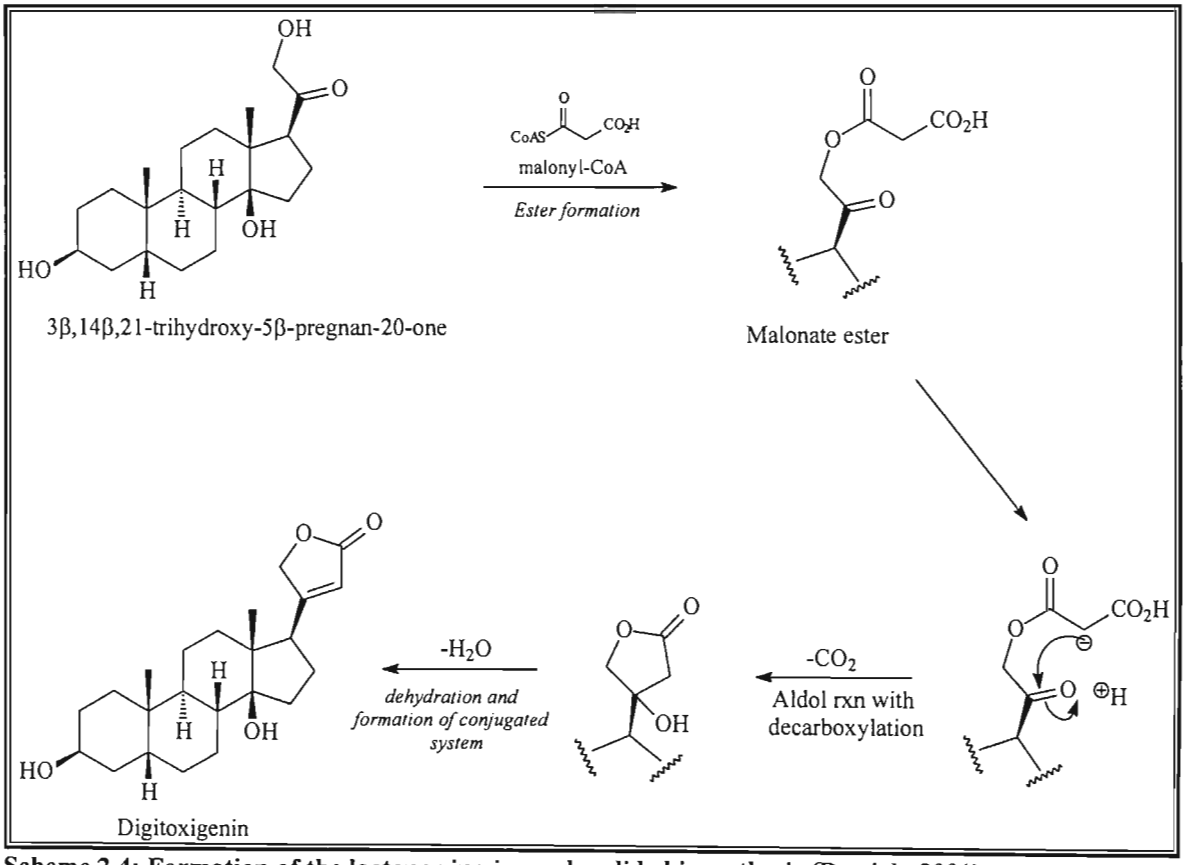

Scheme 2.4: Formation of the lactone ring in cardenolide biosynthesis (Dewick, 2001)

2.4. REFERENCES

Aberhart D.J, Lloyd-Jones J.G, and Caspi E, 1973. Biosynthesis of cardenolides in *Digitalis lantana*. *Phytochemistry*, **12**, 1065-1071.

Anastasia M and Ronchetti F, 1977. Mechanism of the 14β hydroxylation in the biosynthesis of cardenolides: the role of 14β-cholest-5-en-3β-ol. *Phytochemistry*, **16**, 1082-1083.

Begum S, Siddiqui B.S, Sultana R, Zia A, and Suria A, 1999. Bio-active cardenolides from the leaves of *Nerium oleander*. *Phytochemistry*, **50**, 435-438.

Bennett R.D, Sauer H.H, and Heftmann E, 1968. Progesterone metabolism in *Digitalis lantana*. *Phytochemistry*, **7**, 41-50.

Cabrera G.M, Deluca M.E, Seldes A.M, Gros E.G, Oberti J.C, Crockett J, and Gross M.L, 1993. Cardenolide glycosides from the roots of *Mandevilla pentlandiana*. *Phytochemistry*, **32**, 1253-1259.

Caspi E and Lewis D.O, 1968. Biosynthesis of plant sterols-IV. An investigation of a possible mode of 14β-hydroxylation in digitoxigenin. *Phytochemistry*, **7**, 683-691.

Chee Chang L, Gills J, Bhat K, Luyengi L, Farnsworth N, Pezzuto J, and Kinghorn D, 2000. Activity-guided isolation of constituents of *Cerbera manghas* with antiproliferative and anti-estrogenic activities. *Bio-organic & Medicinal Chemistry Letters*, **10**, 2431-2434.

De-Eknamkul W and Potduang B, 2003. Biosynthesis of β-sitosterol and stigmasterol in *Croton sublyratus* proceeds via a mixed origin of isoprene units. *Phytochemistry*, **62**, 389-398.

Dewick, P.M 2001. *Medicinal natural products: A biosynthetic approach*. John Wiley & Sons, Chichester, pp 241-252.

Dinan L, Harmatha J, and Lafont R, 2001. Chromatographic procedures for the isolation of plant steroids. *Journal of Chromatography A*, **935**, 105-123.

Eisenbeib M, Kreis W, and Reinhard E, 1999. Cardenolide biosynthesis in light- and dark-grown *Digitalis lantana* shoot cultures. *Plant Physiology and Biochemistry*, **37**, 13-23.

Elgamal M.H.A, Hanna A.G, Morsy N.A.M, Duddeck H, Simon A, Gati T, and Toth G, 1999. Complete ^{1}H and ^{13}C signal assignments of 5α-cardenolides isolated from *Calotropis procera* R. BR. *Journal of Molecular Structure*, **477**, 201-208.

Grosa G, Allegrone G, and Del Grosso E, 2005. LC-ESI-MS/MS characterization of strophanthin-K. *Journal of Pharmaceutical and Biomedical analysis*, **38**, 79-85.

Hoffmann J and Cole J, 1977. Phytochemical investigation of *Adenium obesum* Forskal (Apocynaceae): isolation and identification of cytotoxic agents. *Journal of Pharmaceutical Sciences*, **66**, 1336-1337.

Kamel M.S, Assaf M.H, Abe Y, Ohtani K, Kasai R, and Yamasaki K, 2001. Cardiac glycosides from *Crytostegia grandiflora*. *Phytochemistry*, **58**, 537-542.

Krenn L and Kopp B, 1998. Bufadienolides from animal and plant sources. *Phytochemistry*, **48**, 1-29.

Langford S and Boor P, 1996. Oleander toxicity: an examination of human and animal toxic exposures. *Toxicology*, **109**, 1-13.

Laphookhieo S, Cheenpracha S, Karalai C, Chantrapromma S, Rat-a-pa Y, Ponglimanont C, and Chantrapromma K, 2004. Cytotoxic cardenolide glycosides from the seeds of *Cerbera odollam*. *Phytochemistry*, **65**, 507-510.

Maier M.S, Seldes A.M, and Gros E.G, 1986. Biosynthesis of the butenolide ring of cardenolides in *Digitalis purpurea*. *Phytochemistry*, **25**, 1327-1330.

Meng Y, Whiting P, Sik V, Rees H.H, and Dinan L, 2001. Ecdysteroids and bufadienolides from *Helleborus torquatus* (Ranunculaceae). *Phytochemistry*, **57**, 401-407.

Mitaine-Offer A, Sauvain M, Petermann C, and Zeches-Hanrot M, 2001. Constituents of the trunk bark of *Maquira coriacea*. *Fitoterapia*, **72**, 841-843.

Paryzec Z and Blaszczyk K, 1999. A new approach to the synthesis of the 17β-butenolide fragment of cardenolides. *Tetrahedron Letters*, **40**, 5913-5914.

Pohl T.S, Koorbanally C, Crouch N.R, and Mulholland D.A, 2001. Bufadienolides from *Drimia robusta* and *Urginea altissima* (Hyacinthaceae). *Phytochemistry*, **58**, 557-561.

Sauer H.H, Bennett R.D, and Heftmann E, 1968. Biosynthesis of *Strophanthus* cardenolides from progesterone. *Phytochemistry*, **7**, 1543-1546.

Saxena V and Albert S, 2005. β-Sitosterol-3-O-β-D-xylopyranoside from the flowers of *Tridax procumbrens* Linn. *Journal of Chemical Sciences*, **117**, 263-266.

Siddiqui B.S, Sultana R, Sabira B, Zia A, and Suria A, 1997. Cardenolides from the methanolic extract of Nerium oleander leaves possessing central nervous system depressant activity in mice. *Journal of Natural Products*, **60**, 540-544.

Singh B and Rastogi R.P, 1970. Cardenolides-glycosides and genins. *Phytochemistry*, **9**, 315-331.

Steyn P, van Heerden F, and Vleggaar R, 1986. Application of high-field NMR spectroscopy to the structural elucidation of natural products. The structure of rubellin, a novel bufadienolide glycoside from *Urginea rubella*. *South African Journal of Chemistry*, **39**, 143-146.

Supratman U, Fujita T, Akiyama K, and Hayashi H, 2001. Insecticidal compounds from *Kalanchoe daigremontiana* x *tubiflora*. *Phytochemistry*, **58**, 311-314.

Tori K and Ishii H, 1973. Carbon-13 nuclear magnetic resonance spectra of cardenolides. *Tetrahedron letters*, **13**, 1077-1080.

Zotzmann J, Hennig L, Welzel P, Muller D, Schafer C, Zillikens S, Pusch H, Glitsch H, and Regenthal R, 2000. A novel cardenolide photoaffinity label for the Na/K-ATPase. *Tetrahedron*, **56**, 9625-9632.

CHAPTER 3: INTRODUCTION TO HOMOISOFLAVANONES

3.1. OCCURRENCE AND CLASSIFICATION

In 1967, Boehler and Tamm isolated a new class of natural products from the bulbs of *Eucomis bicolour*. The compounds were oxygenated heterocycles and were named homoisoflavanones or homoisoflavonoids (Heller and Tamm, 1981). They are predominantly found in the family Hyacinthaceae, and have been isolated in several South African genera, including *Scilla, Veltheimia, Drimiopsis, Resnova* and *Ledebouria*, as well as the genera *Muscari* (Adinolfi *et al.*, 1984; Crouch *et al.*, 1999; Pohl *et al.*, 2000; Koorbanally *et al.*, 2006). Homoisoflavanones have also been isolated previously in the family Leguminosae (Heller and Tamm, 1981; Namikoshi *et al.*, 1987; Geiger, 1988).

Homoisoflavanones are unrelated to isoflavonoids which have a 15-carbon skeleton and are almost entirely restricted to the family Leguminosae (Dewick, 2001). Homoisoflavanones have a 16-carbon backbone and follow a different biosynthetic pathway (**Figure 3.1**). In nature, isoflavonoid formation involves a characteristic 2,3-aryl migration step of the C6-C3-C6 moiety, but the same step is absent in the biosynthesis of homoisoflavanones. Homoisoflavanones seem rather to represent a modification of the unrearranged flavonoid skeleton and therefore the systematic name, 3-benzyl-4-chromanome, is more appropriate (Dewick, 1973).

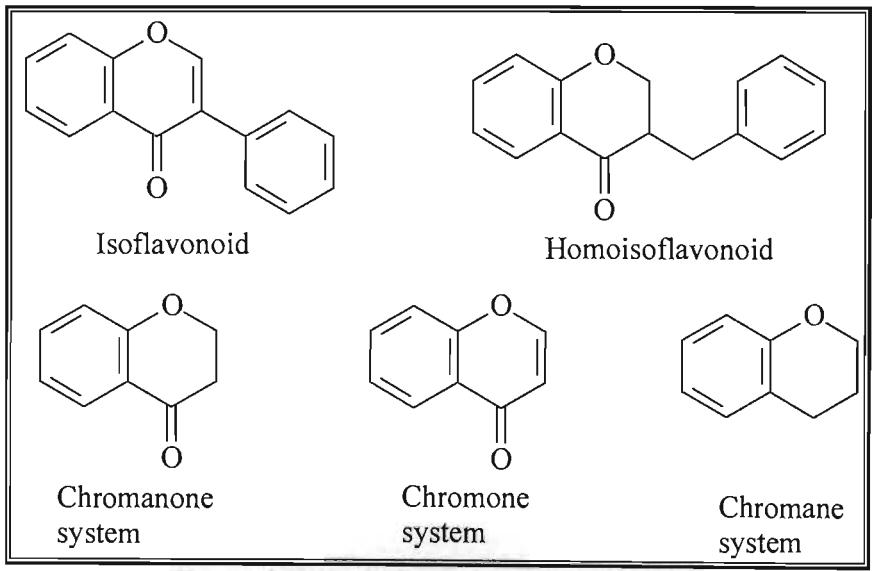

Figure 3.1: Structural difference between isoflavonoids and homoisoflavonoids, and the different skeleton systems of homoisoflavonoids

The skeleton for homoisoflavanones is made up of either a chromanone, chromone or chromane system (**Figure 3.1**) linked with a benzyl or benzylidene group at position C-3. They are usually extensively oxygenated and can have hydroxyl, methoxy or acetate substitution (Pohl *et al.*, 2000). The numbering system used in naming homoisoflavanones utilises the 4-chromanone region as the basic unit; with the benzylic carbon carrying the number nine; and the B-ring numbering starting at the point of benzylic substitution (Heller and Tamm, 1981; **Figure 3.2**).

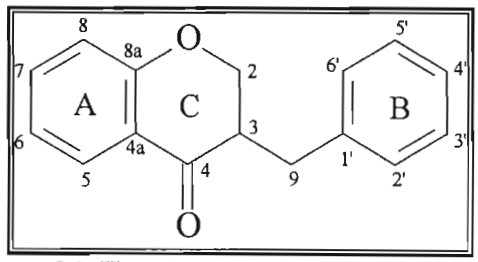

Figure 3.2: Homoisoflavanone numbering system

Homoisoflavanones can be classified into three basic structural types (**Figure 3.3**):

1. 3-benzyl-4-chromanone type or dihydroeucomin type;
2. 3-benzyl-3-hydroxy-4-chromanone type or eucomol type; and
3. 3-benzylidene-4-chromanone type or eucomin type (Kirkiacharian *et al.*, 1984; Namikoshi *et al.*, 1987; Pohl *et al.*, 2000).

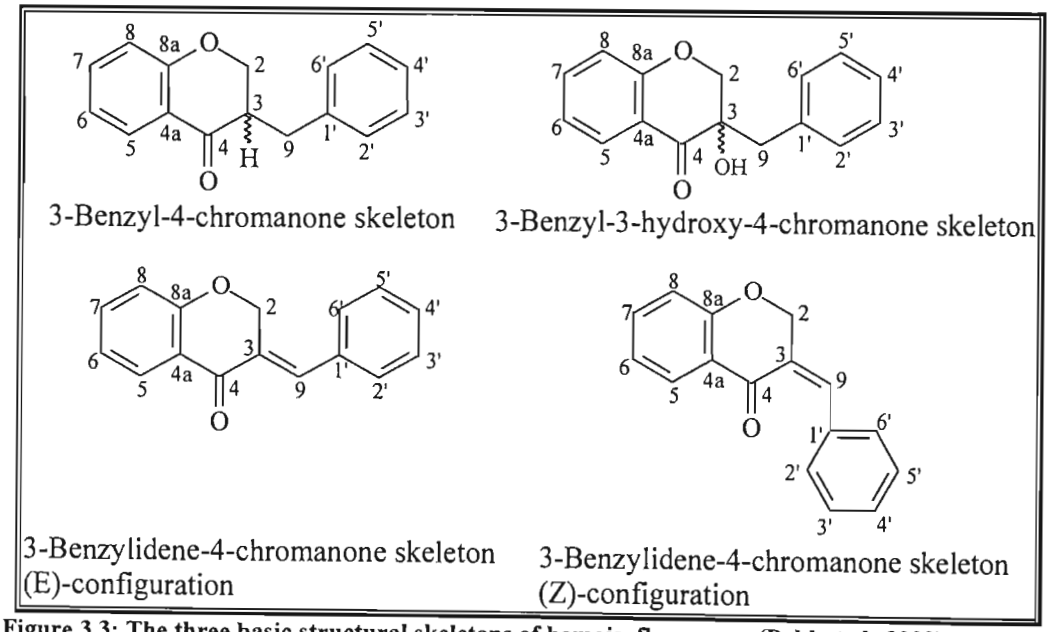

Figure 3.3: The three basic structural skeletons of homoisoflavanones (Pohl *et al.*, 2000)

Besides the three basic types, there are others arising from variations in the biosynthetic pathway. Scillascillin type homoisoflavanones have a characteristic 3-spirocyclobutene ring system; and comosin that does not have a benzylic carbon number 9, but instead is a 3-acetyloxymethyl-3-phenylchroman-4-one. Both these compounds however have a carbonyl function at C-4 (Namikoshi *et al.*, 1987). Brazilin and haematoxylin are homoisoflavanones which contain a cyclopentenyl ring (**Figure 3.4)** and have lost the carbonyl group at C-4 (Dewick, 1975).

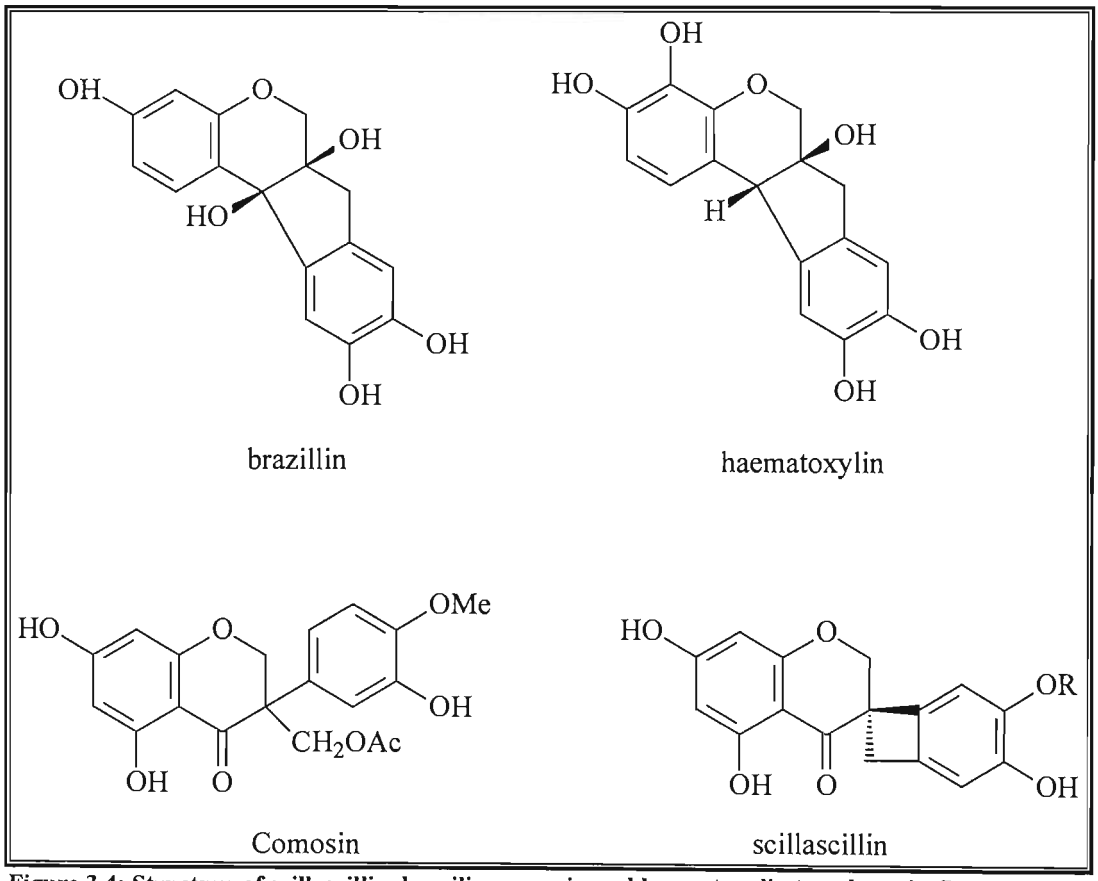

Figure 3.4: Structure of scillascillin, brazilin, comosin and haematoxylin type homoisoflavanones

Structural elucidation of homoisoflavanones is accomplished through the use of ultraviolet (UV), infrared (IR), nuclear magnetic resonance (NMR) and mass spectrometry (MS).

UV spectrometry allows one to easily determine the presence or absence of a double bond between C-3 and C-9. Homoisoflavanones have a uniform absorption, with the only variations occurring if a 3(9)-C double bond is present. In ethanol, the unsaturated system has an absorption maximum occurring between 358nm-367nm, whilst the saturated system has an absorption maximum between 285nm-297nm

(Heller and Tamm, 1981). The addition of sodium acetate induces a bathochromic shift of between 20nm-40nm, if a free hydroxyl group is present at C-7, whilst aluminium chloride produces a similar bathochromic shift (20nm-30nm), if C-5 contains a free hydroxyl group (Sidwell and Tamm, 1970; Heller and Tamm, 1981). These bathochromic shifts help in determining the substitution patterns on the A-ring.

IR spectroscopy also aids in determining whether C-3(9) is saturated or not. Unsaturated compounds have a complex spectral pattern, with four or five maxima located between $1550cm^{-1}$ and $1700cm^{-1}$. Saturated homoisoflavanones however show two to three distinct peaks in this region, with one near or higher than $1640cm^{-1}$, one around $1600cm^{-1}$, and the third around $1590cm^{-1}$. Methylation of the compound at C-7 and/or C-4' does not affect the peak at $1640cm^{-1}$, but methylation at C-5 causes a shift of this peak to $1650cm^{-1}$. If both C-5 and C-7 are methylated, the band is shifted to $1660cm^{-1}$. There are also broad absorption bands between $3000cm^{-1}$ and $3500cm^{-1}$ for hydroxylated homoisoflavanones, and the intensity of these bands depends on the number of hydroxyl groups present (Heller and Tamm, 1981).

Fragmentation patterns from mass spectrometry help in assigning functional groups to both the A and B-rings. The most common fragmentation behaviour of saturated compounds is an A-4 type breakdown of the molecule. This gives rise to a tropylium ion, which is the base peak in the spectrum, and a chromanone fragment. The chromanone fragment may then eliminate water, CO or undergo a *retro*-Diels-Alder (RDA) reaction. In eucomol, a RDA reaction yields a fragment with a mass of *m/z* 152, and an intense peak also occurs at *m/z* 153, which is the result of an effective hydrogen transfer from C-2 to the A-ring (Heller and Tamm, 1981; **Scheme 3.1**).

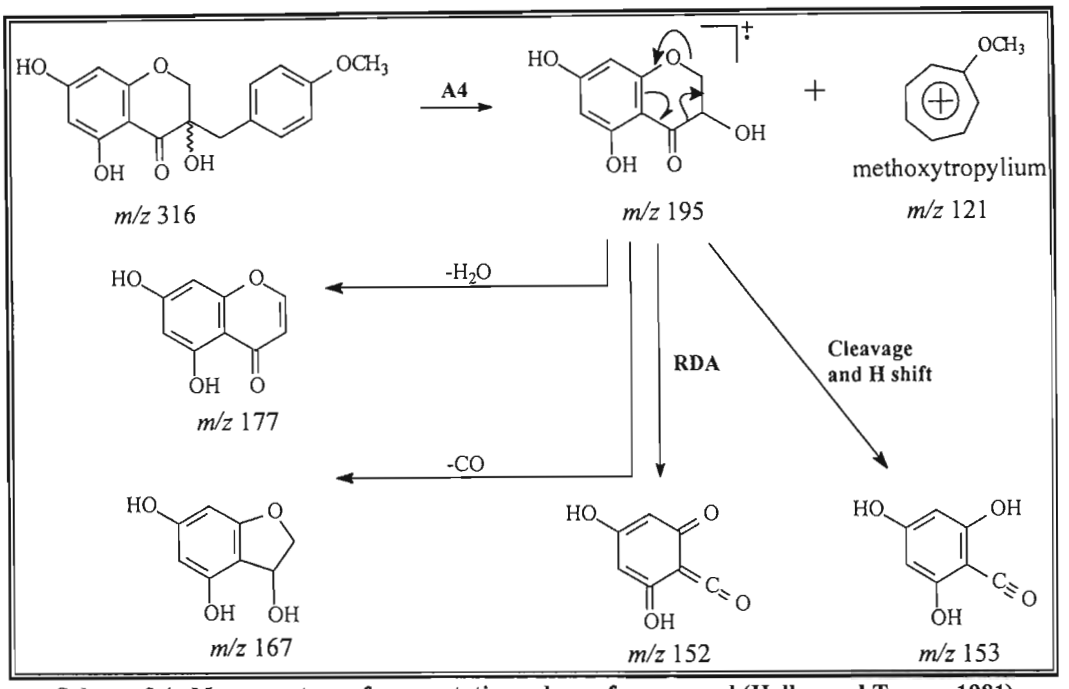

Scheme 3.1: Mass spectrum fragmentation scheme for eucomol (Heller and Tamm, 1981)

Nuclear magnetic resonance (NMR) spectroscopy is an essential tool in the determination of a homoisoflavanone structure. The ^{1}H NMR spectrum of the A and B rings closely resemble those of other flavonoids; whilst the protons associated with the C-ring and C-9 have characteristic splitting patterns for each of the three main types of homoisoflavanones.

1. 3-Benzyl-4-chromanone type: The coupling between the H-2, H-3, and H-9 protons results in a complex pattern, which is characterised by two AB-systems that form part of an ABX-system. The coupling of the two unequivalent H-2 protons with the H-3 proton results in a pair of double doublets typically at δ_H 4.3 and δ_H 4.1 with a coupling constant of approximately 12 Hz. The two unequivalent benzylic H-9 protons also form a pair of double doublets typically at δ_H 3.2 and δ_H 2.7 with the coupling constant being approximately 14 Hz; whilst coupling between H-3 and H-2a/b, and H-9a/b results in a multiplet resonance typically between δ_H 2.7 - 2.9 (Heller and Tamm, 1981; Silayo *et al.*, 1999).

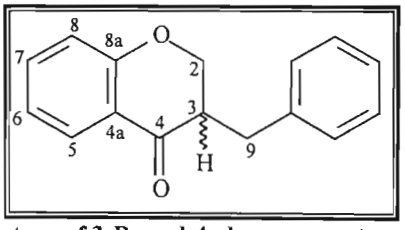

Structure 3.1: Structure of 3-Benzyl-4-chromanone type homoisoflavanone

2. 3-Benzyl-3-hydroxy-4-chromanone type: The ^{1}H NMR spectra for this type of homoisoflavanone is characterised by a pair of doublets for both the two H-2 protons and the two H-9 protons. The doublets due to the coupling of the two unequivalent H-2 protons occurs typically around δ_H 4.2-4.4 and δ_H 4.1-4.2; and the pair of doublets from the two H-9 protons are typically found at δ_H 3.1-3.2 and δ_H 2.65-2.75. The multiplet previously found at δ_H 2.7-2.9 is absent in this spectrum due to the presence of the hydroxyl group (Heller and Tamm, 1981).

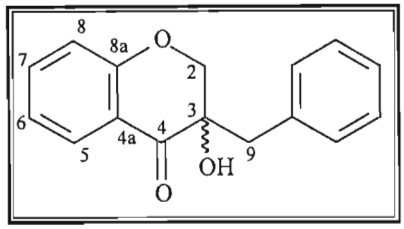

Structure 3.2: Structure of 3-Benzyl-3-hydroxy-4-chromanone type homoisoflavanone

3. 3-Benzylidene-4-chromanone type: Spectra for the 3(9)-unsaturated homoisoflavanones show clear signals for the protons on C-2 and C-9 near δ_H 5.0. The unequivalent H-2 protons occur as a pair of doublets typically around δ_H 5.2-5.5 ppm, whilst the chemical shift for the H-9 proton singlet depends on which isomer is present. In the (*E*)-isomeric form, the resonance occurs typically around δ_H 7.6-7.7 due to anisotropic effects of the carbonyl group and the adjacent aromatic B-ring; whilst the (*Z*)-isomer has the H-9 resonance shifted downfield typically to δ_H 5.5 ppm, as this configuration places H-9 away from the anisotropic region of the carbonyl group (Heller and Tamm, 1981).

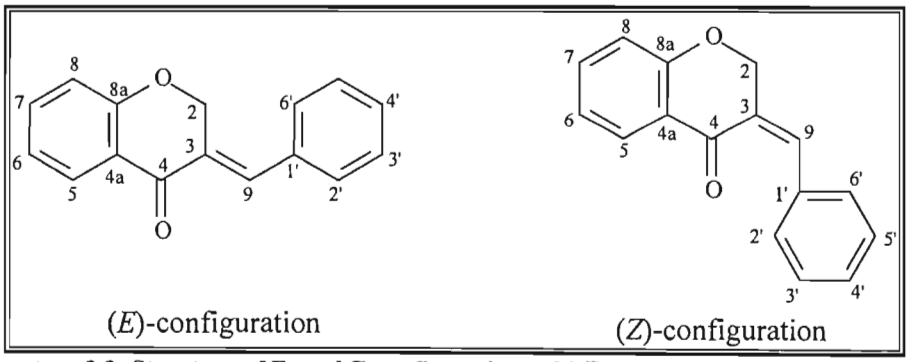

Structure 3.3: Structure of E- and Z-configurations of 3-Benzylidene-4-chromanone type homoisoflavanones

The ^{1}H NMR spectra of homoisoflavanones also display other characteristic features useful in the structural elucidation of compounds. Signals found between δ_H 6.50-

7.20 are generally resonances due to substitution patterns on the B-ring. The patterns observed are due to either an ABX or AA'BB' system. The ABX system arises if substituents are attached to C-3' and C-4', and the proton resonances of C-1', C-2' and C-3' all appear as double doublet resonances. In the AA'BB' system, there is substitution at C-4' and this results in the appearance of a pair of double doublets, each integrating to two protons.

Substitution on the A-ring results in resonances occurring between δ_H 5.80-6.30 on the ^{1}H NMR spectrum. There are usually only a few proton resonances in this region which are due to H-6 and/or H-8. A NOESY spectrum is usually necessary for the assignment of these protons.

^{13}C NMR spectra of homoisoflavanones have characteristic chemical shifts of the C-2, C-3, and C-4 atoms depending on the type of homoisoflavanone present. The C-2 chemical shifts for each homoisoflavanone type can be used to unambiguously distinguish one type from another. At C-3 there is wider variation in chemical shift due to the different chemical environments at this position. The resonance for the 3-benzyl-4-chromanone type is that of an aliphatic methine group and typically occurs at between δ_C 46-48; whist C-3 in 3-benzyl-3-hydroxy-4-chromanone types occurs as an oxygenated, aliphatic resonance, typically found at δ_C 73.5; and for 3-benzylidene-4-chromanone types, the C-3 resonance occurs as a quaternary resonance in the double bond region, typically found at δ_C 129-131. There are also significant differences between the C-4 chemical shifts for the three different types of homoisoflavanones. ^{13}C NMR spectra of C-2, C-3, and C-4 however does not allow for unambiguous differentiation between homoisoflavones, isoflavones, and homoisoflavanones (Kirkiacharian *et al.*, 1984).

Table 3.1: Characteristic ^{13}C NMR chemical shifts for the three main classes of homoisoflavanones (Kirkiacharian *et al.*, 1984).

Homoisoflavanone type	C-2 / ppm	C-3 / ppm	C-4 / ppm
3-benzyl-4-chromanone	69	46-47.5	194
3-benzyl-3-hydroxy-4-chromanone	73	73.5	195
3-benzylidene-4-chromanone	67.5	129-131	182

3.2. BIOLOGICAL ACTIVITY

Plants species within the Hyacinthaceae have wide-ranging ethnomedicinal uses, ranging from treatment of hangovers, sprains, rheumatic fever, cancer and syphilis (Pohl *et al.*, 2000), however there is rarely scientific evidence that accounts for such use. Homoisoflavanones are commonly found in Hyacinthaceae, and previous screenings of homoisoflavanones have shown that they possess anti-inflammatory, anti-mutagenic, anti-allergenic, anti-histaminic, anti-bacterial, antioxidant, and phosphodiesterase inhibition activity (Saitoh *et al.*, 1985; Della Loggia *et al.*, 1989; Wall *et al.*, 1989; Amschler *et al.*, 1996; Crouch *et al.*, 1999; Taylor and van Staden, 2001; du Toit *et al.*, 2005; O'Donnell *et al.*, 2006).

The homoisoflavanones intricatin and intricatinol (**Structure 3.4**), isolated from the roots of *Hoffmanosseggia intricata*, have been shown to possess antimutagenic activity against the mutagenesis caused by 2-aminoanthracene, acetylaminofluorine and ethyl methanesulfonate in *Salmonella typhimurium* cultures. Intricatin was shown to be inhibitory against mutagenesis induced by 2-aminoanthracene, but not against acetylaminofluorine and ethyl methanesulfonate whilst intricatinol had moderate inhibition against 2-aminoanthracene and acetylaminofluorine induced mutagenesis, and greater inhibition for ethyl methanesulfonate induced mutagenesis. The superior potency of intricatinol could be due to the presence the two hydroxyl groups in the A-ring, as previous studies have shown that hydroxylated flavonoids are generally more active than methylated analogues (Wall *et al.*, 1989).

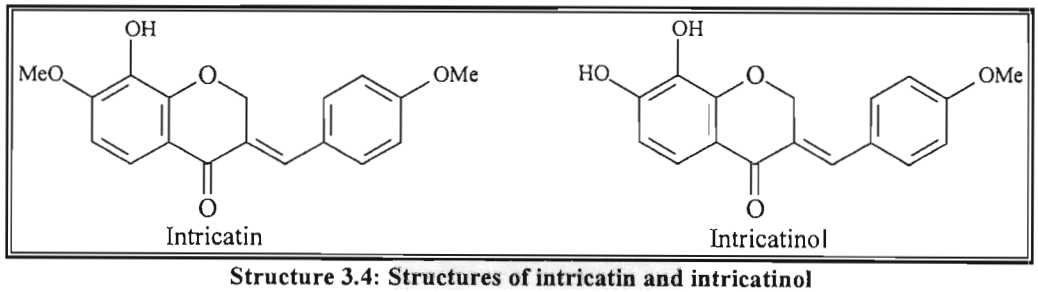

Structure 3.4: Structures of intricatin and intricatinol

The homoisoflavanone, 3-(4'-hydroxybenzyl)-5-hydroxy-6,7,8-trimethoxychroman-4-one (**Structure 3.5**), from *Veltheimia viridifolia*, has been tested for phosphodiesterase inhibition, antioxidant, and bronchospasmolytic activity on

respiration and its influence on the cardiac system of guinea pigs. It was found to have weak, short-lived biological activity in this test system (Amschler *et al.*, 1996)

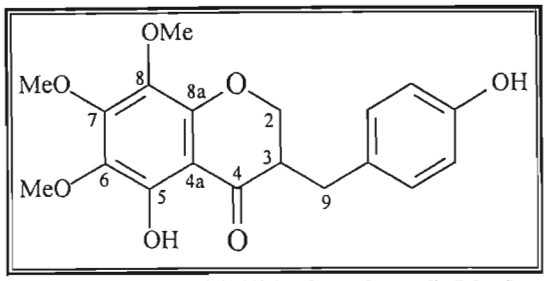

Structure 3.5: Structure of 3-(4'-hydroxybenzyl)-5-hydroxy-6,7,8-trimethoxychroman-4-one

Homoisoflavanones have been found to possess anti-inflammatory properties. Extracts from *Merwilla plumbea, Ledebouria ovatifolia, Drimiopsis maculata* and *Muscari comosum* have been previously shown to exhibit anti-inflammatory activity (Della Loggia *et al.*, 1989; Pohl *et al.*, 2000). The molecular size of the homoisoflavanone affects the anti-inflammatory activity due to steric or bulk effects. Larger molecules are subject to steric hindrance at the receptor site of participating enzymes. Electrostatic potentials on C-3, C-4, C-4a and C-5 also play an important role in the anti-inflammatory activity of homoisoflavanones, as it affects the local attraction between the compound and the receptor (Pohl *et al.*, 2000).

The genus *Mycobacterium* is responsible for tuberculosis and other infections, and has developed resistance to common antibiotics/drug therapies. The homoisoflavanone, 3-(4'-methoxybenzyl)-7,8-methlenedioxy-chroman-4-one, and its metabolite, 7-(1'-hydroxyethyl)-2-(2"-hydroxyethyl)-3,4-dihydrobenzopyran, from *Chlorophytum inornatum* has been shown to be active in inhibiting various *Mycobacterium* species, with minimum inhibitory concentration (MIC) values comparing favourably with control antibiotics ethambutol and isoniazid. This is the first report of a homoisoflavanone having anti-mycobacterial activity (O'Donnell *et al.*, 2006).

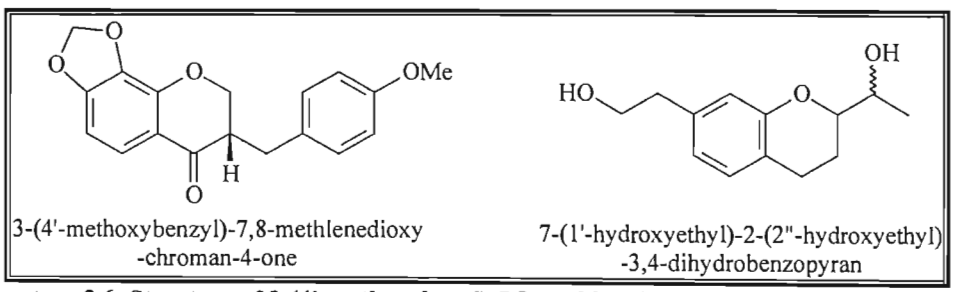

Structure 3.6: Structure of 3-(4'-methoxybenyl)-7,8-methlenedioxy-chroman-4-one and 7-(1'-hydroxyethyl)-2-(2"-hydroxyethyl)-3,4-dihydrobenzopyran)

3.3. BIOSYNTHESIS.

Homoisoflavanones follow a mixed biosynthetic pathway, with the phenolic A-ring being derived via a polyketide pathway, whilst the B-ring is derived from the shikimate pathway (**Figure 3.5**). Phenols derived through the shikimate pathway result in para-substituted oxidation products, but further oxidations may yield substitutions at adjacent sites. The polyketide pathway produces phenols that have a 1,3,5-oxygenation substitution pattern, which is very common amongst natural polyphenols. One or more of these groups can be lost during further biosynthesis (Ebel and Hahlbrock, 1982; Heller and Forkmann, 1988a; Heller and Forkmann, 1988b; Mann *et al.*, 1994).

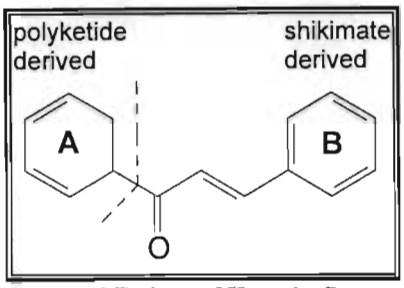

Figure 3.5: Origins of the A and B rings of Homoisoflavanones (Mann *et al.*, 1994)

In the biosynthesis of homoisoflavanones, the first step involves the formation of a chalcone (Dewick, 1975). The first step of chalcone formation is the conversion of L-phenylalanine into cinnamic acid. This reaction is catalysed by the enzyme L-phenylalanine ammonia lyase. Ammonia is enzymatically eliminated in this reaction to produce (*Z*)-cinnamic acid. Hydroxylation by cinnamate 4-hydroxylase at the para-position results in the formation of 4-coumaric acid, and this is subsequently acted upon by the enzyme 4-coumarate: CoA ligase, in the presence of ATP and the co-factor Mg^{2+} to form 4-coumaryl-CoA (Ebel and Hahlbrock, 1982; Heller and Forkmann, 1988a; Heller and Forkmann, 1988b; Bhandari *et al.*, 1992; Dewick, 2001; **Scheme 3.2**).

Oxidation at C-4 occurs via epoxidation and the migration of the H-4 proton to C-3 (**Scheme 3.3**). This shift was first established through tritium-labelling experiments at the National Institute of Health (NIH) in the U.S.A, and was therefore termed the NIH-shift (Ebel and Hahlbrock, 1982; Heller and Forkmann, 1988a; Heller and Forkmann; 1988b; Bhandari *et al.*, 1992).

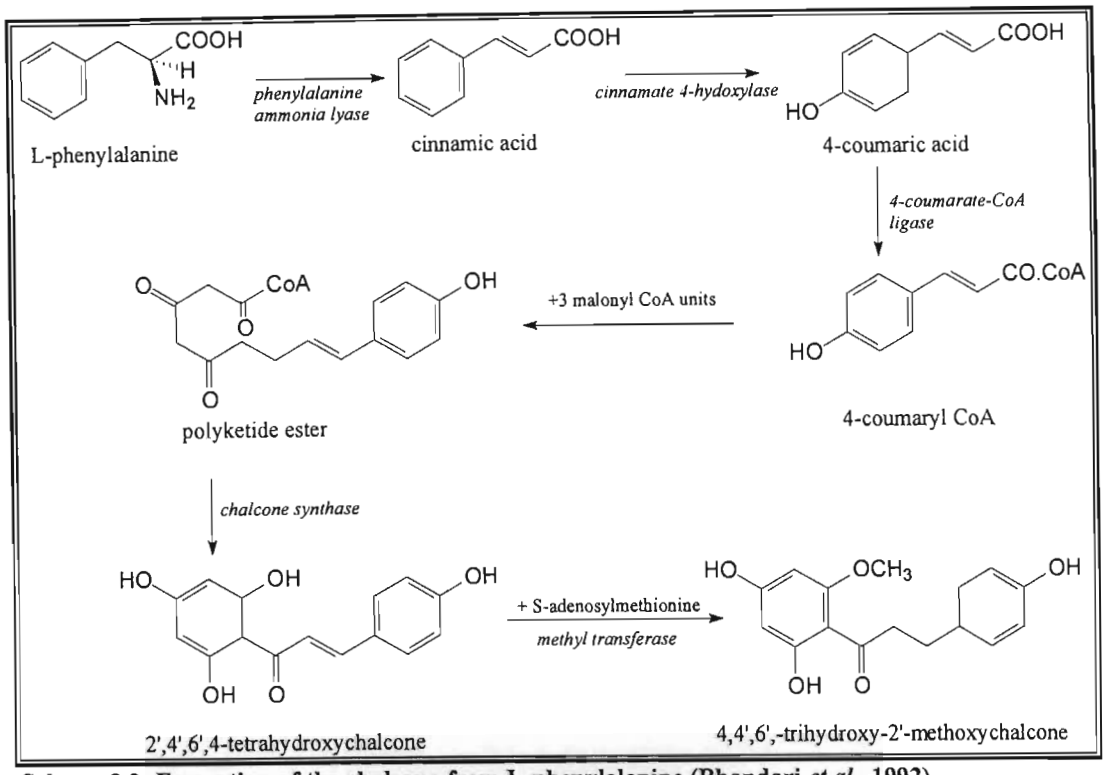

Scheme 3.2: Formation of the chalcone from L-phenylalanine (Bhandari *et al.*, 1992)

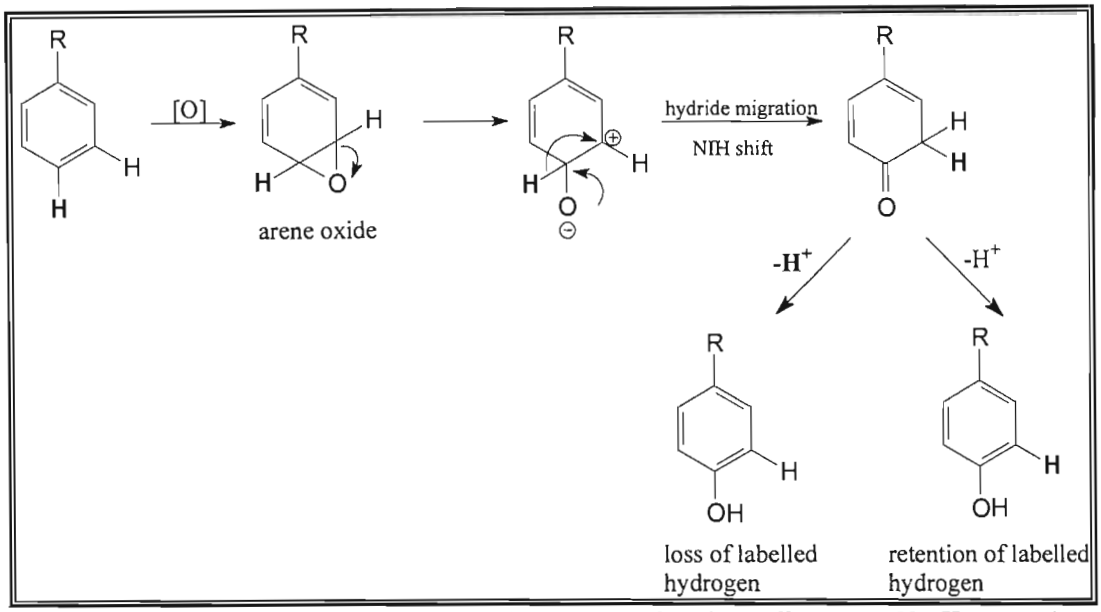

Scheme 3.3: Mechanism illustrating the NIH shift (Ebel and Hahlbrock, 1982; Heller and Forkmann, 1988; Heller and Forkmann, 1988)

A condensation reaction between 4-Coumaryl-CoA and three acetate units derived from malonyl-CoA gives rise to a polyketide ester. The result is the elongation of the aliphatic side chain of 4-coumaryl-CoA by six carbon atoms. Cyclization of the polyketide ester occurs via a postulated *Claisen*-type condensation and results in the

formation of tetrahydroxychalcone (**Scheme 3.2**). This cyclization is catalysed by the enzyme chalcone synthase. Chalcones are the intermediates to all flavonoids, and as such, the enzyme chalcone synthase is regarded as the key enzyme in flavonoid biosynthesis (Ebel and Hahlbrock, 1982; Heller and Forkmann, 1988a; Heller and Forkmann, 1988b; Bhandari *et al.*, 1992).

The chalcone formed has 15 carbons in its skeleton, and the additional carbon for the formation of 16-carbon homoisoflavanones is provided by methionine. In many biosynthetic pathways, a methyl group from methionine provides additional carbons, and in this pathway, 2',4',6',4-tetrahydroxychalcone is methylated at the 2' position by S-adenosylmethionine to form 4,4',6'-trihydroxy-2'-methoxychalcone (**Scheme 3.2**). Methyl transferase catalyses the reaction (Ebel and Hahlbrock, 1982; Heller and Forkmann, 1988a; Heller and Forkmann, 1988b; Bhandari *et al.*, 1992).

The mechanism for the conversion of the chalcone into a homoisoflavanone was first proposed by Dewick (1975). The cyclization of 2'-methoxy-4',6',4-trihydroxychalcone is brought about by the oxidation of the 2'-methoxy group, and this produces the three basic types of homoisoflavanones. The formation of the 3-benzyl-4-chromanone type is through the addition of a hydride ion, whilst the loss of a proton leads to the formation of the 3-benzylidene-4-chromanone type. Hydration of 3-benzylidene-4-chromanone or oxidation of 3-benzyl-4-chromanone leads to the formation of the 3-benzyl-3-hydroxy-4-chromanone type of homoisoflavanone (Dewick, 1975; **Scheme 3.4**).

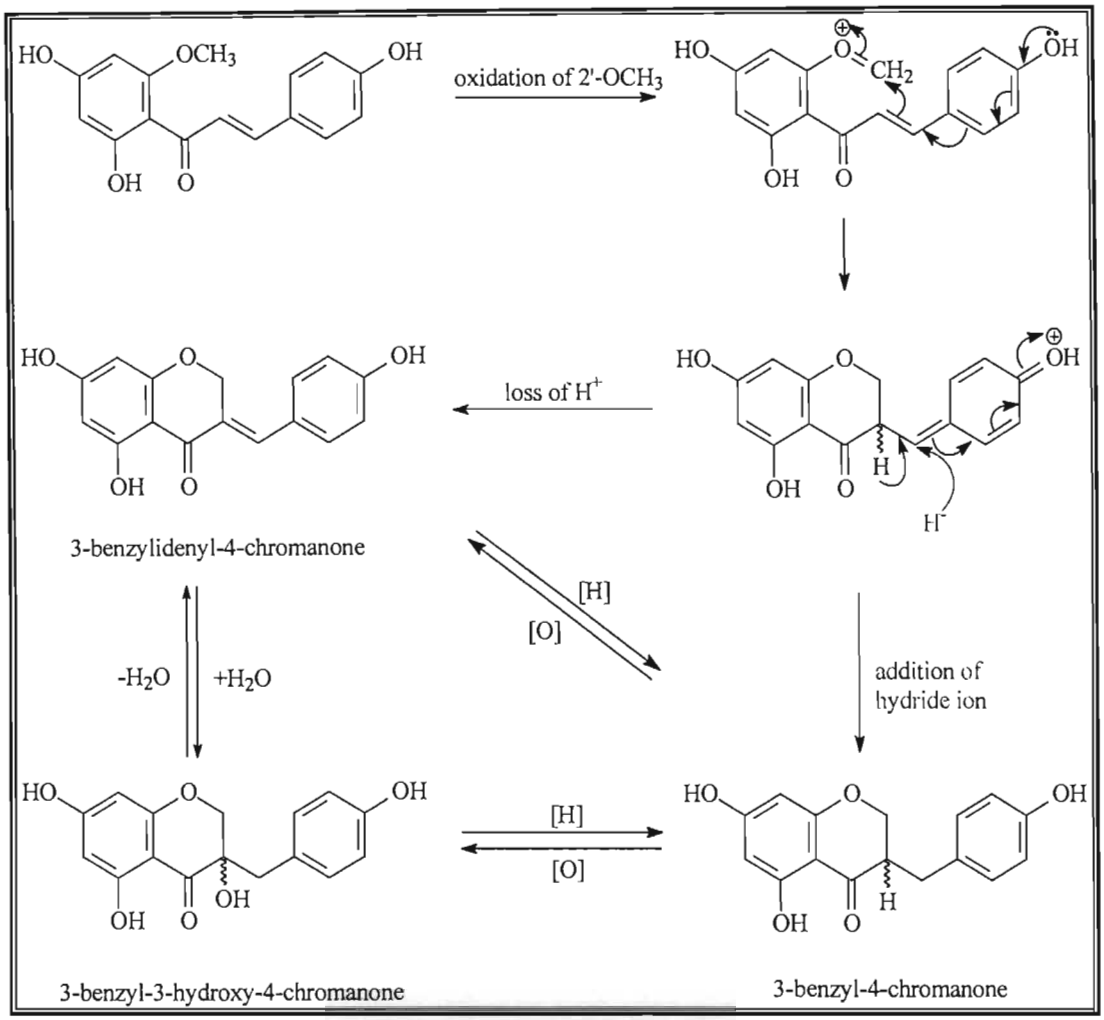

Scheme 3.4: The proposed biosynthetic pathway for the conversion of chalcones to homoisoflavanones (Dewick, 1975)

Scillascillin-type homoisoflavanones, which contain a 3-spirocyclobutenyl ring, are derived from 3-benzyl-3-hydroxy-4-chromanone type homoisoflavanones through a more complex mechanism (**Scheme 3.5**), whilst a similar mechanism in used for the formation of brazilin and haematoxylin type compounds (**Scheme 3.6**) (Dewick, 1975).

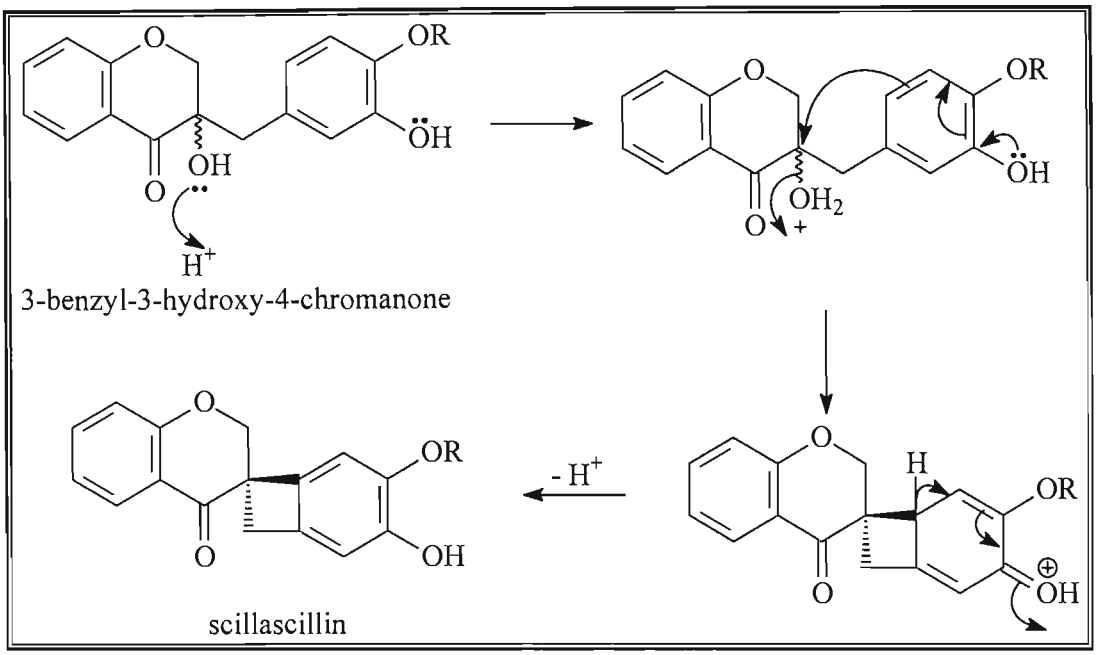

Scheme 3.5: Proposed biosynthetic pathway for the formation of scillascillin (Dewick, 1975)

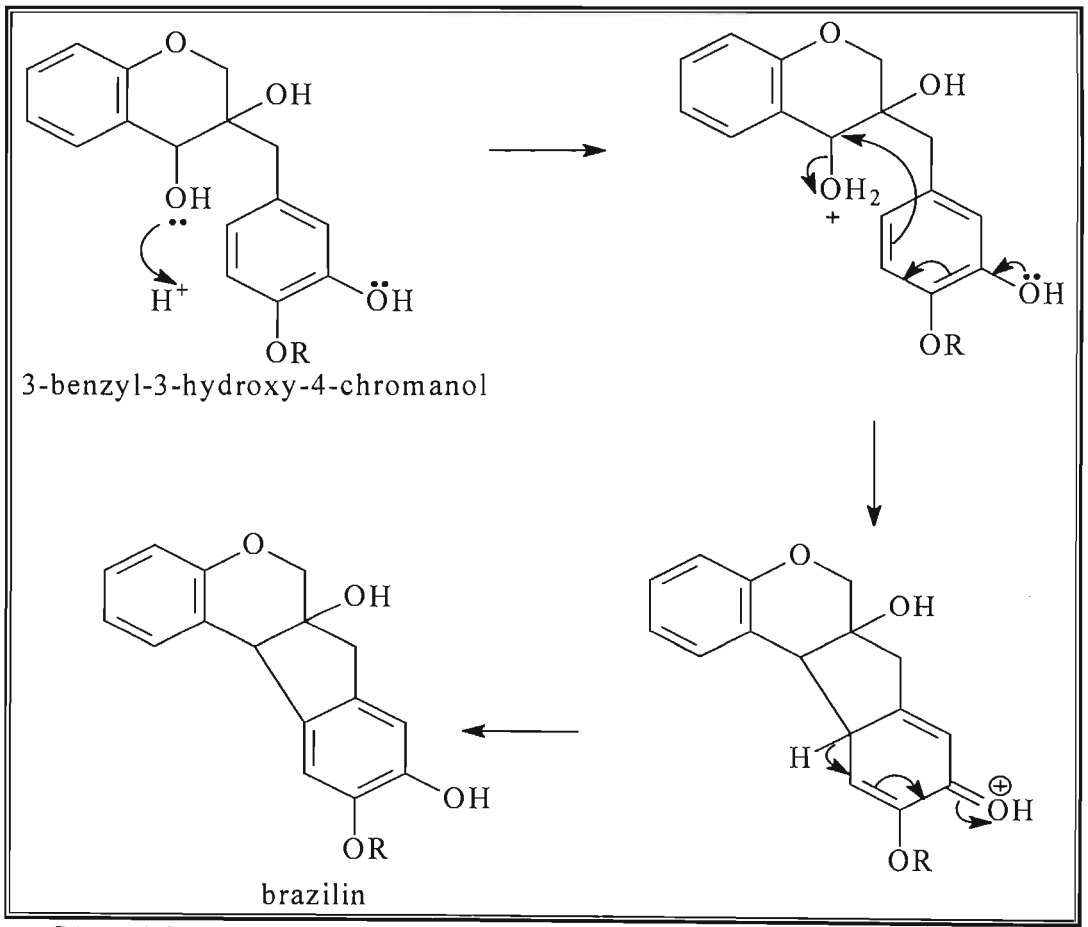

Scheme 3.6: Proposed biosynthetic pathway for the formation of brazilin (Dewick, 1975)

3.4. REFERENCES

Adinolfi M, Barone G, Belardini M, Lanzetta R, Laonigro G, and Parrilli M, 1984. 3-Benzyl-4-chromanones from *Muscari comosum*. *Phytochemistry*, **23**, 2091-2093.

Amschler G, Frahm A.W, Killan U, Muller-Doblies D, and Muller-Doblies U, 1996. Constituents of *Veltheimia viridifolia*; I. Homoisoflavanones of the bulbs. *Planta Medica*, **62**, 534-539.

Bhandri P, Crombie L, Daniels P, Holden I, Van Bruggen N, and Whiting D.A, 1992. Biosynthesis of the A/B/C/D-ring system of the rotenoid amorphigenin by *Amorpha fruticosa* seedlings. *Journal of the Chemical Society Perkin Transactions*, **1**, 839-849.

Crouch N.R, Bangani V, and Mulholland D.A, 1999. Homoisoflavanones from three South African *Scilla* species. *Phytochemistry*, **51**, 943-946.

Della Loggia R, Del Negro P, Tubaro A, Barone G, and Parrilli M, 1989. Homoisoflavanones as anti-inflammatory principles of *Muscari comosum*. *Planta Medica*, **55**, 587.

Dewick P.M, 1973. Biosynthesis of the 3-benzylchroman-4-one Eucomin. *Journal of the Chemical Society-Chemical communications*, 438-439.

Dewick P.M, 1975. Biosynthesis of the 3-benzylchroman-4-one eucomin in *Eucomis bicolor*. *Phytochemistry*, **14**, 983-988.

Dewick P.M, 2001. *Medicinal Natural Products: a biosynthetic approach*. John Wiley and Sons, Chichester, pp 154-155.

du Toit K, Elgorashi E.E, Malan S.F, Drewes S.E, van Staden J, Crouch N.R, and Mulholland D.A, 2005. Anti-inflammatory activity and QSAR studies of compounds isolated from Hyacinthaceae species and *Tachiadenus longiflorus* Griseb. (Gentianaceae). *Bioorganic & Medicinal Chemistry*, **13**, 2561-2568.

Ebel J, and Hahlbrock, 1982. In: *The Flavonoids: Advances in research*. Eds: Harborne J.B, Mabry T.J. Chapman and Hall, London, pp 641-665.

Geiger H, 1988. Miscellaneous flavonoids. In: *The flavonoids: advances in research since 1980*. Ed. Hanbome J.B. Chapman & Hall, London. pp 389-397.

Heller W, and Tamm C, 1981. Homoisoflavanones and biogenetically related compounds. *Fortschritte der Chemie Organischer Naturstoffe*, **40**, 106-152.

Heller W, and Forkmann G, 1988a. In: *The Flavonoids: Advances in research since 1980*. Ed: Harborne J.B, Chapman and Hall, London, pp 399-420.

Heller W, and Forkmann G, 1988b. In: *The Flavonoids: Advances in research since 1986*. Ed: Harborne J.B, Chapman and Hall, London, pp 499-522.

Kirkiacharian B.S, Gomis M, Tongo H.G, Mahuteau J, and Brion J.D, 1984. The ^{13}C NMR spectra of homoisoflavonoids. *Organic Magnetic Resonance*, **22**,106-108.

Koorbanally N.A, Crouch N.R, Harilal A, Pillay B, Mulholland D.A, 2006. Coincident isolation of a novel homoisoflavonoid from *Resnova humifusa* and *Eucomis Montana* (Hyacinthoideae: Hyacinthaceae). *Biochemical Systematics and Ecology*, **34**, 1-5.

Mann J, Davidson R.S, Hobbs J.B, Banthorpe D.B, and Harborne J.B, 1994. In *Natural Products: Their chemistry and biological significance*. Longmans, Essex, pp 372.

Namikoshi M, Nakata H, Yamada H, Nagai M, and Saitoh T, 1987. Homoisoflavonoids and related compounds. II. Isolation and absolute configurations of 3,4-dihydroxylated homoisoflavans and brazilins from *Caesalpinia sappan* L. *Chemical and Pharmaceutical Bulletin,* **35**, 2761-2773.

O'Donnell G, Bucar F, and Gibbons S, 2006. Phytochemistry and antimycobacterial activity of Chlorophytum inornatum. *Phytochemistry*, **67**, 178-182.

Pohl T.S, Crouch N.R, and Mulholland D.A, 2000. Southern African Hyacinthaceae: chemistry, bioactivity and ethnobotany. *Current Organic Chemistry,* **4**, 1287-1324.

Saitoh T, Sakashita S, Nakata H, Shimokawa T, Kinjo J, Yamahara J, Yamasaki M, and Nohara T, 1985. 3-Benzylchroman derivatives related to brazilin from *Sappan lignum*. *Chemical and Pharmaceutical Bulletin*, **34**, 2506-2511.

Sidwell W and Tamm C, 1970. The homo-isoflavanones II. Isolation and structure of 4'-O-methylpunctatin, autumnalin and 3,9-dihydroautumnalin. *Tetrahedron letters*, **7**, 475-478.

Silayo A, Ngadjui B.T, and Abegaz B.M, 1999. Homoisoflavonoids and stilbenes from the bulbs of *Scilla nervosa subsp. Rigidifolia*. *Phytochemistry*, **52**, 947-955.

Taylor J.L.S and Van Staden J, 2001. COX-1 inhibitory activity in extracts from Eucomis L'Herit. species. *Journal of Ethnopharmacology*, **75**, 257-265.

Wall M.E, Wani M.C, Manikumar G, Taylor H, and McMivney R, 1989. Plant antimutagens, 6. Intricatin and intricatinol, new antimutagenic homoisoflavonoids from *Hoffmanosseggia intricata*. *Journal of Natural Products*, **52**, 774-778.

CHAPTER 4: STRUCTURAL ELUCIDATION OF EXTRACTED COMPOUNDS

4.1. EXTRACTIVES FROM *STROPHANTHUS SPECIOSUS*

4.1.1. INTRODUCTION

There have been previous studies of *Strophanthus speciosus* (Chen *et al.*, 1951; Schindler and Reichstein, 1952), with some early reports dating back to 1887 (Budd, 1887), but previous works concentrated on the seeds and roots of the plant, where numerous cardiac glycosides were found (see chapter 1). *Strophanthus speciosus* has been used ethnomedicinally to treat snakebite and hysteria, and has also been used as an arrow poison and homicidal agent (Hutchings, 1996). In this study, the leaves and stems of *Strophanthus speciosus* were examined with the aim of finding cardiac glycosides to be screened for muscle relaxant activity, as part of a collaborative project with the University of Sienna, Italy. The leaves were dried and crushed, and then Soxhlet extracted for 24 hours with hexane, dichloromethane, ethyl acetate, and methanol successively using a Soxhlet apparatus. The stems were dried and chipped and extracted in the same manner, with the same solvents.

One cardenolide was isolated in the dichloromethane extract of the stem, and it was identified as 3β-O-(6'-deoxy-3'-O-methyl-D-galactopyranose)-14β-hydroxy-16β-acetoxy-5β-card-20(22)-enolide, more commonly know as neritaloside or oleandrigenin digitaloside. Neritaloside has been previously isolated in *Nerium oleander*, *Nerium indicum, Phyrygilanthus celatroides*, *Dendrophtoe falcata*, *Amyema congener* (parasitic *on Nerium oleander*) and *Mandevilla pentlandiana* (Jager *et al.*, 1959; Boonsong and Wright, 1961; Cabrera *et al.*, 1993), but there are no previous reports of it being isolated in *Strophanthus speciosus*. Unfortunately, the amount isolated (14.4mg) was insufficient to be used in the muscle relaxant screen, where at least 20mg of sample is required.

Neritaloside has been reported as having central nervous system depressant activity in mice at doses of 50mg neritaloside per kilogram mouse. It was shown to decrease motor activity in mice at 25mg/kg, and at 50mg/kg, the mice had increased rates of respiration, abduction of limbs, and tremors on movement (Siddiqui *et al.*, 1997; Begum *et al.*, 1999).

4.1.2. STRUCTURAL ELUCIDATION OF COMPOUND 1: NERITALOSIDE

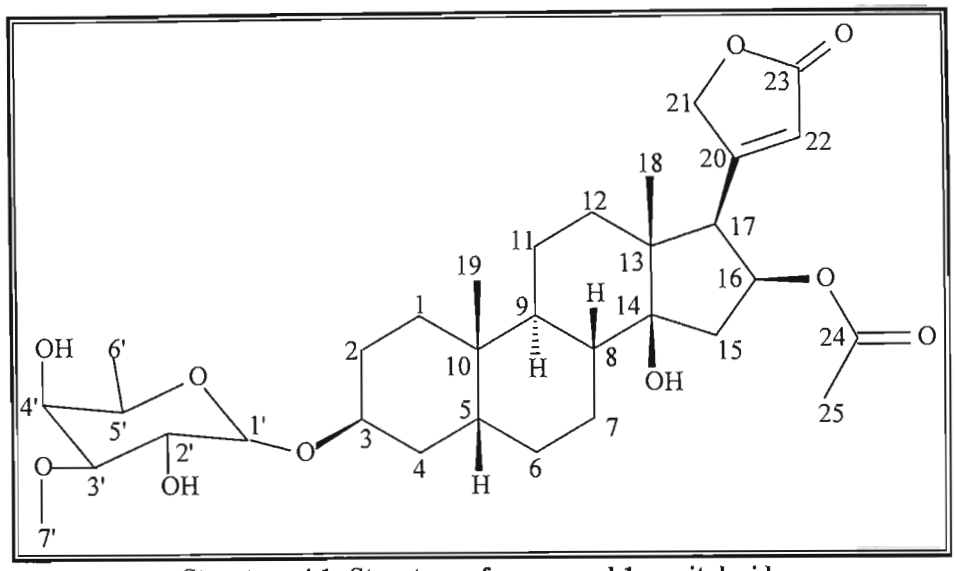

Structure 4.1: Structure of compound 1, neritaloside

Compound **1**, neritaloside (**Structure 4.1**), was isolated as off-white coloured crystals with a melting point of 134-140°C. This compared favourably with the literature value of 135-140°C (Jager *et al.*, 1959). The mass spectrum of compound **1** (**Spectrum 1g**) gave a peak at *m/z* 372, which corresponded with a molecular formula of $C_{23}H_{32}O_4$, with a double bond equivalence of 7. This fragment does not have the sugar or acetyl moieties attached. The NMR spectra indicated that the cardenolide however was present as the glycoside, with a sugar attached at C-3, and an acetyl group attached at C-16. The molecular formula of the glycoside is $C_{32}H_{48}O_{10}$.

^{1}H NMR, ^{13}C NMR, DEPT, COSY, NOESY, HMBC, HSQC and mass spectra were used for the structural elucidation.

The ^{1}H NMR spectrum (**Spectrum 1a**) indicated that the compound isolated was a cardenolide because of the characteristic resonances of the α,β-unsaturated lactone ring attached at C-17. The DEPT spectra (**Spectrum 1j**) indicated that there were five methyl groups present, with two being present on the sugar moiety, and three on the aglycone. There were two double doublets of one proton each at δ_H 4.96 and δ_H 4.83 which were assigned as H-21a (J = 18.13 and 1.83 Hz) and H-21b (J = 18.13 and 1.65 Hz)

respectively; and a single proton singlet at δ_H 5.95, assigned to H-22 because of HMBC correlations (**Spectrum 1d**) with the 2H-21 protons. W-coupling could be seen in the COSY spectrum (**Spectrum 1e**) between H-21 and H-22. Two resonances on the ^{13}C NMR spectrum (**Spectrum 1b**), δ_C 167.76 and δ_C 174.05, showed HMBC correlations with the 2H-21 and H-22 protons, indicating that these were either C-20 or C-23. The resonance at δ_C 167.76 also had an HMBC correlation with a proton resonance on the steroid backbone, indicating that the resonance was that of C-20, whilst the proton resonance on the steroid backbone was that of H-17. The resonance at δ_C 174.05 was therefore assigned C-23 as it did not have any correlations with the steroid backbone.

The corresponding C-17 resonance at δ_C 56.06 showed an HMBC correlation to the multiplet proton resonance at δ_H 5.43, which was then assigned to H-16. The 2H-15 protons had two separate resonances on the ^1H NMR spectrum; a double doublet at δ_H 2.70 (J = 15.75 and 9.71 Hz), and a broad multiplet at δ_H 1.64. These assignments were made due to COSY correlations with the H-16 proton. There were two overlapping singlets on the ^1H NMR spectrum, integrating to three protons each at δ_H 0.903 and δ_H 0.905, which were due to the C-18 and C-19 methyl groups respectively. An HMBC correlation between one of the overlapping resonances with C-17 indicated that it was the 3H-18 resonance. The 3H-18 protons also had HMBC correlations with δ_C 39.18 and δ_C 49.95, and after comparison with literature, these were assigned to C-12 and C-13 respectively (Begum *et al.*, 1999). The resonance at δ_C 84.22, was assigned C-14 after HMBC correlations with H-15a, H-17, and 3H-18.

The H-16 resonance was deshielded, and also showed a NOESY correlation (**Spectrum 1f**) with the three- proton singlet at δ_H 1.95, indicating that an acetyl group was attached at C-16. The resonance at δ_H 1.95 showed an HMBC correlation with the deshielded resonance at δ_C 170.42, and this carbon resonance was therefore assigned as the acetyl carbonyl. The resonance atδ_H 1.95 was assigned to the acetyl methyl group.

The remaining carbon and proton resonances were assigned using DEPT and literature data.

In the sugar moiety, the anomeric proton, H-1', was identified on the ^{1}H NMR spectrum as a doublet at δ_H 4.22 (J = 7.87 Hz) as it had an HMBC correlation with C-3 (δ_C 74.01) on the aglycone. COSY correlations between H-1' and the multiplet resonance at δ_H 3.62 indicated that this resonance was due to H-2'. The H-2' resonance in turn had a COSY correlation with δ_H 3.19, which was then assigned H-3'. On the ^{1}H NMR spectrum, a three-proton methoxy singlet (δ_C 57.52) at δ_H 3.50 showed HMBC correlation with C-3', indicating that the methoxy group was attached at C-3'. A broad singlet resonance at δ_H 3.82 was assigned to H-4' because of a COSY correlation with H-3'. The H-5' resonance was assigned to δ_H 3.54 due to HMBC correlations with C-1' and C-4', and occurred as a double quartet (J = 5.49 and 0.92 Hz). A three proton doublet at δ_H 1.32 (J = 6.59 Hz) was identified as a methyl group using the HSQC (**Spectrum 1c**) and DEPT spectra, and was positioned on C-5' due to HMBC correlations with C-5' and a COSY correlation with H-5'.

The orientation of the sugar moiety's functional groups was determined using NOESY spectra and a model of the compound. From these correlations (**Table 4.1**) it was determined that the sugar moiety was 6-deoxy-3-O-methyl-D-galactopyranose, also known as D-digitalosyl. The H-3' resonance had a NOESY correlation with H-5' indicating that these protons were axial in orientation. H-2' had NOESY correlations with H-1' and H-3', but not with H-5', indicating that the H-2' was equatorial, and similarly, H-4' did not have NOESY correlations with H-3' or H-5', indicating that it was equatorial in orientation. Comparison of literature values with ^{13}C NMR spectra agreed with this assignment and identification, with the slight variations in some of the resonances being attributed to the literature compound being the aglycone only (Cabrera *et al.*, 1993).

The mass spectrum supported this structure, as can be seen in the proposed fragmentation pattern in **scheme 4.1**. The major peaks from the mass spectrum were *m/z* 177, *m/z* 192, and *m/z* 372, with minor peaks at *m/z* 162, and *m/z* 207. The peaks at *m/z* 177 and *m/z*

162 correlated with the sugar moiety, either with the linking oxygen present or absent. Peak *m/z* 372 represents the aglycone with neither the sugar or acetyl moieties being present, whilst *m/z* 192 and *m/z* 207 are fragments of the aglycone.

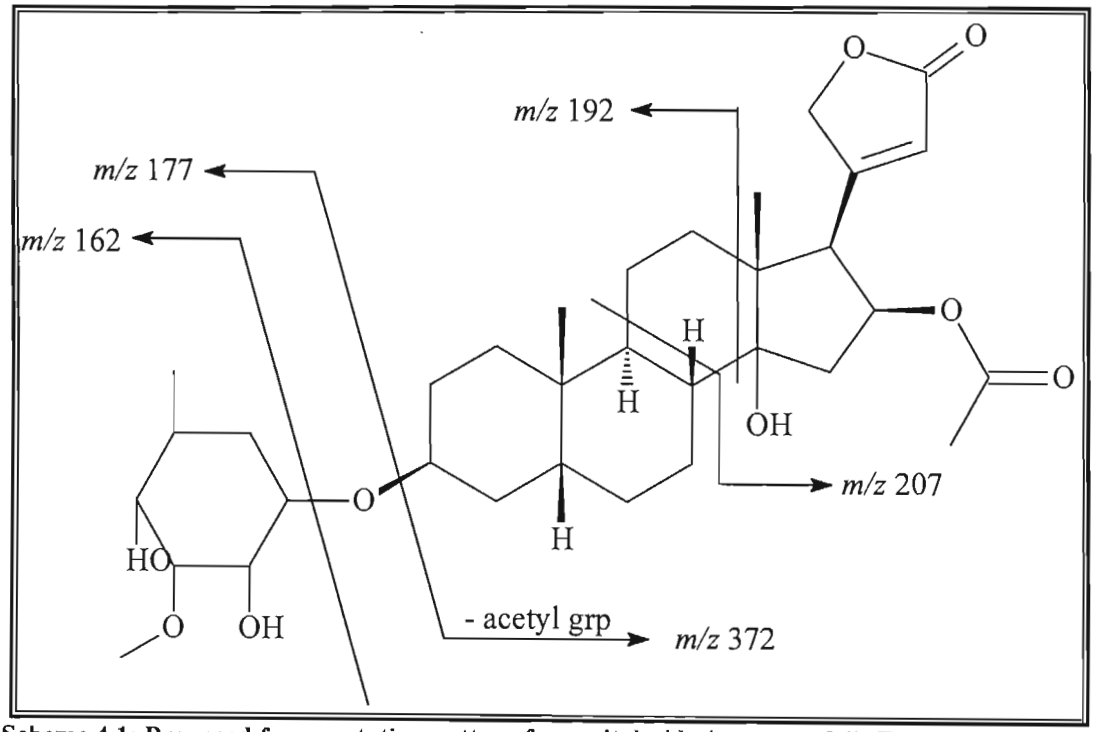

Scheme 4.1: Proposed fragmentation pattern for neritaloside (compound 1) (Begum *et al.*, 1999)

Table 4.1: ^{1}H, ^{13}C, HMBC, COSY and NOESY data for compound 1 ($CDCl_3$).

	^{1}H/ ppm	^{13}C/ ppm	^{13}C/ ppm lit.	HMBC C→H	COSY	NOESY
1a	1.81 m	26.36	30.4	-	*	*
1b	~ 1.2 m				*	*
2a	~ 1.6 m	26.41	26.8	-	*	*
2b	~ 1.43 m				*	*
3	4.02 s	74.01	75.0	H-1'; H-4b	*	H-1'
4a	~ 1.6 m	30.03	30.5	-	*	*
4b	~1.40 m				*	*
5	~ 1.67m	36.36	36.8	H-4b; H-6a	*	*
6a	~1.64 m	29.67	27.1	-	*	*
6b	~ 1.2 m				*	*
7a	~ 1.4 m	20.73	21.3	-	*	*
7b	~ 1.2 m				*	*
8	~ 1.46 m	41.73	42.0	-	*	*
9	~ 1.53 m	35.68	36.1	H-8; H-19	*	*
10	-	35.03	35.5	H-19	-	-
11a	~1.2 m	20.96	21.3	H-12b	*	*
11b	~1.6 m				*	*
12a	~1.53 m	39.18	40.7	H-18	*	*
12b	~ 1.22 m				*	*
13	-	49.95	50.7	H-15b; H-17; H-18	-	-
14	-	84.22	84.2	H-15b; H-17; H-18	-	-
15a	2.70 dd: 15.75, 9.71 Hz	41.19	39.4	H-17	H-15b; H-16	H-5b, H-16
15b	1.64 m				H-15a; H-16	H-15a
16	5.43 m	73.89	75.3	H-15b; H-17	H-15a,b; H-17	H-15a
17	3.17 dd: 8.79, 6.96 Hz	56.06	56.7	H-15a; H-18; H-22	H-16	H-16, H-22
18	0.903 s	15.91	15.8	-	*	H-17; H-21
19	0.905 s	23.61	23.4	-	*	*
20	-	167.76	175.8	H-17; H-21a,b; H-22	-	-
21a	4.96 dd: 18.13, 1.83 Hz	75.62	76.8	H-17; H-22	H-21b; H-22	H-18;H- 21b
21b	4.83 dd: 18.13, 1.65 Hz				H-21a; H-22	H-21a
22	5.95 s	121.34	120.9	H-17; H-21a,b	H-21a,b	H-17; H-18; H-25
23	-	174.05	171.3	H-21b; H-22	-	-
24	-	170.42	170.7	H-25	-	-
25	1.95 s	21.03	20.3	-	-	H-16; H-22
1'	4.22 d: 7.87 Hz	101.29	102.5	H-2'; H-5'; H-3	H-2'	H-3;H-2';H-3';H-5'
2'	3.62 m	70.73	70.8	H-3'; H4'	H-1'; H-3'	H-1'; H-3'
3'	3.19 td: 10.81, 7.51, 1.83 Hz	82.80	84.0	H-2'; H-4'; H-7'	H-2'; H-4'; H-5'	H-1'; H-2'; H-4'; H-5
4'	3.82s	68.11	68.1	H-3'; H-6'; H-7'	H-3'	H-5'; H-6'
5'	3.54 dq: 5.49, 0.92 Hz	70.34	70.6	H-4'; H-6'	H-6'	H-1'; H-3'; H-4'; H-6'
6'	1.32 d: 6.59 Hz	16.44	16.8	H-5'	H-5'; H-7'	H-4'; H-5'
7'	3.50 s	57.52	55.7	H-3'	H-6'	H-3'; H-4'

* Spectrum too clustered to differentiate couplings. Literature values from Cabrera *et al.* (1993).

4.2. EXTRACTIVES FROM *EUCOMIS MONTANA*

4.2.1. INTRODUCTION

Eucomis montana was recently investigated by Koorbanally *et al.* (2006). In that study the dichloromethane, ethyl acetate, and methanol extracts of the bulbs were examined. One nortriterpenoid and eleven homoisoflavanones were found (see chapter 1 for list of compounds and structures, page 21-23). In this study the methanol extract was re-examined to obtain samples for the anti-inflammatory screens setup in this project. Three homoisoflavanones were found. The three homoisoflavanones isolated in this study were previously isolated in the work by Koorbanally *et al.* (2006), but in that study, two of the compounds were found in different extracts; 3,9-dihydroeucomin was isolated in the dichloromethane extract, and 4'-demethyl-5-O-methyl-3,9-dihydroeucomin was isolated in the ethyl acetate extract .

The compounds isolated were:

1. 3,9-dihydroeucomin (5,7-dihydroxy-3-(4'-methoxybenzyl)-4-chromanone), (compound **2**).
2. 4'-demethyl-3,9-dihydroeucomin (5,7-dihydroxy-3-(4'hydroxybenzyl)-4-chromanone), (compound **3**).
3. 4'-demethyl-5-O-methyl-3,9-dihydroeucomin (7-hydroxy-3-(4'-hydroxybenzyl)-5-methoxy-4-chromanone, (compound **4**).

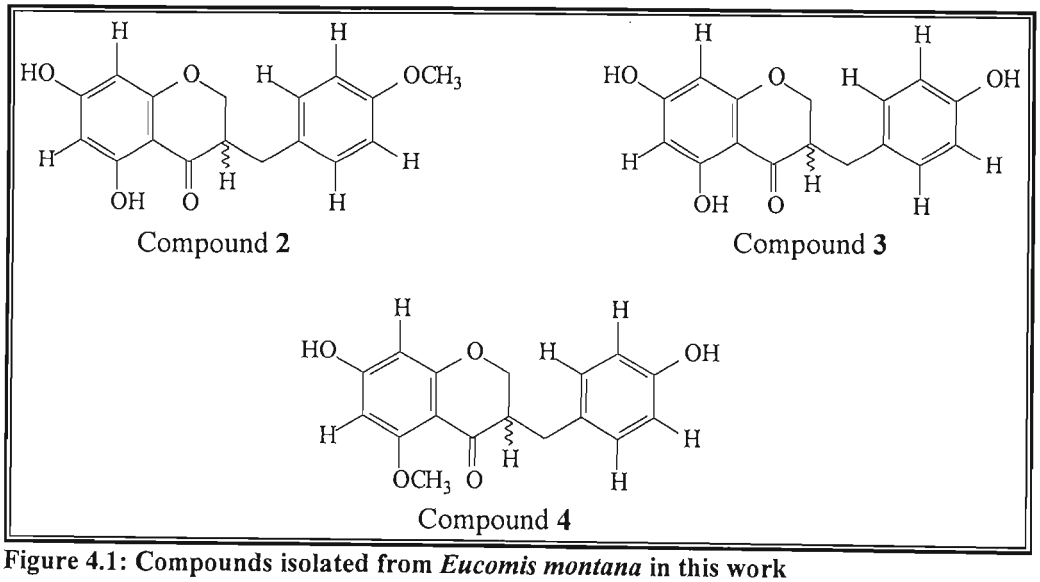

Figure 4.1: Compounds isolated from *Eucomis montana* in this work

4.2.2. STRUCTURAL ELUCIDATION OF COMPOUND 2: 3,9-DIHYDROEUCOMIN

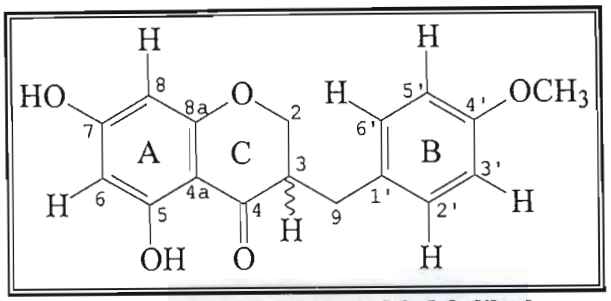

Structure 4.2: Structure of compound 2, 3,9-dihydroeucomin

Compound **2**, 3,9-dihydroeucomin or 5,7-dihydroxy-3-(4'-methoxybenzyl)-4-chromanone (**Structure 4.2**), was isolated as off-white coloured crystals with a melting point of 156-158°C. The mass spectrum (**Spectrum 2g**) of compound **2** gave a molecular ion [M^+] peak at *m/z* 300, which corresponded to a molecular formula of $C_{17}H_{16}O_5$. From the molecular formula, a double bond equivalence of 10 was deduced.

The IR data (**Spectrum 2j**) indicated the presence of hydroxyl groups (3313cm^{-1}, O-H stretching), aromatic rings (1511cm^{-1}, aromatic C=C stretching), and carbonyl groups (1634cm^{-1}, C=O stretching) (Crews *et al.*, 1998).

The ^{1}H NMR (**Spectrum 2a**) spectrum showed the characteristic splitting pattern of 3-benzyl-4-chromanone type homoisoflavanones for the two H-2, H-3, and two H-9 protons (Heller and Tamm, 1981; Adinolfi *et al.*, 1984; Pohl *et al.*, 2000). Each of the two H-2 protons was split by coupling with each other and by coupling with the H-3 proton, resulting in a pair of double doublet resonances at δ_H 4.07 (dd, J = 11.50 and 6.75 Hz) and δ_H 4.23 (dd, J = 11.50 and 4.17 Hz). A similar double doublet splitting pattern was seen at δ_H 3.13 (dd, J = 13.69 and 4.17 Hz) and δ_H 2.66 (dd, J = 13.69 and 10.51 Hz). These were assigned to the two H-9 protons and were split by coupling with each other and the H-3 proton. A multiplet resonance at δ_H 2.77 was assigned to H-3, and the resonance pattern was due to coupling to the H-2a, H-2b, H-9a, and H-9b protons. These coupling patterns were confirmed by correlations in the COSY spectrum, where coupling between 2H-2 and H-3; and between H-3 and 2H-9 could be seen. The 2H-2 proton resonances were shifted downfield due to deshielding by the adjacent oxygen atom.

During mass spectrometry (MS), homoisoflavanones undergo an A-4 type fragmentation, resulting in the formation of a tropylium ion which forms the base peak of the spectrum (Heller and Tamm, 1981). In the mass spectrum of compound **2**, the base peak occurred at *m/z* 121, corresponding to the methoxytropylium ion. The chromanone fragment at *m/z* 179 indicated that there were two hydroxyl groups present on the chromanone fragment.

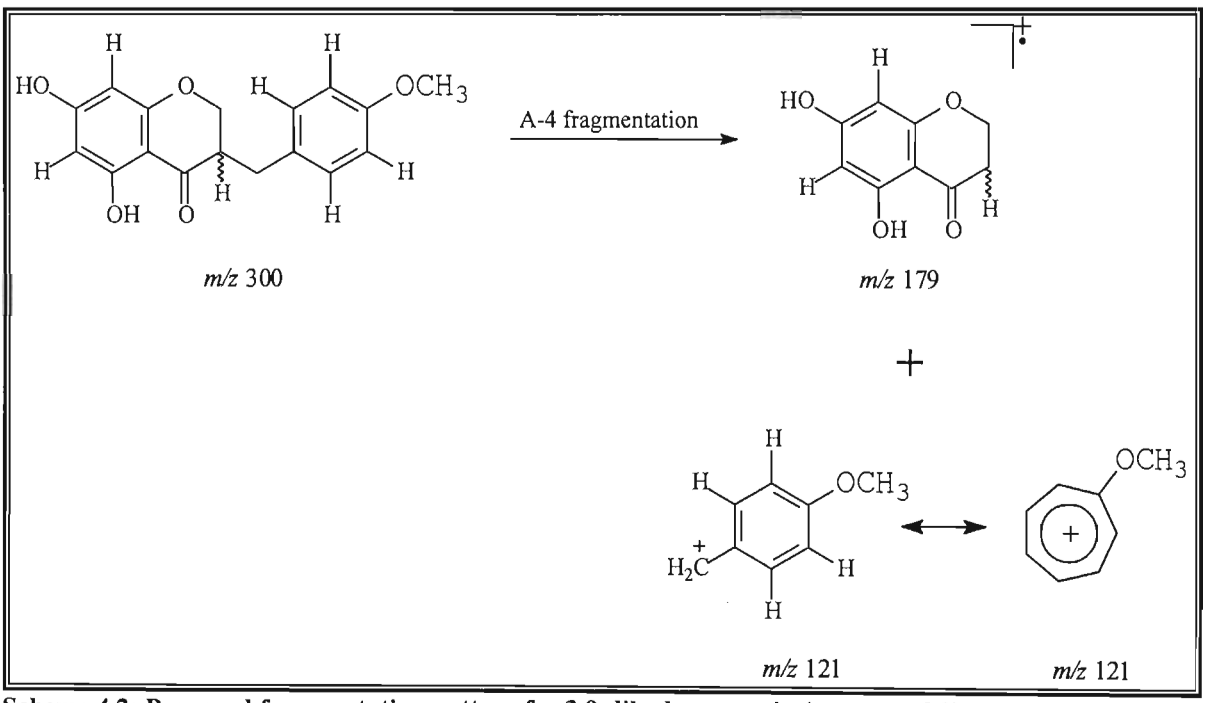

Scheme 4.2: Proposed fragmentation pattern for 3,9-dihydroeucomin (compound 2)

On the A-ring, protons H-6 and H-8 were indicated by doublet resonances at δ_H 5.96 (J = 2.18 Hz) and δ_H 5.89 (J = 2.18 Hz) in the ^{1}H NMR spectrum, and were *meta*-coupled as indicated by the coupling constant. The MS fragmentation pattern (**scheme 4.2**) indicated that the A-ring contained two hydroxyl groups and these were assigned to C-5 and C-7 based on biosynthetic grounds (Dewick, 1975). These assignments were confirmed by UV absorption as a bathochromic shift was seen upon the addition of both NaOAc (36nm) (**Spectrum 2h**) and $AlCl_3$ (23nm) (**Spectrum 2i**) (Sidwell and Tamm, 1970; Heller and Tamm, 1981; Adinolfi *et al.*, 1984). An HMBC correlation (**Spectrum 2d**) between δ_C 164.67 and H-6 allowed this carbon to be assigned to C-5, whilst HMBC correlations δ_C 164.38 and both H-6 and H-8 indicated that this resonance was that of C-7. The C-8a resonance was assigned as δ_C 163.19 as there was a HMBC correlation

between this resonance and H-8, as well as a correlation with the two protons on C-2. HMBC correlations between δ_C 102.65 and H-6, H-8 and the C-5 hydroxyl proton indicated that this resonance was due to C-4a.

A pair of doublet resonances at δ_H 6.83 (d, J = 7.53 Hz) and δ_H 7.12 (d, J = 8.73 Hz), each integrating to 2 protons, indicated a *para*-disubstituted aromatic system for the B-ring. NOESY correlations (**Spectrum 2f**) between the doublet resonance at δ_H 7.12 with the 2H-2, H-3 and 2H-9 protons, and a HMBC correlation with C-9, indicated that this resonance was due to the H-2'/6' protons, and hence the δ_H 6.83 resonance was assigned H-3'/5'. The methoxytropylium ion in the mass spectrum indicated that a methoxyl group was attached to the ring system, and with the system being *para*-substituted, it was placed at C-4'. This was confirmed by a NOESY correlation between the methoxyl peak (δ_H 3.78) and H-3'/5'. The resonance at δ_C 158.44 showed HMBC correlations to both H-3'/5' and the methoxy proton resonance and was therefore assigned to C-4'. The resonance at δ_C 129.73 was assigned to C-1' because it showed HMBC correlations with H-3, H-9, and H-3'/5'.

Table 4.2: ^{1}H, ^{13}C, HMBC, COSY and NOESY data for compound 2 and ^{13}C literature values ($CDCl_3$) (Heller et al., 1976)

	^{1}H/ ppm	^{13}C/ ppm	^{13}C/ ppm Lit	HMBC C→H	COSY	NOESY
2a	4.07 dd: 11.50, 6.75 Hz	68.93	68.94	H-3; H-9a,b	H-2b; H-3	H-2b; H-3; H-2'/6'
2b	4.23 dd: 11.50, 4.17 Hz				H-2a; H-3	H-2a; H-3
3	2.77 m	46.82	46.82	H-2a; H-9a,b	H-2a,b; H-9a,b	H-2a,b; H-9a,b; H-2'/6'
4		197.98	197.93	H-2a,b; H-3; H-9a,b		
4a		102.65	102.65	H-6; H-8, OH-5	5-OH	
5	12. 12s (OH)	164.67	164.68	H-6		
6	5.96 d: 2.18 Hz	96.61	96.60	H-8	H-8;5-OH	
7		164.33	164.26	H-6; H-8		
8	5.89 d: 2.18 Hz	95.02	95.99	H-6	H-6	
8a		163.19	163.17	H-2a,b; H-8		
9a	2.66 dd: 13.69, 10.51 Hz	31.98	31.95	H-2a,b; H-3	H-3; H-9b	H-2a; H-3; H-9b; H-2'/6'
9b	3.13 dd: 13.69, 4.17 Hz				H-3; H-9a	H-3; H-9a; H-2'/6'
1'		129.73	130.06	H-9a,b		
2'/6'	7.12 d: 8.73 Hz	130.11	130.10	H-3, H-9b	H-3'/5'	H-3; H-9a,b; H-3'/5'
3'/5'	6.83 d: 7.53	114.13	114.12	H-2'/6'	H-2'/6'	H-2'/6'; 4'-OCH_3
4'		158.44	158.43	H-2'/6'; H-3'/5' 4'-OCH_3		
4'-OCH_3	3.78	55.23	55.27			H-3'/5'

4.2.3. STRUCTURAL ELUCIDATION OF COMPOUND 3:4'-DEMETHYL-3,9-DIHYDROEUCOMIN

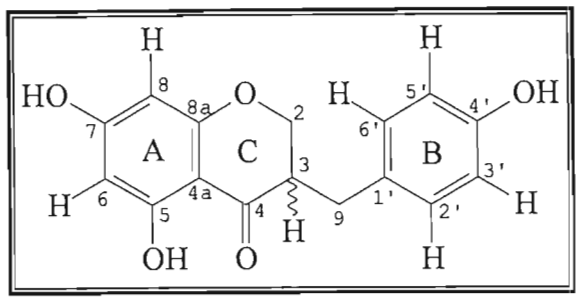

Structure 4.3: Structure of Compound 3, 4'-demethyl-3,9-dihydroeucomin

Compound **3**, 4'-demthyl-3,9-dihydroeucomin or 5,7-dihydroxy-3-(4'-hydroxybenzyl)-4-chromanone (**Structure 4.3**), was isolated as a yellow crystalline solid with a melting point of 94-97°C. The mass spectrum (**Spectrum 3g**) gave a molecular ion [M^+] peak of *m/z* 286, which corresponded to a molecular formula of $C_{16}H_{14}O_5$. From the molecular formula, a double bond equivalence of 10 was deduced.

The IR data (**Spectrum 3j**) indicated the presence of hydroxyl groups (3357cm^{-1}, O-H stretching), aromatic rings (1515cm^{-1}, aromatic C=C stretching), and carbonyl groups (1639cm^{-1}, C=O stretching) (Crews *et al.*, 1998).

The mass spectrum showed strong peaks at *m/z* 107 and *m/z* 179. A-4 type cleavage results in this fragmentation pattern, where the *m/z* 107 fragment was due to a hydroxytropylium ion. The peak at *m/z* 179 can undergo a *retro*-Diels-Alder (RDA) cleavage to yield a fragment with a mass of *m/z* 152, or form a fragment with a mass of *m/z* 153 through cleavage of the chromanone fragment followed by an effective hydrogen transfer from C-2 to the A-ring (Heller and Tamm, 1981, **Scheme 4.3**). The presence of the hydroxytropylium peak at *m/z* 107 indicated that there was one hydroxyl group present on the B-ring.

The only difference between the ^{1}H NMR (**Spectrum 3a**) spectra of compound **2** and compound **3** was the disappearance of the methoxy resonance. The ^{1}H NMR spectrum showed the same characteristic splitting pattern for a 3-benzyl-4-chromanone type

homoisoflavanones as compound **2**, with reference to the splitting pattern of the two H-2, H-3, and two H-9 protons.

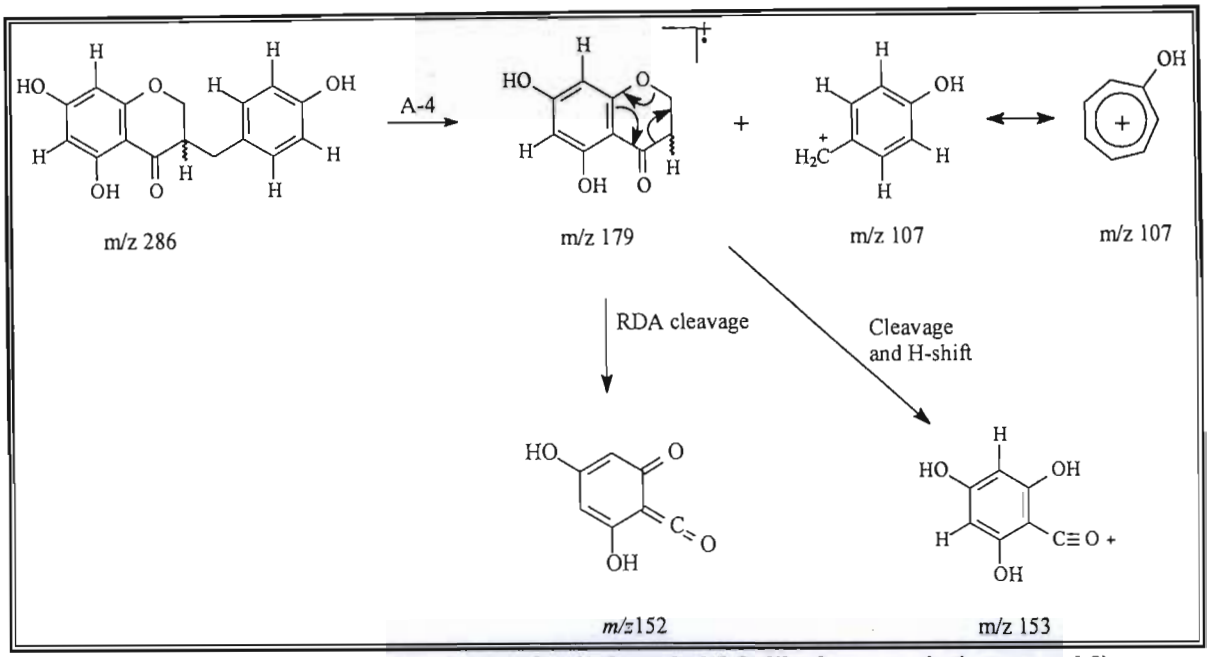

Scheme 4.3: Proposed fragmentation pattern for 4'-demethyl-3,9-dihydroeucomin (compound 3)

The difference between compound **2** and compound **3**, as suggested by the MS spectrum, occurred on the B-ring. As in compound **2**, a pair of doublet resonances at δ_H 6.74 (d, J = 6.41 Hz) and δ_H 7.03 (d, J = 8.61 Hz), each integrating to two protons, indicated a *para*-disubstituted aromatic ring system. NOESY correlations (**Spectrum 3f**) allowed these to be assigned to H-3'/5' and H-2'/6' respectively. The difference between compound **2** and **3** however occurred at C-4'. A hydroxyl group was placed at C-4' in compound **3** as indicated by the hydroxytropylium ion in the mass spectrum.

The NMR and MS spectra indicated identical substitution on the A-ring as in compound **2**. This was confirmed by the pair of doublets at δ_H 5.93 (d, J = 1.7 Hz) and δ_H 5.87 (d, J = 1.3 Hz), with the coupling constants indicating *meta*-coupled protons as in compound **2**, and were therefore assigned to H-6 and H-8 respectively. Bathochromic shifts in the UV spectrum on the addition of both $AlCl_3$ (22nm) (**Spectrum 3i**) and NaOAc (37nm) (**Spectrum 3h**) confirmed the presence of hydroxyl groups on C-5 and C-7 (Sidwell and Tamm, 1970; Heller and Tamm, 1981; Adinolfi *et al.*, 1984). Assignments of the other protons and carbons on the A-ring were made as in compound **2**.

Table 4.3 ^{1}H, ^{13}C, HMBC, COSY and NOESY data for compound 3 ($CDCl_3$)

	^{1}H/	^{13}C/	HMBC C→H	COSY	NOESY
2a	4.20 dd: 11.54, 4.03 Hz	68.78	H-9b	H-2b; H-3	H-2b; H-3; H-2'/6'
2b	4.04 dd: 11.54, 6.59 Hz			H-2a; H-3	H-2a; H-3;H-2'/6'
3	2.71m	46.81	H-9a,b	H-2a,b; H9a,b	H-2ab; H-9a,b; H2'/6'
4		197.81	H-2a,b; H-3; H-9a		
4a		101.98	H-6; H-8		
5		164.27	H-6		
6	5.93 d:1.7 Hz	96.42		H-8	
7		166.10	H-6; H-8		
8	5.87 d: 1.3 Hz	95.12		H-6	
8a		163.05			
9a	3.09 dd: 13.55, 4.03 Hz	32.04	H-2a,b; H-2'/6'	H-3; H-9b	H-3; H-9b; H-2'6'
9b	2.61 dd: 13.37,10.44 Hz			H-3; H-9a	H-3; H-9a; H-2'/6'
1'		129.16	H-9a,b; H-3'/5'		
2'/6'	7.02 d: 8.61 Hz	130.15	H-9a,b	H-3'/5'	H-2b; H-3; H-9a,b; H-3'5'
3'/5'	6.74 d: 6.41 Hz	115.47		H-2'/6'	H-2'/6'
4'		155.09	H-2'/6'; H-3'/5'		

4.2.4. STRUCTURAL ELUCIDATION OF COMPOUND 4: 4'-DEMETHYL-5-O-METHYL-3,9-DIHYDROEUCOMIN.

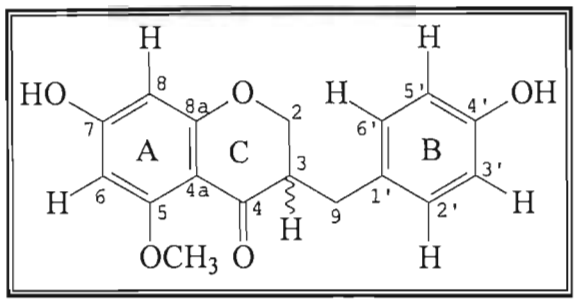

Structure 4.4: Structure of Compound 4, 4'-demethyl-5-O-methyl-3,9-dihydroeucomin

The structure of compound **4** was elucidated to be that of 4'-demethyl-5-O-methyl-3,9-dihydroeucomin or 7-hydroxy-3-(4'-hydroxybenzyl)-5-methoxy-4-chromanone (**Structure 4.4**). However in determining the structure there was conflicting data, *viz.* the melting point. However the NMR, MS, IR and UV data does not allow for any other possible structure as will be discussed.

The IR data (**Spectrum 4j**) indicated the presence of hydroxyl groups (3285cm^{-1}, O-H stretching), aromatic rings (1515cm^{-1}, aromatic C=C stretching), and carbonyl groups (1652cm^{-1}, C=O stretching) (Crews *et al.*, 1998).

The compound, 4'-demethyl-5-O-methyl-3,9-dihydroeucomin, was isolated as yellow/orange crystals that had a melting point of 103-104°C. This melting point however did not correspond with the literature value of 196-197°C (Finckh and Tamm, 1970). The mass spectrum (**Spectrum 4g**) gave a molecular ion [M^+] peak of *m/z* 300, which corresponded to a molecular formula of $C_{17}H_{16}O_5$. From the molecular formula, a double bond equivalence of 10 was deduced.

The NMR data indicated that compound **4** was structurally very similar to compound **2**, and the ^{1}H NMR spectrum (**Spectrum 4a**) showed the characteristic 2H-2, H-3, 2H-9 splitting pattern for 3-benzyl-4-chromanone type homoisoflavanones (Heller and Tamm, 1981; Adinolfi *et al.*, 1984; Pohl *et al.*, 2000).

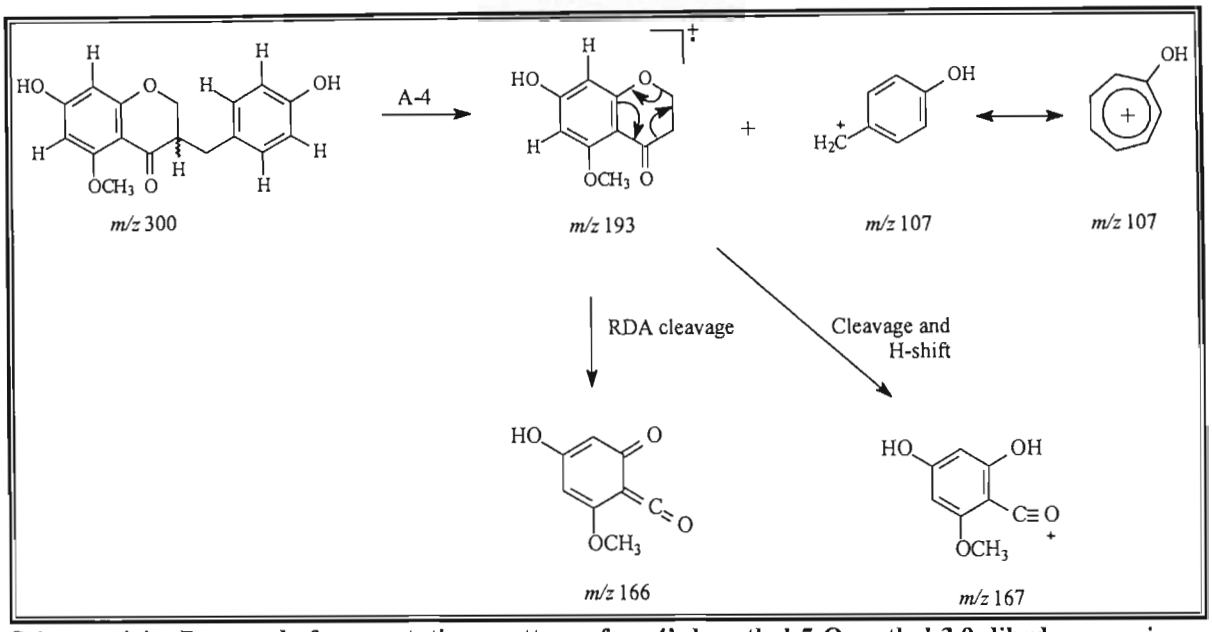

Scheme 4.4: Proposed fragmentation pattern for 4'-demethyl-5-O-methyl-3,9-dihydroeucomin (compound 4)

As in compound **3**, the presence of the hydroxytropylium ion in the mass spectrum indicated a hydroxyl group at C-4' on the B-ring (Adinolfi *et al.*, 1985). The fragmentation pattern of the mass spectrum (**Scheme 4.4**) indicated that the methoxyl group observed in the ^{1}H NMR spectrum (δ_H 3.71) was on the A-ring, as the A-4 type fragmentation resulted in molecular ion peaks of *m/z* 193 and *m/z* 107. The *m/z* 193 peak is representative of an A-ring containing both methoxyl and hydroxyl groups, and the *m/z* 107 peak represents a hydroxytropylium ion. The peak at *m/z* 167 is due to cleavage and hydrogen shift of the chromanone fragment (Heller and Tamm, 1981).

As in compounds **2** and **3**, the ^{1}H NMR spectrum indicated the meta-coupled protons of H-6 and H-8. The C-5 and C-7 resonances were identified as in compound **2**, based on HMBC correlations between C-7 and H-6 and H-8, and HMBC correlations (**Spectrum 4d**) between C-5 and H-6. The methoxyl and hydroxyl groups indicated in the mass spectrum were placed at C-5 and C-7 respectively, as the methoxyl protons had an HMBC correlation with C-5. This assignment was confirmed by a NOESY correlation (**Spectrum 4f**) between the methoxyl protons and H-6 (**Figure 4.2**). A bathochromic shift in the UV spectrum of 35nm upon the addition of NaOAc (**Spectrum 4h**) confirmed that a hydroxyl group was present at C-7, whilst the absence of a bathochromic shift with

the addition of $AlCl_3$ (**Spectrum 4i**) indicated that there was no hydroxyl group attached at C-5 (Sidwell and Tamm, 1970; Heller and Tamm, 1981; Adinolfi *et al.*, 1984), which confirmed the assignment of the methoxyl group at C-5. The position of the carbonyl resonance at C-4 (δ_C 192.52) also indicated that the methoxyl group was attached at C-5 as if a hydroxyl group was attached at this position then the C-4 resonance would be found further down field due to chelating effects (Adinolfi *et al.*, 1985).

The IR data also supported this structural assignment. Heller and Tamm (1981) reported that the IR spectrum of saturated homoisoflavanones have two to three distinct peaks occurring around 1640cm^{-1}, 1600cm^{-1}, and 1590cm^{-1}. Methylation at C-5 causes a shift of the peak at 1640cm^{-1} to 1650cm^{-1}. The C=O stretching band occurred at 1652cm^{-1}, showing greater double bond character than compounds **2** and **3** (1634cm^{-1} and1639cm^{-1} respectively), indicating that C-5 was methylated as there was no chelating effect occurring.

Comparison of ^{1}H NMR data with literature values (**Table 4.6)** agrees with this structural assignment. The inconsistent melting point is however unexplainable.

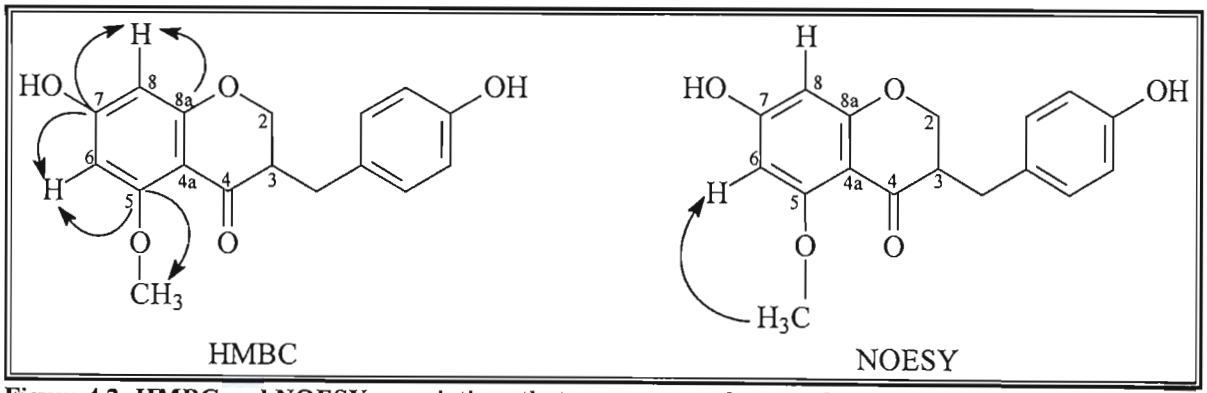

Figure 4.2: HMBC and NOESY correlations that support attachment of methoxyl group to C-5

Table 4.4: ^{1}H, ^{13}C, HMBC, COSY and NOESY data for compound 4 ($CDCl_3$)

	^{1}H /	^{13}C /	HMBC C→H	COSY	NOESY
2a	3.91 dd: 11.17, 6.04 Hz	68.26	H-3; H-9a,b; 5-OCH_3	H-2b; H-3; H-9a	H-2b; H-3; H-9a; H-2'/6'
2b	4.06 dd: 11.35, 3.48 Hz			H-2a; H-3	H-2a; H-3
3	2.50m	48.45	H-2a,b; H-3; H9a,b	H-2a,b; H9a,b	H2a,b; H-9b; H-2'/6'
4		192.52	H-2a,b; H-3; H-9a,b		
4a		104.11	H-6; H-8		
5		162.87	H-6; 5-OCH_3		
6	5.92 d:1.47 Hz	93.10	H-8		5-OCH_3
7		164.61	H6-; H-8		
8	5.88 d:1.28 Hz	95.69	H-6		
8a		164.66	H-2a,b; H-8		
9a	2.44 dd: 10.99, 5.13 Hz	32.11	H-2a,b; H-3	H-3; H-9b	H-3; H-9b; H-2'/6'
9b	2.92 dd: 14.01, 7.33 Hz			H-3; H-9a	H-3; H-9a; H-2'/6'
1'		129.23	H-3; H-9a,b; H-3'/5'		
2'/6'	6.91 d: 8.42 Hz	129.91	H-3; H-9a,b; H-3/'5'	H-3'/5'	H-2b; H-3; H-9a; H-3'/5'
3'/5'	6.64 d: 8.42 Hz	115.31	H-2'/6'	H/2'/6'	H-2'/6'
4'		155.06	H-2'/6'; H-3'/5'		
5-OCH_3	3.71	55.49			H-6

Table 4.5 Comparison of ^{1}H NMR data for compound 4 with 4'-demethyl-5-O-methyl-3,9-dihydroeucomin (CD_3OD) (Finckh and Tamm, 1970).

	^{1}H NMR - literature	^{1}H NMR -compound 4
2a	4.07 dd	4.09 dd
2b	4.23 dd	4.23 dd
3	2.65 m	2.66 m
6	6.09 d	6.10 d
8	5.98 d	5.99 d
9a	2.65 m	2.62 m
9b	3.04 dd	3.04 dd
2'/6'	7.07 d	7.06 d
3'/5'	6.75 d	6.74 d
5-OCH_3	3.84 s	3.85 s

4.3. REFERENCES:

Adinolfi M, Barone G, Lanzetta R, Belardini M, Lanzetta R, Laonigro G, and Parrilli M, 1984. 3-Benzyl-4-chromanones from *Muscari comosum*. *Phytochemistry*, **23**, 2091-2093.

Adinolfi M, Barone G, Lanzetta R, Laonigro G, Mangoni L, and Parrilli M, 1985. Three 3-benzyl-4-chromanones from *Muscari comosum*. *Phytochemistry*, **24**, 624-626.

Begum S, Siddiqui B.S, Sultana R, Zia A, and Suria A, 1999. Bio-active cardenolides from the leaves of *Nerium oleander*. *Phytochemistry*, **50**, 435-438.

Boonsong C and Wright S.E, 1961. The cardiac glycosides present in mistletoes growing on *Nerium oleander*. *Australian Journal of Chemistry*, **14**, 449-457.

Budd W, 1887. *Strophanthus* as a heart tonic and diuretic. *The Lancet*, **130**, 513.

Cabrera G.M, Deluca M.E, Seldes A.M, Gros E.G, Oberti J.C, Crockett J, and Gross M.L, 1993. Cardenolide glycosides from the roots of *Mandevilla pentlandiana*. *Phytochemistry*, **32**, 1253-1259.

Chen K.K, Henderson F.G, and Anderson R.C, 1951. Comparison of forty-two cardiac glycosides and aglycones. *Journal of Pharmacology and Experimental Therapeutics*, **103**, 420-430.

Crews P, Rodriguez J, and Jaspars M, 1998. *Topics in organic chemistry: organic structure analysis*. Oxford University Press, Oxford.

Dewick P.M, 1975. Biosynthesis of the 3-benzylchroman-4-one eucomin in *Eucomis bicolor*. *Phytochemistry*, **14**, 983-988.

Finckh R and Tamm C, 1970. The homoisoflavanones III. Isolation and structure of punctatin, 3,9-dihydropunctatin, 4'-O-methyl-3,9-dihydropunctatin, 4'-demethyl-eucomin and 4'-demethyl-5-O-methyl-3,9-dihydroeucomin. *Experientia*, **26**, 472-473.

Heller W, Andermatt P, Schaad W, and Tamm C, 1976. Homoisoflavanone. IV. Neue inhaltsstoffe der eucomoin-reihevon *Eucomis bicolor*. *Helvetica Chimica Acta*, **59**, 2048-2058.

Heller W and Tamm C, 1981. Homoisoflavanones and biogenetically related compounds. *Fortschritte der Chimie Organischer Naturstoffe*, **40**, 106-152.

Hutchings A, 1996. *Zulu medicinal plants: an inventory*. University of Natal Press, Pietermarizburg, South Africa, pp 242.

Jager H, Schindler O, and Reichstein T, 1959. Die glycoside der samen von *Nerium oleander* L.glycoside und aglykone. *Helvetica Chimica Acta*, **42**, 977-1013.

Koorbanally N.A, Crouch N.R, Harilal A, Pillay B, and Mulholland D.A, 2006. Coincident isolation of a novel homoisoflavanoid from *Resnova humifusa* and *Eucomis Montana* (Hyacinthoideae: Hyacinthaceae). *Biochemical Systematics and Ecology,* **34**, 1-5.

Pohl T.S, Crouch N.R, and Mulholland D.A, 2000. Southern African Hyacinthaceae: chemistry, bioactivity and ethnobotany. *Current Organic Chemistry*, **4**, 1287-1324.

Schindler O, and Reichstein T, 1952. Identification of substance no. 763 from *Strophanthus speciosus* and *S. boivinii* as stropeside (desglucodigitalinum verum). *Helvetica Chimica Acta,* **35**, 442-446.

Siddiqui B.S, Sultana R, Begum S, Zia A, and Suria A, 1997. Cardenolides from the methanolic extract of *Nerium oleander* leaves possessing central nervous system depressant activity in mice. *Journal of Natural Products*, **60**, 540-544.

Sidwell W and Tamm C, 1970. The homoisoflavanones II. Isolation and structure of 4'-O-methyl-punctatin, autumnalin and 3,9-dihydro-autumnalin. *Tetrahedron Letters*, **7**, 475-478.

CHAPTER 5: EXPERIMENTAL

5.1. FOREWORD TO EXPERIMENTAL

5.1.1. NUCLEAR MAGNETIC RESONANCE SPECTROSCOPY (NMR SPECTROSCOPY)

NMR spectroscopy was carried out on a 400MHz Varian UNITY-INOVA spectrophotometer. All spectra were recorded at room temperature in deuteriochloroform ($CDCl_3$), except for 4'-demethyl-5-O-methyl-3,9-dihydroeucomin (Compound **4**), which was additionally carried out in deuteriomethanol (CD_3OD) for literature comparison. The chemical shifts (δ) were recorded in ppm relative to the internal standard, tetramethylsilane (TMS), and coupling constants (*J*) are given in Hertz (Hz).

5.1.2. INFRARED SPECTROSCOPY (IR SPECTROSCOPY)

IR spectra were recorded using a Nicolet Impact 400D Fourier-Transform Infrared Spectrometer. Compounds were dissolved in dicloromethane and analysed on a sodium window. Spectra were calibrated against an air background.

5.1.3. ULTRAVIOLET ABSORPTION SPECTROSCOPY (UV SPECTROSCOPY)

UV absorption spectroscopy was measured using a Varian DMS 300 UV-vis spectrometer. Samples were dissolved in dichloromethane (neritaloside, compound **1**) or methanol (3,9-dihydroeucomin, 4'-demethyl-3,9- dihydroeucomin and 4'-demethyl-5-O-methyl-3,9-dihydroeucomin, compounds **2,3 and 4** respectively). Bathochromic shifts were recorded by adding NaOAc and $AlCl_3$ solutions to the samples. NaOAc and $AlCl_3$ solutions were prepared by dissolving 0.5g of the anhydrous salts in 100mL of methanol.

5.1.4. OPTICAL ROTATIONS

Optical rotations were measured at room temperature in either dichloromethane (compound **1**) or methanol (compounds **2-4**) using an Optical Activity AA-5 Polarimeter together with a series A2 stainless steel (4 x 200mm) unjacketed flow tube.

5.1.5. MELTING POINTS

Melting points were determined using an Ernst Leitz Weltzlar melting point apparatus and are uncorrected.

5.1.6. MASS SPECTROMETRY

The mass spectra for the compounds were recorded on an Agilent MS 5973 instrument connected to a GC 6890.

5.1.7. GENERAL CHROMATOGRAPHY

The isolation of the pure compounds employed column and thin layer chromatographic techniques. In column chromatography, different sized columns, ranging from 1-4cm in diameter depending on the purification stage, were used. Separation of the extracts was carried out on a column using Merck Art. 9385 silica gel (particle size 40-63μm). All separations were carried out under gravity. Final purifications, where necessary, were performed using a 0.75cm diameter Pasteur pipette packed with Merck Art. 9385 silica gel. Both the column and thin layer chromatography made use of varying ratios of hexane, dichloromethane, ethyl acetate and methanol. Thin layer chromatography was carried out on 0.2mm SiO_2, aluminium-backed plates (Merck Art. 5554). The plates were developed using anisaldehyde: H_2SO_4(conc): methanol (1:2:97) spray reagent and developed with heat.

5.2. ISOLATION OF COMPOUNDS 1-4

The extracts were eluted using various solvent systems. Neritaloside (Compound **1**) was isolated in the dichloromethane extract of the stem of *Strophanthus speciosus* (1.89g loaded onto column), and the homoisoflavonones (Compounds **2-4**) were isolated in the methanol extract of the bulbs of *Eucomis montana* (2.12g loaded onto column, 10.58g initially extracted). The dichloromethane extract of the stem of *Strophanthus speciosus* was eluted using a step gradient solvent system (5%, 10%, 20%, 40%, 60%, 80% and 100%) of ethyl acetate in hexane. Thirty fractions of 40mL each were collected at each stage.

Neritaloside (Compound **1**) was eluted in fractions 187-210 of the dichloromethane extract of the stems when eluted through a 4cm diameter column. Repeat column chromatography was performed in order to isolate the pure compound. The sample

was loaded onto a 1cm diameter column and eluted with 100% ethyl acetate. Fractions of 5mL were collected and neritaloside was eluted in fractions 6, 7, and 8.

The methanol extract of the bulbs of *Eucomis montana* was eluted using a step gradient solvent system (100% dichloromethane; 5%, 10%, 20%, 40%, 60%, 80%, 100%) of ethyl acetate in dichloromethane. Thirty fractions of 40mL each were collected at each stage.

Compound **2**, 3,9-dihydroeucomin, was eluted in fraction 44-60 on a 4cm diameter column, and repeat chromatography was performed to isolate the pure compound. The sample was loaded onto a 1cm column and eluted with 5% ethyl acetate in dichloromethane. Fractions of 5mL were collected and the compound was eluted in fractions 4-10. These fractions were further purified on a 0.75cm diameter Pasteur pipette, using a solvent system of 2:7:12 ethyl acetate:dichloromethane:hexane, and the pure compound was eluted in fractions 11 and 12.

Compound **3**, 4'-demethyl-3,9- dihydroeucomin, was eluted in fractions 78-85 on a 4cm diameter column, and the sample was loaded onto a 1cm diameter column for further purification. The column was eluted using a 12% ethyl acetate in dichloromethane solvent system and 5mL fractions were collected. The sample was eluted in fractions 8-10 and was pure off this column.

Compound **4**, 4'-demethyl-5-O-methyl-3,9-dihydroeucomin, was eluted off the crude column in fractions 121-130 on a 4cm diameter column. It was loaded onto a 1cm diameter column and eluted with 40% ethyl acetate in dichloromethane in order to further purify the compound. Fractions of 5mL were collected and the pure compound was isolated in fractions 7-15.

5.3. PHYSICAL DATA

5.3.1. COMPOUND 1

Systematic name:	3β-O-(6'-deoxy-3'-O-methyl-D-galactopyranose)-16β-acetoxy-14β-hydroxy-5β-card-20(22)-enolide
Alternate name:	Neritaloside; or oleandrigenin digitaloside.
Yield:	14.4mg
Physical description:	Off-white crystals
Melting point:	134-140°C; lit: 135-140°C (Jager *et al.*, 1959)
Optical rotation:	$[\alpha]_D$ +1.04° dichloromethane
Lit:	$[\alpha]_D$ +11.4° methanol (Jager *et al.*, 1959)
Mass spectrum:	*m/z* 372, $C_{23}H_{32}O_4$ requires 372g.mol^{-1}
	fragments: *m/z* 207, *m/z* 192, *m/z* 177,
IR data:	ν_{max} cm^{-1}: 3464, 2921, 2853, 1739, 1456, 1244
UV data:	λ_{max} (log ε) 235nm (4.21)
^{1}H NMR data:	See Table 4.1 ($CDCl_3$) (see p 63)
^{13}C NMR data:	See Table 4.1 ($CDCl_3$) (see p 63)

5.3.2. COMPOUND 2

Systematic name:	5,7-dihydroxy-3-(4'-methoxybenzyl)-4-chromanone
Alternate name:	3,9-dihydroeucomin
Yield:	5.1mg
Physical description:	Off-white crystals
Melting point:	156-158°C; lit: 161-163°C (Heller *et al.*, 1976).
Optical rotation:	$[\alpha]_D$ +42.0° MeOH
Lit:	$[\alpha]_D$ +38° $CHCl_3$ (Heller *et al.*, 1976)
Mass spectrum:	$[M^+]$ at *m/z* 300; m/z $C_{17}H_{16}O_5$ requires 300g.mol^{-1}
	fragment: *m/z* 121
IR data:	ν_{max} cm^{-1}: 3313, 2924, 1634, 1511
UV data:	λ_{max} (log ε) 289nm (4.24)
	Bathochromic shift: $AlCl_3$: 23nm, NaOAc: 36nm
^{1}H NMR data:	See Table 4.2 ($CDCl_3$) (p 68)
^{13}C NMR data:	See Table 4.2 ($CDCl_3$) (p 68)

5.3.3. COMPOUND 3

Name:	5,7-dihydroxy-3-(4'hydroxybenzyl)-4-chromanone
Alternate name:	4'-demethyl-3,9- dihydroeucomin
Yield:	6.1mg
Physical description:	Orange crystals
Melting point:	94-97°C; lit: 103-104°C (Adinolfi *et al.*, 1985)
Optical rotation:	$[\alpha]_D$ -15.0° MeOH
Lit:	$[\alpha]_D$ -34° MeOH (Adinolfi *et al.*, 1985)
Mass spectrum:	$[M^+]$ at *m/z* 286. $C_{16}H_{14}O_5$ requires 286g.mol^{-1}
	fragments: *m/z* 179, *m/z* 153, *m/z* 107
I.R. data:	ν_{max} cm^{-1}: 3357, 2924, 1639, 1515
UV data:	λ_{max} (log ε) 289nm (4.22)
	Bathochromic shift: $AlCl_3$: 22nm, NaOAc 37nm
^{1}H NMR data:	See Table 4.3 ($CDCl_3$) (p 71)
^{13}C NMR data:	See Table 4.3 ($CDCl_3$) (p 71)

5.3.4. COMPOUND 4

Name:	7-hydroxy-3-(4'-hydroxybenzyl)-5-methoxy-4-chromanone
Alternate name:	4'-demethyl-5-O-methyl-3,9-dihydroeucomin
Yield:	25.9mg
Physical description:	yellow/orange crystals
Melting point:	103-106°C; lit: 196-197°C (Finckh and Tamm, 1970)
	(Discrepancy unexplainable, see Chapter 4).
Optical rotation:	$[\alpha]_D$ -1.54° MeOH
Lit:	$[\alpha]_D$ -38° dioxane (Finckh and Tamm, 1970)
Mass spectrum:	$[M^+]$ at *m/z* 300, $C_{17}H_{16}O_5$ requires 300g.mol^{-1}
	fragments: *m/z* 193; *m/z* 167; *m/z* 107
I.R. data:	ν_{max} cm^{-1}: 3285, 2918, 1652, 1515
UV data:	λ_{max} (log ε) 291nm (4.52)
	Bathochromic shift: $AlCl_3$: 0nm, NaOAc 35nm
^{1}H NMR data:	See Table 4.4 ($CDCl_3$) and Table 4.5 (CD_3OD) (p 75)
^{13}C NMR data:	See Table 4.4 ($CDCl_3$) (p 75)

5.4. REFERENCES:

Adinolfi M, Barone G, Lanzetta R, Laonigro G, Mangoni L, and Parrilli M, 1985. Three 3-benzyl-4-chromanones from *Muscari comosum*. *Phytochemistry*, **24**, 624-626.

Finckh R and Tamm C, 1970. The homoisoflavanones III. Isolation and structure of punctatin, 3,9-dihydropunctatin, 4'-O-methyl-3,9-dihydropunctatin, 4'-demethyl-eucomin and 4'-demethyl-5-O-methyl-3,9-dihydroeucomin. *Experientia*, **26**, 472-473.

Heller W, Andermatt P, Schaad W, and Tamm C, 1976. Homoisoflavanone. IV. Neue inhaltsstoffe der eucomoin-reihevon *Eucomis bicolor*. *Helvetica Chimica Acta*, **59**, 2048-2058.

Jager H, Schindler O, and Reichstein T, 1959. Die glycoside der samen von *Nerium oleander* L.glycoside und aglykone. *Helvetica Chimica Acta*, **42**, 977-1013.

CHAPTER 6: ANTI-INFLAMMATORY BIOASSAY BACKGROUND

6.1. INTRODUCTION

This chapter will provide a brief biological background to the cellular basis of inflammatory responses, and conclude by providing the theoretical background for the basis of the bioassay technique reported in this study (Chapter 7).

A large percentage of the world's population relies on traditional medicines as their primary source of health care (Cordell and Colvard, 2005; Alcorn, 1995; Bojor, 1991); this is evident in South Africa, where up to 60% of the population consult traditional healers, and a large part of the medications used are plant derived (van Wyk *et al.*, 1997).

Biological screening of plants has several purposes, with the objective being the discovery and development of new medicines (Dhawan, 1991). There are several approaches used to assess plants for biological activity: *viz.* phytochemical, pharmacological and ethnopharmacological. The ethnopharmacological approach utilises traditional knowledge as a selection tool, and often involves field observations and descriptions. Ethnopharmacological screening is often used to select plants for further screening. Phytochemical screening is the examination of a plant to determine its chemical composition. Phytochemical screening often goes hand-in-hand with pharmacological screening, where various extracts and isolated compounds are examined for possible medicinal effects through the use of bioassay systems (Wagner, 1989; Bruhn and Sandberg, 1991; Dhawan, 1991).

6.2. THE INFLAMMATION PATHWAY

Inflammation is a normal tissue response to mechanical, chemical or infectious injury. Whether acute or chronic, it is regulated by humoral and cellular responses (Winrow *et al.*, 1993). The response is due to the affected tissue responding to chemical mediators produced after injury. It is characterised by an increase in the blood flow to the affected tissue, and this results in increased temperature, redness, swelling, and pain in the affected region (Sipe 1990; Winrow *et al.*, 1993; Kimball, 2006). The inflammatory response is a vital regulating mechanism as it isolates the damaged/infected area, mobilises effector cells to the site of injury, and promotes

healing, but if the response is aggravated and prolonged it can have adverse effects and result in damage (Kimball, 2006).

6.2.1. ACUTE INFLAMMATORY REACTION

Inflammation is a complex process with many different mediators involved. One of the key mediators in the initiation of an inflammatory response are mast cells. Mast cells are found throughout the body in connective tissue and are granular in nature. They are able to bind both complement fragments, and pathogen-associated molecular patterns (PAMPs) such as lipopolysaccharides and peptidoglycans, which activate the mast cells, and trigger the release of many other mediators. These mediators recruit polymorphonuclear neutrophils, lymphocytes and further plasma complement components to the site of inflammation. Restoration is achieved through the containment of the injury and infection, removal of any debris, and the repair of damaged tissue. An acute inflammatory response is generally completed within a few days of the injury occurring (Sipe, 1990; Roitt, 1994; Kimball, 2006).

Mast cells are important initiators of inflammation and can be activated by a group of glycoproteins present in the plasma of vertebrates. These glycoproteins are known as complement and can interact with immunoglobulins, bacteria, and viruses to produce a rapid, highly amplified response that triggers a stimulus-mediated cascade of events. The complement system is made up of thirty five soluble and cell-bound proteins, numbered according to their order of discovery. The complement system is divided into three biochemical pathways, the classical complement pathway, the alternate complement pathway, and the mannose-binding lectin pathway. The alternate pathway does not rely on pathogen-binding protein for its activation, but is rather activated by the direct hydrolysis of C3 on the surface of the pathogen to form a reactive intermediate C3b, and is the pathway utilised during an inflammation response. C3b is able to bind to acceptor sites on the surface of pathogens, and in the presence of Mg^{2+} ions, can combine with another complement component (factor B). After cleavage by the plasma enzyme factor D, it forms the complex C3bBb. This complex is enzymatically active and acts as a C3 convertase, splitting other C3 molecules to form C3a and C3b. The C3a fragment is released, but the C3b molecules continue to bind to the surface of micro-organisms, as well as giving rise to C3bBC3b, which is also known as the alternate pathway C5 convertase. This

complex triggers the next step in the cascade and hydrolyses C5 into C5a and C5b. C5b together with C6, C7, C8 and C9 (C5b6789) complex to form the membrane attack complex, whilst C3a together with C5a trigger mast cell degranulation. These two complexes, C3a and C5a, and the mediators they trigger from the mast cells, are responsible for the recruitment polymorphonuclear neutrophils and further plasma complement components to the site of trauma. Some of the mediators involved are tumour necrosis factor-alpha (TNF-α), chemotactic cytokines (chemokines), reactive oxygen species (ROS), histamine, interleukin-1 (IL-1), leukotrienes and prostaglandins. Associated with the release of these mediators is increased blood flow and vascular leakage, which manifests as redness and swelling in the affected tissue (Borsos and Leonard, 1990; Sipe, 1990; Roitt, 1994; Kimball, 2006).

TNF-α is rapidly released by stimulated mast cells. All of the cells involved in the inflammatory response contain receptors for TNF-α and, upon binding TNF-α, they amplify the inflammatory reaction. Chemokines are secreted proteins that attract other leukocytes into the affected area. ROS are released by activated phagocytes and are used to destroy microorganisms, but they can lead to tissue injury. Histamine is the mediator responsible for the increased blood flow to the trauma site, and is also responsible for the leakage of plasma and plasma proteins into the tissue space (Kimball, 2006).

IL-1 is a cytokine produced by macrophages and monocytes that are recruited to the site of inflammation. IL-1 affects surrounding cells in two ways. The first mechanism is a paracrine effect on the surrounding cells, causing them to produce tissue factor that triggers a blood-clotting cascade, which stimulates the secretion of other interleukins, and activates T-cells that initiate a further immune response. The second mechanism is hormonal. IL-1 is carried throughout the body in the blood causing a decrease in blood pressure, and induces fever by stimulating the release of prostaglandins. Prostaglandins and leukotrienes are formed through the metabolism of arachidonic acid and are potent mediators of inflammation, causing bronchoconstriction, vasodilation, and inhibition of platelet aggregation (Kimball, 2006).

Mast cell mediators can therefore have two origins. The first is the direct release of preformed mediators that will cause an inflammatory response, whilst the second is through the metabolism of arachidonic acid, which is produced through the activation of phospholipase A_2 (Roitt, 1994; **Figure 6.1**; **Table 6.1**).

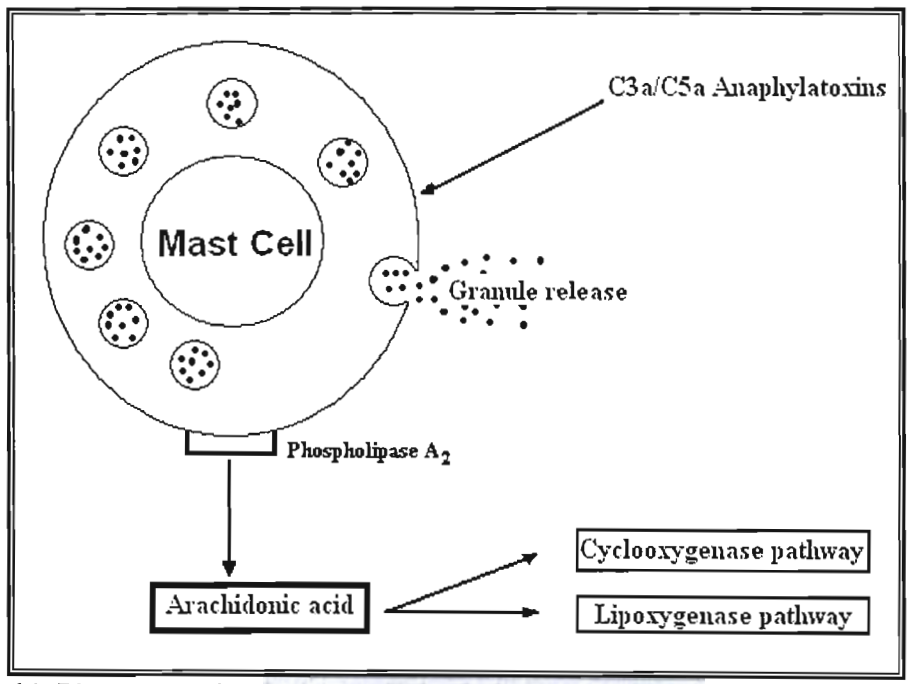

Figure 6.1: Diagram showing the two methods of release of mediators by mast cells. (i) Release of preformed mediators present in granules. (ii) Release of mediators formed through the metabolism of arachidonic acid (from Roitt, 1994)

Table 6.1: Inflammatory mediators released by mast cells (Roitt, 1994)

	PRE-FORMED	EFFECT
Granule release	Histamine	Vasodilation, increase capillary permeability, bronchoconstriction
	Proteoglycan	Binds granule protease
	Neutral proteases β-glucosamineidase	Activates C3 Cleaves glucosamine
	Eosinophil chemotactic factor Neutrophil chemotactic factor	Eosinophil chemotaxis Neutrophil chemotaxis
	Platelet activating factor	Mediator release
	Interleukins 3, 4, 5, & 6 Tumour necrosis factor	Macrophage activation, trigger acute phase proteins
	NEWLY SYNTHESIZED	**EFFECT**
Lipoxygenase pathway	Leukotrienes	Bronchoconstriction, chemotaxis
Cyclooxygenase pathway	Prostaglandins	Vasodilation, platelet aggregation,

Resolution of the inflammatory response is brought about through the modulation of the activated macrophages by proteinase inhibitors and other acute-phase proteins. This results in the gradual cessation of the numerous inflammatory reactions. If the

acute-inflammatory response does not subside, then a physiological state referred to as the chronic inflammatory state may set in (Sipe, 1990).

6.2.2. REACTIVE OXYGEN SPECIES

Oxygen metabolism in biological organisms is associated with the formation of ROS such as superoxide anions (O_2^-), singlet oxygen (O_2^{Δ}), hydrogen peroxide (H_2O_2), and hydroxyl radicals ($OH^{\cdot}$). In the electron transport chain in mitochondria, four electrons are used sequentially to reduce O_2 to H_2O, but this process is not fully efficient. Under normoxic conditions, one to two percent of the mitochondrial electron-flow "leaks off" to form superoxide anions. Superoxide anions may then be dismutased to form hydrogen peroxide. Hydrogen peroxide may be reduced to hydroxyl anions, facilitated by Fe^{2+} or Cu^{+} that act as electron donors (**Figure 6.2**), but in normal conditions the enzyme catalase reduces H_2O_2 to H_2O and O_2 (Molsen, 1994).

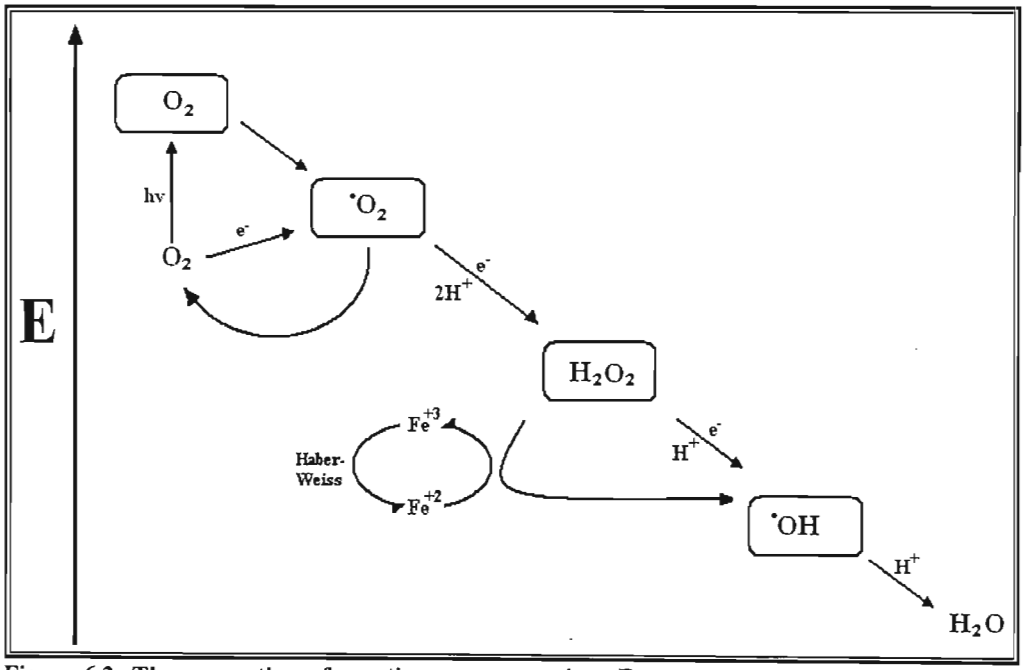

Figure 6.2: The generation of reactive oxygen species. E represents associated energy levels of components. Diagram does not show oxygen side products produced during the reactions (Baker and Orlandi, 1995)

The respiratory burst from polymorphonuclear leukocytes during an inflammatory response is catalysed by the NADPH oxidase enzyme system. During phagocytosis, cells consume more oxygen, and produce more NADPH via the hexose monophosphate shunt (pentose pathway or 6-phosphogluconate pathway), and

NADPH reduces molecular oxygen to superoxide anions that gives rise to hydrogen peroxide, hydroxyl radicals, and hypochlorous acid. Hydrogen peroxide is formed through the dismutation of superoxide anions, and is the substrate for the generation of hypochlorous acid via myeloperoxidase (Allen *et al.*, 1986; Badwey and Karnovsky, 1986; Winrow *et al.*, 1993).

The released ROS can act in a variety of ways and exert an anti-microbial action. The hydroxyl radical can lead to breakdown of plasma membranes, nuclear membranes, and chromosome damage. Hydrogen peroxide can readily cross membranes and then give rise to other, more reactive ROS; hypochlorous acid is a powerful oxidising agent that can act at various sites on cellular molecules. The killing of invading organisms by ROS is, however, a late-stage activity in the inflammatory pathway, and in order for ROS production, chemoattractants are necessary to attract the polymorphonuclear leukocytes to the site of injury. Prostaglandins and leukotrienes, produced from arachidonic acid, are powerful chemoattractants that cause the aggregation and adhesion of leukocytes to venular endothelium, which precedes the emigration of leukocytes into the extravascular space (Moslen, 1994).

6.2.3. PROSTAGLANDINS AND LEUKOTRIENES

Leukotrienes and prostaglandins are potent mediators of inflammation and are derived from arachidonic acid (**Structure 6.1**), a 20-carbon unsaturated fatty acid present in membrane phospholipids (Mathews and Van Holde, 1996; Garrett and Grisham, 2005; Kimball, 2006). Prostaglandins and leukotrienes act as local hormones by inhibiting platelet aggregation, inducing vasodilation, and causing bronchoconstriction (Roitt, 1994).

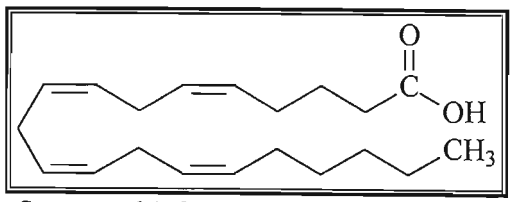

Structure 6.1: Structure of arachidonic acid

There are two important biosynthetic pathways in the formation of prostaglandins and leukotrienes: the 5-lipoxygenase (LOX) pathway that leads to the formation of

leukotrienes, and the cyclooxygenase (COX) pathway that forms prostaglandins and thromboxanes.

Prostaglandins are formed through the action of a bifunctional enzyme called prostaglandin endoperoxide synthase. The first activity of this enzyme is the addition of two oxygen molecules to arachidonic acid to form a ring structure and a hydroperoxy group. This is the cyclooxygenase activity of the enzyme. The second activity involves the reduction of the peroxide to form stable prostaglandins PGE_2, PGD_2 and $PGF_{2\alpha}$, prostacyclin (PGI_2), and thromboxane B_2, via the unstable prostaglandins PGG_2 and PGH_2 (Wagner, 1989; Mathews and Van Holde, 1996). There are two isoforms of COX in animals: COX-1 that is responsible for normal, physiological production of prostaglandins; and COX-2, which is induced by cytokines and endoxins to produce prostaglandins during inflammatory responses (**Figure 6.3**) (Garrett and Grisham, 2005).

Figure 6.3: Crystallographic model of ovine COX-1 and murine COX-2 regions of prostaglandin endoperoxide synthase (from Protein Data Bank, file 1PRH and COX5 respectively). Yellow = membrane binding domain; light green = dimerisation domain; red = heme. Peroxidase active site visible as cleft at top of diagram (from Simmons *et al.*, 2004)

Leukotrienes are formed through the attack of 5-lipoxygenase on arachidonic acid, which adds O_2 to carbon-5, forming 5-hydroperoxyeicosatetraenoic acid (5-HPETE). Dehydration follows to form an epoxide, and isomerisation of the double bonds leads to the formation of the leukotriene LTA_4. Hydrolysis of the epoxide forms LTB_4. The sulphopeptide leukotrienes LTC_4, LTD_4 and LTE_4 are formed if there is a transfer of a thiol group from glutathione to leukotriene LTB_4 (Lewis and Austen, 1987; Wagner, 1989; Mathews and Van Holde, 1996). The steps in this process are illustrated in **Figure 6.4**.

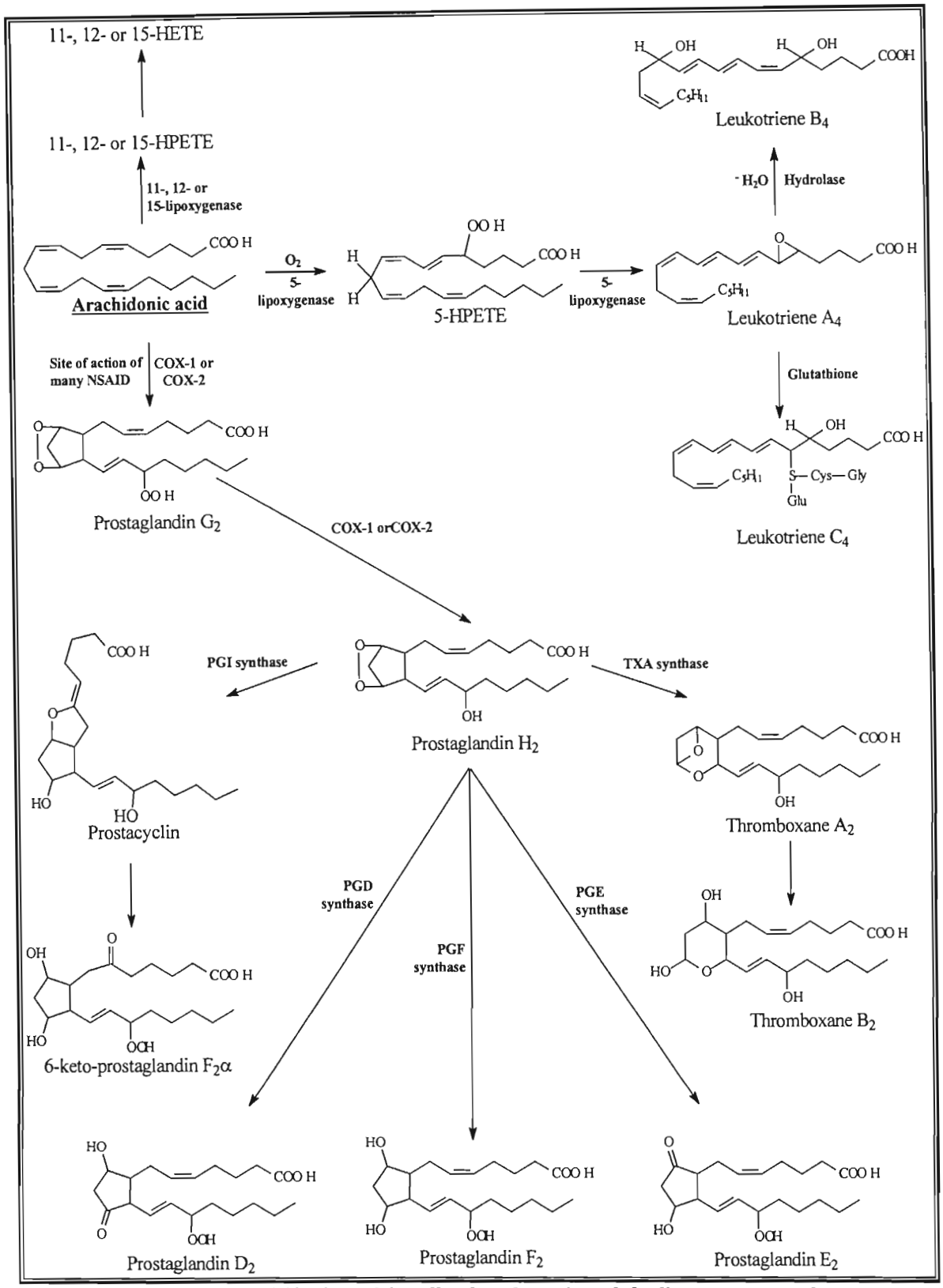

Figure 6.4: The fates of arachidonic acid in cells after the action of the lipoxygenases to form leukotrienes and HPETEs, or by cyclooxygenases to prostaglandins. Many NSAIDs block the synthesis of prostaglandin G_2 (Matthews and Van Holde, 1996; Simmons *et al.*, 2004)

6.2.4. NON-STEROIDAL ANTI-INFLAMMATORY DRUGS

Prostaglandins and leukotrienes are known to enhance inflammation in animal tissues, and thus inhibiting their synthesis is a common mode of action in commercial anti-inflammatory medications. Non-steroidal anti-inflammatory drugs (NSAIDs) are one of the most highly utilised pharmaceuticals in medicine and act by inhibiting prostaglandin synthesis. One of the earliest and most popular NSAIDs was aspirin (**Structure 6.2**). Aspirin inhibits prostaglandin synthesis by affecting the prostaglandin endoperoxide synthase enzyme. By O-acetylating $serine_{530}$ on the enzyme it destroys the COX activity of the enzyme and, in doing so, prevents the formation of prostaglandins (Gibbon and Swanepoel, 1997; Simmons *et al.*, 2004; Garrett and Grisham, 2005).

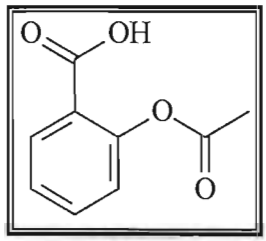

Structure 6.2: Structure of aspirin or acetyl salicylic acid

The NSAID ibuprofen (**Structure 6.3**) works by reversibly competing for the active site on the enzyme, but it is readily washed out of the active site. Consequently, once the NSAID concentration lessens in the environment of the enzyme, anti-inflammatory activity decreases. Ibuprofen does not react in a time-dependent manner. (Gibbon and Swanepoel, 1997; Simmons *et al.*, 2004; Garrett and Grisham, 2005).

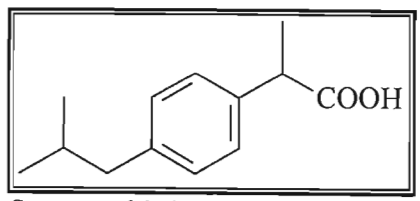

Structure 6.3: Structure of ibuprofen

Diclofenac and indomethacin (**Structure 6.4**) inhibit COX-1 and COX-2 in a time-dependent mechanism where it may take seconds to minutes to bind to the active site. Once bound, however, it may take several hours before they are released from the active site. The mechanism through which they work is the apparent formation of a salt bridge between the carboxyl group of the NSAIDs and the guanidinium moiety of

arginine$_{120}$ in COX-1. Hydrophobic interactions between the aromatic rings of the NSAIDs and the hydrophobic amino acids in the active site further stabilises the bonding of the drug within the active site. These interactions prevent the binding of arachidonic acid to the enzyme (Gibbon and Swanepoel, 1997; Simmons *et al.*, 2004; Garrett and Grisham, 2005).

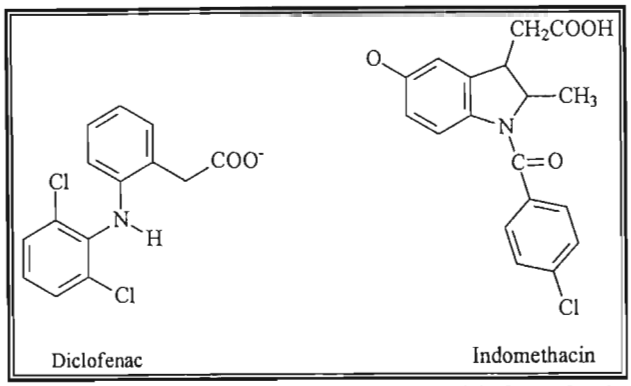

Structure 6.4: Structures of diclofenac and indomethacin

A new class of NSAIDs, such as rofecoxib (Vioxx), celecoxib (Celebrix), and meloxicam (Mobic) (**Structure 6.5**), differ from other NSAID in that they selectively inhibit COX-2. These COX-2 inhibitors are medically preferable, as they do not have the associated side effects of stomach lesions and renal toxicity that COX-1 inhibitors have. Celecoxib and rofecoxib are diaryl compounds that are weak time-dependent inhibitors of COX-1, but potent time-dependent inhibitors of COX-2. Because the compounds do not have carboxyl groups, they do not form carboxyl-arginine$_{120}$ bonds for stabilisation of the drug within the active site, but instead they are stabilised in the active site through hydrophobic interactions and hydrogen bonding (Gibbon and Swanepoel, 1997; Simmons *et al.*, 2004; Garrett and Grisham, 2005).

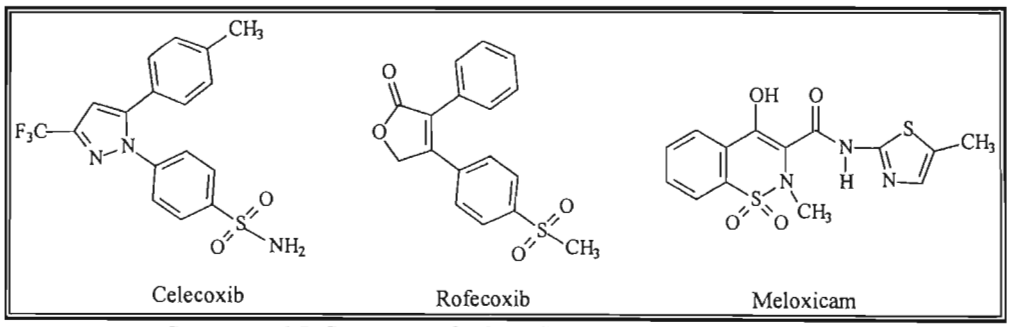

Structure 6.5: Structure of celecoxib, rofecoxib and meloxicam

The screening for anti-inflammatory activity can have several approaches since there are many pathways involved (**Figure 6.4**), and molecular sites and modes of action, as

has been described. One approach is to examine the conversion of C^{14}-arachidonic acid into prostaglandins PGG_2 and PGE_2 via the COX pathway, with COX being obtained from the seminal vesicles of sheep microsomes (White and Glassman, 1974). Inhibition of the 5-lipoxygenase pathway is another method used when screening for anti-inflammatory activity (Adams *et al.*, 2004), and examining the chemiluminescence generated by stimulated leukocytes is a third technique used in screening for anti-inflammatory activity. In this study, the chemiluminescent assay was used to screen compounds for anti-inflammatory activity as it offered a high throughput, and was effective with small amounts of test compound.

6.3. THE CHEMILUMINESCENT ASSAY

Chemiluminescence (CL) in cells can be defined as the production of light in cells as a result of a chemical reaction. The light generated during such a reaction is generally in the visible range (400-600nm), however, it can also be in the ultraviolet or infrared range. The cells that are responsible for the CL are usually single cells such as neutrophils, monocytes or macrophages (Van Dyke *et al.*, 1986; Van Dyke and Van Dyke, 1986). These phagocytic leukocytes play several essential roles in the immune response, such as receptor-mediated phagocytosis, which results in the destruction of the invading pathogen inside the phagosome or phagolysosome (**Figure 6.5**).

Phagocytic leukocytes produce a number of ROS such as superoxide anions (O_2^-), hydrogen peroxide (H_2O_2), and hydroxyl radicals (OH^-). The ROS are released in the respiratory burst during phagocytosis, and are responsible for killing the invading pathogens. The respiratory burst is the main mechanism through which phagocytic leukocytes destroy pathogens, and also accompanies anti-tumour activity as well as inflammatory reactions. It is the degradation of the ROS that results in CL (Gabig and Lefker, 1986; De Baetseilier and Schram, 1986).

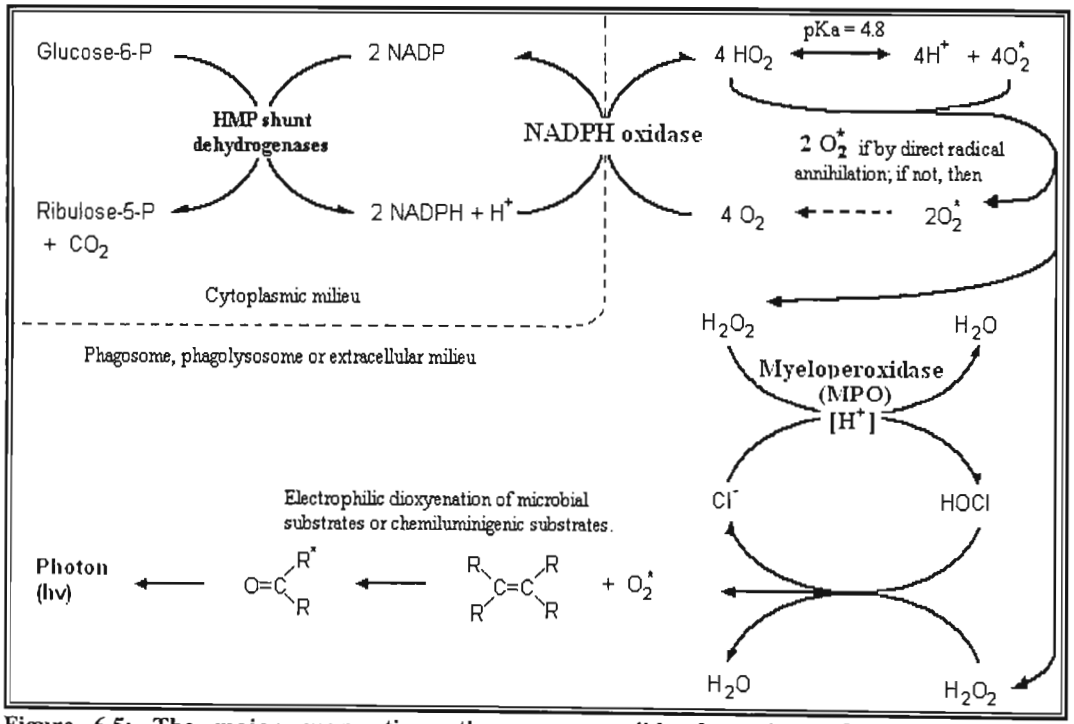

Figure 6.5: The major enzymatic pathways responsible for microbial metabolism and oxygenation, and the relationship between these activities and chemiluminescence. The cytoplasmic milieu is separated from those of the phagosome-phagolysosome-extracellular milieu (Allen *et al.*, 1986)

The amount of light produced during phagocytosis varies depending on the pathogen load of the organism and its disease state, and therefore, measuring the changes in detected CL can provide a quantifiable means of detecting disease states such as inflammatory processes, infections, degenerative diseases, and cancer (Van Dyke and Van Dyke, 1986). This provides an *in vitro* model system that allows the mechanisms of the humoral immune system to be studied (Allen, 1986).

The amount of light generated during phagocytosis is also dependent upon the number of cells present. This introduces a sensitivity problem, as relatively large numbers of phagocytic cells are needed to produce sufficient CL. This problem can be overcome through the use of 'by-stander' molecules that aid the production of CL. These by-stander molecules are chemicals that are oxidised by the ROS of the respiratory burst, resulting in their attaining an excited state. The relaxation of the excited product is responsible for the emission of light (Chasteen, 1995). By utilising by-stander molecules, the sensitivity of the assay can be increased and fewer phagocytes can be used (Allen, 1986; De Baetseilier and Schram, 1986; Van Dyke and Van Dyke, 1986).

It was reported that the chemical luminol, or 5-amino-2,3-dihydrophthalazine-1,4-dione, produced an intense chemiluminescence when treated with alkaline solutions of H_2O_2 (**Figure 6.6**). This triggered research into the use of luminol as a luminescent probe for the detection of oxidants. Luminol was found to have a high chemiluminescent quantum yield, suggesting that it could be effectively used to measure the oxidative activity of phagocytes (Allen *et al.*, 1986). Allen and Loose (1976) showed that the luminescence produced by leukocytes could be increased by several orders of magnitude through the use of luminol as a by-stander molecule. Luminol has a relatively low toxicity, which adds to its usefulness as a bystander molecule (Allen *et al.*, 1986).

Luminol can be oxidised by a number of compounds including perborate, permanganate, and iodine, but the most effective oxidant is H_2O_2. The oxidation of luminol results in the formation of 3-aminophthalate, which is the light-emitting species. Many metal cations can be used to catalyse this oxidation, and cobalt has been found to be the most effective (Chasteen, 1995).

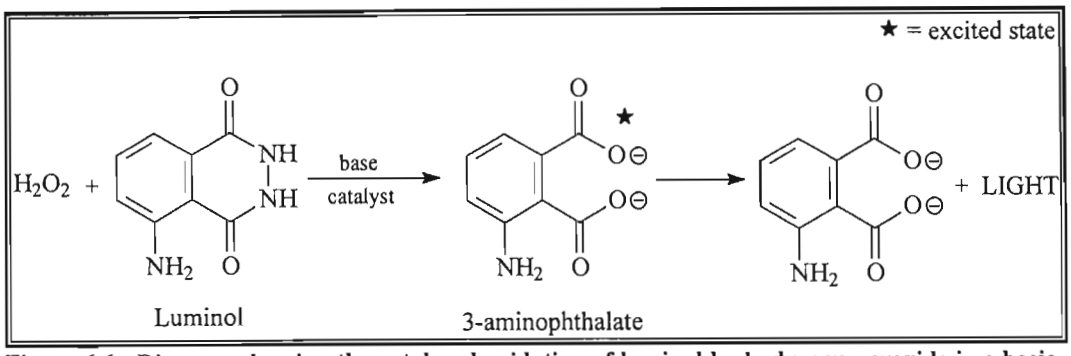

Figure 6.6: Diagram showing the catalysed oxidation of luminol by hydrogen peroxide in a basic solution resulting in the generation of light (Chasteen, 1995)

At physiological pH luminol does not directly react with hydrogen peroxide to yield luminescence. The enzyme myeloperoxidase (MPO), i.e. Cl^-:H_2O_2 oxidoreductase, which is found in neutrophil leukocytes and monocytes, is responsible for the peroxide dependent oxidation of chloride ions (Cl^-) to hypochlorous acid (HOCl) (Allen et al., 1986; Andrews and Krinsky, 1986). Hypochlorous acid can directly dehydrogenate luminol under physiological pH to yield a luminol diazaquinone (**Figure 6.7**). This reaction however does not liberate sufficient energy to produce electron excitement and luminescence. However the diazaquinone is susceptible to attack by hydrogen peroxide, and this reaction yields an excited 3-aminophthalate molecule. Relaxation of the electronically excited 3-aminophthalate to its ground state results in photon emission and luminescence (Allen *et al.*, 1986; **Figure 6.7**).

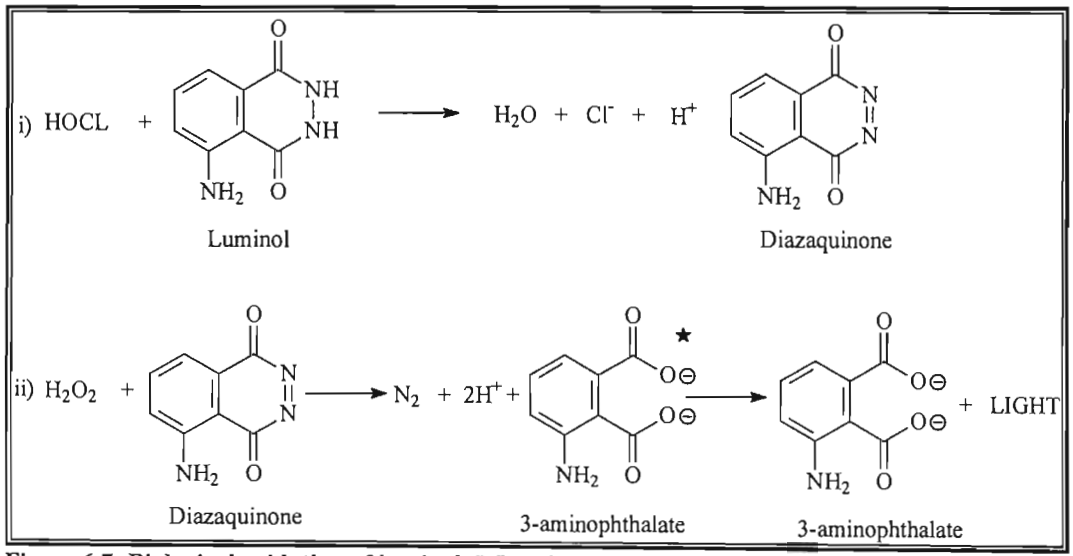

Figure 6.7: Biological oxidation of luminol. i) Luminol is dehydrogenated by hypochlorous acid to form diazaquinone; ii) diazaquinone is dioxygenated by hydrogen peroxide to give an excited 3-aminophthlate that liberates light upon relaxation (Allen *et al.*, 1986)

Hypochlorous acid can also form singlet oxygen when it reacts with hydrogen peroxide. The singlet oxygen generated can react directly with luminol to form the electronically excited 3-aminophthalate, accompanied by the associated release of photons upon relaxation. Superoxide anions are also capable of dioxygenating luminol to form 3-aminophthalate and luminescence (Allen *et al.*, 1986; **Figure 6.8**).

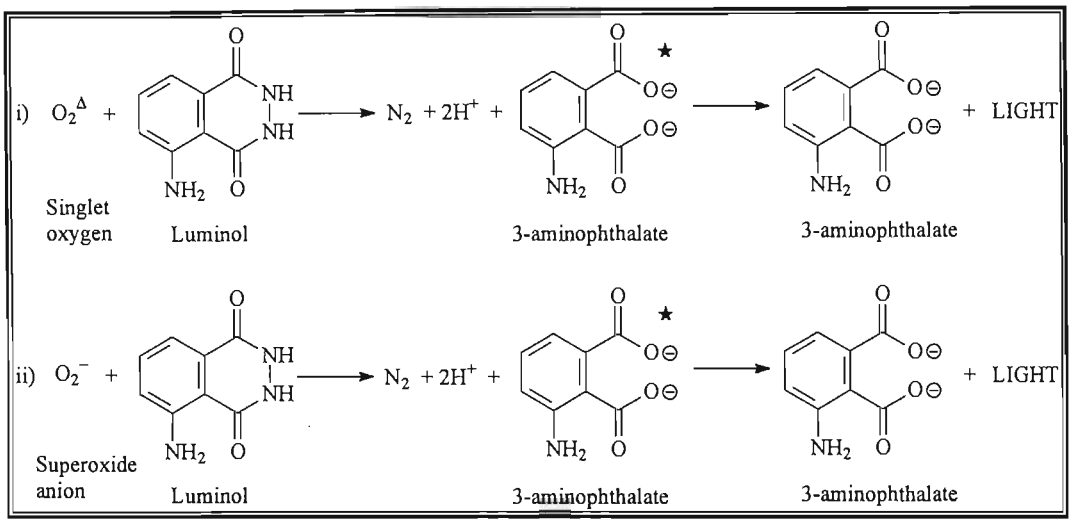

Figure 6.8: Oxidation of luminol to 3-aminophthalate resulting in chemiluminescence by i) singlet oxygen; and ii) superoxide anions in biological systems (Allen *et al.*, 1986)

The basis of a chemiluminescence bioassay is that if the quantity and functional capacity of phagocytic leukocyte populations are held constant, then the degree of phagocyte oxygenating activity, and resultant chemiluminescence, will reflect the stimulating capacity of a triggering agent, as in the following equation:

Phagocyte + triggering agent → phagocyte oxygenation activity + luminol → CL

If the triggering agent is held constant then one can analyse qualitatively and quantitatively the effects of various compounds for phagocyte inhibiting effects, i.e. anti-inflammatory activity (De Baetseiler and Schram, 1986).

When selecting a triggering agent there are several important considerations, as different phagocytes do not respond to all soluble stimulants. Blood granulocytes, monocytes, peritoneal macrophages and leukocytes require serum factors for proper recognition of particles (Van Dyke *et al.*, 1986). For optimum phagocytic ingestion of invading particles, the particles need to be treated with blood serum. This treatment of particles with serum is termed opsonization, and the elements in the

serum that produce the effect are called opsonins. Opsonization results in the adsorption of certain proteins from the serum onto the surface of triggering agents, and these adsorptions facilitate the phagocytosis of the particles (Absolom, 1986).

A popular triggering agent is zymosan, an insoluble carbohydrate extracted from the cell wall of *Saccharomyces cerevisiae*. Contact of opsonized zymosan with phagocytic leukocytes results in recognition via complement and/or IgG Fc receptors on the leukocyte, and leads to activation of redox metabolism, phagocytosis, azurophilic degranulation, and formation of phagolysosomes. This response is preferable to that of treatment with a chemical stimulus, such as phorbol myristate acetate (PMA), as PMA stimulation does not recreate a full inflammatory response. In addition, there is no azurophilic degranulation and phagolysosomes formation, and as a result does not generate the same intensity of chemiluminescence. Although the initial response is similar between opsonized zymosan and PMA, the peak luminescence obtained from PMA is reached after about 35 minutes and is followed by rapid deceleration (**Figure 6.9**), whilst opsonized zymosan produces a peak in CL activity after around 40 minutes, which thereafter gradually declines (Allen, 1986; **Figure 6.10**).

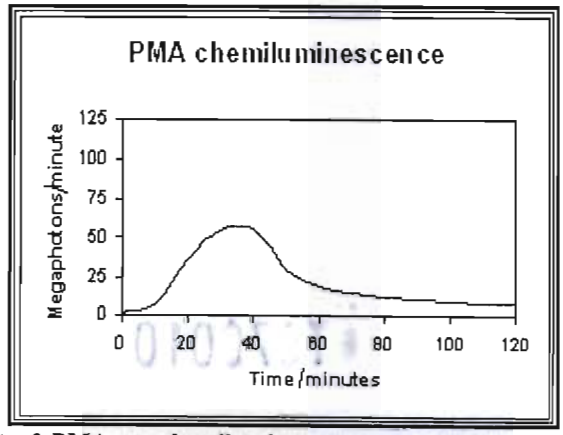

Figure 6.9: The effect of PMA on chemiluminescence. Conditions for the test was ~20 000 leukocytes in 50µL phosphate buffered saline; 80µL luminol; 100µg opsonized zymosan (Results from Allen, 1986)

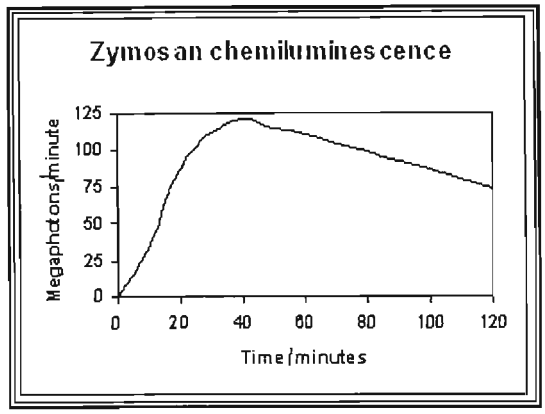

Figure 6.10: The effect of zymosan on chemiluminescence. Conditions for the test was ~20 000 leukocytes in 50µL phosphate buffered saline; 80µL luminol; 50µL PMA (Results from Allen, 1986)

Luminol is not the only bystander molecule available. Lucigenin, or 10,10'-dimethyl-9,9'-biacridium dinitrate (DBA), is a water soluble acridium salt that has a quantum yield similar to that of luminol. In alkaline solutions DBA reacts with H_2O_2 to yield electronically excited N-methylacridone that releases photons upon relaxation. The physical properties and chemical reactivity of DBA however differs from luminol. Both luminol and DBA yield chemiluminescence when reacted with H_2O_2 but the mechanisms for the dioxygenation differs. Luminol reacts with oxygen to form 3-aminophthalate and photons; DBA also undergoes a dioxygenation reaction, but it also undergoes a two-electron reduction. The DBA reaction with H_2O_2 is therefore a reductive-dioxygenation. This difference in reaction mechanism may explain why DBA does not yield luminescence in the myeloperoxidase system (Allen 1986).

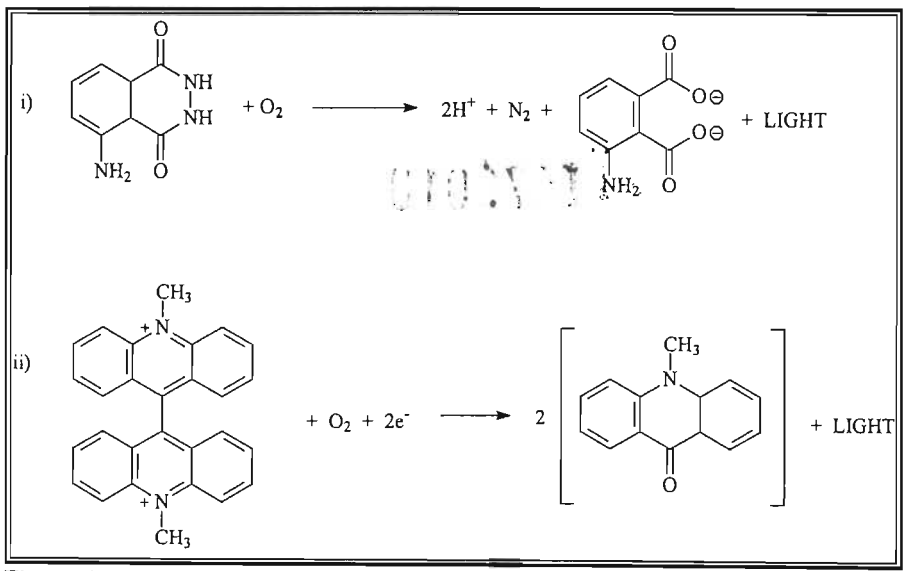

Figure 6.11: Luminol versus DBA dioxygenation. (i) Shows the general dioxygenation of luminol; (ii) the reductive-dioxygenation of DBA (Allen, 1986)

The classical method for the dioxygenation of DBA is through reaction with alkaline H_2O_2. H_2O_2 under these conditions is able to divalently reduce DBA to yield a moloxide (dioxetane) intermediate, which then breaks down to yield two molecules of N-methylacridone, one of which is in an excited state. Relaxation of the excited N-methylacridone results in the release of photons (**Figure 6.11**). However, under biological conditions of neutral-to-slightly-acidic pH, DBA is only weakly reactive with H_2O_2. An alternative dioxygenation route involves the univalent reduction of DBA, catalysed by either a metal or metalloprotein, producing a cation radical that is free to react with superoxide anions in a radical-radical, anion-cation annihilation reaction to yield the monoxide intermediate. The monoxide molecule again could undergo disintegration to yield an excited N-methylacridone molecule. A third possible route for dioxygenation involves the divalent reduction of DBA, again catalysed by a metal or metalloprotein, followed by reaction with singlet oxygen. This again produces a moloxide intermediate that disintegrates to yield two N-methylacridone molecules, with one being in an excited state. Relaxation of the excited molecule produces chemiluminescence (Allen, 1986; **Figure 6.12**).

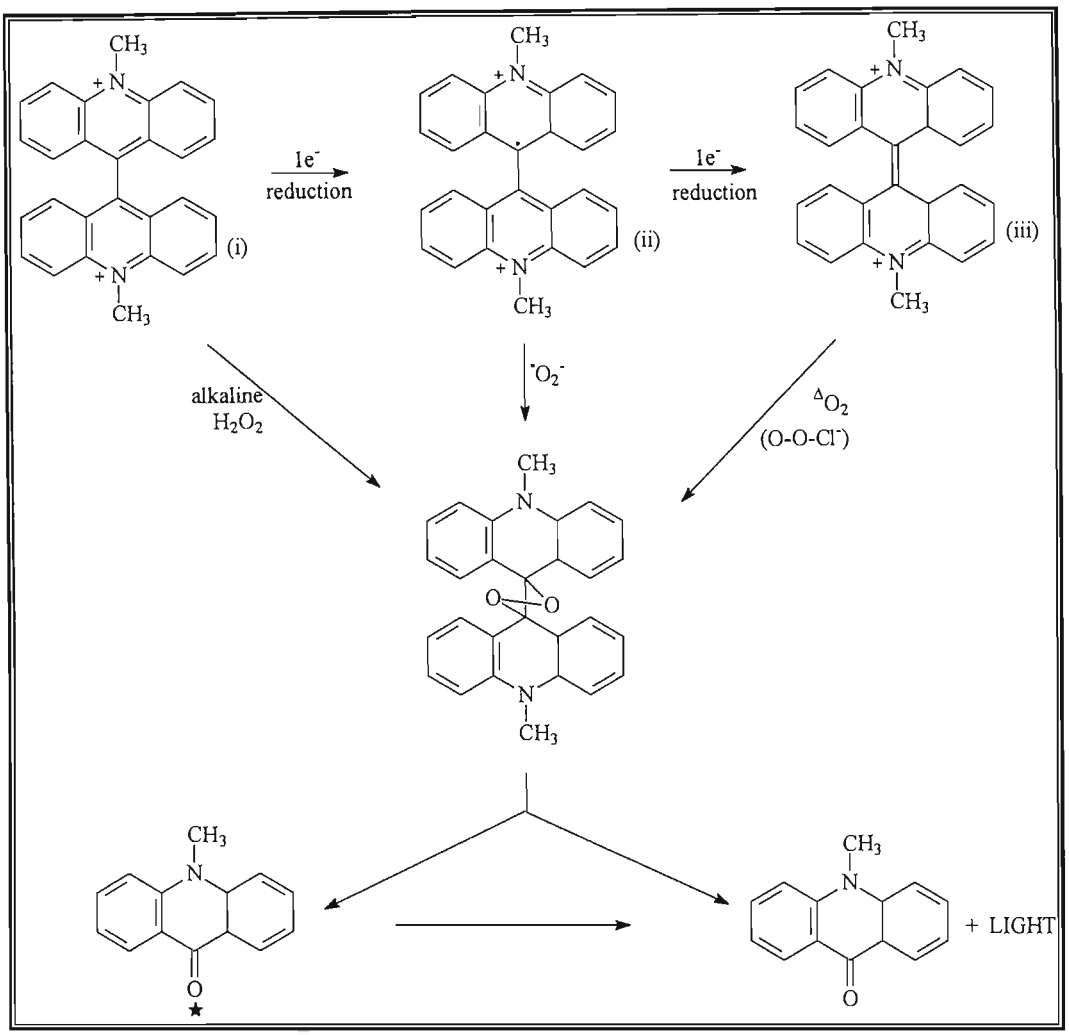

Figure 6.12: Possible pathways to DBA dioxygenation. (i) Classical pathway involving divalent reduction and dioxygenation by H_2O_2; (ii) univalent reduction resulting in a radical-radical, cation-anion annihilation reaction with superoxide anions; (iii) divalent reduction catalysed by metals or metalloproteins followed by dioxygenation by singlet oxygen (Allen, 1986)

6.4. REFERENCES

Absolom D.R, 1986. Opsonins and dysopsonins: an overview. *Methods in Enzymology*, **132**, 281-306.

Adams M, Kunert O, and Bauer R, 2004. Inhibition of leukotriene biosynthesis by quinolone alkaloids from the fruit of *Evodia rutaecarpa*. *Planta Medica*, **70**, 904–908.

Alcorn J.B, 1995. The scope and aims of ethnobotany in a developing world. In: *Ethnobotany: evolution of a discipline*. Eds. Schultes R.E and von Reis S. Dioscorides Press, Portland, Oregon, pp 23-39.

Allen R.C and Loose L.D, 1976. Phagocytic activation of a luminol-dependent chemiluminescence in rabbit alveolar and peritoneal macrophages. *Biochemical and Biophysical Research Communications*, **69**, 242-252.

Allen R.C, 1986. Phagocytic leukocyte oxygenation activities and chemiluminescence: a kinetic approach to analysis. *Methods in Enzymology*, **133**, 449- 493.

Allen R.C, Dale D, and Tayor F Jnr, 1986. Blood phagocyte luminescence: gauging systemic immune activation. *Methods in Enzymology*, **133**, 591-629.

Andrews P.C and Krinsky N.I, 1986. Human myeloperoxidase and hemi-myeloperoxidase. *Methods in Enzymology*, **132**, 369-378.

Badwey J.A and Karnovsky M.L, 1986. NADH oxidase from guinea pig polymorphonuclear leukocytes. *Methods in Enzymology*, **132**, 365-369.

Baker C.J and Orlandi E.W, 1995. Active oxygen in plant pathogenesis. *Annual Review of Phytopathology*, **33**, 299-321.

Bojor O, 1991. Methodology of economic mapping of medicinal plants in the spontaneous flora. In: *Medicinal plant industry*. Ed: Wijesekera R.O.B. CRC Press, Boca Raton, USA, pp 18.

Borsos T, and Leonard E, 1990. Physiologic functions of complement. In: *Immunophysiology: Role of cells and cytokines in immunity and inflammation*. Eds: Oppenheim J and Shevach E. Oxford University Press, Oxford, pp 152-165.

Bruhn J.G and Sandberg F, 1991. Screening and processing of plant material for potential pharmaceutical needs: experience and applications in three continents. In: *Medicinal plant industry*. Ed: Wijesekera R.O.B. CRC Press, Boca Raton, USA, pp 223-235.

Chasteen T, 1995. The chemiluminescence of luminol and bis(2,4,5-trichlorphenyl)oxalate (TCPO). Found at: www.shsu.edu/~chm_tgc/JPPdir/JPP1999. Accessed November 2004.

Cordell G.A and Colvard M.D, 2005. Some thoughts on the future of ethnopharmacology. *Journal of Ethnopharmacology,* **100**, 5-14.
De Baetseilier P and Schram E, 1986. Luminescent bioassays based on macrophage cell lines. *Methods in Enzymology*, **133**, 507-527.

Dhawan B.N, 1991. Methods for biological assessment of plant medicines. In: *Medical plant industry*. Ed: Wijesekera R.O.B. CRC Press, Boca Raton, USA, pp 77-81.

Gabig T.G and Lefker B.A, 1986. NADPH oxidase from polymorphonuclear cells. *Methods in Enzymology*, **132**, 355-364.

Garrett R.H and Grisham C.M, 2005. *Biochemistry*. Thompson Learning Inc, California, pp 788-790.

Gibbon C.J, and Swanepoel C.R (eds), 1997. *South African Medicines Formulary*. Medical Association of South Africa, Pioneer Press, Cape Town, pp 301-307.

Kimball J, 2006. Kimball's biology pages. Found at: http://users.rcn.com/jkimball.ma.ultranet/BiologyPages/I/Inflammation.html. Accessed May 2006.

Lewis R.A and Austen K.F, 1987. Regulatory modulators of the 5-lipoxygenase pathway. In: *Allergy and inflammation.* Ed: Kay A.B. Academic Press, London, England, pp 71-81.

Mathews C.K, and Van Holde K.E, 1996. *Biochemistry, 2nd edition.* The Benjamin/Cummings Publishing Company, California, USA, pp 692-696.

Moslen M.T, 1994. Reactive oxygen species in normal physiology, cell injury and phagocytosis. In: *Free radicals in diagnostic medicine*. Ed: Armstrong D. Plenum Press, New York, USA, pp 17-27.

Roitt I.M, 1994. *Essential immunology*. Blackwell Scientific Publications, Oxford, England, pp 5-20.

Simmons D.L, Botting R.M, and Hla T, 2004. Cyclooxygenase isozymes: the biology of prostaglandin synthesis and inhibition. *Pharmacological reviews*, **56**, 387-437.

Sipe J.D, 1990. The acute-phase response. In: *Immunophysiology: role of cells and cytokines in immunity and inflammation.* Eds: Oppenheim J.J and Shevach E.M. Oxford University Press, Oxford, pp 259-273.

Van Dyke K, Van Scott, M.R, and Castranova V, 1986. Measurement of phagocytosis and cell-mediated cytotoxicity by chemiluminescence. *Methods in Enzymology*, **132**, 498-507.

Van Dyke K and Van Dyke C, 1986. Cellular Chemiluminescence associated with disease states. *Methods in Enzymology*, **133**, 493-507.

van Wyk B-E, van Oudtshoorn B, and Gericke N, 1997. Medicinal plants of South Africa. Briza, Pretoria, pp 8-22.

Wagner H, 1989. Search for new plant constituents with potential antiphlogistic and anti-allergic activity. *Planta Medica*, **55**, 235-241.

White H.L and Glassman A.T, 1974. A simple radiochemical assay for prostaglandin synthetase. *Prostaglandins*, **7**, 123-129.

Winrow V.R, Winyard P.G, Morris C.J and Blake D.R, 1993. Free radicals in inflammation: second messengers and mediators of tissue destruction. *British Medical Bulletin*, **49**, 506-522.

CHAPTER 7: SCREENING OF COMPOUNDS FOR BIOLOGICAL ACTIVITY

7.1. REAGENTS

7.1.1. DEXTRAN SOLUTION:

A dextran solution was made according to the method used by the National Referral Laboratory for Lysomal, Peroxisomal and Related Genetic Disorders of the University of Adelaide (2005). Dextran (5g) (MW ~ 200 000 Daltons) and NaCl (0.7g) was dissolved in 100mL deionised water. Solution was made up freshly on the day of use.

7.1.1. HEPES BUFFER:

A HEPES buffer (4-(2-hydroxyethyl)piperazine-1-ethanesulfonic acid) was made using the method of Van Dyke and Van Dyke (1986). The buffer contained 145mM NaCl, 5mM KCl, 10mM HEPES and 5.5mM glucose; 4.235g NaCl, 0.1865g KCl, 1.19g HEPES, and 0.495g glucose, which were dissolved in 450mL deionised water. The pH was adjusted to 7.4 and the volume made up to 500mL. The solution was autoclaved and stored at 4°C. HEPES buffer is preferable over phosphate-based buffers, as the phosphates can interact with calcium, resulting in the precipitates (Van Dyke and Van Dyke, 1986).

7.1.3. LYSIS BUFFER:

Lysis buffer was made according to the method of the National Referral Laboratory for Lysomal, Peroxisomal and Related Genetic Disorders of the University of Adelaide (2005). The lysis buffer contained 155mM NH_4Cl, 10mM $NaHCO_3$, 0.1mM EDTA; 8.3g NH_4Cl, 0.84g $NaHCO_3$ and 29.3mg EDTA, which were dissolved in 900mL deionised water and adjusted to a pH of 7.4. The volume was then made up to one litre, the solution autoclaved, and stored at 4°C.

7.1.4. LUMINOL SOLUTION:

A 3mM luminol solution in 1% dimethyl sulphoxide (DMSO) and HEPES buffer was made up. Luminol (0.051g) (Fluka) was dissolved in 1mL of DMSO, and 100μL of this solution was added to 9.9mL HEPES buffer. This solution was made up fresh, immediately before use.

7.1.5. OPSONIZED ZYMOSAN:

Opsonized zymosan particles were prepared using a modification of the method of Tosi and Hamedani (1992). Zymosan (Sigma-Aldrich) was incubated in fresh human serum at 37°C for one hour with gentle agitation at a concentration of 25mg zymosan per millilitre human serum. After incubation, the solution was centrifuged at 1000xg for 10 minutes to pellet the opsonized zymosan. The opsonized zymosan was then washed three times with phosphate-buffered saline, pH 7.4 (Highveld Biological), and resuspended at a concentration of 10mg/mL in PBS and stored at –80°C in 0.5mL aliquots.

Human serum was prepared by allowing whole fresh human blood to clot in centrifuge tubes for thirty minutes at room temperature. The blood clots were removed and the remaining solution was centrifuged for ten minutes at 1000xg. The serum was then removed and stored on ice for immediate use.

7.1.6. ANTIOXIDANT/ FREE RADICAL SCAVENGING ASSAY REACTION MEDIUM

The antioxidant assay reaction medium was prepared by adding 2.4g sodium bicarbonate, 0.08g ammonium carbonate monohydrate, and 0.04g copper (II) sulphate pentahydrate to 100mL of distilled water.

7.2. METHODOLOGY

7.2.1. LEUKOCYTE SEPARATION AND PREPARATION.

Leukocytes were isolated from human buffy coat cells using modifications of the methods of Boyum (1984) and the National Referral Laboratory for Lysomal, Peroxisomal and Related Genetic Disorders of the University of Adelaide (2005). Dextran solution (5mL) was placed in a 15mL centrifuge tube and 5mL of buffy coat, obtained from the South African National Blood Service, was gently layered on top of the dextran solution. The solution was left to sediment for one hour at room temperature in a sterile environment. The pale upper layer was retained and the sedimented erythrocytes discarded. The upper layer (5mL) was mixed with 5mL of ice-cold lysis buffer in 15mL centrifuge tubes, and left to stand for ten minutes on ice with occasional shaking. The solution was centrifuged at 290xg at 4°C for ten minutes, the supernatant discarded and the pellet resuspended in 5mL lysis buffer. The solution was recentrifuged at 290xg for ten minutes at 4°C, the supernatant discarded and the pellet washed in 5mL HEPES buffer. The solution was again centrifuged at 290xg for ten minutes at 4°C, with the supernatant being discarded and the pellet of isolated leukocytes retained.

The leukocyte pellet was resuspended in RPMI culture media (Highveld Biological), with 10% bovine calf serum (Highveld Biological) and 2% streptomycin/penicillin antibiotic (Highveld Biological), at a concentration of $\sim 10^7$ cells per millilitre. Cultured leukocytes were aliquoted into a 24-well culture plate and stored at 37°C in an incubator with 5% CO_2 atmosphere. Cultured cells could be stored for approximately three days without any significant loss in chemiluminescent activity.

7.2.2. ANTI-INFLAMMATORY CHEMILUMINESCENT SCREENING.

The anti-inflammatory bioassay was based on a modification of the method of Van Dyke and Van Dyke (1986). Leukocyte solution (400µL) was placed into the well of a black, 24-well microplate (NUNC™, Apogent) together with 100µL 3mM luminol solution, and 50µL test compound dissolved in HEPES buffer. Immediately before screening 50µL of the opsonized zymosan was added to the well and the microplate was placed in a pre-heated fluorescent/luminescent spectrophotometer (BioTek FL_X 800i Microplate Fluorescent reader) and monitored every two minutes for 1 hour.

Different blanks and controls were used during the screening protocols: an uninhibited luminescence negative control was performed where the chemiluminescent reaction was left to proceed normally; positive controls where commercial NSAIDs were added to the reaction mixtures; and two background blanks where no luminescence occurred, as one solution did not have any luminol solution added to the reaction mixture, and the other did not have any opsonized zymosan added to the reaction mixture. The volumes of all test wells were kept constant by adding HEPES buffer to the blanks and negative controls wells.

7.2.3. ANTIOXIDANT/ FREE RADICAL SCAVENGING SCREENING.

The assay was performed by mixing 500μL of antioxidant assay reaction medium, 100μL of 97μM H_2O_2, and 50μL test compound (dissolved in DMSO) in the well of black microplates. 100μL of 3mM luminol solution was added immediately before recording the chemiluminescence. Two controls were used: one containing 500μL reaction medium, 100μL H_2O_2, 50μL DMSO, and 100μL luminol solution; and the second, a background blank, contained 500μL reaction medium, 100μL DMSO, and 100μL H_2O_2. Chemiluminescence was recorded every ten seconds for three minutes.

7.3. ANTI-INFLAMMATORY ASSAY OPTIMISATION

The reaction was optimised for concentration of luminol, optimal volumes of leukocyte solution, and opsonized zymosan. Assays were run in triplicate and the graphs plotted represent the average values. Standard deviations are not shown on graphs, but can be seen in the Appendix (page 135). Variations in overall maximal luminescence between experiments were due to the relative age, and activity of blood cells. Two commercial non-steroidal anti-inflammatory drugs (NSAIDs), diclofenac and meloxicam, were used as positive controls for comparative purposes with test compounds.

7.3.1. OPTIMISATION OF LUMINOL CONCENTRATION

Assays were performed using various concentrations of luminol solution to find the concentration for maximal luminescence. Concentrations tested were 1mM, 3mM, 5mM, and 12mM luminol solution (**Figure 7.1**).

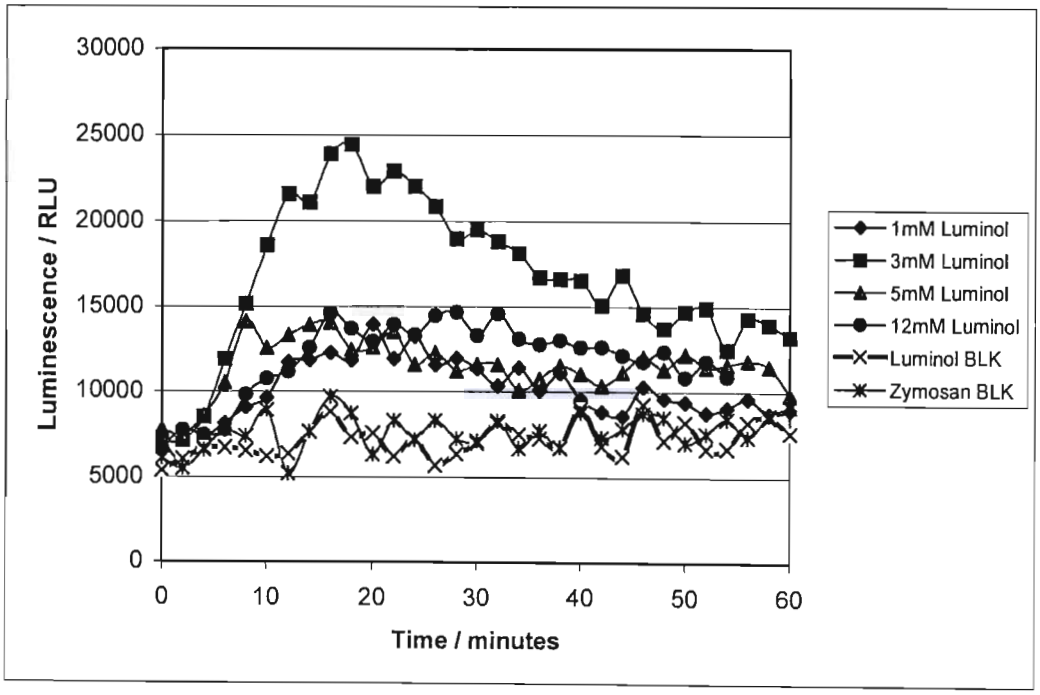

Figure 7.1: Graph of varying concentrations of luminol solution. Volume of blood cells and opsonized zymosan stimulant were kept constant at 400uL and 100uL respectively.

As can be seen from **Figure 7.1**, a 3mM luminol solution concentration produced maximal luminescence, whilst 1mM, 5mM and 12mM solutions showed some apparent reduction or inhibition of CL.

7.3.2 Optimisation of luminol, opsonized zymosan, and leukocyte solution volumes.

Having established the optimal concentration, the assay was optimised to determine ideal volumes of luminol solution, opsonized zymosan and leukocyte solution for use in the microplate wells. Two different volumes of each component were tested: 50μL and 100μL were tested for both luminol solution and opsonized zymosan; and 400μL and 500μL volumes for the leukocyte cells. The concentration of leukocytes in solution was typically adjusted to ~10^7 cells/mL. Background blanks for both luminol and opsonized zymosan volumes were also run. The volumes of all wells were kept constant at 600μL for the wells containing 400μL leukocyte, and 700μL for the wells containing 500μL leukocyte solution with HEPES buffer.

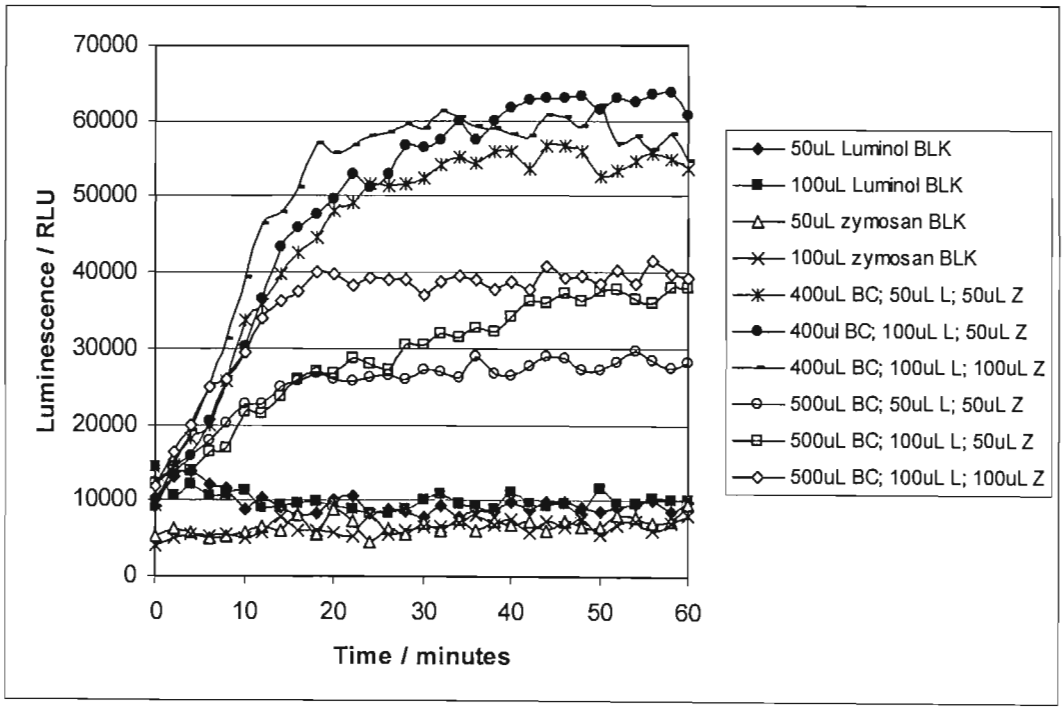

Figure 7.2: Graph of varying volumes of luminol solution, opsonized zymosan, and blood cells. In legend: LC = leukocyte solution; L = luminol solution; Z = opsonized zymosan, BLK = blank.

The results (**Figure 7.2**) indicated that a volume of 400μL blood cell solution and 100μL luminol solution produced maximum chemiluminescence over the 60 minute time span. The volume of opsonized zymosan however did not significantly affect the overall luminescence. A higher volume of opsonized zymosan caused a more rapid onset of luminescence but the maximum luminescence was not however affected. Due to the time and cost involved in opsonizing zymosan, the lower volume of

opsonized zymosan was chosen for all further experiments and optimal assay conditions were 400µL blood cell solution, 100µL luminol solution, and 50µL opsonized zymosan.

7.3.2. COMMERCIAL ANTI-INFLAMMATORY CONTROLS.

Two commercial NSAIDs were utilised as positive controls and to act as references against which to measure the anti-inflammatory activity of plant extracts. Diclofenac (Panamor® 25mg/mL) and meloxicam (Mobic® 10mg/mL) intramuscular injectable NSAIDs were selected (diclofenac a COX-1 inhibitor and meloxicam a COX-2 inhibitor). Optimisation assays were performed to determine the concentration and volume of these anti-inflammatories that completely inhibited chemiluminescence (**Figures 7.3-7.6** for diclofenac; **7.7-7.10** for meloxicam).

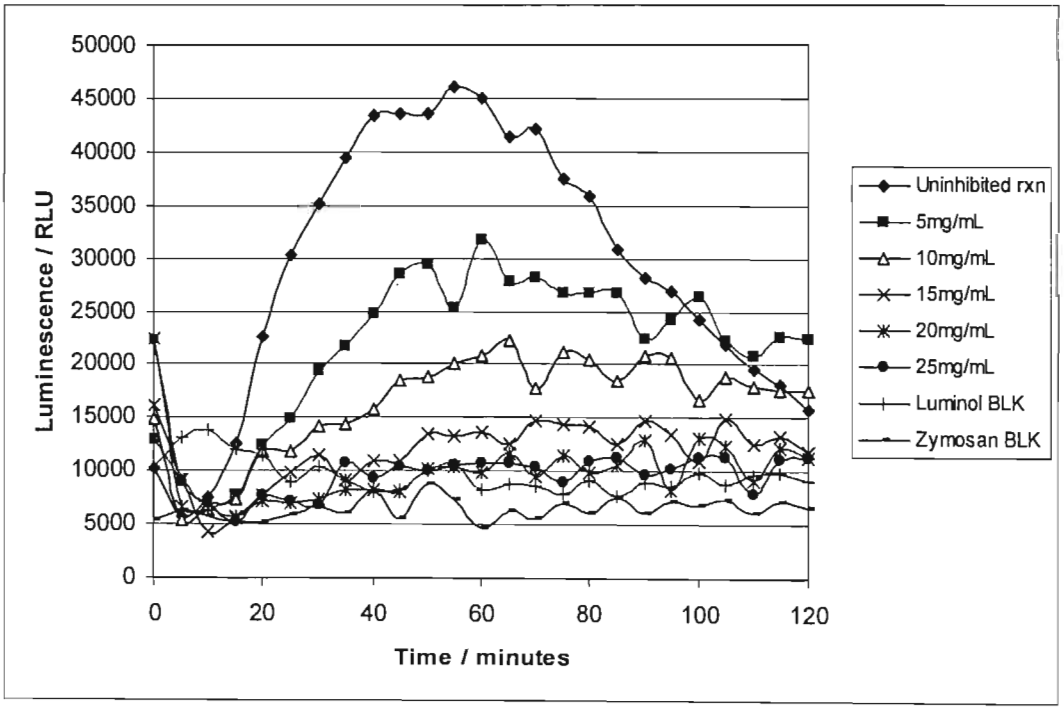

Figure 7.3: Graph illustrating the inhibition of chemiluminescence by diclofenac. 5µL of five different concentration of diclofenac solution were added to each well and compared with an uninhibited reaction. BLK = blank.

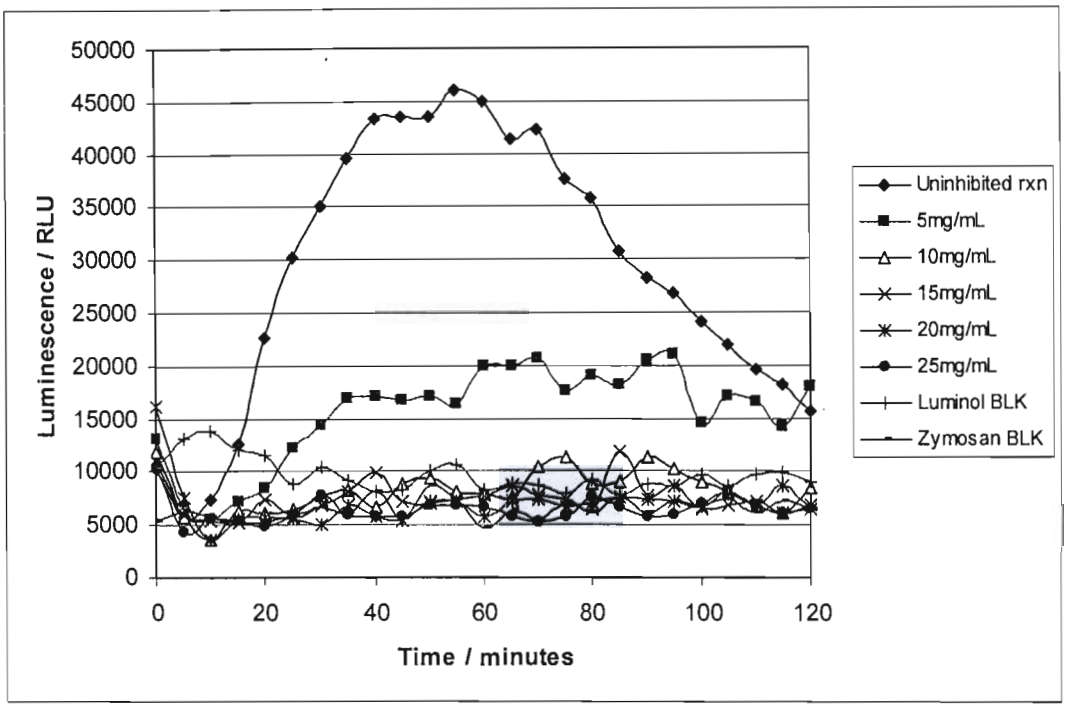

Figure 7.4: Graph illustrating the inhibition of chemiluminescence by diclofenac. 15µL of five different concentration of diclofenac solution were added to each well and compared with an uninhibited reaction. BLK = blank.

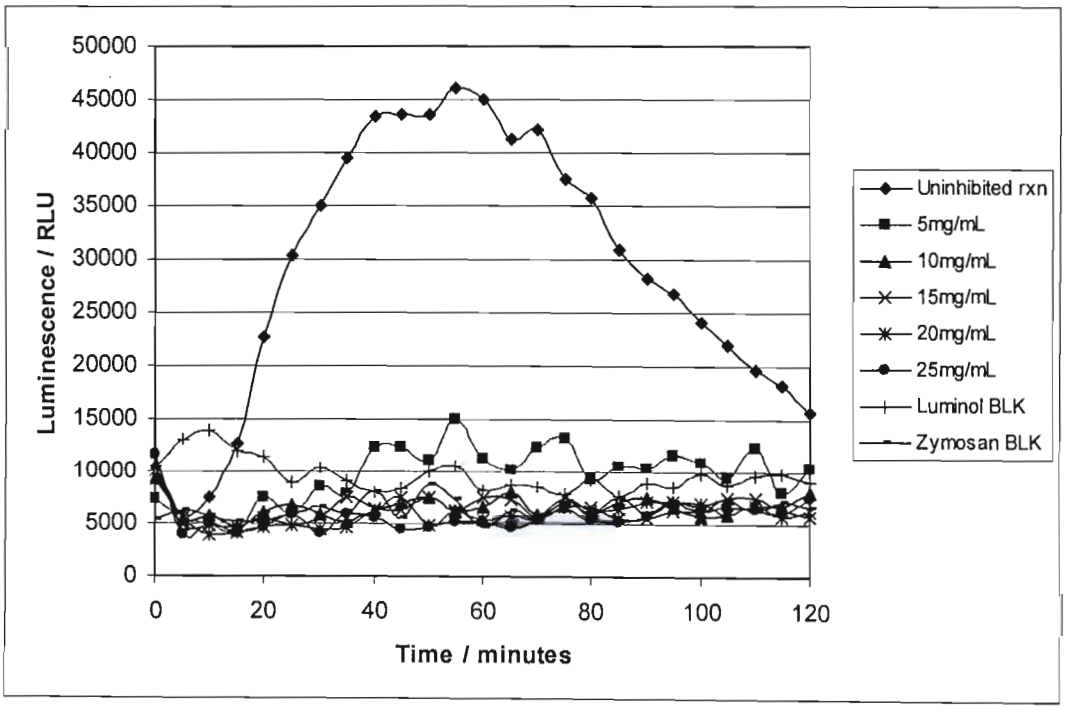

Figure 7.5: Graph illustrating the inhibition of chemiluminescence by diclofenac. 30µL of five different concentration of diclofenac solution were added to each well and compared with an uninhibited reaction. BLK = blank.

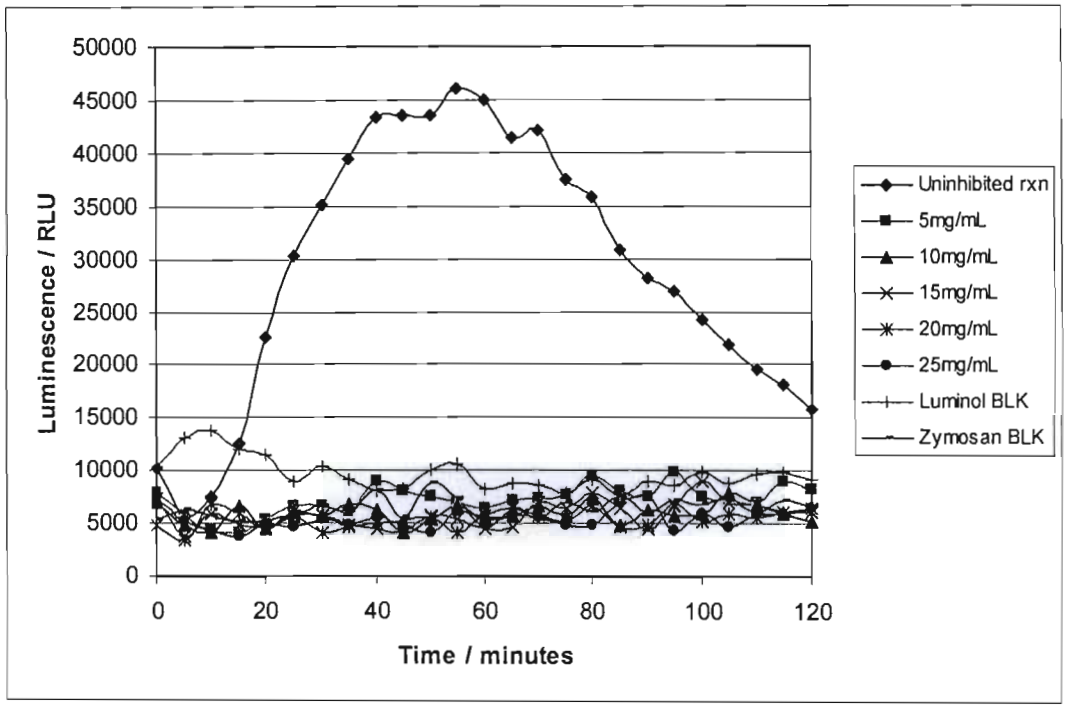

Figure 7.6: Graph illustrating the inhibition of chemiluminescence by diclofenac. 50µL of five different concentration of diclofenac solution were added to each well and compared with an uninhibited reaction. BLK = blank.

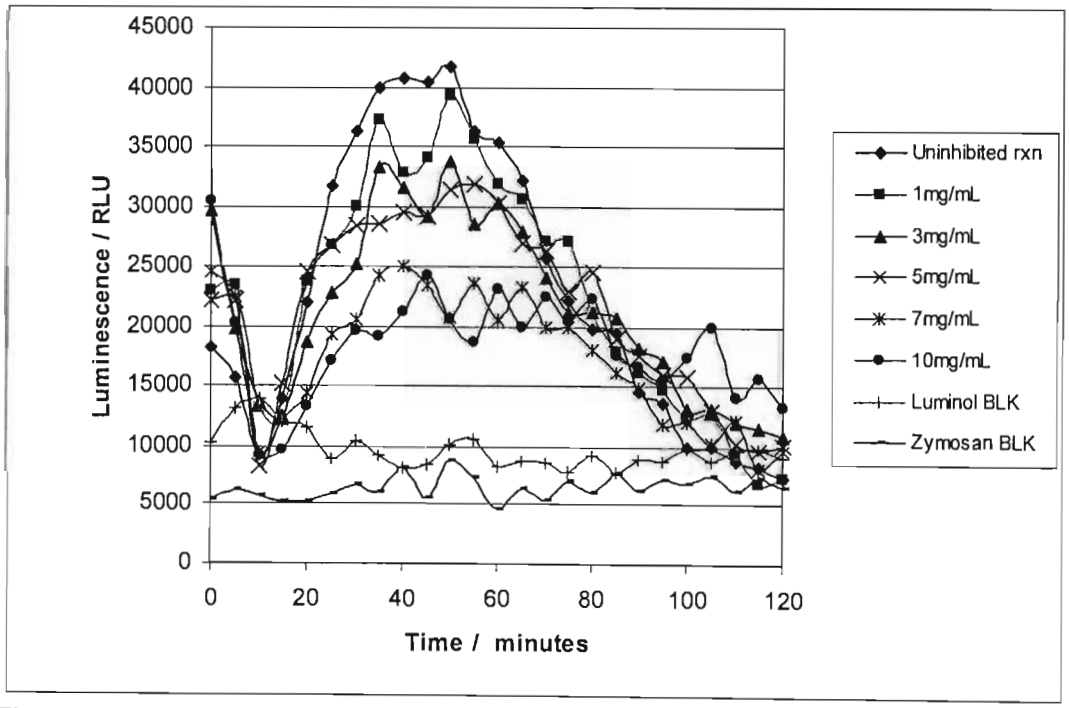

Figure 7.7: Graph illustrating the inhibition of chemiluminescence by meloxicam. 5µL of five different concentration of diclofenac solution were added to each well and compared with an uninhibited reaction. BLK = blank.

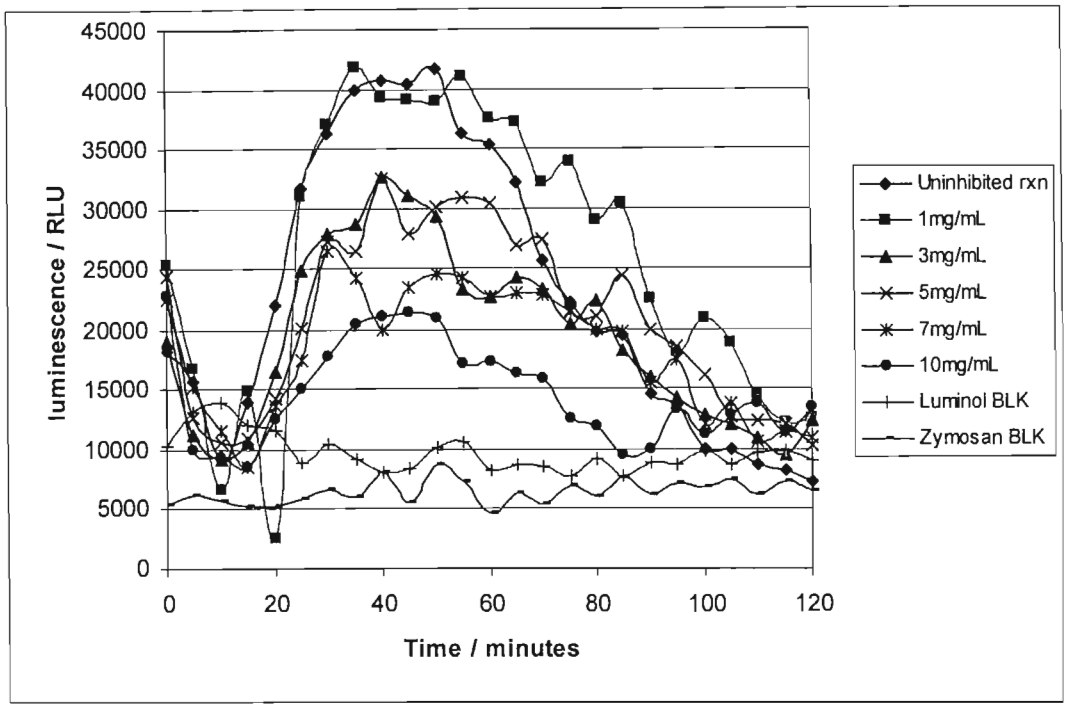

Figure 7.8: Graph illustrating the inhibition of chemiluminescence by meloxicam. 15µL of five different concentration of diclofenac solution were added to each well and compared with an uninhibited reaction. BLK = blank.

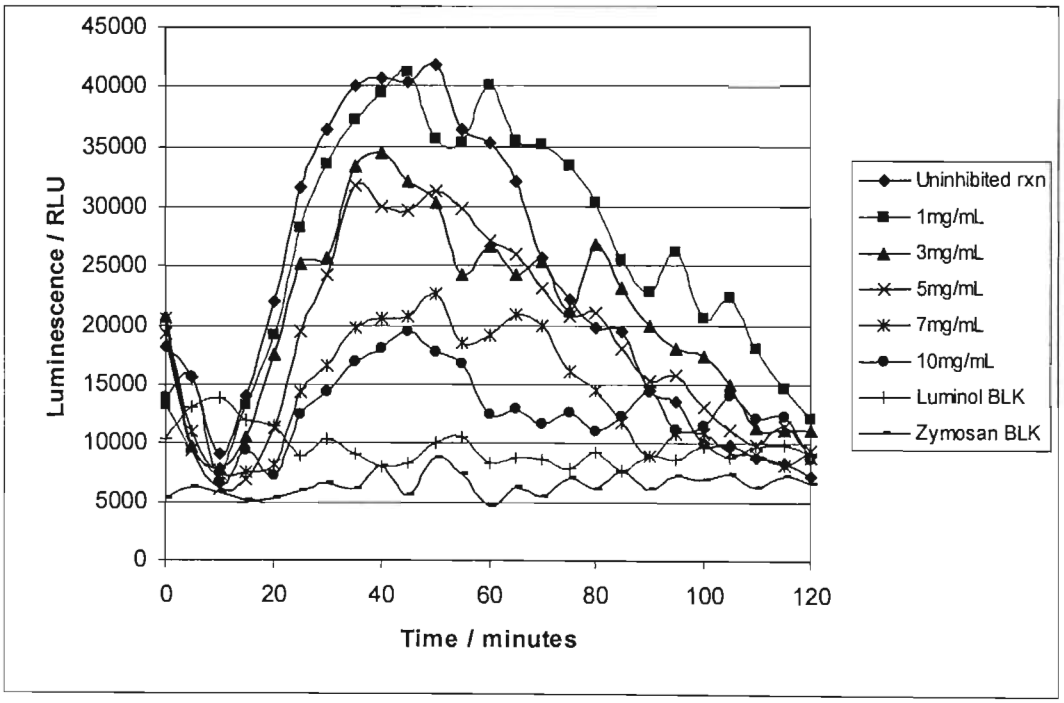

Figure 7.9: Graph illustrating the inhibition of chemiluminescence by meloxicam. 30µL of five different concentration of diclofenac solution were added to each well and compared with an uninhibited reaction. BLK = blank.

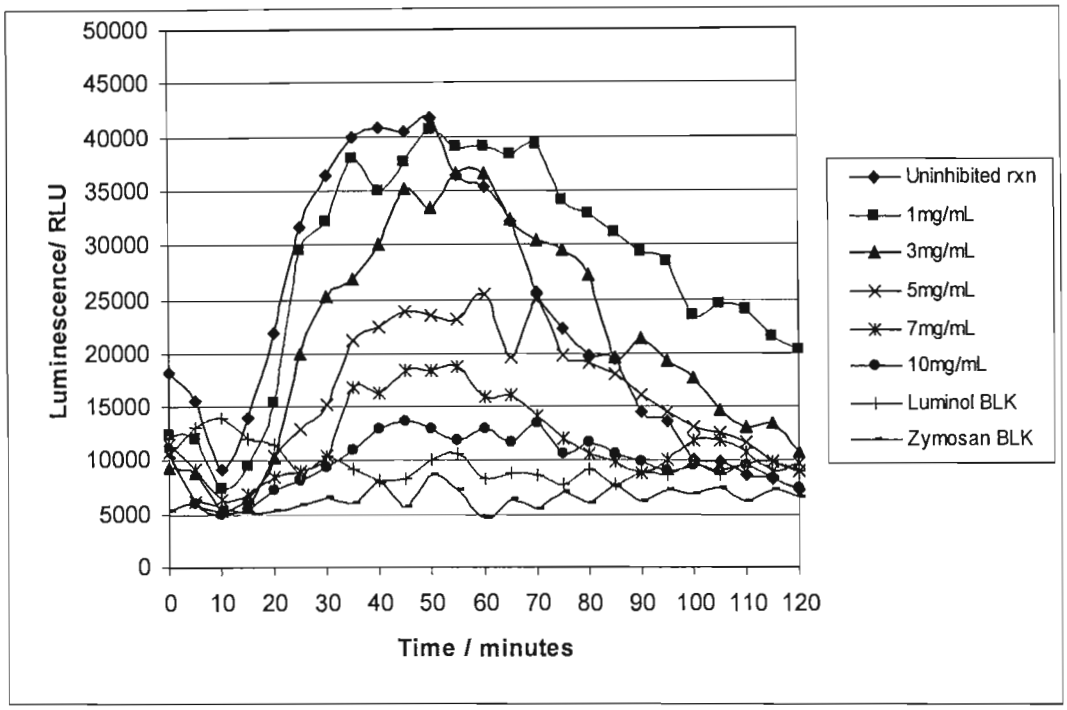

Figure 7.10: Graph illustrating the inhibition of chemiluminescence by meloxicam. 50µL of five different concentration of diclofenac solution were added to each well and compared with an uninhibited reaction. BLK = blank.

Overall, the above results clearly indicated that diclofenac had a greater capacity to inhibit chemiluminescence than meloxicam, with concentrations of 10mg/mL and above completely inhibiting the reaction, at volumes of only 15µL. Meloxicam, on the other hand, almost completely inhibited the production of chemiluminescence when 50µL at a concentration of 10mg/mL was added. To standardise volumes, it was decided that 50µL of both NSAIDs would be used at a concentration of 10mg/mL.

7.4. ANTI-INFLAMMATORY ACTIVITY OF ISOLATED HOMOISOFLAVANONES

Through the optimisation of the assay it was determined that the ideal reaction medium contained: 400µL cultured leukocyte solution; 100µL of 3mM luminol solution; and 50µL opsonized zymosan solution; background blanks were determined using either: leukocyte solution and opsonized zymosan, or leukocyte solution and luminol. Only two controls were used, with the positive controls containing 50µL of 10mg/mL NSAIDs added to the reaction medium, and the negative control containing only the reaction medium (leukocyte solution, luminol and zymosan). Different concentrations of the test compounds were assayed, with the volume of test compound being kept constant at 50µL. A concentration of 1mg/mL was used additionally for 4'-demethyl-3,9-dihydroeucomin (compound **3**) but not for the other compounds. At a concentration of 5mg/mL there was too great an inhibition of chemiluminescence for 4'-demethyl-3,9-dihydroeucomin (compound **3**), and therefore IC_{50} values could not be calculated when the minimum concentration used was 5mg/mL.

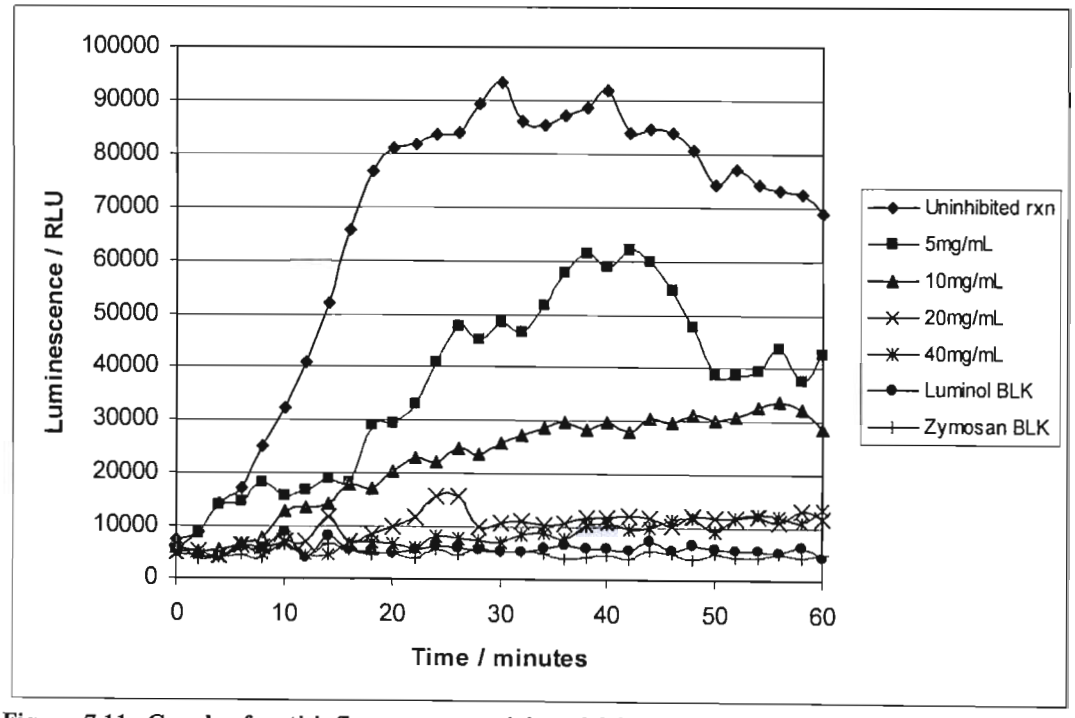

Figure 7.11: Graph of anti-inflammatory activity of 3,9-dihydroeucomin (compound 2) in the standardized assay system. 50µL of compound 2 at varying concentrations was added to each well. BLK = blank, rxn = reaction.

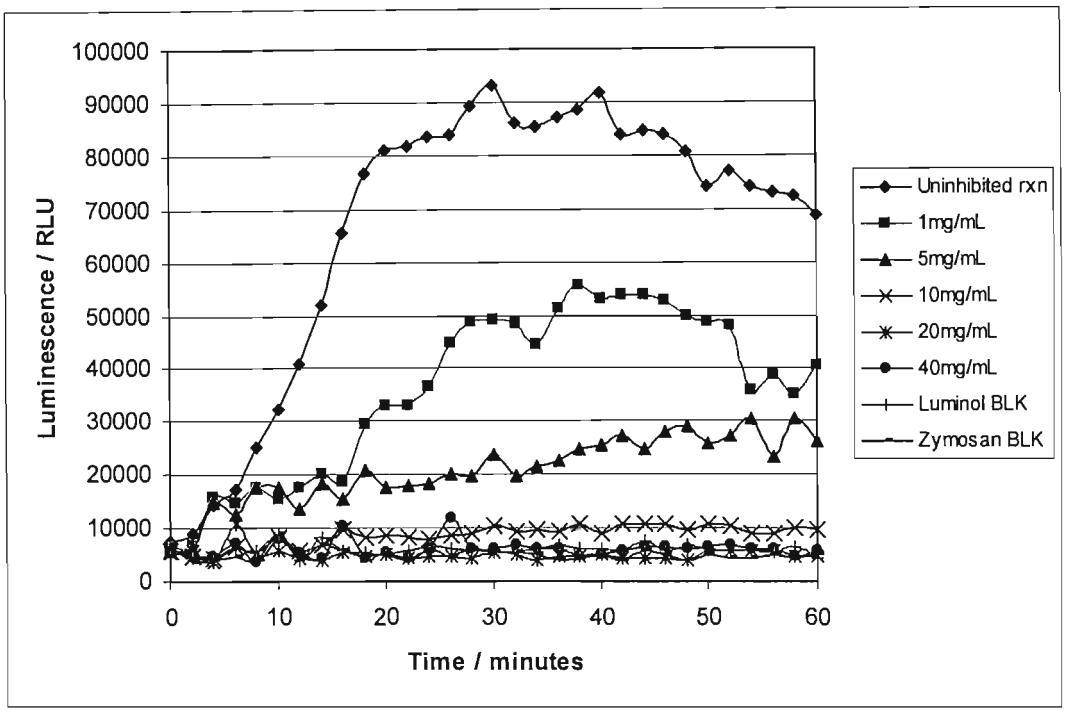

Figure 7.12: Graph of anti-inflammatory activity of 4'-demethyl-3,9-dihydroeucomin (compound 3) in the standardized assay system. 50μL of compound 3 at varying concentrations was added to each well. BLK = blank, rxn = reaction.

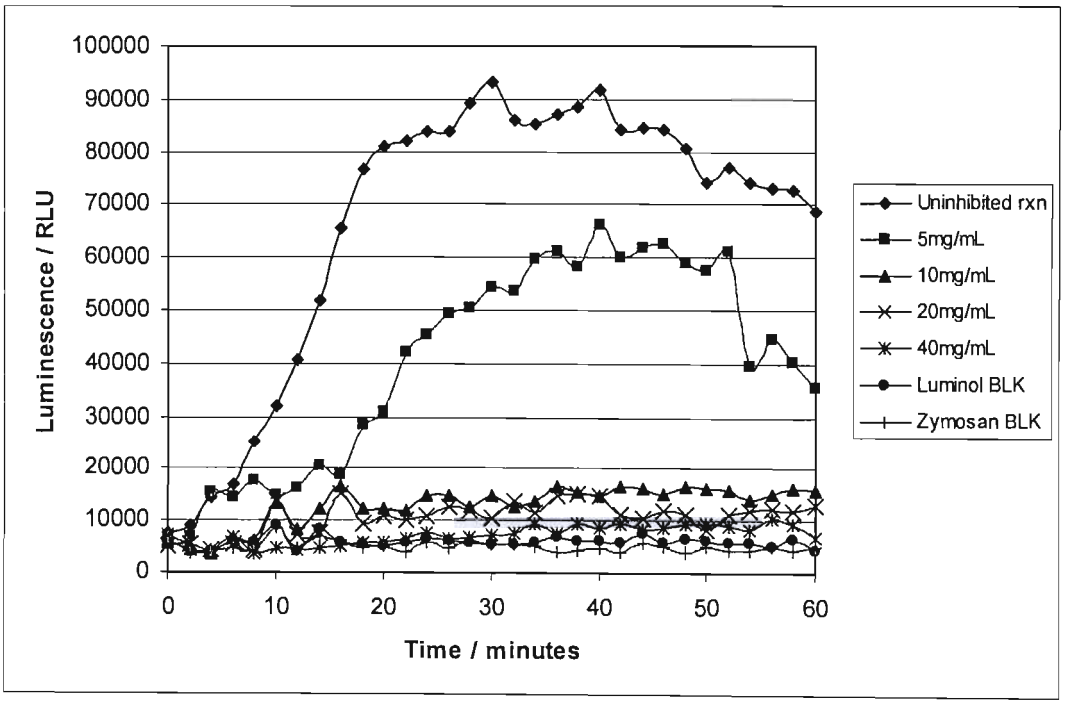

Figure 7.13: Graph of anti-inflammatory activity of 4'-demethyl-5-O-methyl-3,9-dihydroeucomin (compound 4) in the standardized assay system. 50μL of compound 4 at varying concentrations was added to each well. BLK = blank, rxn = reaction.

7.4.1. Calculation of IC_{50}

In order to make meaningful comparisons between the test compounds, IC_{50} values were determined using regression analysis of the data obtained in the assays. The IC_{50} values were defined as the concentration of compound that inhibited fifty percent of the luminescence. From the regression analysis, IC_{50} values were calculated as 14mg/mL, 7mg/mL, and 13mg/mL for 3,9-dihydroeucomin (compounds **2**), 4'-demethyl-3,9-dihydroeucomin (compound **3**) and 4'-demethyl-5-O-methyl-3,9-dihydroeucomin (compound **4**) respectively (structures given on page 63), and 1mg/mL for diclofenac, and 6mg/mL for meloxicam.

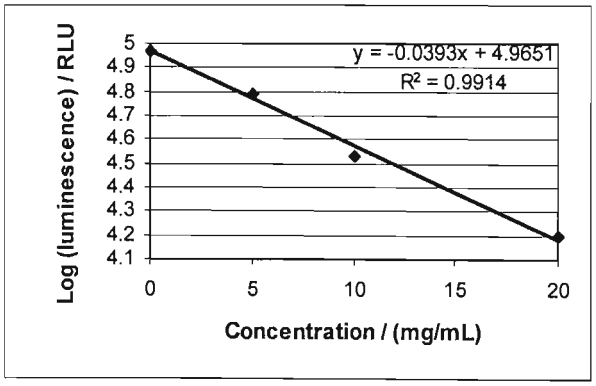

Figure 7.14: Calculation of IC_{50} for 3,9-dihydroeucomin (compound 2)

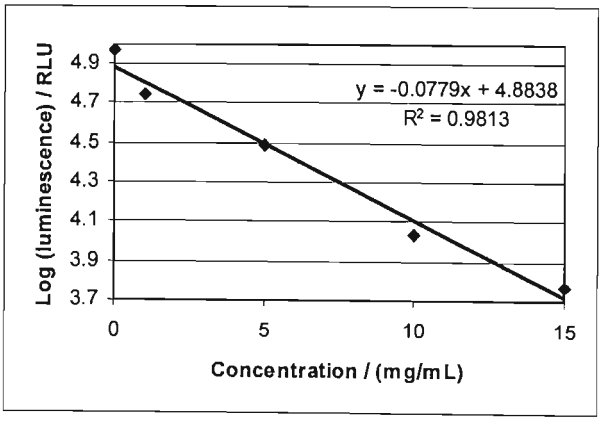

Figure 7.15: Calculation of IC_{50} for 4'-demethyl-3,9-dihydroeucomin (compound 3)

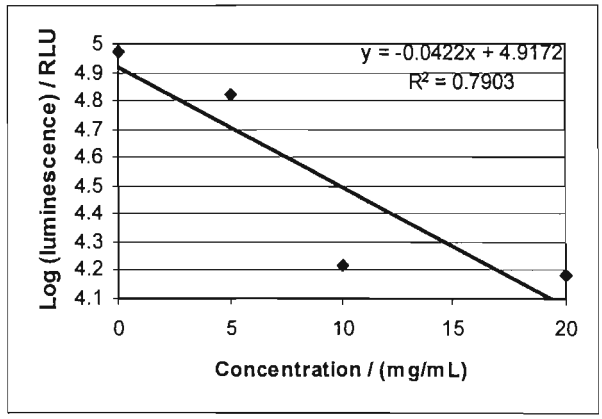

Figure 7.16: Calculation of IC_{50} for 4'-demethyl-5-O-methyl-3,9-dihydroeucomin (compound 4)

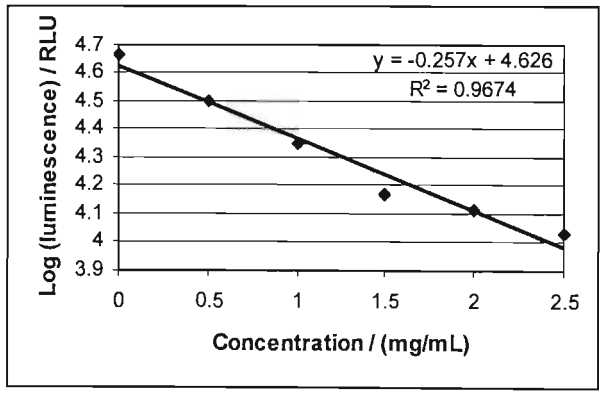

Figure 7.17 Calculation of IC_{50} for diclofenac

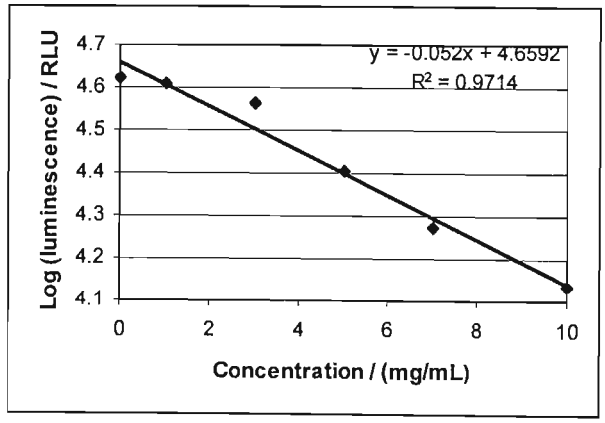

Figure 7.18: Calculation of IC_{50} meloxicam

7.5. ANTIOXIDANT/ FREE RADICAL SCAVENGING ACTIVITY OF ISOLATED HOMOISOFLAVANONES.

Antioxidant/ free radical scavenging activity was also investigated using a chemiluminescent method, similar to the one used for the screening of anti-inflammatory activity. Various concentrations of test compounds were used, with the volumes being fixed at 50μL to make direct comparisons with the anti-inflammatory results. The luminol concentration was also kept the same as that used in the anti-inflammatory assay.

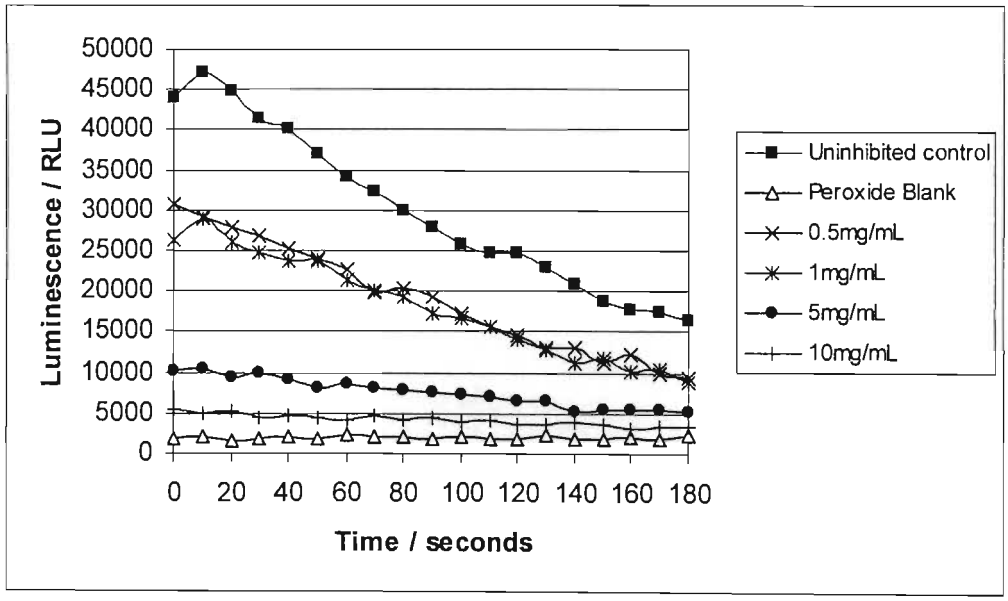

Figure 7.19: Results of antioxidant/ free radical scavenging activity of 3,9-dihydroeucomin (compound 2) at four concentrations using the luminol CL assay..

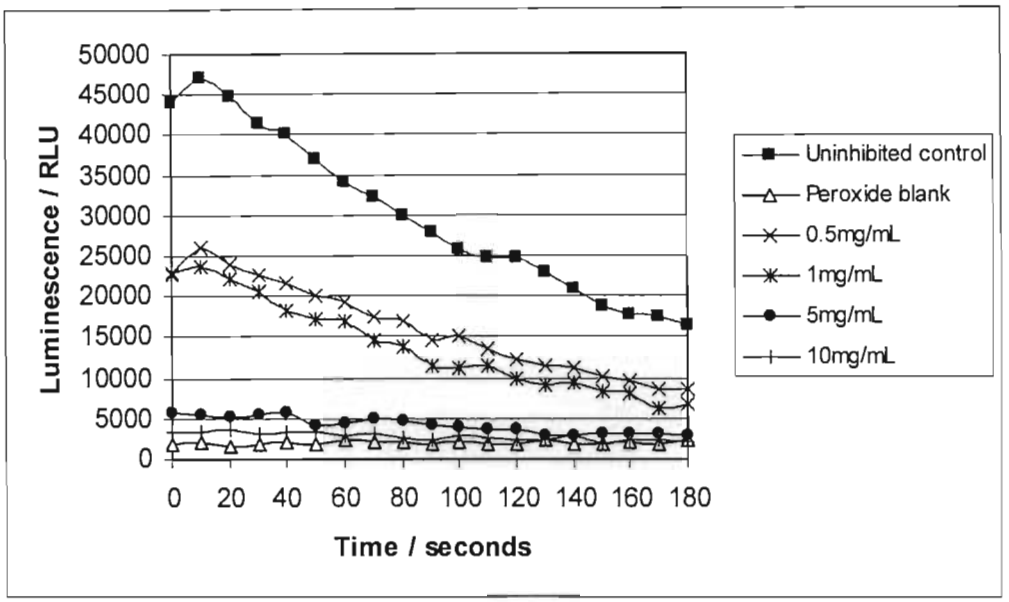

Figure 7.20: Results of antioxidant/ free radical scavenging activity of 4'-demethyl-3,9-dihydroeucomin (compound 3) at four concentrations using the luminol CL assay..

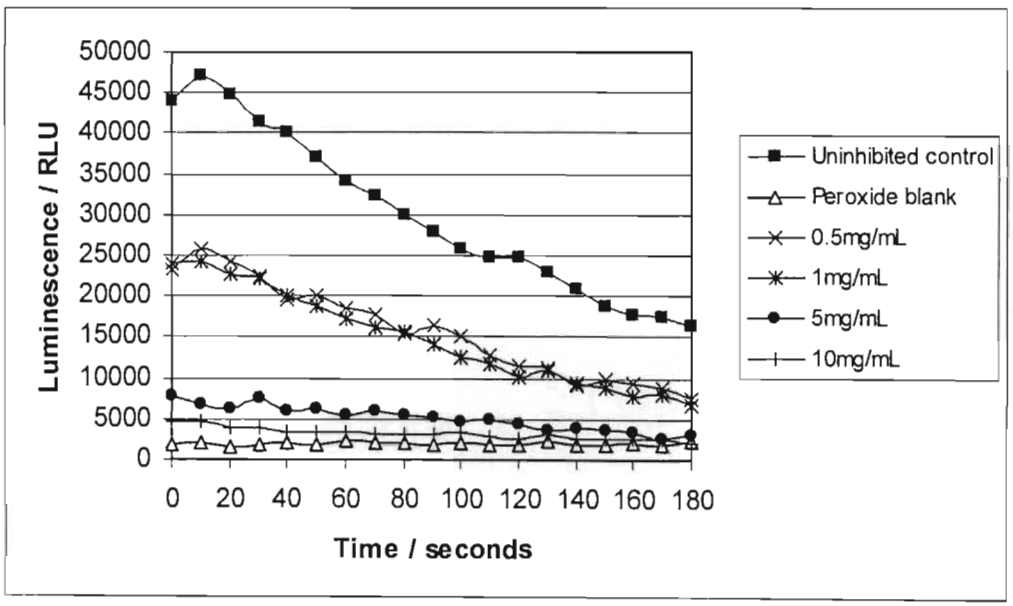

Figure 7.21: Results of antioxidant/ free radical scavenging activity of 4'-demethyl-5-O-methyl-3,9-dihydroeucomin (compound 4) at four concentrations using the luminol CL assay.

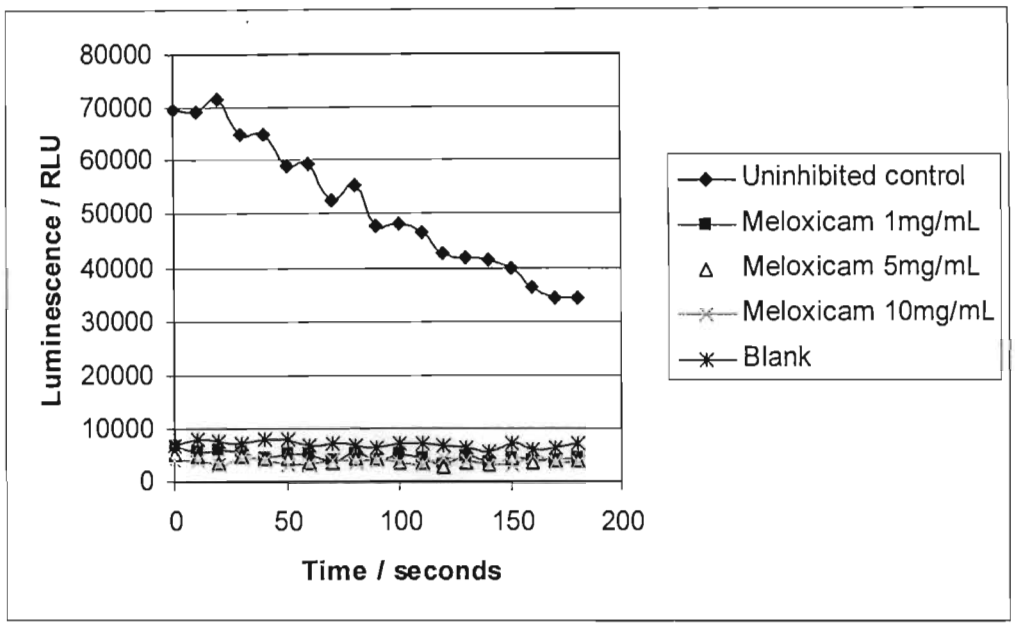

Figure 7.22: Results of antioxidant/ free radical scavenging activity of meloxicam at four concentrations using the luminol CL assay.

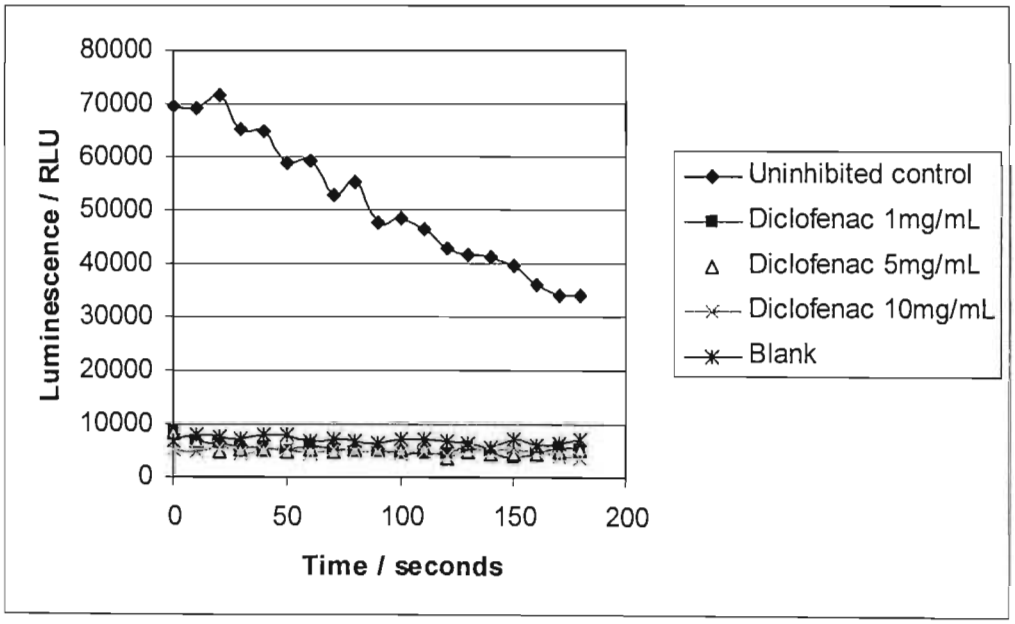

Figure 7.23: Results of antioxidant/ free radical scavenging activity of diclofenac at four concentrations using the luminol CL assay.

7.6. DISCUSSION

The testing of purified compounds is preferable to that of crude extract testing, as any positive results can be attributed solely to the compound. The screenings in this study tested the pure compounds only and showed that all three compounds displayed anti-inflammatory activity in the bioassay developed. 4'-Demethyl-3,9-dihydroeucomin (compound **3**) had the highest inhibitory effect, with an IC_{50} value of 7mg/mL, almost half that of the other two compounds (**Figures 7.14- 7.16**). These results compared favourably with the IC_{50} of meloxicam, which was 6mg/mL (50μL volume, 10mg/mL concentration). The other two compounds were less effective, with IC_{50} values being 14mg/mL and 13mg/mL for 3,9-dihydroeucomin (compound **2**) and 4'-demethyl-5-O-methyl-3,9-dihydroeucomin (compound **4**) respectively.

From the results, percentage inhibition of chemiluminescence was calculated for each compound using the following formula:

$$\% \text{ inhibition} = \left[1 - \left[\frac{(Lum_{compound} - Lum_{background})}{(Lum_{unhibited\ rxn} - Lum_{background})} \right] \right] \times 100$$

where the background luminescence (luminol blank) was subtracted from the maximum luminescence of the test compound, and this was then divided by the difference between the maximum luminescence of the uninhibited reaction and the luminescence of the background. Two of the compounds, 4'-demethyl-3,9-dihydroeucomin (compound **3**) and 4'-demethyl-5-O-methyl-3,9-dihydroeucomin (compound **4**), showed a very high percentage inhibition of the chemiluminescent reaction at concentrations of 10mg/mL, with 4'-demethyl-3,9-dihydroeucomin (compound **3**) having an inhibitory percent of 94% and 4'-demethyl-5-O-methyl-3,9-dihydroeucomin (compound **4**) being 88%. Compound **2**, 3,9-dihydroeucomin, had the lowest percent inhibition, at 71%. These results compared very favourably with the NSAID controls used, with diclofenac having 100% inhibition and meloxicam 90% inhibition of chemiluminescence at equivalent concentrations.

Table 7.1: Comparison of percentage inhibition of luminescence of the various compounds and controls in the anti-inflammatory assay.

Concentration	Compound 2	Compound 3	Compound 4	Diclofenac	Meloxicam
1mg/mL	-	43%	-	-	4%
5mg/mL	36%	72%	31%	99%	51%
10mg/mL	71%	94%	88%	100%	90%

Of the three test compounds, 4'-demethyl-3,9-dihydroeucomin (compound **3**) was the best inhibitor of the CL reaction, having a greater inhibitory effect than meloxicam. 4'-Demethyl-5-O-methyl-3,9-dihydroeucomin (compound **4**) also had a very high inhibitory effect on the CL reaction, with its percentage inhibition being only slightly lower than that of meloxicam. Of the three compounds, 3,9-dihydroeucomin (compound **2**) had the lowest inhibitory effect. Looking at the structures of the compounds, it appears that the presence of a hydroxyl group on the B-ring is of importance for the inhibition of the CL reaction, as both 4'-demethyl-3,9-dihydroeucomin (compound **3**) and 4'-demethyl-5-O-methyl-3,9-dihydroeucomin (compound **4**) had a hydroxyl substitution at the 4'-position, whilst 3,9-dihydroeucomin (compound **2**) did not. A higher number of hydroxyl groups also seemed to impart greater CL inhibitory effect, as could be seen by the trihydroxy substituted 4'-demethyl-3,9-dihydroeucomin (compound **3**) having the highest CL inhibitory capabilities.

In vitro studies on biological activity, although informative, do not however mimic the *in vivo* situation. *In vivo* there are numerous interacting factors that are incorporated, such as binding of compounds to proteins, enzyme inhibition/activation, and the presence of co-factors. These are factors that cannot be predicted from *in vitro* assays (Morrow and Roberts, 2001). Biological assays generally only screen for one type of activity, and the results can sometimes be misleading. Although this assay gave a good indication of anti-inflammatory activity, there is nonetheless the possibility of false positives. The assay depends on the oxidation of luminol by the ROS produced by the respiratory burst of leukocytes, but compounds that have good antioxidant/free radical scavenging activities could mimic the results of anti-inflammatory compounds. Even though they are not inhibiting the COX-1 or COX-2 enzymes, that are partly responsible for mediating the respiratory burst associated

with inflammation, they would produce results suggesting they were. For this reason it was decided to test the compounds for antioxidant/free radical scavenging activity.

The antioxidant/ free radical scavenging assay was performed in a solution designed to mimic the anti-inflammatory assay reaction system but without any leukocytes present in the assay wells. The solution was adjusted to contain similar concentrations of H_2O_2 as that would approximate to those released by the phagocytic burst. Luminol is susceptible to H_2O_2 oxidation, resulting in the formation of 3-aminophthalate, the light emitting species in the anti-inflammatory assay (Chasteen, 1995; Allen et al., 2000). In the presence of Fe^{2+} or Cu^{+}, H_2O_2 is readily reduced to hydroxyl radicals, with the transition metals serving as electron donors (Moslen, 1994). The H_2O_2 scavenging/peroxidative screening method developed by Baker *et al.* (1995) involves the use of horseradish peroxidase to catalyse the oxidation of luminol by H_2O_2. However, the presence of peroxidase might have introduced a further complicating factor in the assay system. It was therefore decided to utilize a purely inorganic reaction, with no enzymatic catalysts. The inorganic oxidation of luminol however requires an alkaline reaction medium and the presence of a catalyst (Chasteen, 1995). On the other hand, the anti-inflammatory assays were performed at biological pH, whilst this assay was performed under alkaline conditions, using Cu^{2+} as the catalyst for the reaction.

The results of the antioxidant/ free radical scavenging assay indicated that the positive anti-inflammatory results were at least partly due to antioxidant or free radical scavenging activity of the compounds, rather than inhibition of the COX-1 and COX-2 enzymes, as all the compounds exhibited high percentage inhibition of the luminescence reaction. The NSAIDs however also had very high antioxidant activities with almost all concentrations totally inhibiting the production of luminescence. The NSAIDs even inhibited background luminescence produced by the reaction medium and peroxide blank, to levels lower than that of the blanks.

Table 7.2: Comparison of percentage inhibition of luminescence of the various compounds and controls in the Antioxidant/ free radical scavenging assay.

Concentration	Compound 2	Compound 3	Compound 4	Diclofenac	Meloxicam
1mg/mL	41%	52%	51%	97%	100%
5mg/mL	82%	92%	87%	100%	100%
10mg/mL	92%	96%	94%	100%	100%

Antioxidant activity is of biological importance as unchecked ROS can cause cell damage. The plasma membrane of cells is one of the first targets of ROS, and any lipid peroxidation that occurs has particularly dangerous consequences. Lipid peroxidation does not occur as a once-off reaction but, rather, occurs as a chain reaction that results in the formation of conjugated dienes, lipid peroxyl radicals and hydroperoxides. The peroxyl radicals can further react with new lipid molecules, propagating the process further. The hydroperoxides can decompose forming secondary free radicals that can cause further peroxidative damage. Lipid peroxidation can also affect the activity and function of membrane bound proteins. Eventually, it results in changes in membrane permeability and can lead to the destruction of the whole cell (Krasowska *et al.*, 2000).

The antioxidant and free-radical scavenging activity of flavonoids has been well-documented (Rice-Evans *et al.*, 1996; Cos *et al.*, 1998), but to date not much research has been conducted on the antioxidant activity homoisoflavonoids. Phenolic compounds have been shown to be natural antioxidants and free-radical scavengers, and there are two possible reducing pathways (Trouillas *et al.*, 2006):

1. H-transfer from the molecule to the radical via direct O-H bond breaking:
   $ROH + OH^{\cdot} \rightarrow RO^{\cdot} + HOH$
2. Electron transfer from the molecule to the radical resulting in direct H-abstraction:
   $ROH + OH^{\cdot} \rightarrow ROH^{+\cdot} + OH^{-} \rightarrow RO^{\cdot} + HOH.$

For compounds to have antioxidant activity, the above reactions must be thermodynamically favourable in the sense that the removal a hydrogen atom from ROH occurs more readily than from HOH, and the resulting radical ($RO^{\cdot}$) must be

relatively stable so that it only reacts slowly with neighbouring molecules without adding to oxidative stress (Trouillas *et al.*, 2006).

Of all the naturally occurring phenolic antioxidants, it has been shown that the flavonoid family is the most important. Studies on flavonoid antioxidant activity have shown that the B-ring of flavonoids is the most important in terms of structure-function relationships, as it is readily performs H-transfers, and consequently has antioxidant capacity. This is particularly true when the B-ring is a catechol moiety (Cos *et al.*, 1998; Trouillas *et al.*, 2006). The A-ring seems to be less important in terms of antioxidant activity, but the presence of an ortho-dihydroxy structure in the A- or B-rings leads to greater antioxidant activity (Wagner, 1989). A 2,3-double bond contributes to antioxidant activity as it ensures π-electron delocalisation between the B- and C-rings, which contributes to the stability of the resultant radical after H-abstraction. The presence of a 3-OH group also adds to antioxidant activity, although the effectiveness of this group depends somewhat on the presence of the 2,3-double bond and the 4-carbonyl group (Trouillas *et al.*, 2006).

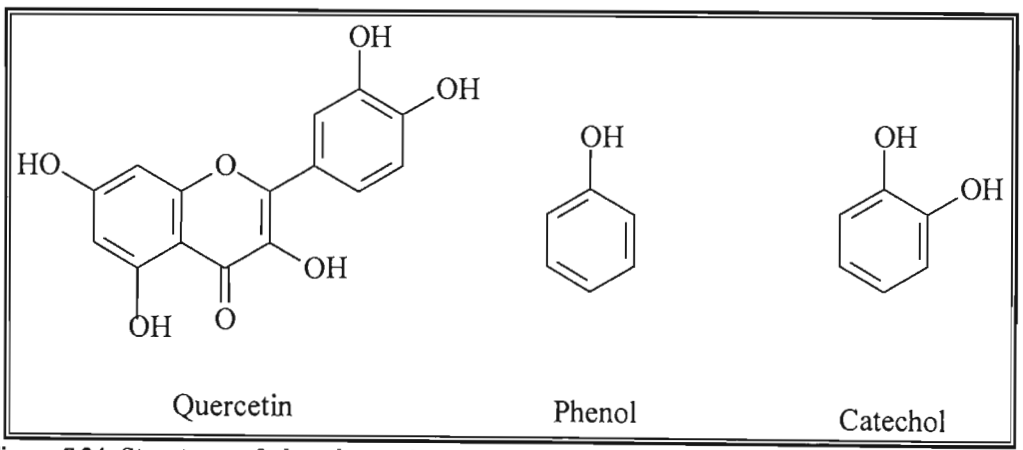

Figure 7.24: Structures of phenol, catechol and quercetin, a flavonoid with good antioxidant activity

Homoisoflavonoids are structurally very similar to flavonoids, but one of the main differences is the C-9 bridge between the B-ring and the chromanone fragment, and thus similar structure-function activities would be expected between flavonoids and homoisoflavonoids. 4'-Demethyl-3,9-dihydroeucomin (compound **3**) and 4'-demethyl-5-O-methyl-3,9-dihydroeucomin (compound **4**) both had a B-ring which was a phenol moiety, suggesting good antioxidant activity, which was confirmed by the bioassays, whereas 3,9-dihydroeucomin (compound **2**), did not have a phenolic B-

ring, and displayed poorer antioxidant activity. In both the anti-inflammatory and antioxidant assays, 4'-demethyl-3,9-dihydroeucomin (compound **3**) had the highest levels of inhibition and lowest IC_{50} values. Although it does not have an ortho-dihydroxy substitution on the A-ring, it is meta-dihydroxy substituted and the additional hydroxy group could be a possible contributing factor to its higher anti-inflammatory and antioxidant activity. Following the theoretical structure-function relationships with regard to antioxidant activity, the ranking of the test compounds should place 4'-demethyl-3,9-dihydroeucomin (compound **3**) as having the highest activity, as it has a phenolic moiety B-ring and has dihydroxy substitution on the A-ring. 4'-Demethyl-5-O-methyl-3,9-dihydroeucomin (compound **4**) with its phenolic B-ring moiety and single C-7 hydroxy group should hypothetically have the second-best antioxidant activity, and 3,9-dihydroeucomin (compound **2**), which does not have a phenolic B-ring, should exhibit the lowest antioxidant activity, as indeed was the case, although there was not sufficient variation to be signify a definite trend.

It is suggested that other anti-inflammatory assays of these compounds be performed to obtain a better understanding of the complex nature of the inflammatory response and possible levels of interaction. COX-1 and COX-2 inhibitory assays such as those of White and Glassman (1974), and Noreen *et al.* (1998), which analyse the conversion of ^{14}C-arachidonic acid into prostaglandins through the actions of COX-1 and COX-2, would indicate whether the compounds were inhibiting the enzymes responsible for mediating inflammation, or if they were acting purely as antioxidants. Previous work on several *Eucomis* species by Taylor and Van Staden (2001, 2002) showed that the crude ethanolic bulb extracts from *E. comosa-punctata*, *E. humulis*, and *E. pole-evansii* produced high COX-1 and COX-2 inhibitory activity at concentrations of 250μg/mL. Pure homoisoflavonoid analysis by du Toit (2004) of compounds from *E. comosa* and *E. pole-evansii* however did not agree with these results, with the compounds only having a moderate inhibitory effect. This clearly indicates the potential pitfalls of using crude extracts in bioassays.

Due to structural similarities of homoisoflavonoids and flavonoids, and the high antioxidant activity of flavonoids, further investigations in the antioxidant activity of these compounds should also be performed. Previous work by Siddaiah *et al.* (2006) showed that some homoisoflavonoids, such as 5,7-dihydroxy-3[(3',4',5'-

trihydroxyphenyl)methylene]-4-chromanone had very high antioxidant activity (IC_{50} 6.5μM), higher than that of important biological antioxidants such as ascorbic acid (IC_{50} 852μM) and tocopherol (IC_{50} 726μM). In view of the possible importance of antioxidants in the prevention of degenerative diseases such as cancer, Alzheimer's, Parkinson's and cardiovascular disease, the potential of dietary antioxidants from plant sources should be thoroughly investigated.

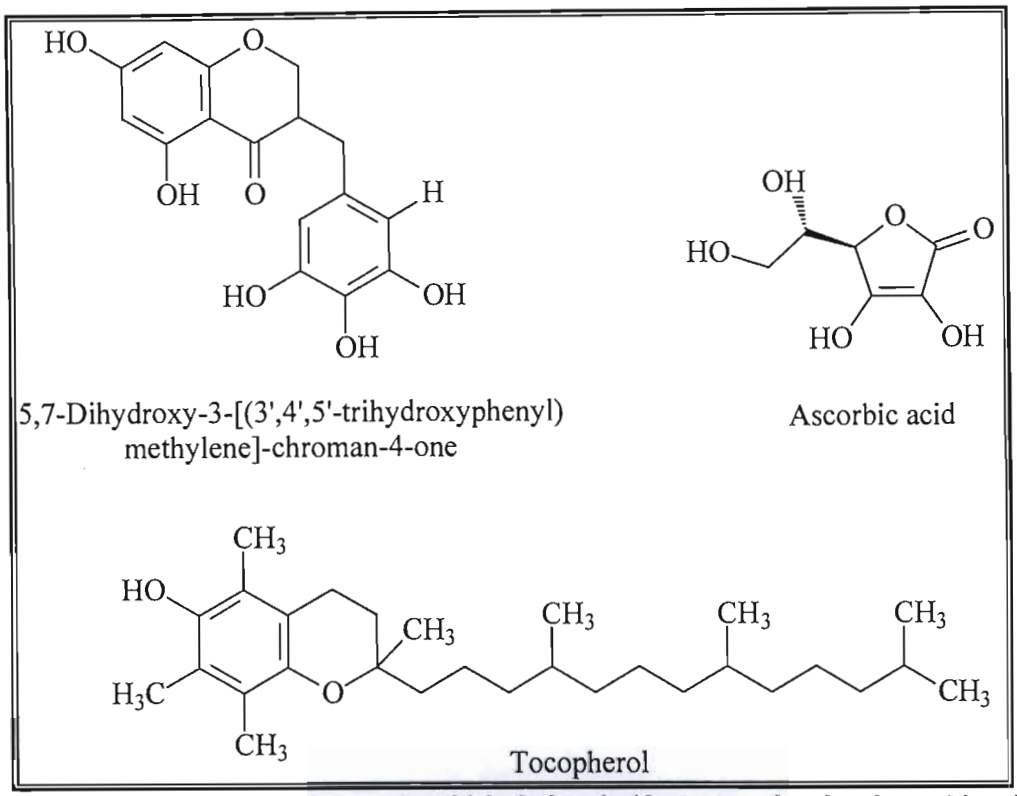

Figure 7.25: Structures of two important biological antioxidants, tocopherol and ascorbic acid, and 5,7-dihydroxy-3[(3',4',5'-trihydroxyphenyl)methylene]-4-chromanone, a homoisoflavanone with high antioxidant activity.

Although *Eucomis montana* has not been previously reported as having ethnomedicinal uses, *Eucomis* species are widely used by the Southern Sotho, Tswana, Xhosa and Zulu people for the treatment of pain and inflammation (Hutchings and Terblanche, 1989). *Eucomis comosa* has also been reported as being used as an anti-rheumatic agent (Hutchings, 1996). The anti-inflammatory/antioxidant activity of the homo-isoflavonoids isolated in this study from *Eucomis montana* seems to validate the ethnomedicinal usage of *Eucomis* species in the treatment of pain, inflammation and rheumatism.

REFERENCES

Allen R.C, Dale D.C, and Taylor F.B, 2000. Blood phagocyte luminescence: gauging systemic immune activation. *Methods in Enzymology*, **305**, 591-629.

Baker C.J, Harmon G.L, Glazner J.A, and Orlandi E.W, 1995. A non-invasive technique for monitoring peroxidative and H_2O_2-scavenging activities during interactions between bacterial plant pathogens and suspension cell. *Plant physiology*, **108**, 353-359.

Boyum A, 1984. Separation of lymphocytes, granulocytes and monocytes from human blood using iodinated density gradient media. *Methods in Enzymology*, **108**, 88-102.

Chasteen T, 1995. The chemiluminescence of luminol and bis(2,4,5-trichlorphenyl)oxalate (TCPO). Found at: www.shsu.edu/~chm_tgc/JPPdir/JPP1999. Accessed November 2004.

Cos L, Ying M, Hu J.P, Cimanga K, and Van Poel B, 1998. Structure-activity relationships and classification of flavonoids as inhibitors of xanthine oxidase and superoxide scavengers. *Journal of Natural Products*, **61**, 71-76.

du Toit K, 2004. *A phytochemical investigation of members of the Hyacinthaceae family and biological screening of homoisoflavanones and structurally related compounds*. University of KwaZulu-Natal, PhD thesis, pp 127-152.

Hutchings A and Terblanche S, 1989. Observations on the use of some known and suspected toxic Liliflorae in Zulu and Xhosa medicine. *South African Medical Journal*, **75**, 62-69.

Hutchings A, 1996. *Zulu medicinal plants: an inventory*. University of Natal Press, Pietermarizburg, pp 242.

Krasowska A, Rosiak D, Szkapiak K, and Lukaszewcz M, 2000. Chemiluminescence detection of peroxyl radicals and comparison of antioxidant activity of phenolic compounds. *Current Topics in Biophysics*, **24**, 89-95.

Morrow J and Roberts, L, 2001. Lipid-derived autacoids. In: *The pharmacological basis of therapeutics, 10th edition*. Eds: Hardman J.G and Limbird L.E. McGaw-Hill, New York, pp 687-733.

Moslen M.T, 1994. Reactive oxygen species in normal physiology, cell injury and phagocytosis. In: *Free radicals in diagnostic medicine*. Ed: Armstrong D. Plenum Press, New York, pp 17-27.

National Referral Laboratory for Lysomal, Peroxisomal and Related Genetic Disorders of the University of Adelaide, 2005. Found at: www.health.adelaide.edu.au/NRL/methods2.htm. Accessed February 2005.

Noreen Y, Ringbom T, Perera P, Danielson H, and Bohlin L, 1998. Development of a radiochemical cyclooxygenase-1 and –2 *in vitro* assay, for identification of natural

products as inhibitors of prostaglandin biosynthesis. *Journal of Natural Products*, **61**, 2-7.
Rice-Evans C.A, Miller N.J, and Paganga G, 1996. Structure-antioxidant activity relationships of flavonoids and phenolic acids. *Free Radical Biology and Medicine*, **20**, 933-956.

Siddaiah V, Venkata Rao C, Venkateswarlu S, Krishnaraju A.V, and Subbaraju G.V, 2006. Synthesis, stereochemical assignments, and biological activities of homoisoflavonoids. *Bioorganic and Medicinal Chemistry*, **14**, 2545-2551.

Taylor J.L.S and Van Staden J, 2001. COX-1 inhibitory activity in extracts from *Eucomis* L'Herit. species. *Journal of Ethnopharmacology*, **75**, 257-265.

Taylor J.L.S and Van Staden J, 2002. COX-1 and COX-2 inhibitory activity in extracts prepared from *Eucomis* species, with reference to extracts from *E. autumnalis autumnalis*. *South African Journal of Botany*, **68**, 80-85.

Tosi M.F and Hamedani A, 1992. A rapid, specific assay for superoxide release from phagocytes in small volumes of whole blood. *American Journal of Clinical Pathology*, **97**, 566-573.

Trouillas P, Marsal P, Siri D, Lazzaroni R, and Duroux J-L, 2006. A DFT study on the reactivity of OH groups in quercetin and taxifolin antioxidants: The specificity of the 3-OH site. *Food Chemistry*, **97**, 679-688.

Van Dyke K and Van Dyke C, 1986. Cellular Chemiluminescence associated with disease states. *Methods in Enzymology*, **133**, 493-507.

Wagner H, 1989. Search for new plant constituents with potential antiphlogistic and antiallergic activity. *Planta Medica*, **55**, 235-241.

White H.L and Glassman A.T, 1974. A simple radiochemical assay for prostaglandin synthetase. *Prostaglandins*, **7**, 123-129.

CHAPTER 8: SUMMARY AND CONCLUSIONS

The research presented in this study had two aims: to isolate and characterize pure compounds from medicinal plants; and to set up suitable screens whereby these compounds could be tested for biological activity. The first aim involved a phytochemical investigation of two South African plants: *Strophanthus speciosus* and *Eucomis montana*. One cardenolide, neritaloside (compound **1**), was isolated in *Strophanthus speciosus*, and three homoisoflavonoids, 3,9-dihydroeucomin, 4'-demethyl-3,9-dihydroeucomin, and 4'-demethyl-5-O-methyl-3,9-dihydroeucomin (compounds **2-4** respectively) were isolated in *Eucomis montana*. All the compounds have been isolated previously, although the cardenolide, neritaloside, has not previously been reported to have been isolated in *Strophanthus speciosus*.

This study also focused on the screening of the isolated compounds for anti-inflammatory activity. A chemiluminescent screen for anti-inflammatory activity was used, as the bioassay afforded a high-throughput, cost effective method for screening compounds for anti-inflammatory activity. The three homoisoflavonoids were screened for anti-inflammatory activity as the genus *Eucomis* have been reportedly used for the treatment of inflammatory diseases, and homoisoflavonoids have been reported as having anti-inflammatory activity. All three of the compounds exhibited good anti-inflammatory activity against the bioassay, with 4'-demethyl-3,9-dihydroeucomin (compound **3**) having an IC_{50} value of 7mg/mL, which compared favourably to that of the NSAID meloxicam's value of 6mg/mL. The cardenolide was not tested for biological activity, as the amount isolated was too small to be put through the muscle relaxant assay for which it was intended.

Due to the possibility of false positive results that could be produced by compounds that had good antioxidant/free-radical scavenging activity, an antioxidant/free radical scavenging screen was developed that would indicate whether the compounds were in fact inhibiting the COX enzymes responsible for mediating an inflammation reaction, or rather scavenging the ROS produced by the anti-inflammatory screen. All three of the compounds showed a very high antioxidant/free radical scavenging activity, but as the

control NSAIDs also had high activity in this screen, a definitive anti-inflammatory or antioxidant/free radical scavenging mode of action of the compounds could not be assigned.

To better quantify the anti-inflammatory activity of the compounds, further biological screening needs to be performed. An anti-inflammatory screen that specifically targets the inhibition of the COX enzymes would provide greater insight into the anti-inflammatory activity of the compounds. The chemiluminescent screen used in this research is not however without merit, as it is rapid, reproducible, has a high throughput, and is cost effective, and as such provides a quick method to provisionally screen compounds for anti-inflammatory activity. Compounds that show high levels of chemiluminescence inhibition could then be further screened specifically for COX inhibitory activity.

The high levels of antioxidant/free radical scavenging activity of the homoisoflavonoids are very important as well. ROS play important roles in degenerative diseases such as cancer, Alzheimer's, Parkinson's, and cardiovascular disease, and therefore cheap, effective sources of antioxidants are of importance.

This study provides directions for further investigation, be it further investigation into the anti-inflammatory activity of homoisoflavonoids; or research into the antioxidant/free radical scavenging activity of homoisoflavonoids, as to date very few studies in this direction have been conducted. This study also highlights the importance of an interdisciplinary approach when investigating plants for potential medicinal compounds.

APPENDIX

PAGE

TABLE OF CONTENTS 135

COMPOUND 1: NERITALOSIDE

Spectrum 1a: ^{1}H NMR spectrum of compound **1** ($CDCl_3$) 141

Spectrum 1b:^{13}C NMR spectrum of compound **1** ($CDCl_3$) 142

Spectrum 1c: HSQC spectrum of compound **1** 143

Spectrum 1d: HMBC spectrum of compound **1** 144

Spectrum 1e: COSY spectrum of compound **1** 145

Spectrum 1f: NOESY spectrum of compound **1** 146

Spectrum 1g: Mass spectrum of compound **1** 147

Spectrum 1h: UV spectrum of compound **1** 148

Spectrum 1i: IR spectrum of compound **1** 148

Spectrum 1j: DEPT spectrum of compound **1** 149

COMPOUND 2: 3,9-DIHYDROEUCOMIN

Spectrum 2a: ^{1}H NMR spectrum of compound **2** ($CDCl_3$) 150

Spectrum 2b:^{13}C NMR spectrum of compound **2** $CDCl_3$) 151

Spectrum 2c: HSQC spectrum of compound **2** 152

Spectrum 2d: HMBC spectrum of compound **2** 153

Spectrum 2e: COSY spectrum of compound **2** 154

Spectrum 2f: NOESY spectrum of compound **2** 155

Spectrum 2g: Mass spectrum of compound **2** 156

Spectrum 2h: UV spectrum + UV (+NaOAc) spectrum of compound **2** 157

Spectrum 2i: UV spectrum + UV (+$AlCl_3$) spectrum of compound **2** 157

Spectrum 2j: IR spectrum of compound **2** 158

COMPOUND 3: 4'-DEMETHYL-3,9-DIHYDROEUCOMIN

Spectrum 3a: ^{1}H NMR spectrum of compound **3** ($CDCl_3$) 159

Spectrum 3b:^{13}C NMR spectrum of compound **3** ($CDCl_3$) 160

Spectrum 3c: HSQC spectrum of compound **3** 161

Spectrum 3d: HMBC spectrum of compound **3** 162

Spectrum 3e: COSY spectrum of compound **3** 163

Spectrum 3f: NOESY spectrum of compound **3** 164

Spectrum 3g: Mass spectrum of compound **3** 165

Spectrum 3h: UV spectrum + UV (+NaOAc) spectrum of compound **3** 166

Spectrum 3i: UV spectrum + UV (+$AlCl_3$) spectrum of compound **3** 166

Spectrum 3j: IR spectrum of compound **3** 167

COMPOUND 4: 4'-DEMETHYL-5-O-METHYL-3,9-DIHYDROEUCOMIN

Spectrum 4a: ^{1}H NMR spectrum of compound **4** ($CDCl_3$) 168

Spectrum 4b:^{13}C NMR spectrum of compound **4** ($CDCl_3$) 169

Spectrum 4c: HSQC spectrum of compound **4** 170

Spectrum 4d: HMBC spectrum of compound **4** 171

Spectrum 4e: COSY spectrum of compound **4** 172

Spectrum 4f: NOESY spectrum of compound **4** 173

Spectrum 4g: Mass spectrum of compound **4** 174

Spectrum 4h: UV spectrum +UV (+NaOAc) spectrum of compound **4** 175

Spectrum 4i: UV spectrum + UV (+$AlCl_3$) spectrum of compound **4** 175

Spectrum 4j: Infrared spectrum of compound **4** 176

Spectrum 4k: ^{1}H NMR spectrum of compound **4** (CD_3OD) 177

Spectrum 4l: ^{13}C NMR spectrum of compound **4** (CD_3OD) 178

GRAPHS SHOWING STANDARD DEVIATION

Graph 1: Graph of varying concentrations of luminol solution. Volume of blood cells and opsonized zymosan stimulant were kept constant at 400uL and 100uL respectively, 1mM luminol solution 179

Graph 2: Graph of varying concentrations of luminol solution. Volume of blood cells and opsonized zymosan stimulant were kept constant at 400uL and 100uL respectively, 3mM luminol solution 179

Graph 3: Graph of varying concentrations of luminol solution. Volume of blood cells and opsonized zymosan stimulant were kept constant at 400uL and 100uL respectively, 5mM luminol solution 180

Graph 4: Graph of varying concentrations of luminol solution. Volume of blood cells and opsonized zymosan stimulant were kept constant at 400uL and 100uL respectively, 12mM luminol solution 180

Graph 5: Graph of varying volumes of luminol solution, opsonized zymosan, and blood cells. 400μL blood cells, 50μL luminol, 50μL zymosan 181

Graph 6: Graph of varying volumes of luminol solution, opsonized zymosan, and blood cells. 400μL blood cells, 100μL luminol, 50μL zymosan 181

Graph 7: Graph of varying volumes of luminol solution, opsonized zymosan, and blood cells. 400μL blood cells, 100μL luminol, 100μL zymosan 182

Graph 8: Graph of varying volumes of luminol solution, opsonized zymosan, and blood cells. 500μL blood cells, 50μL luminol, 50μL zymosan 182

Graph 9: Graph of varying volumes of luminol solution, opsonized zymosan, and blood cells. 500μL blood cells, 100μL luminol, 50μL zymosan 183

Graph 10: Graph of varying volumes of luminol solution, opsonized zymosan, and blood cells. 500μL blood cells, 100μL luminol, 100μL zymosan 183

Graph 11: Graph of anti-inflammatory activity of compound 2. 50μL of compound 2 at 5mg/mL concentration was added 184

Graph 12: Graph of anti-inflammatory activity of compound 2. 50μL of compound 2 at 10mg/mL concentration was added 184

Graph 13: Graph of anti-inflammatory activity of compound 2. 50μL of compound 2 at 20mg/mL concentration was added 185

Graph 14: Graph of anti-inflammatory activity of compound 2. 50μL of compound 2 at 40mg/mL concentration was added 185

Graph 15: Graph of anti-inflammatory activity of compound 3. 50μL of compound 3at 1mg/mL concentration was added 186

Graph 16: Graph of anti-inflammatory activity of compound 3. 50μL of compound 3at 5mg/mL concentration was added 186

Graph 17: Graph of anti-inflammatory activity of compound 3. 50μL of compound 3at 10mg/mL concentration was added 187

Graph 18: Graph of anti-inflammatory activity of compound 3. 50μL of compound 3at 20mg/mL concentration was added 187

Graph 19: Graph of anti-inflammatory activity of compound 3. 50μL of compound 3at 40mg/mL concentration was added 188

Graph 20: Graph of anti-inflammatory activity of compound 4. 50μL of compound 4at 5mg/mL concentration was added 188

Graph 21: Graph of anti-inflammatory activity of compound 4. 50μL of compound 4at 10mg/mL concentration was added 189

Graph 22: Graph of anti-inflammatory activity of compound 4. 50μL of compound 4at 20mg/mL concentration was added 189

Graph 23: Graph of anti-inflammatory activity of compound 4. 50μL of compound 4at 40mg/mL concentration was added 190

Graph 24: Results of Antioxidant/ free radical scavenging activity of compound 2, 0.5mg/mL concentration 190

Graph 25: Results of Antioxidant/ free radical scavenging activity of compound 2, 1mg/mL concentration 191

Graph 26: Results of Antioxidant/ free radical scavenging activity of compound 2, 5mg/mL concentration 191

Graph 27: Results of Antioxidant/ free radical scavenging activity of compound 2, 10mg/mL concentration 192

Graph 28: Results of Antioxidant/ free radical scavenging activity of compound 3, 0.5mg/mL concentration 192

Graph 29: Results of Antioxidant/ free radical scavenging activity of compound 3, 1mg/mL concentration 193

Graph 30: Results of Antioxidant/ free radical scavenging activity of compound 3, 5mg/mL concentration 193

Graph 31: Results of Antioxidant/ free radical scavenging activity of compound 3, 10mg/mL concentration 194

Graph 32: Results of Antioxidant/ free radical scavenging activity of compound 4, 0.5mg/mL concentration 194

Graph 33: Results of Antioxidant/ free radical scavenging activity of compound 4, 1mg/mL concentration 195

Graph 34: Results of Antioxidant/ free radical scavenging activity of compound 4, 5mg/mL concentration 195

Graph 35: Results of Antioxidant/ free radical scavenging activity of compound 4, 10mg/mL concentration 196

Graph 36: Results of Antioxidant/ free radical scavenging activity of meloxicam, 1mg/mL concentration 196

Graph 37: Results of Antioxidant/ free radical scavenging activity of meloxicam, 5mg/mL concentration 197

Graph 38: Results of Antioxidant/ free radical scavenging activity of meloxicam, 10mg/mL concentration 197

Graph 39: Results of Antioxidant/ free radical scavenging activity of diclofenac, 1mg/mL concentration 198

Graph 40: Results of Antioxidant/ free radical scavenging activity of diclofenac, 5mg/mL concentration 198

Graph 41: Results of Antioxidant/ free radical scavenging activity of diclofenac, 10mg/mL concentration 199

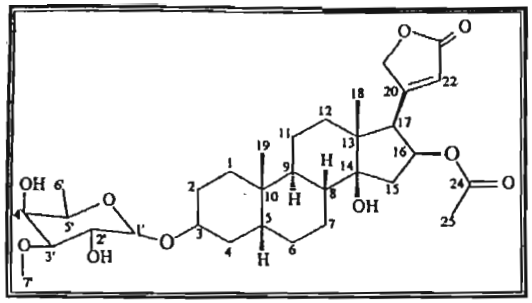

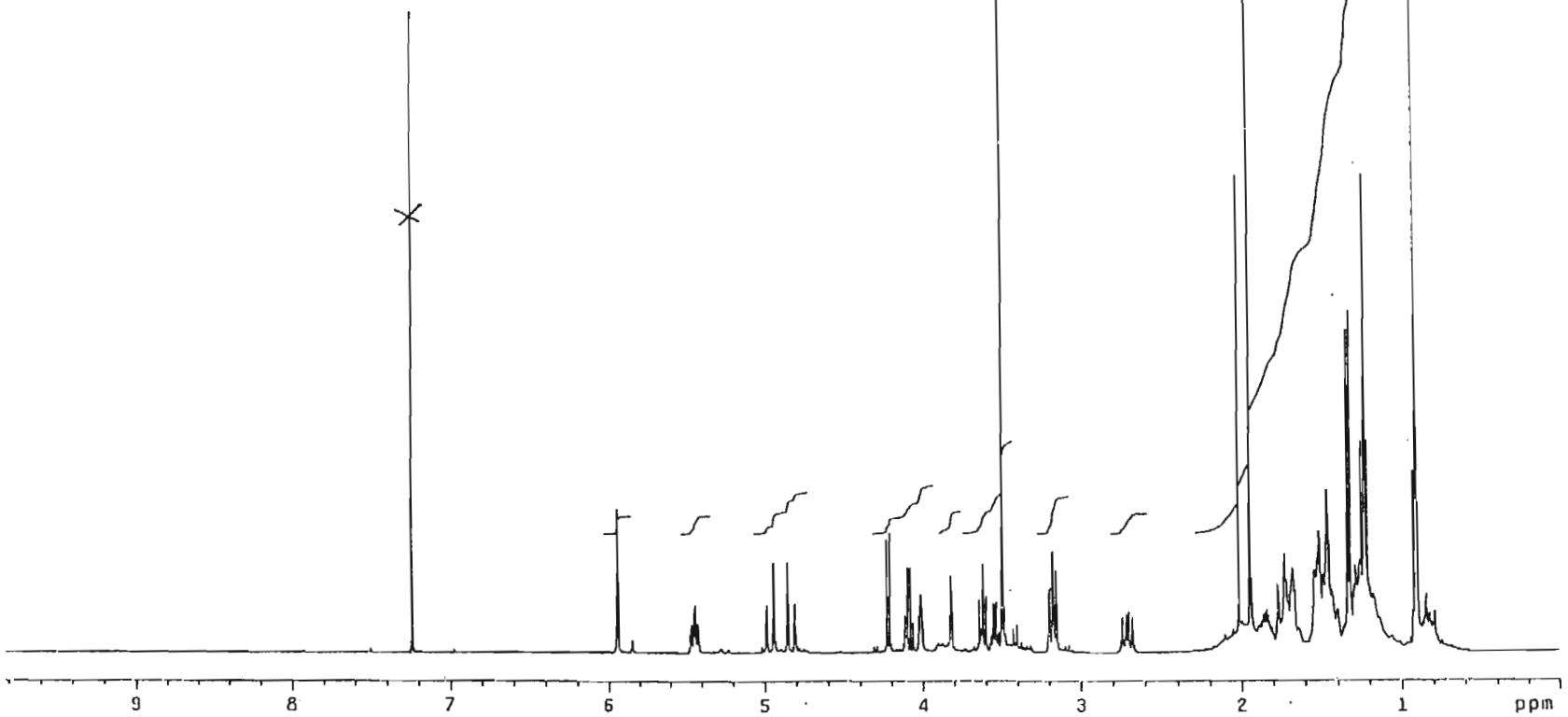

Spectrum 1a: ^{1}H NMR spectrum of compound **1** ($CDCl_3$)

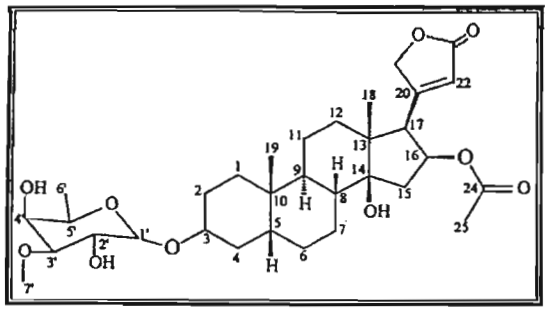

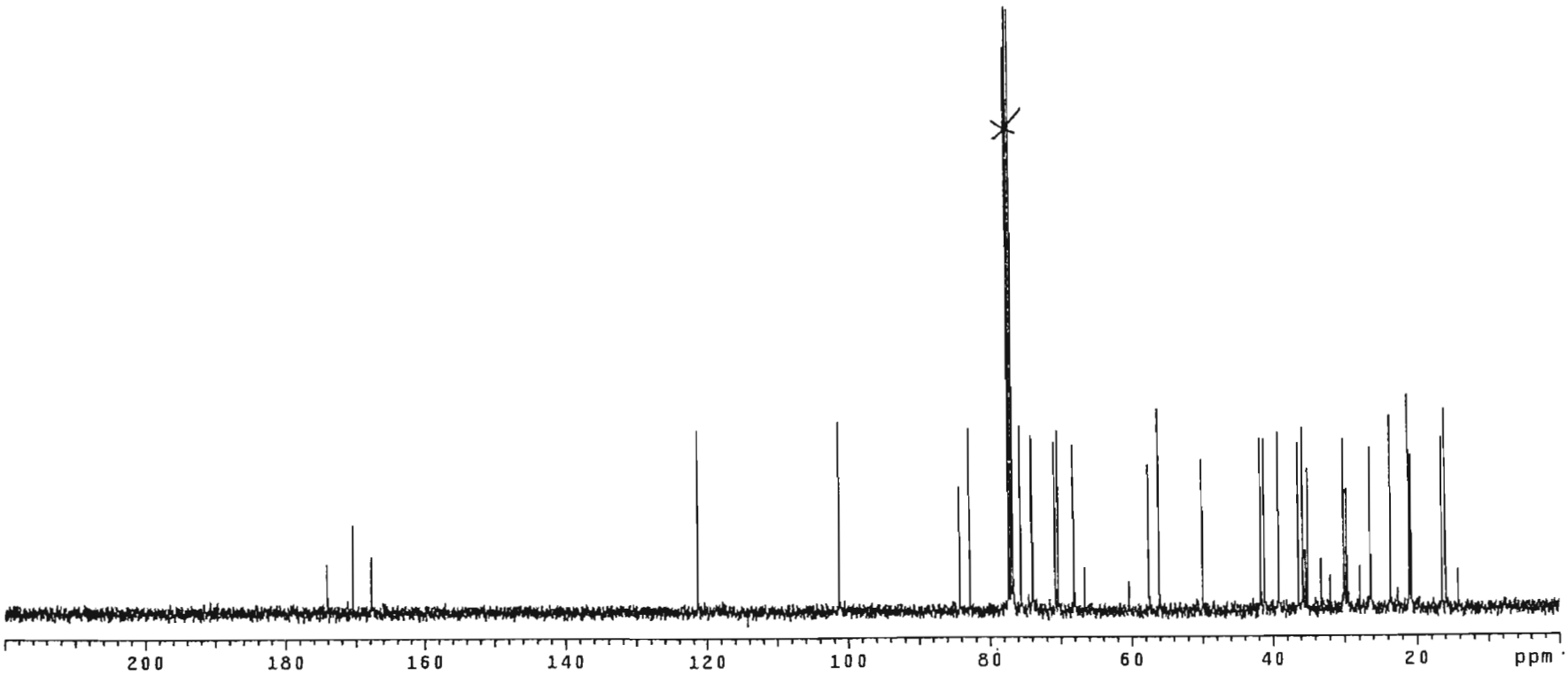

Spectrum 1b: ^{13}C NMR spectrum of compound 1 ($CDCl_3$)

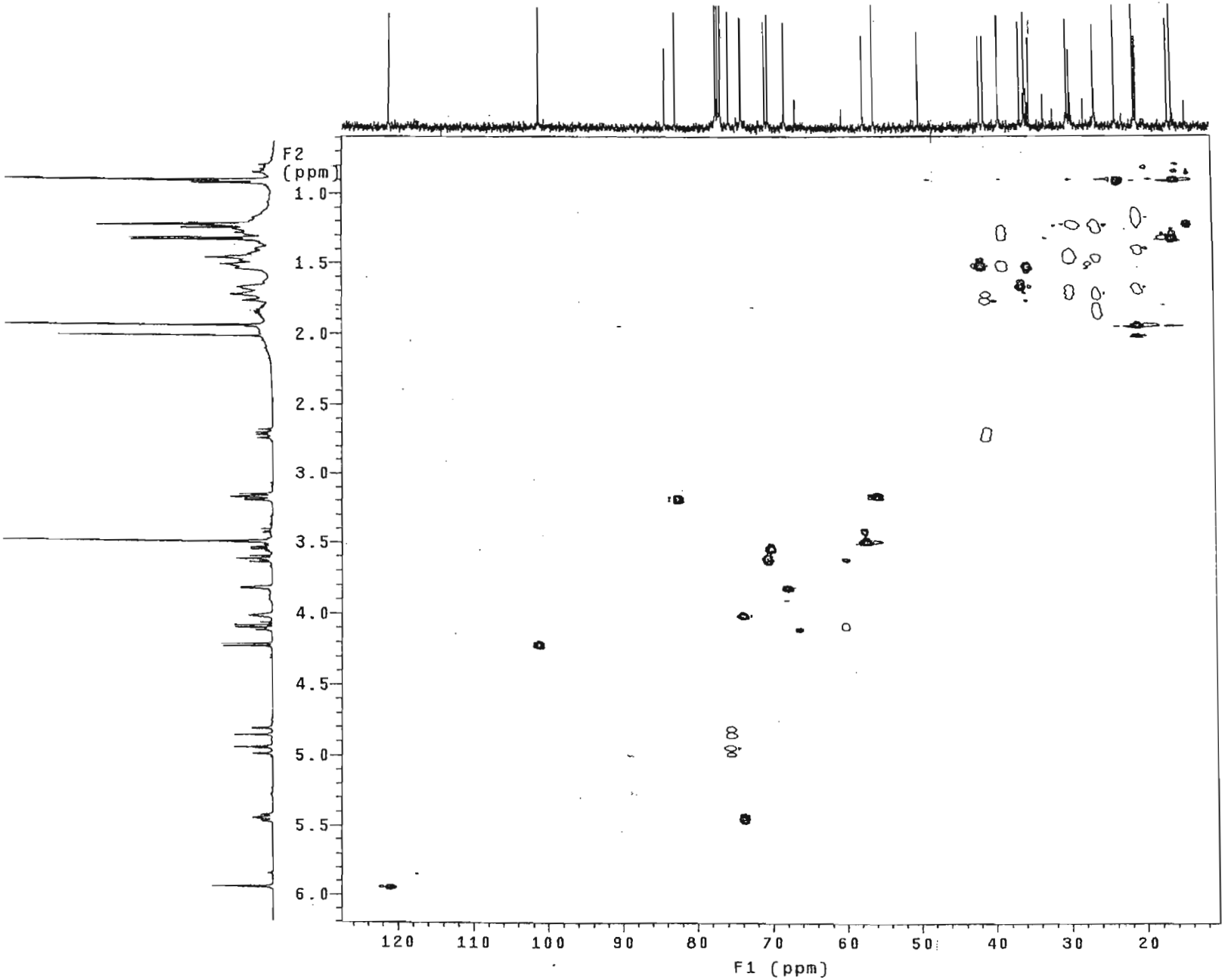

Spectrum 1c: HSQC spectrum of compound 1

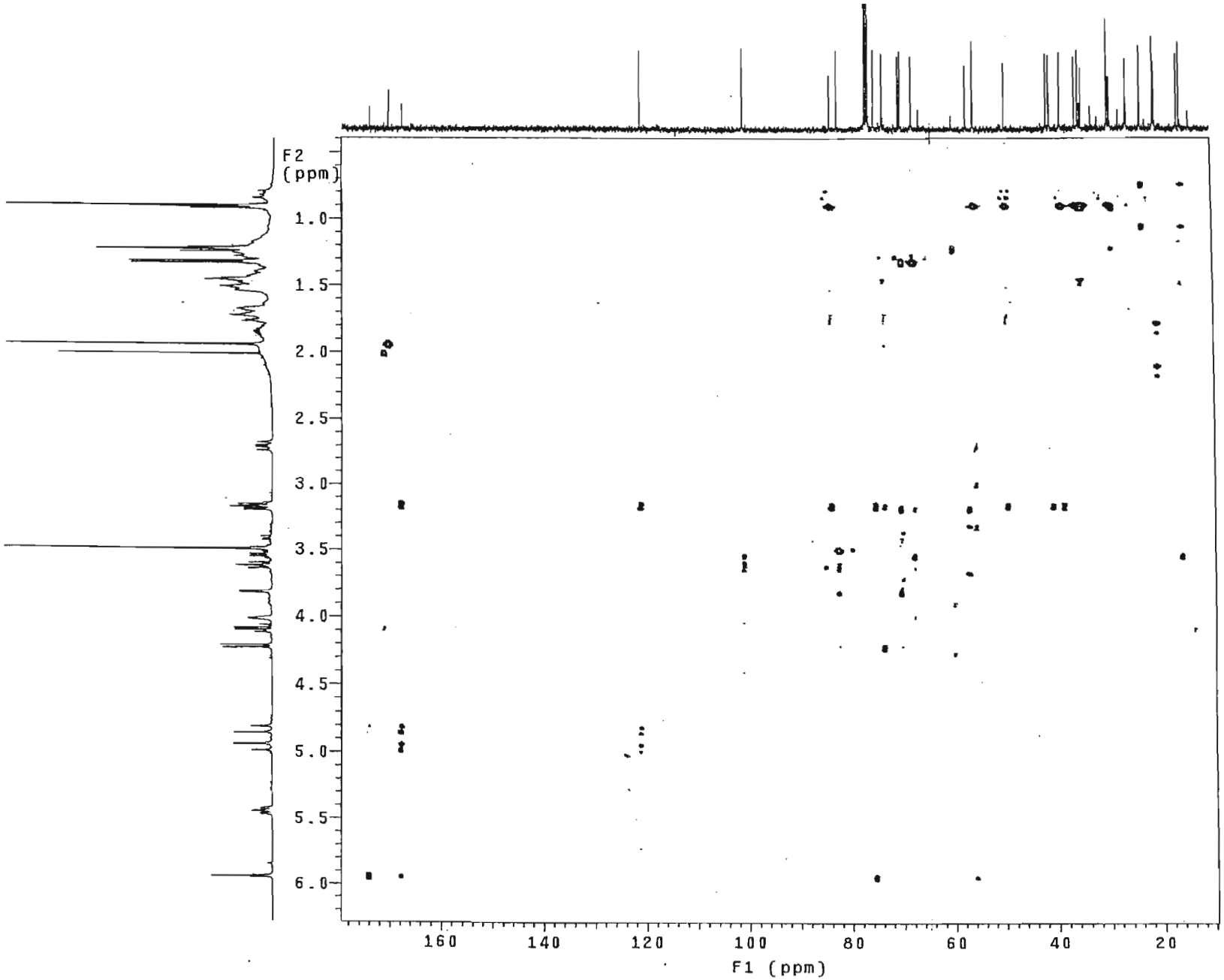

Spectrum 1d: HMBC spectrum of compound **1**

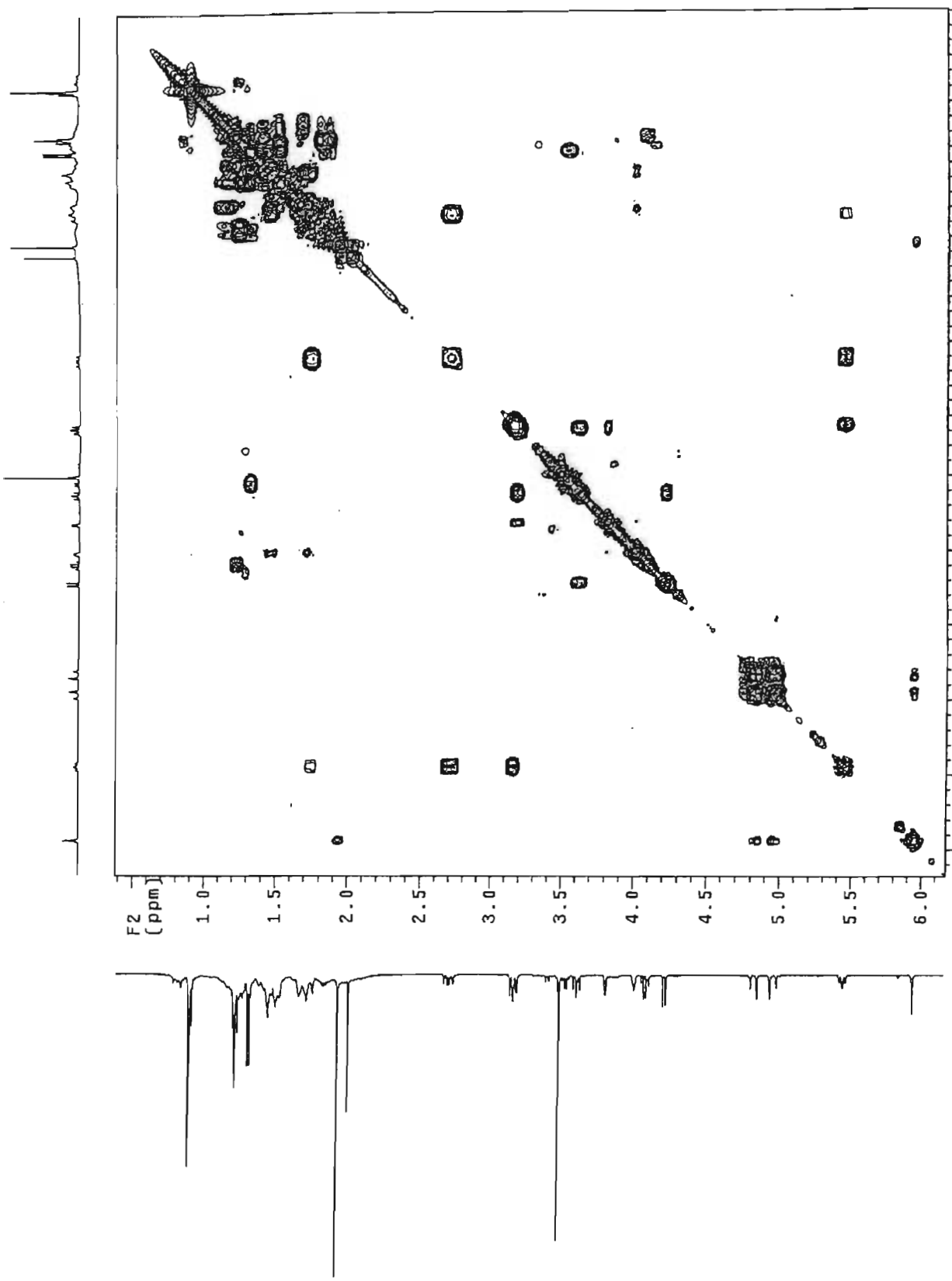

Spectrum 1e: COSY spectrum of compound 1

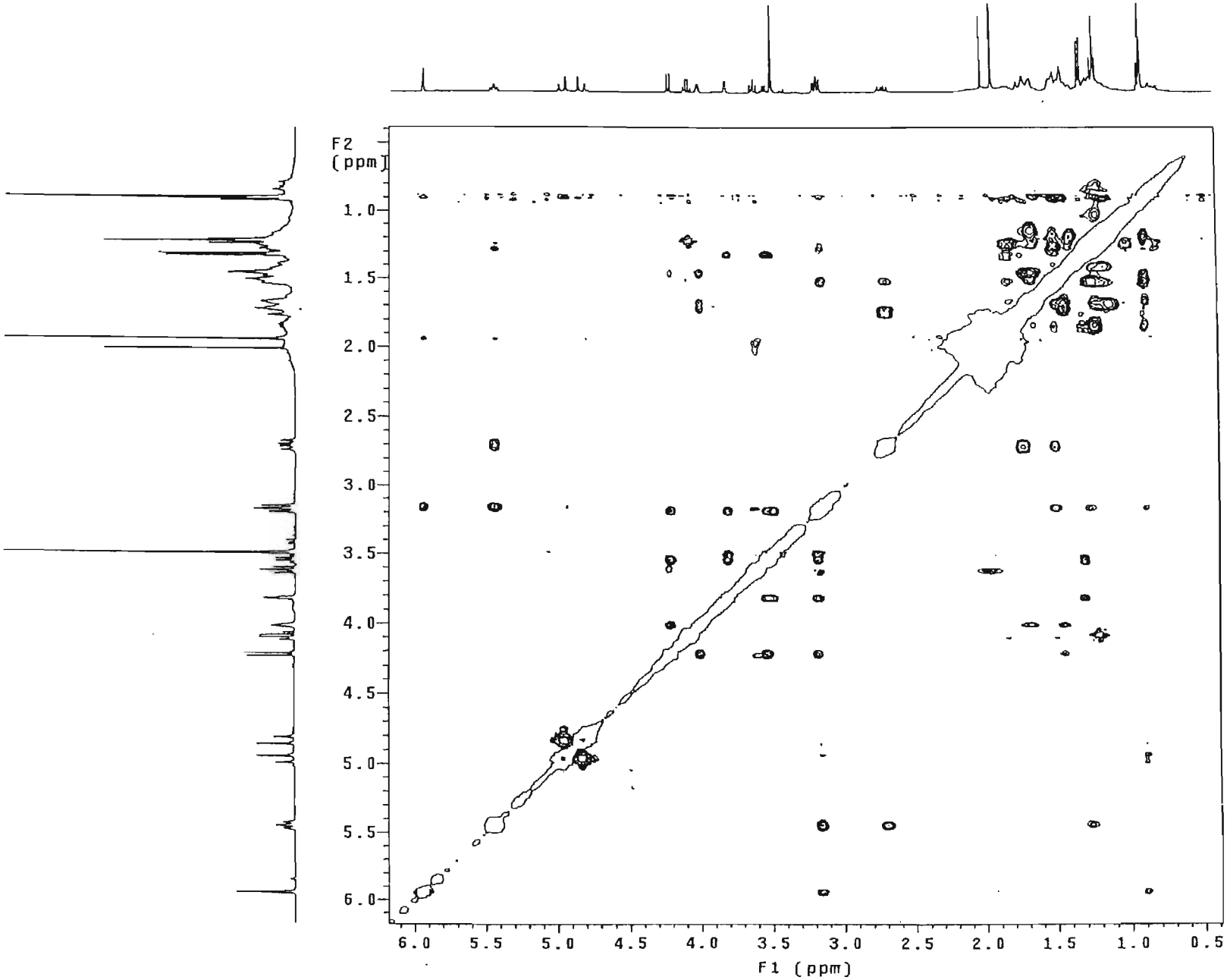

Spectrum 1f: NOESY spectrum of compound 1

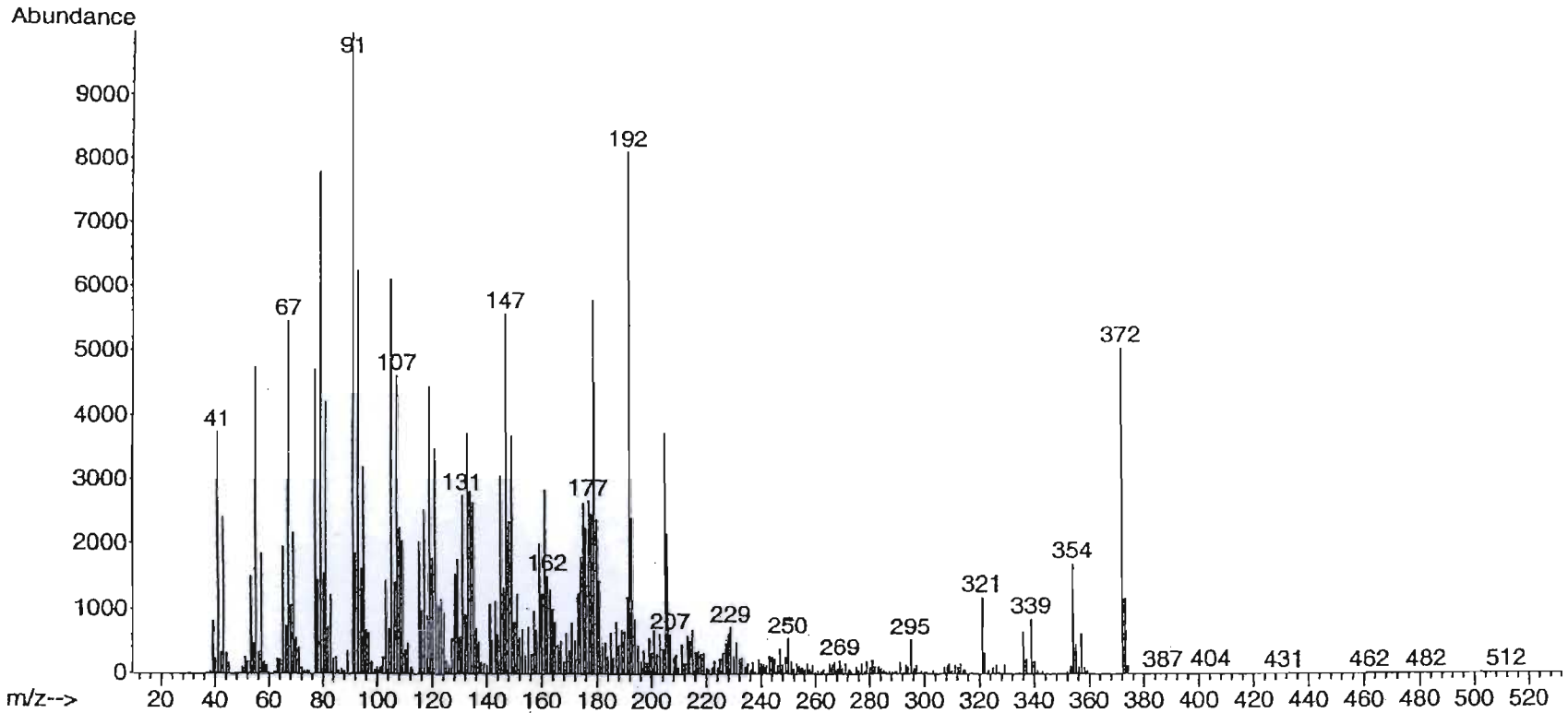

Spectrum 1g: Mass spectrum of compound **1**

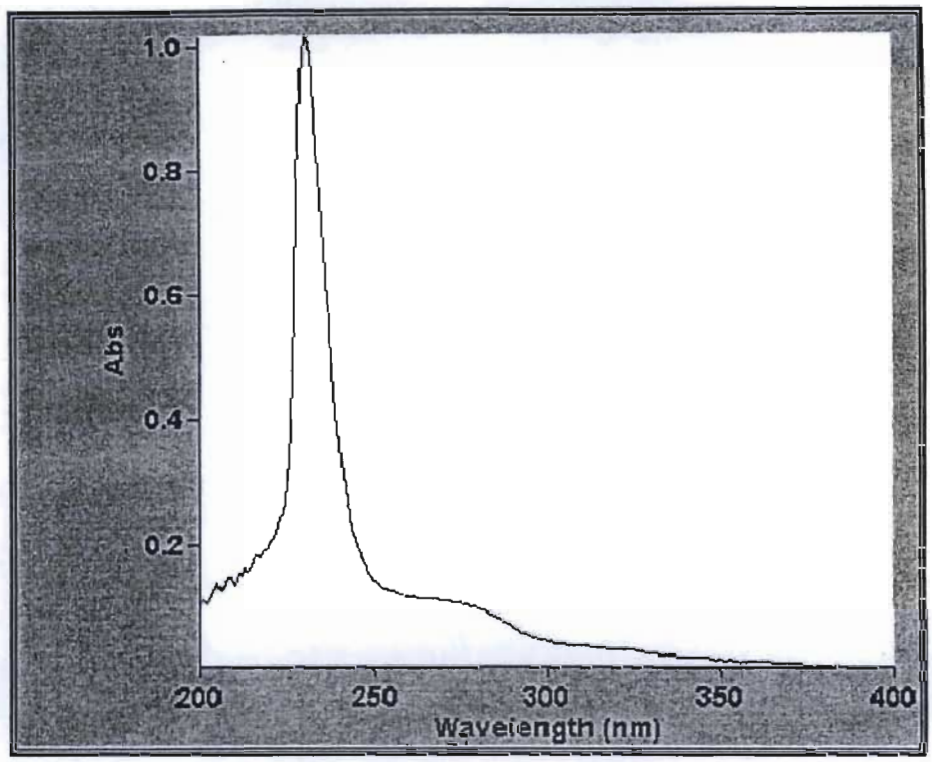

Spectrum 1h: UV spectrum of compound **1**

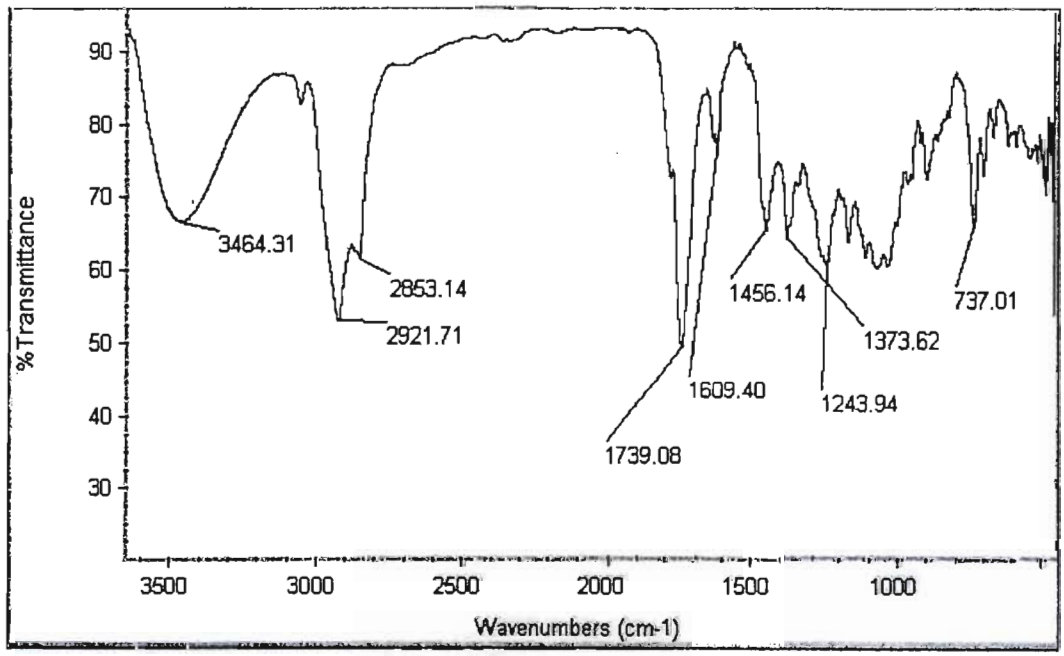

Spectrum 1i: IR spectrum of compound **1**

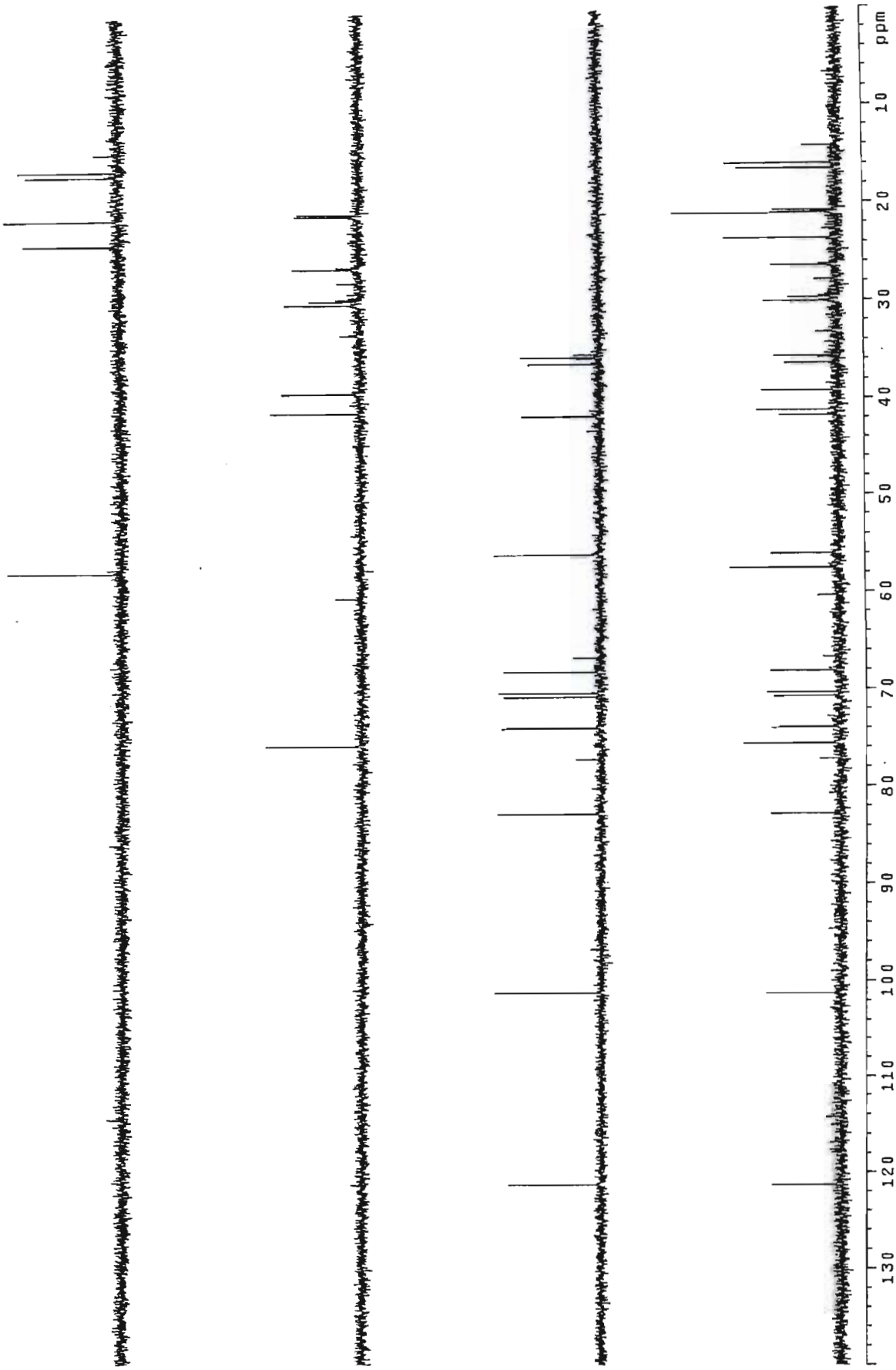

Spectrum 1j: DEPT spectrum of compound **1**

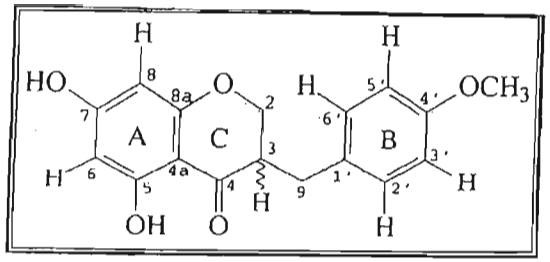

Spectrum 2a: ^{1}H NMR spectrum of compound **2** ($CDCl_3$)

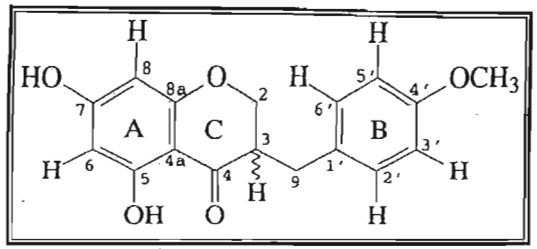

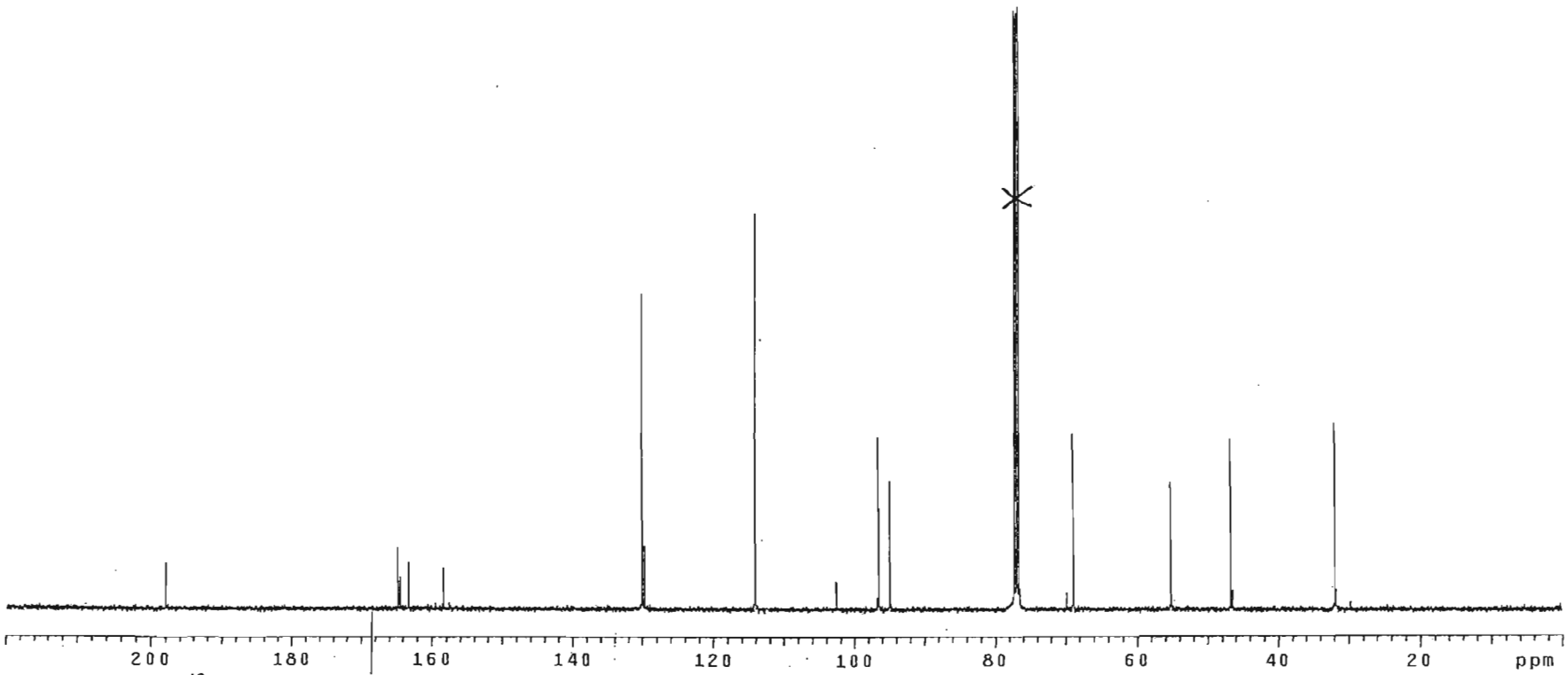

Spectrum 2b: ^{13}C NMR spectrum of compound **2** ($CDCl_3$)

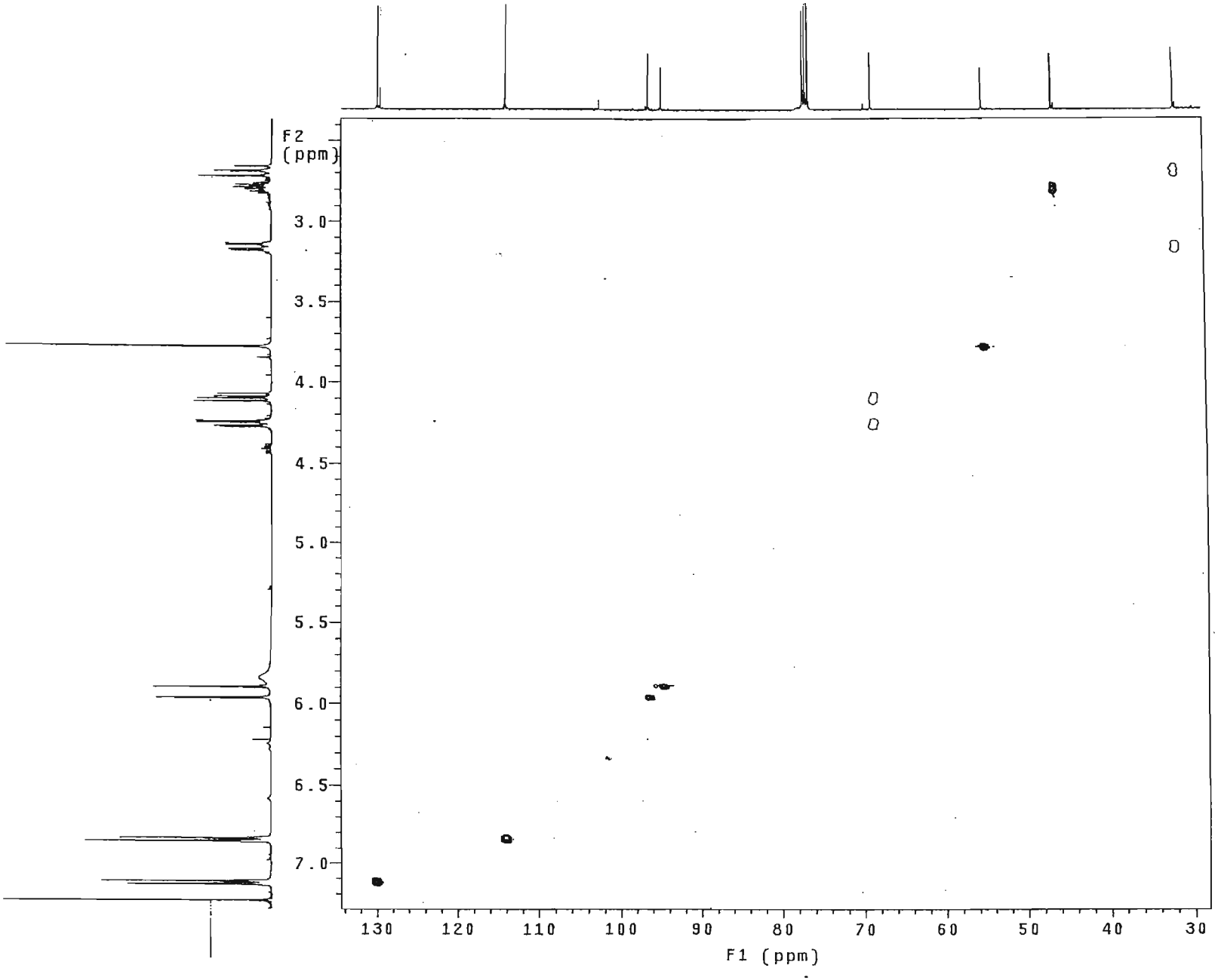

Spectrum 2c: HSQC spectrum of compound **2**

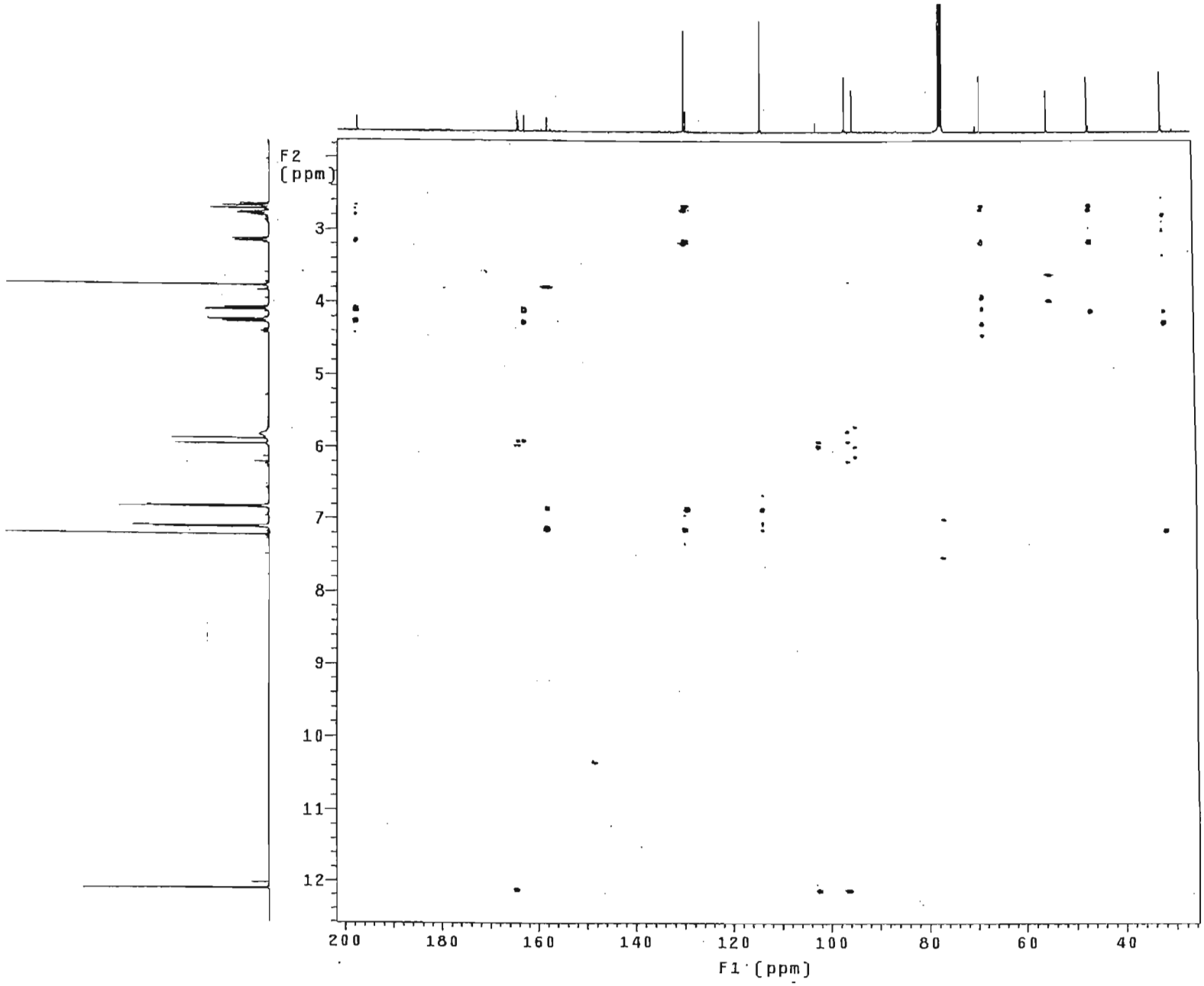

Spectrum 2d: HMBC spectrum of compound **2**

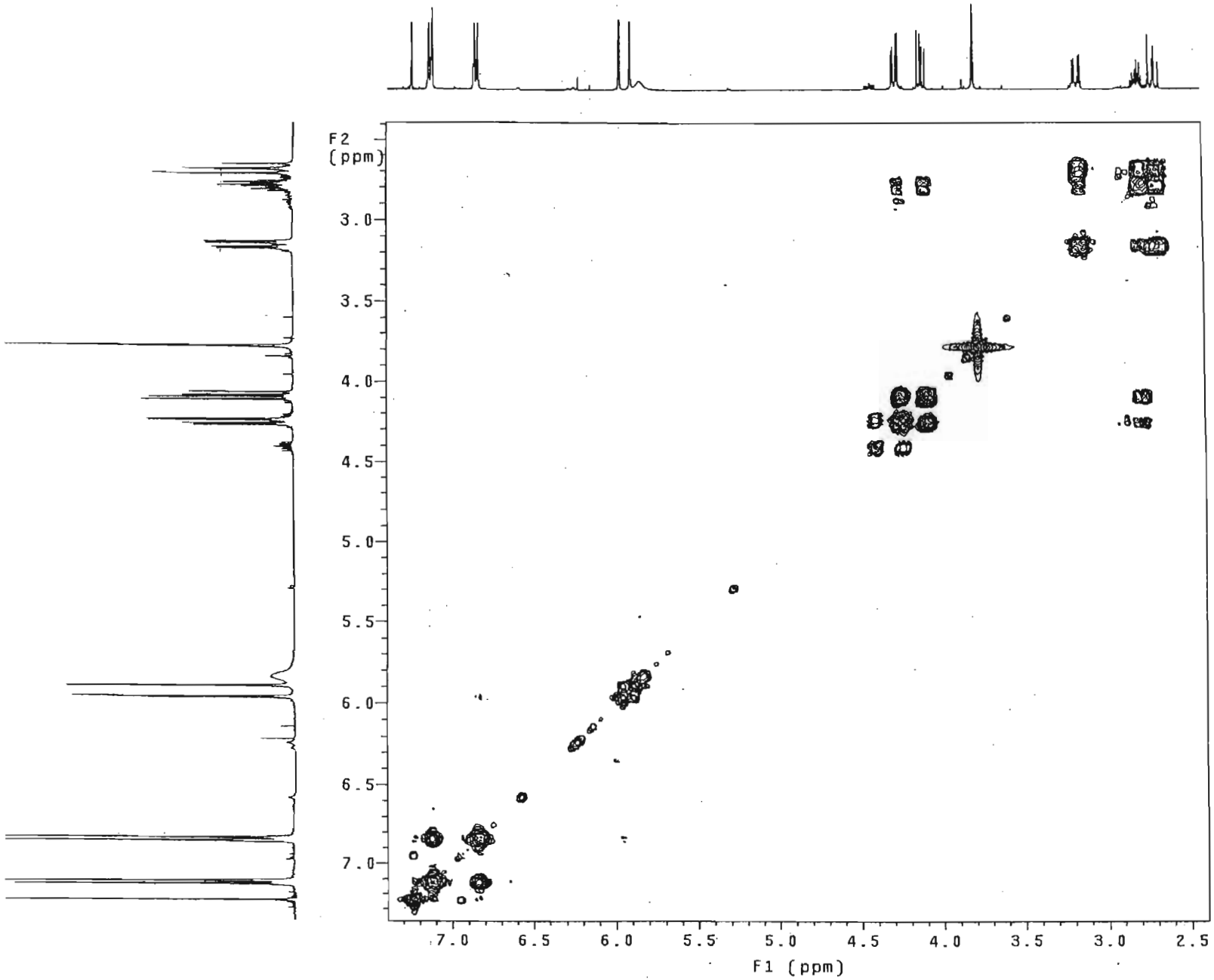

Spectrum 2e: COSY spectrum of compound **2**

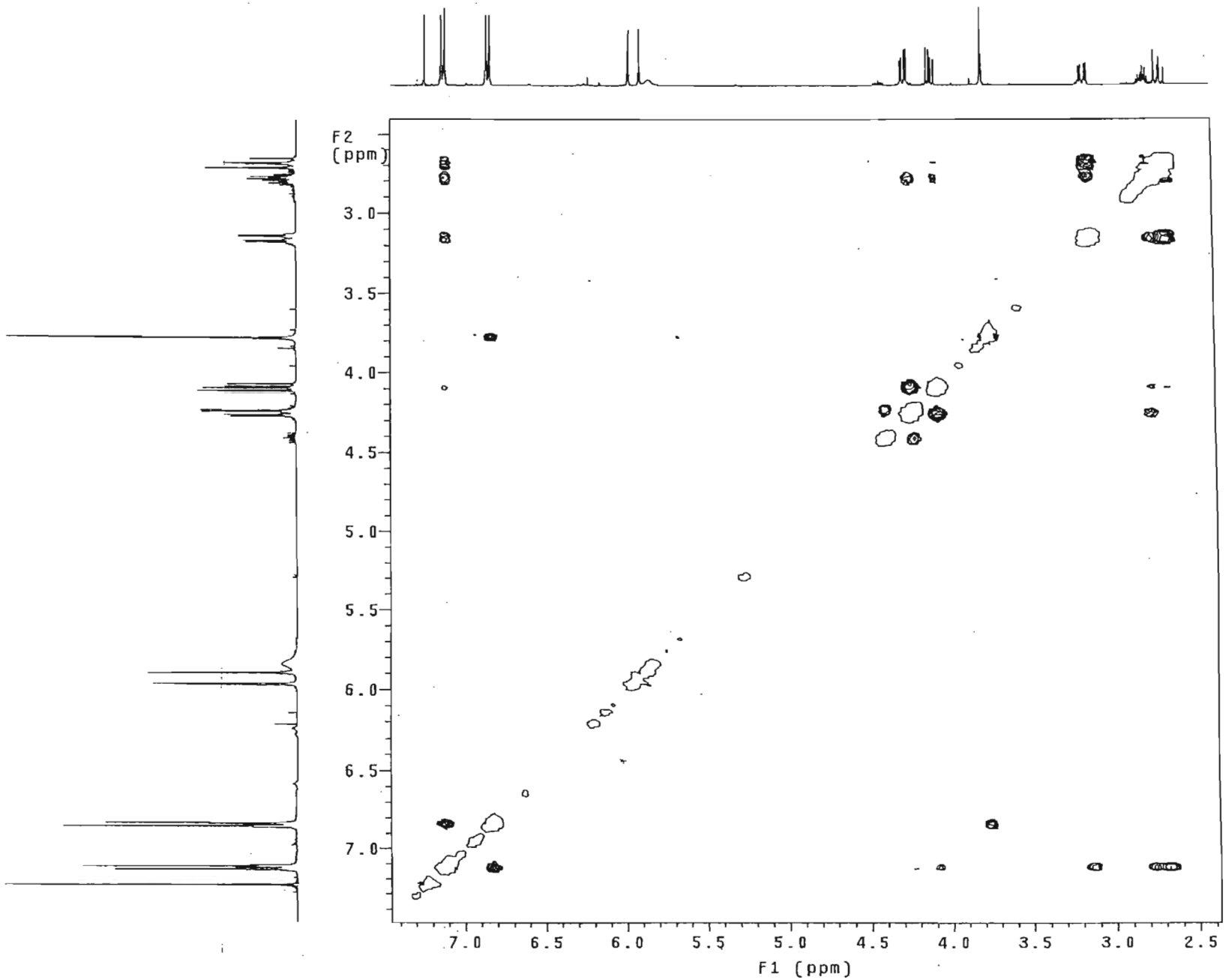

Spectrum 2f: NOESY spectrum of compound **2**

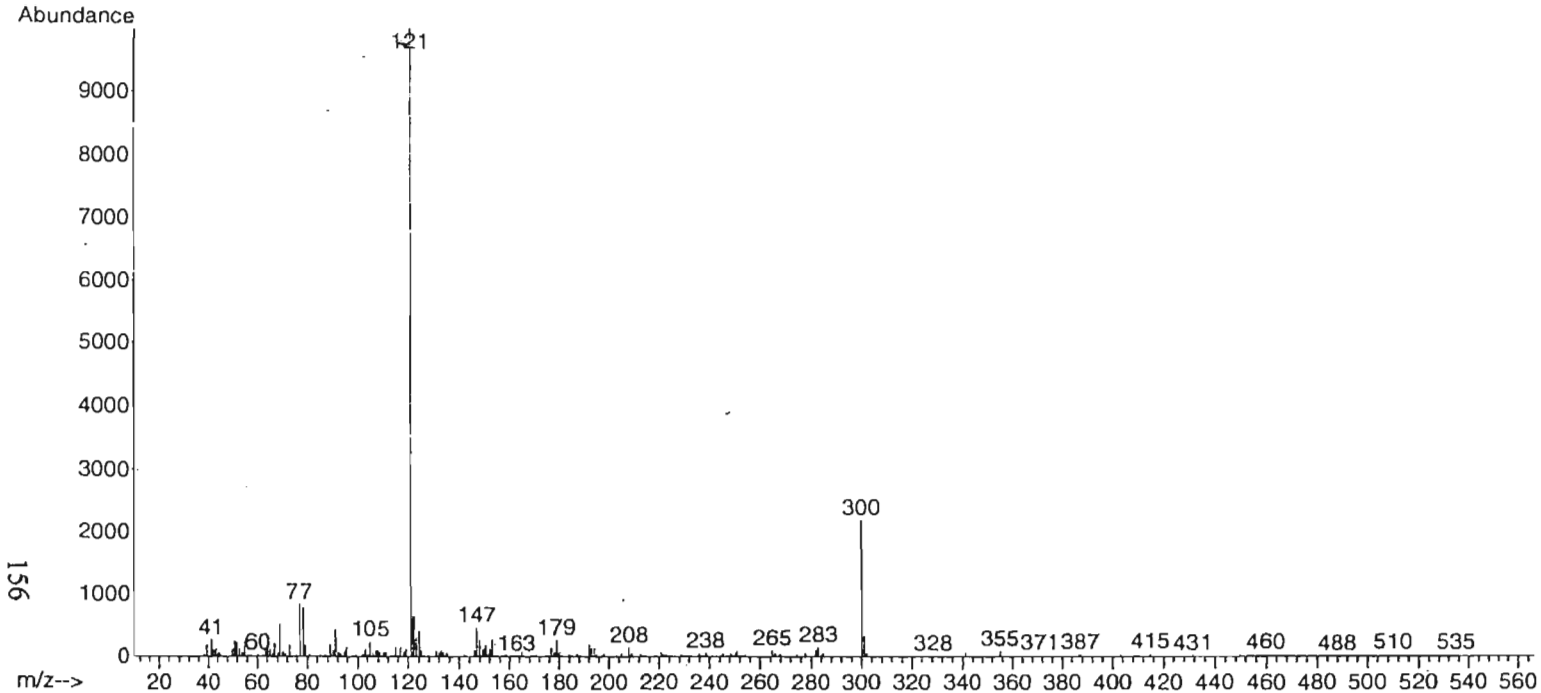

Spectrum 2g: Mass spectrum of compound **2**

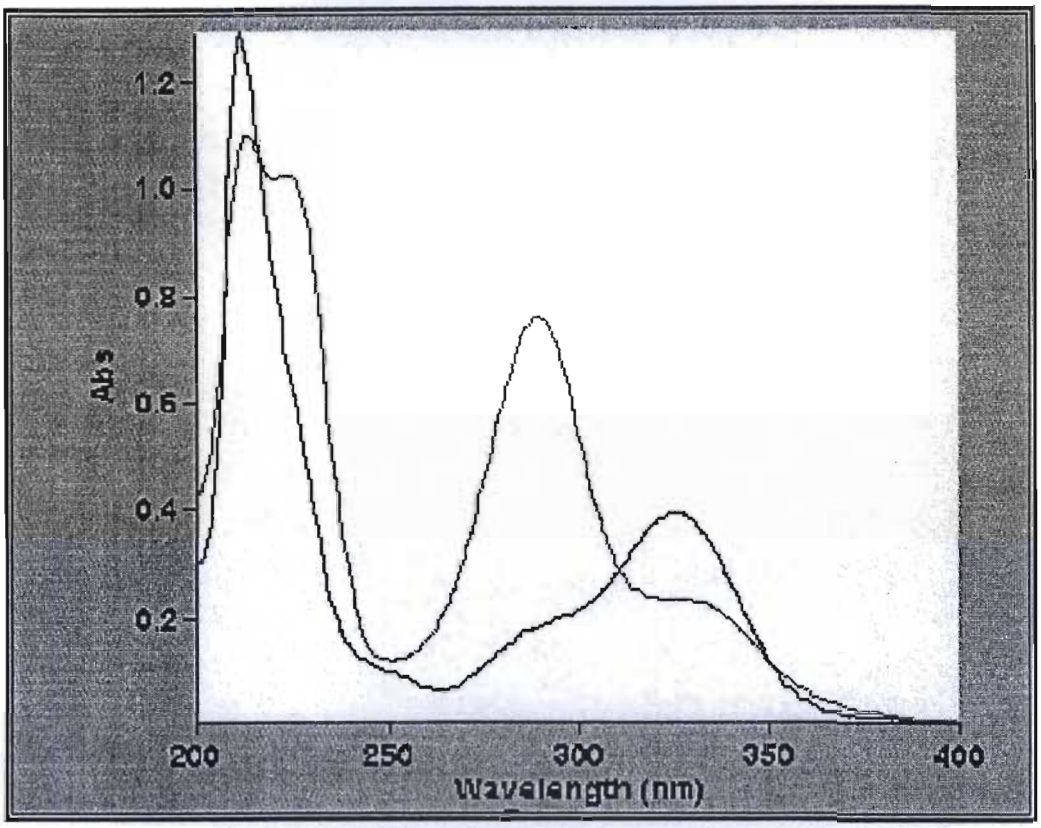

Spectrum 2h: UV spectrum + UV (NAOAc) spectrum of compound 2

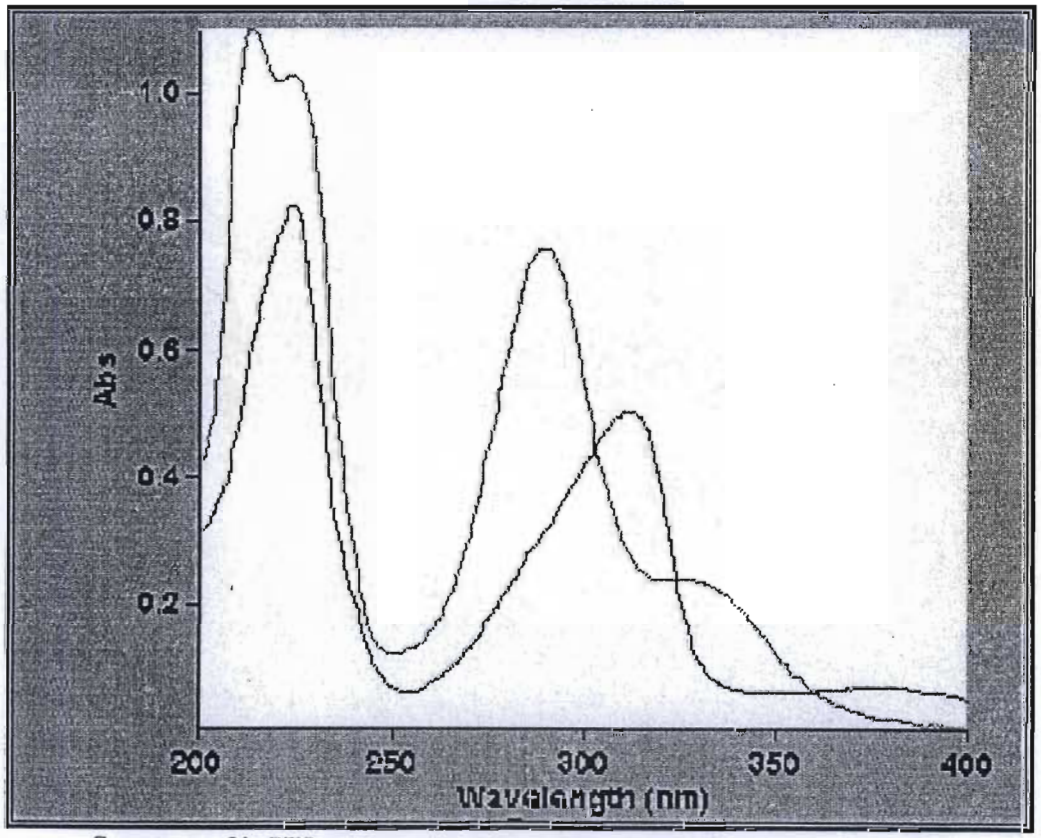

Spectrum 2i: UV spectrum + UV ($AlCl_3$) spectrum of compound 2

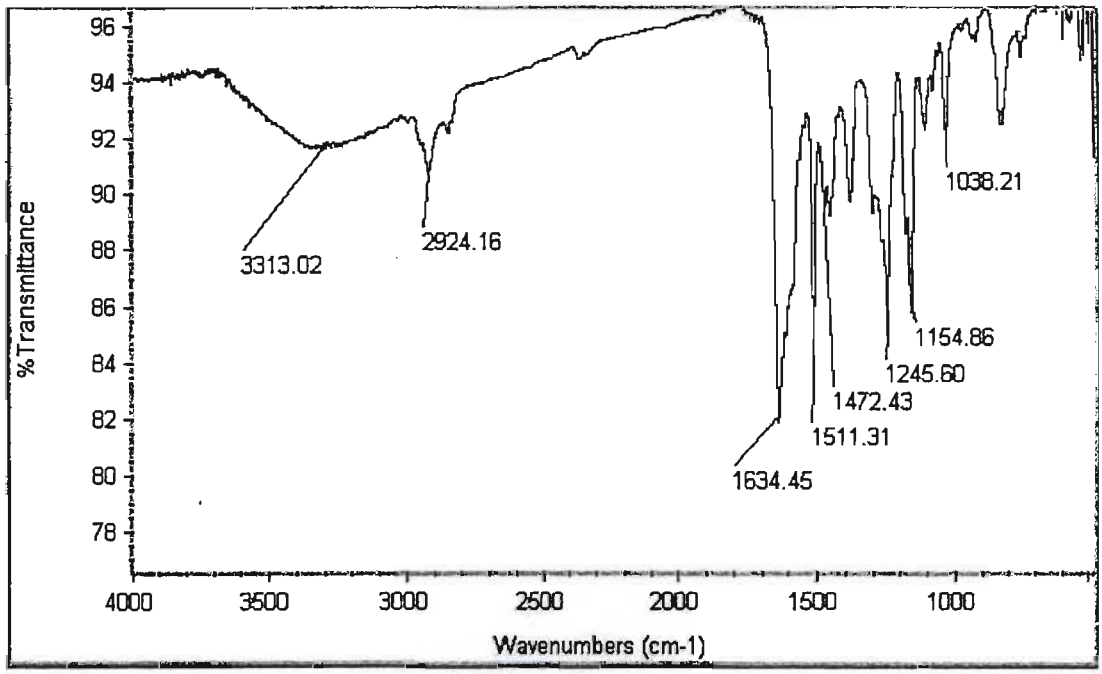

Spectrum 2j: IR spectrum of compound **2**

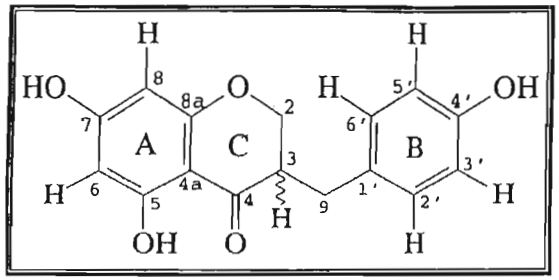

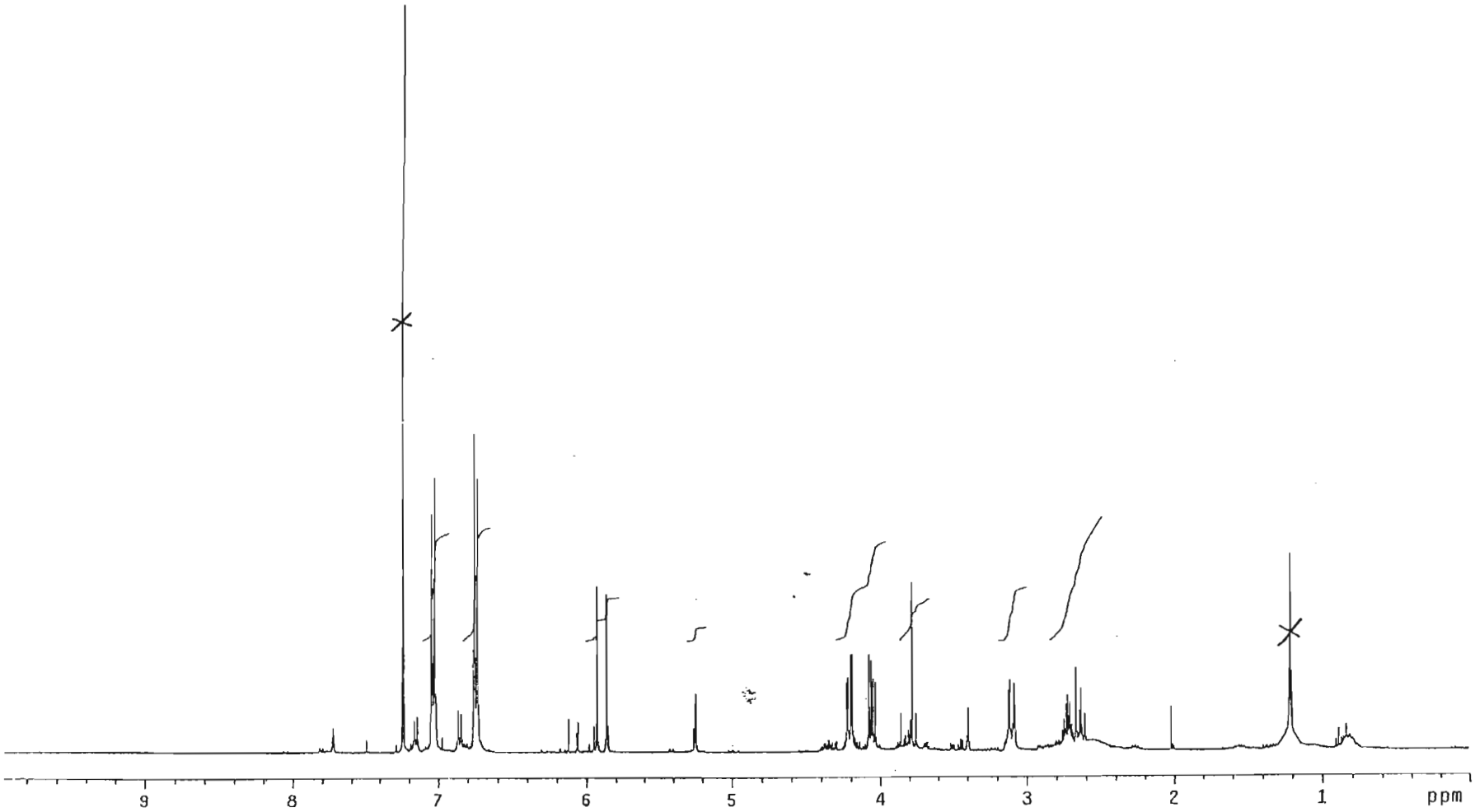

Spectrum 3a: ^{1}H NMR spectrum of compound **3** ($CDCl_3$)

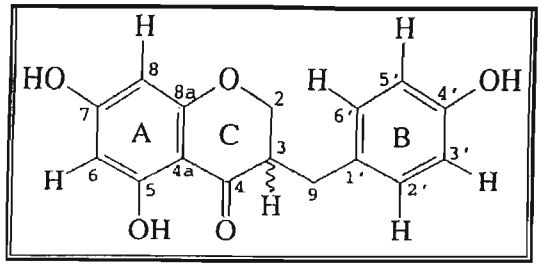

Spectrum 3b: ^{13}C NMR spectrum of compound **3** ($CDCl_3$)

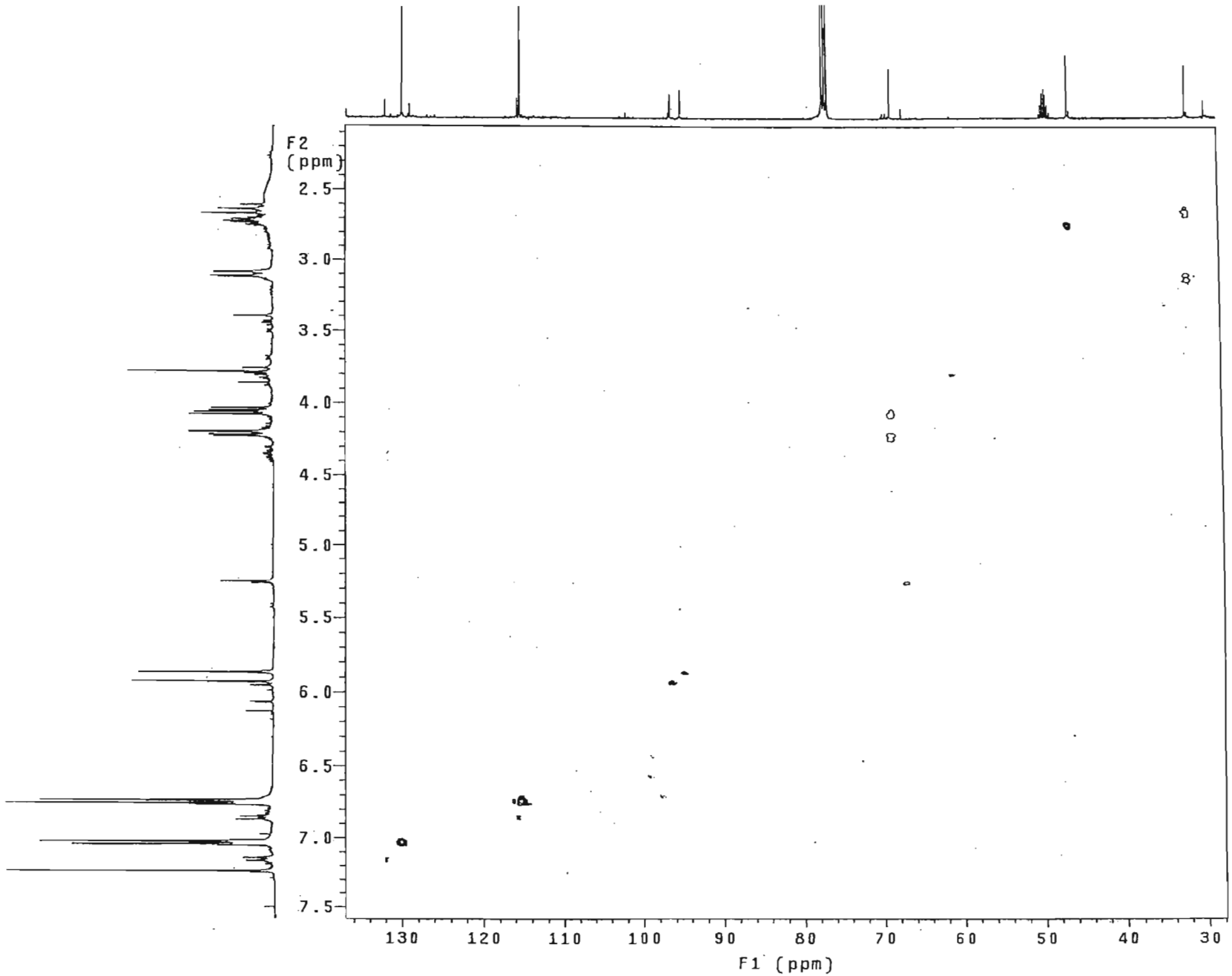

Spectrum 3c: HSQC spectrum of compound **3**

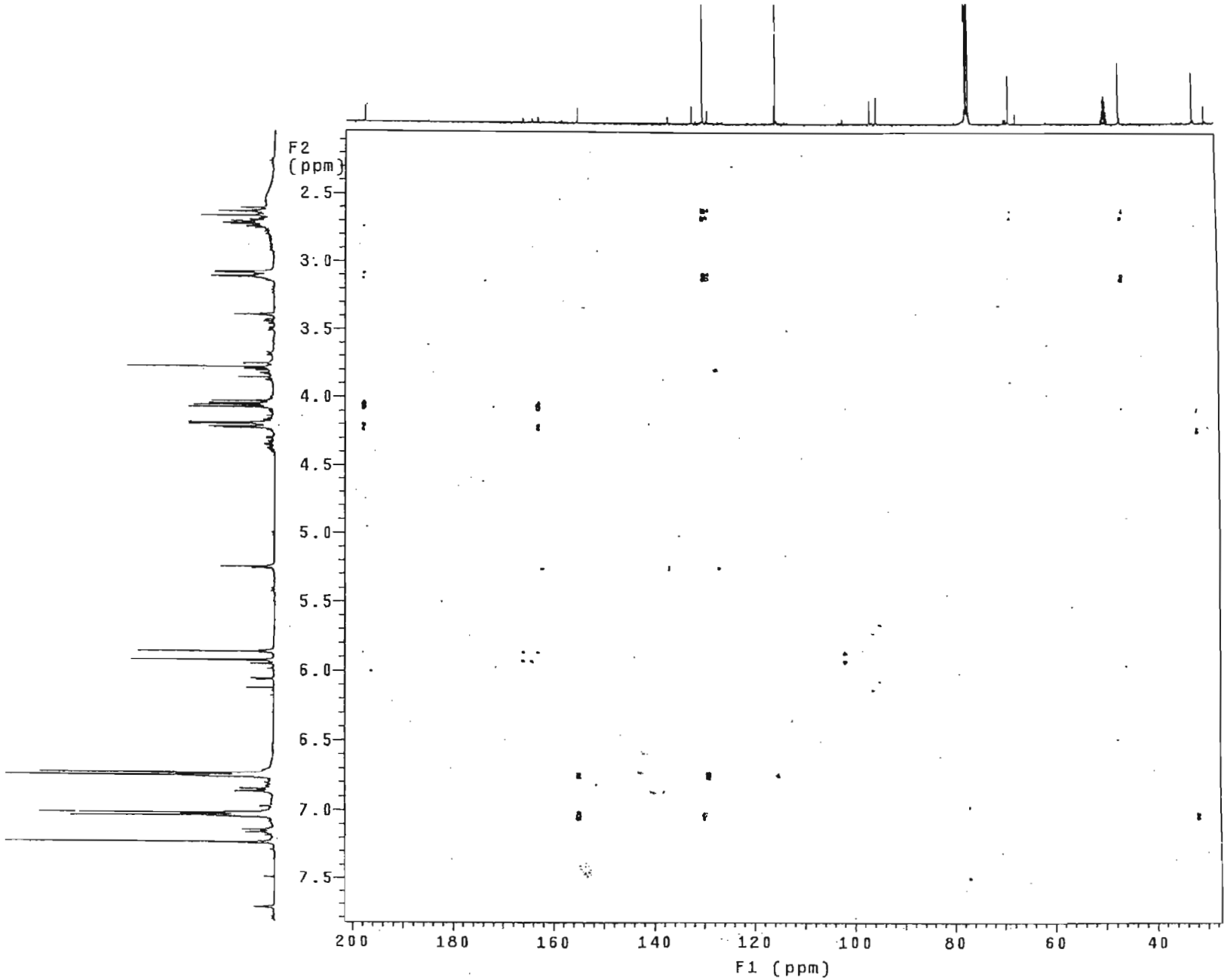

Spectrum 3d: HMBC spectrum of compound **3**

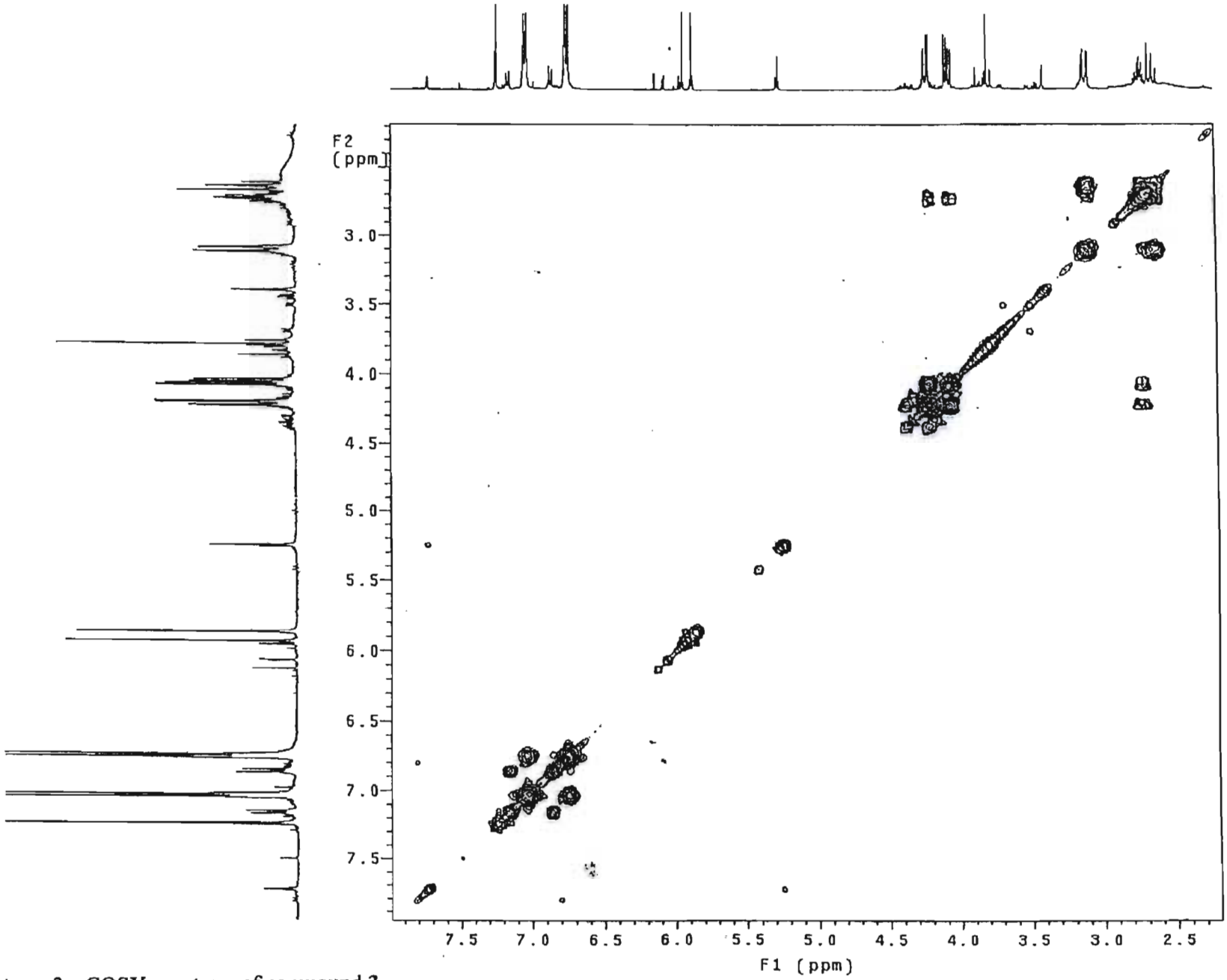

Spectrum 3e: COSY spectrum of compound 3

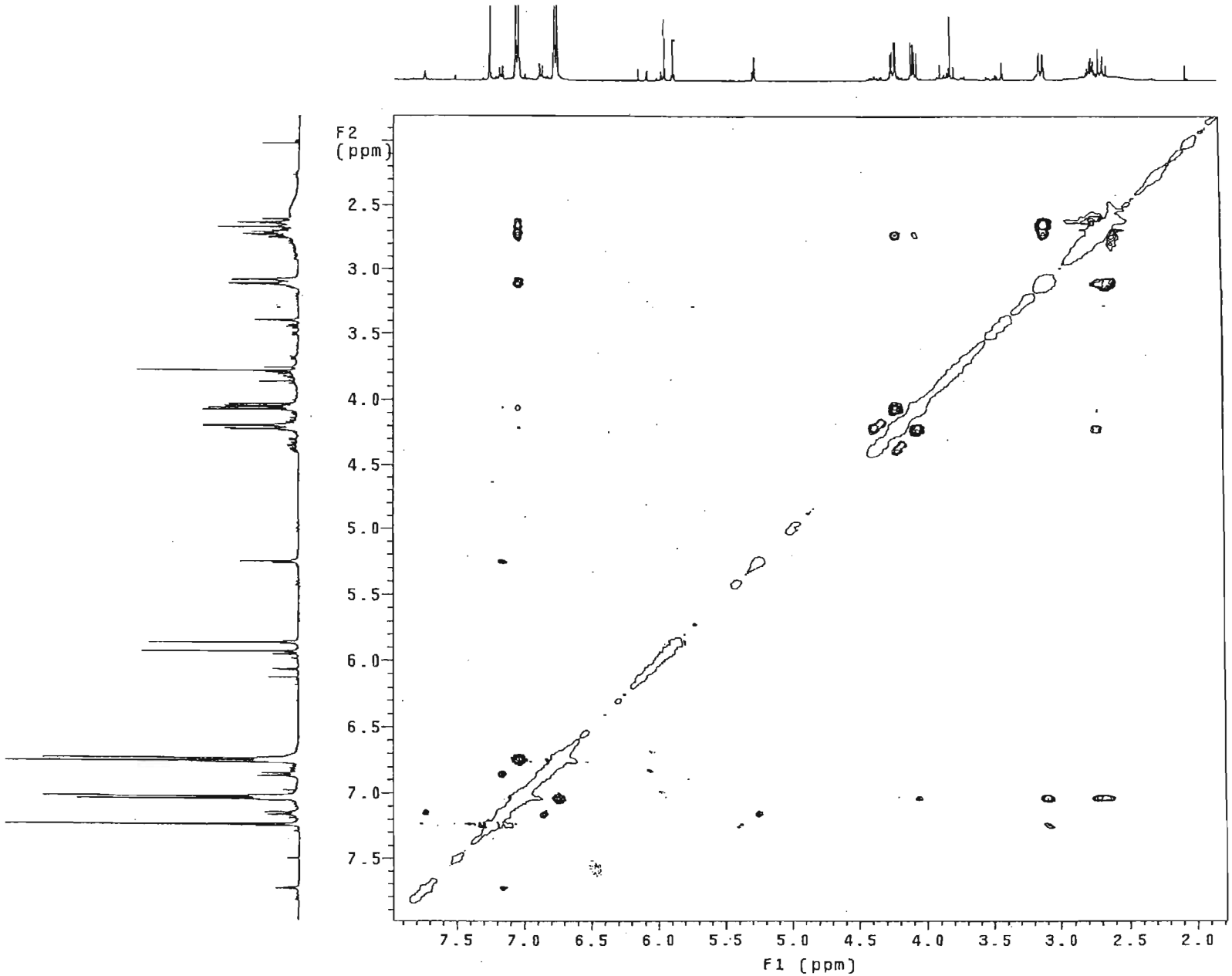

Spectrum 3f: NOESY spectrum of compound **3**

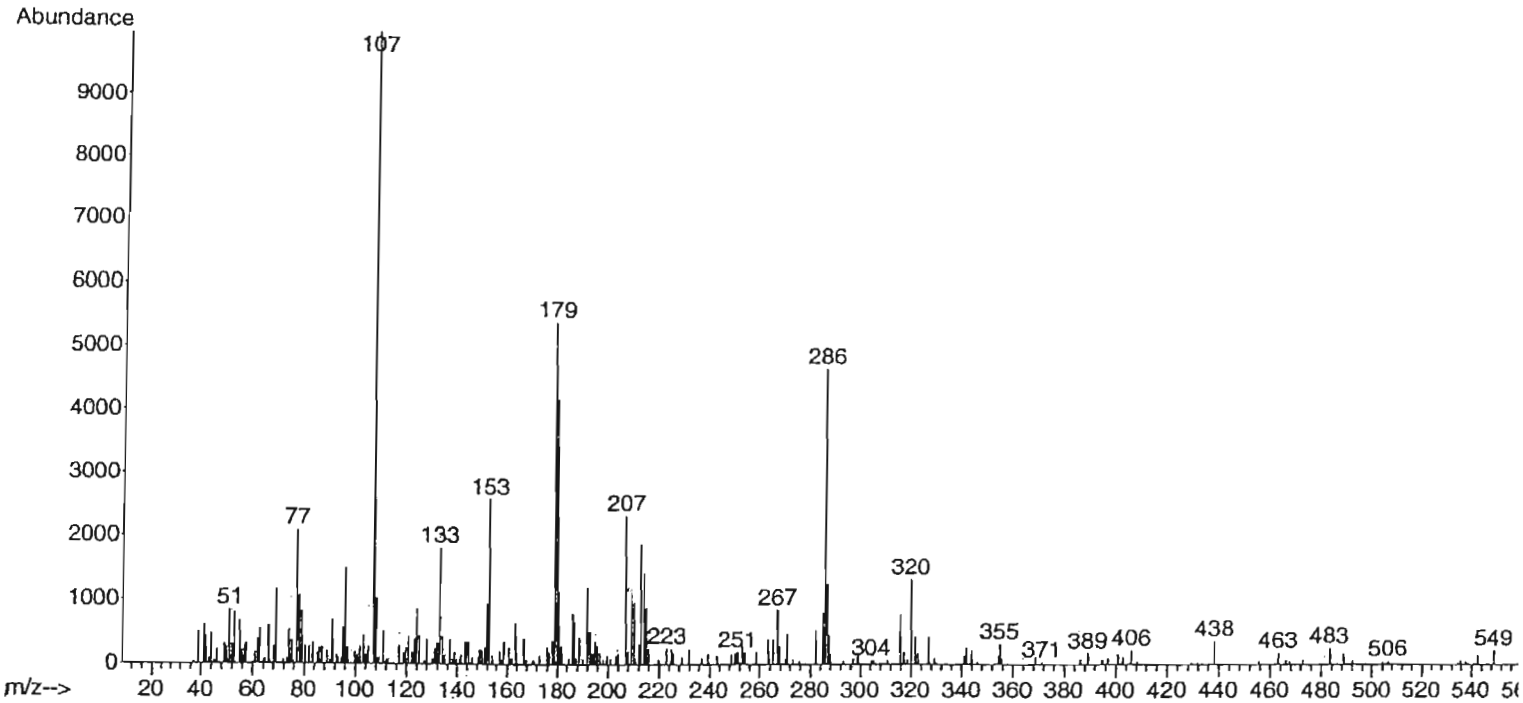

Spectrum 3g: Mass spectrum of compound **3**

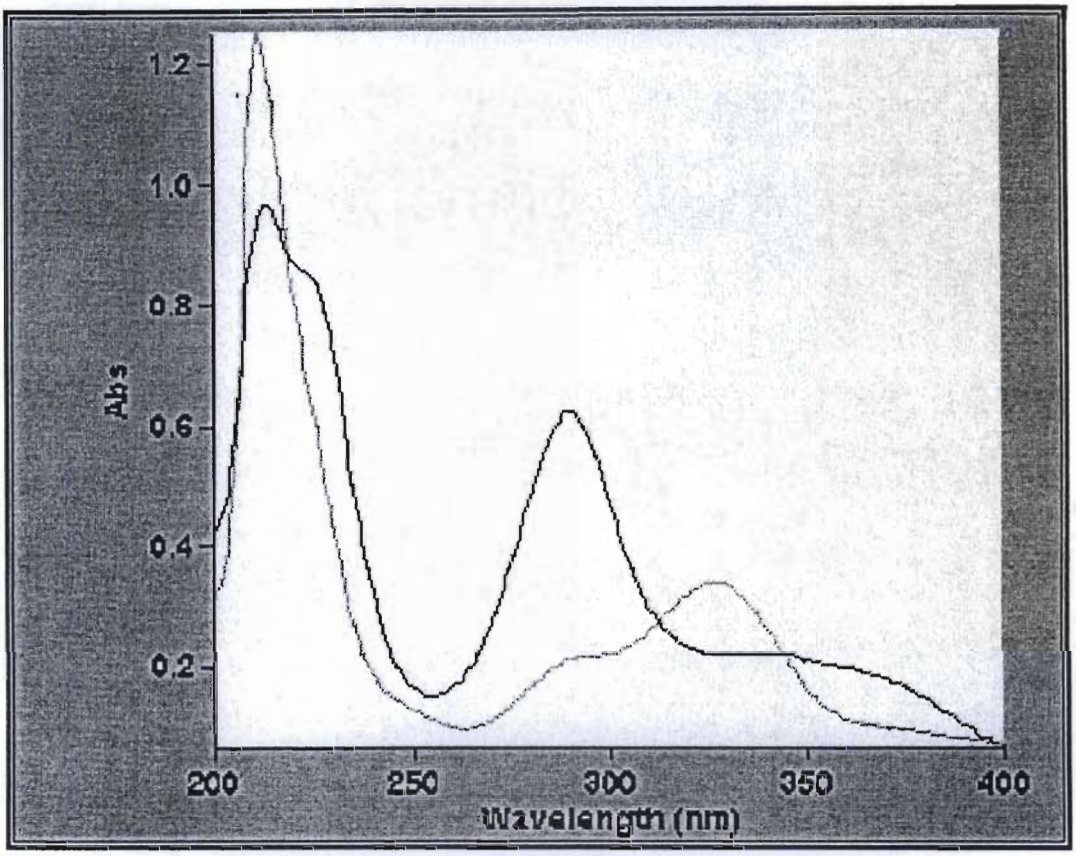

Spectrum 3h: UV spectrum + UV (NAOAc) spectrum of compound 3

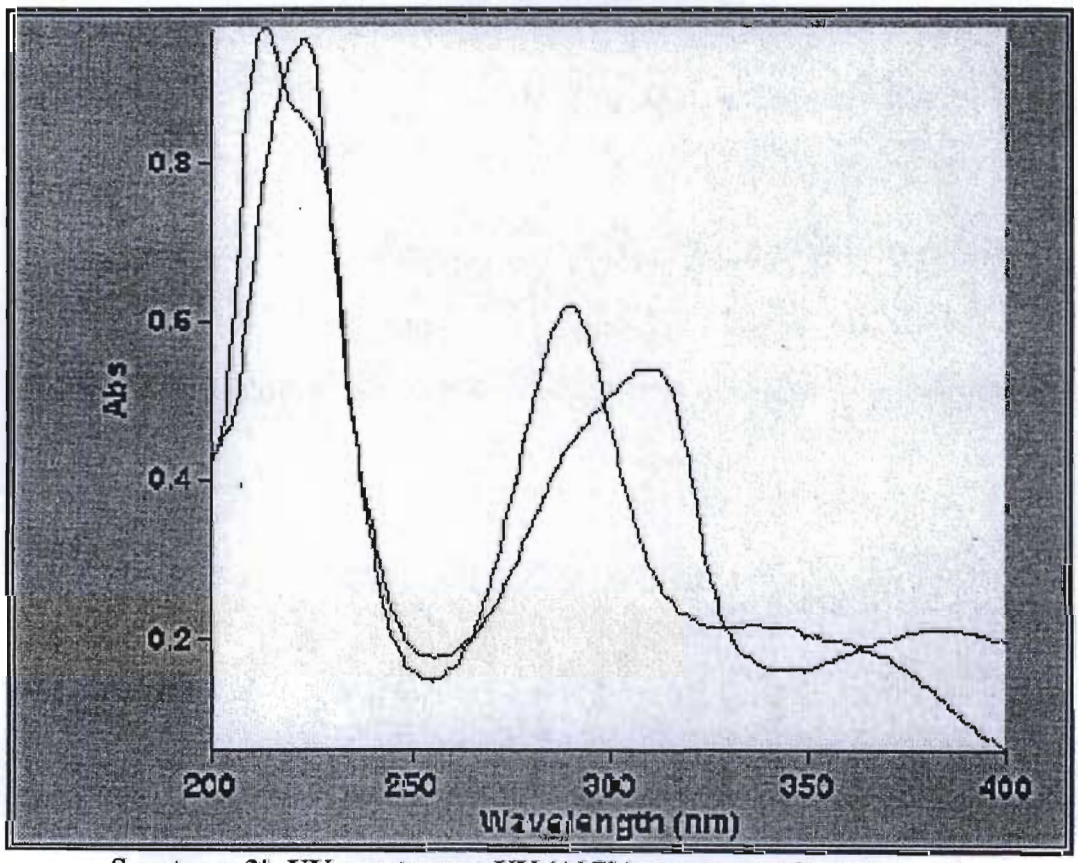

Spectrum 3i: UV spectrum + UV ($AlCl_3$) spectrum of compound 3

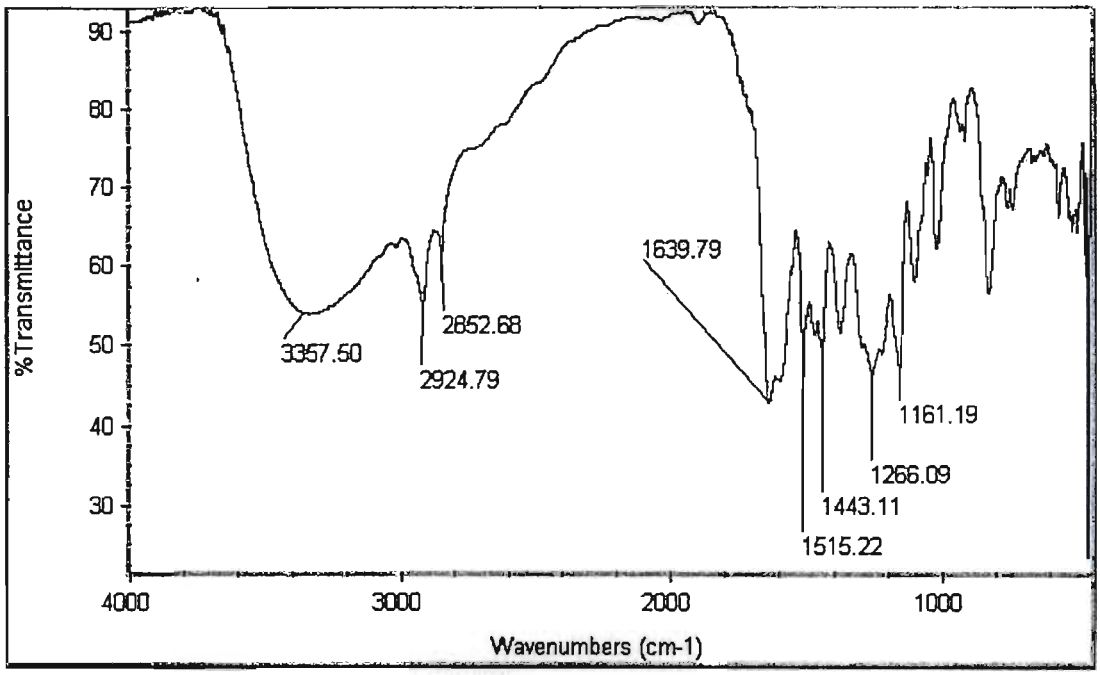

Spectrum 3j: IR spectrum of compound **3**

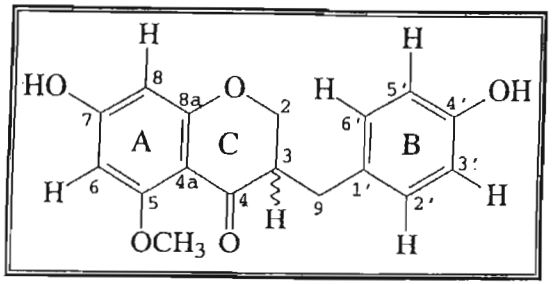

Spectrum 4a: ^{1}H NMR spectrum of compound **4** ($CDCl_3$)

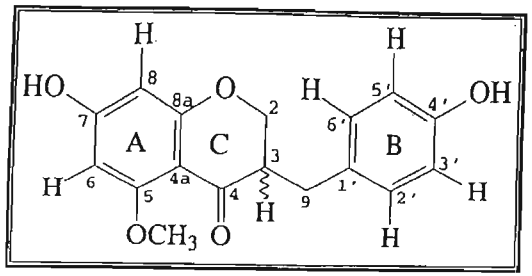

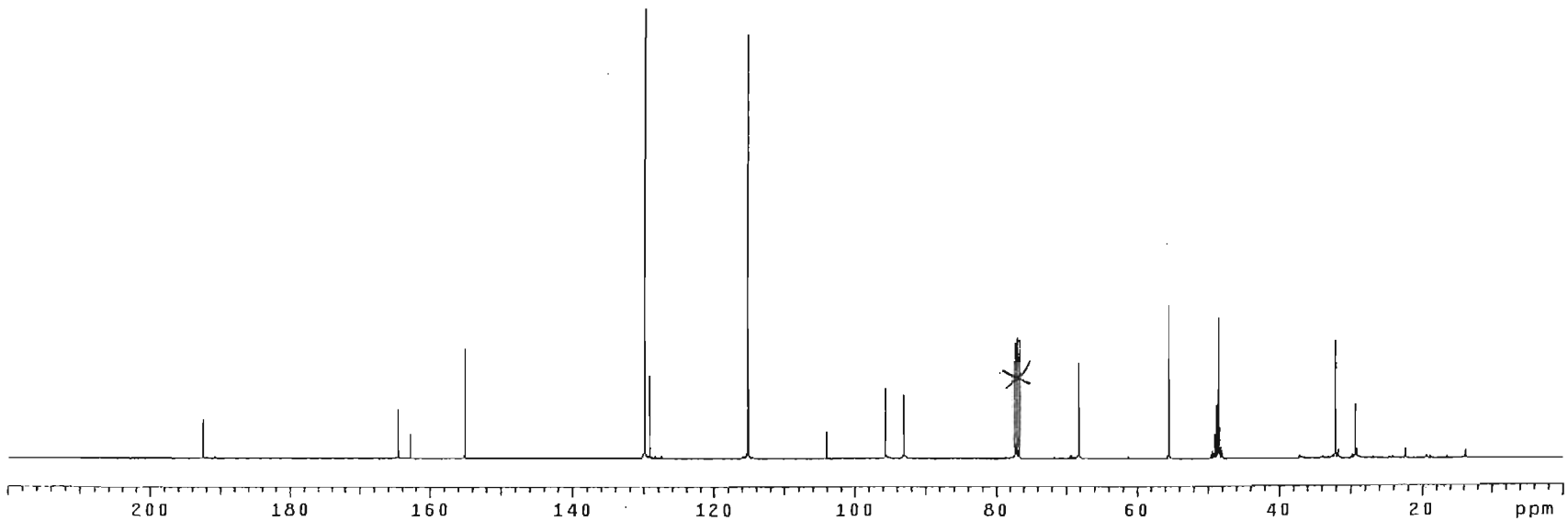

Spectrum 4b: ^{13}C NMR spectrum of compound **4** ($CDCl_3$)

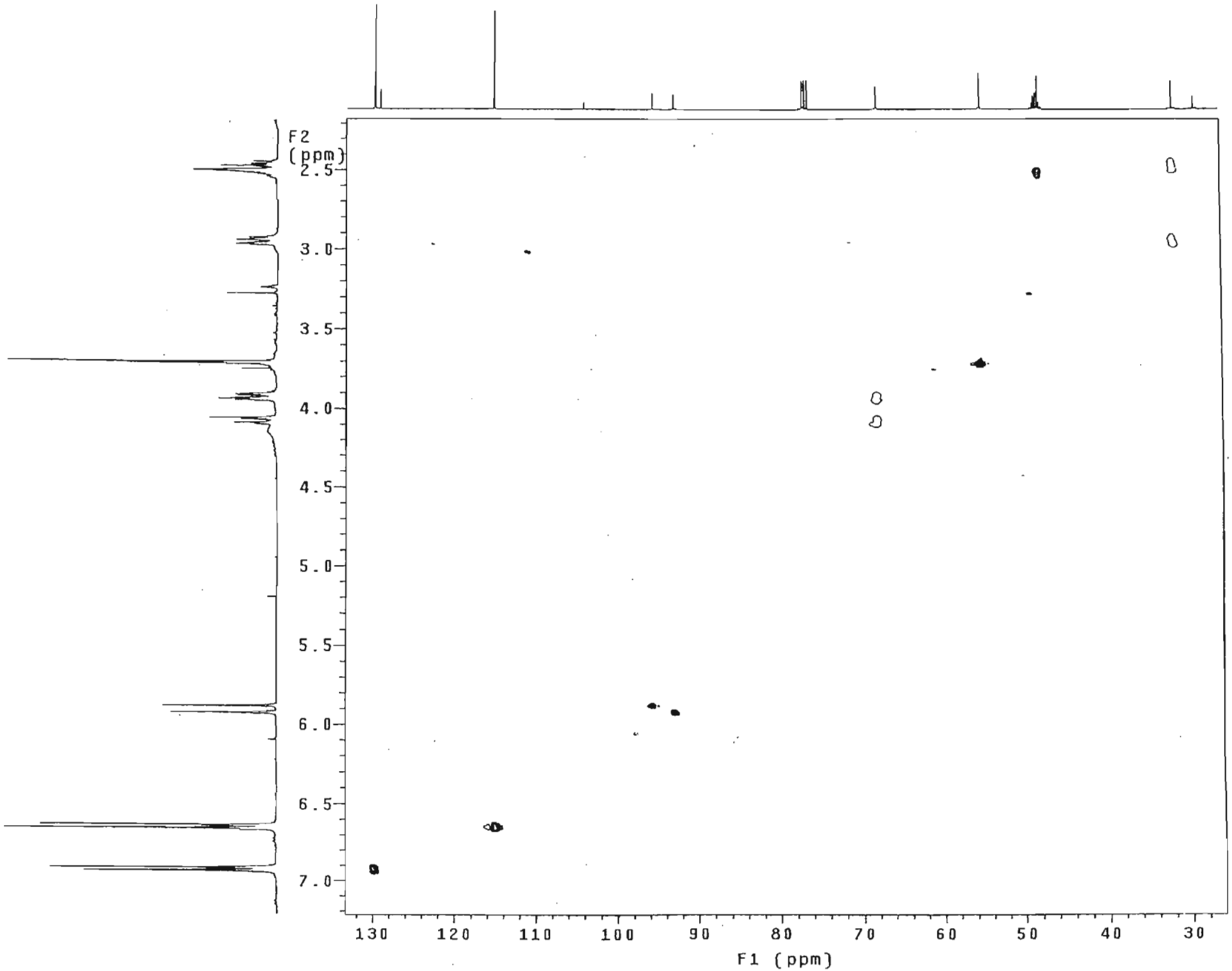

Spectrum 4c: HSQC spectrum of compound **4**

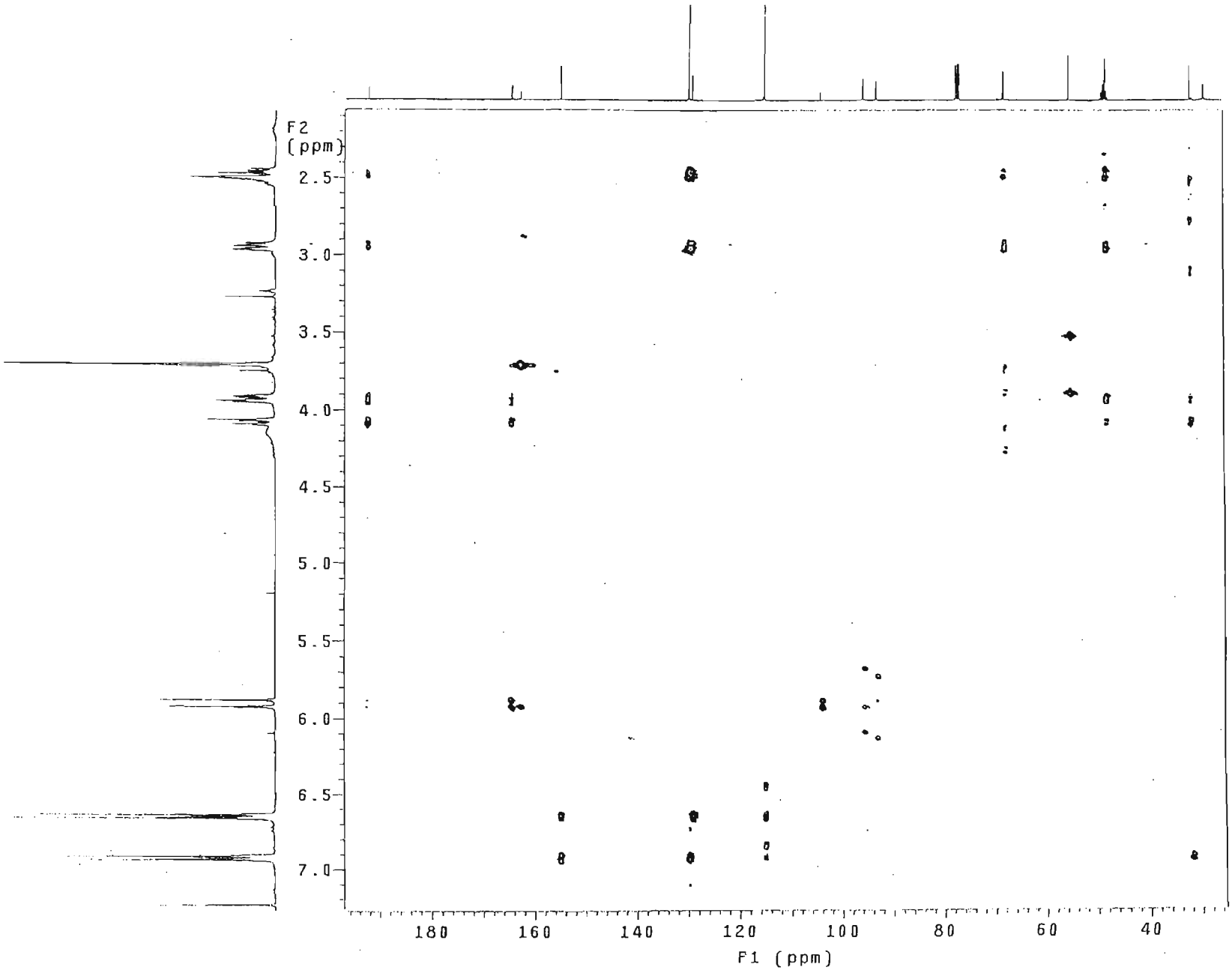

Spectrum 4d: HMBC spectrum of compound 4

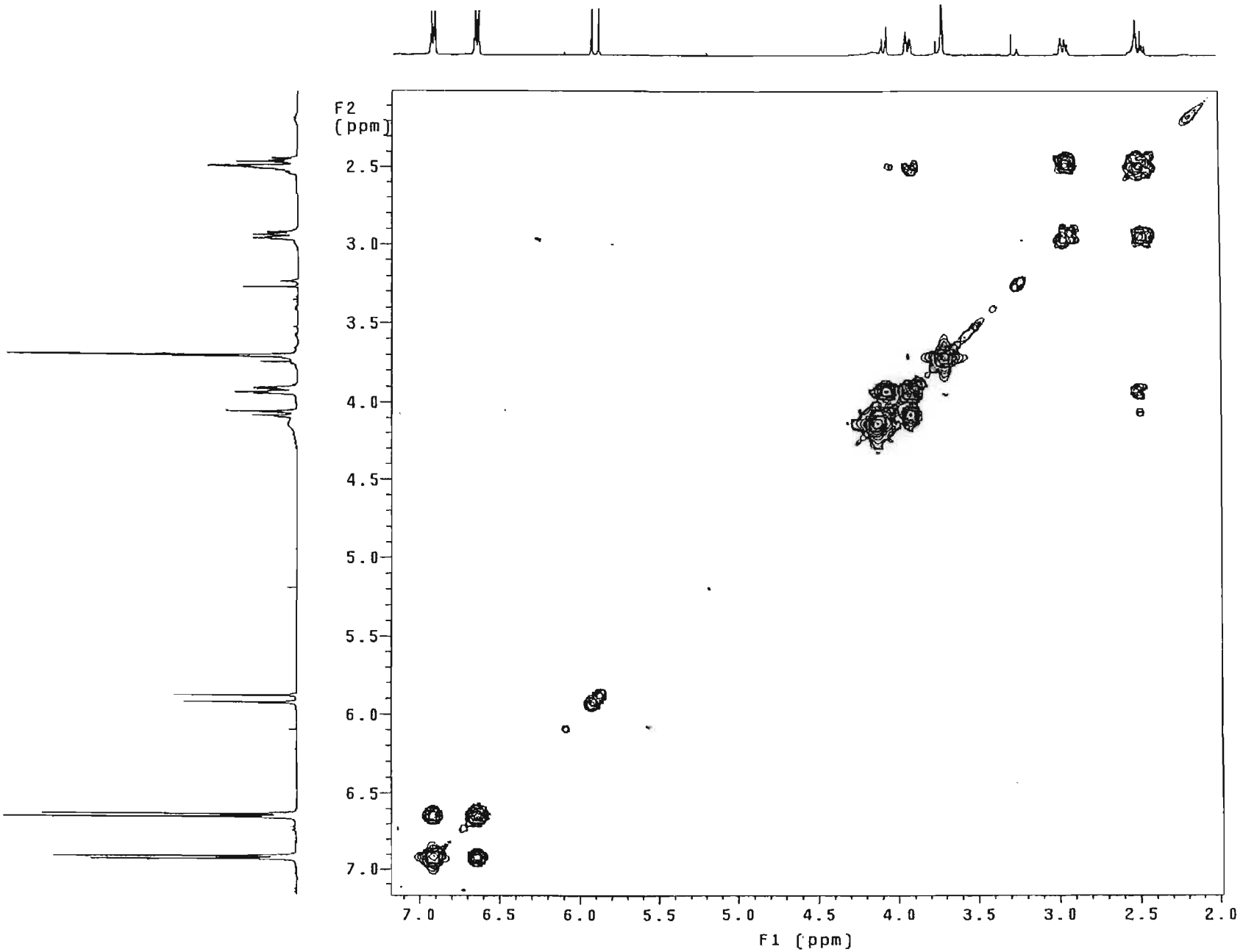

Spectrum 4e: COSY spectrum of compound 4

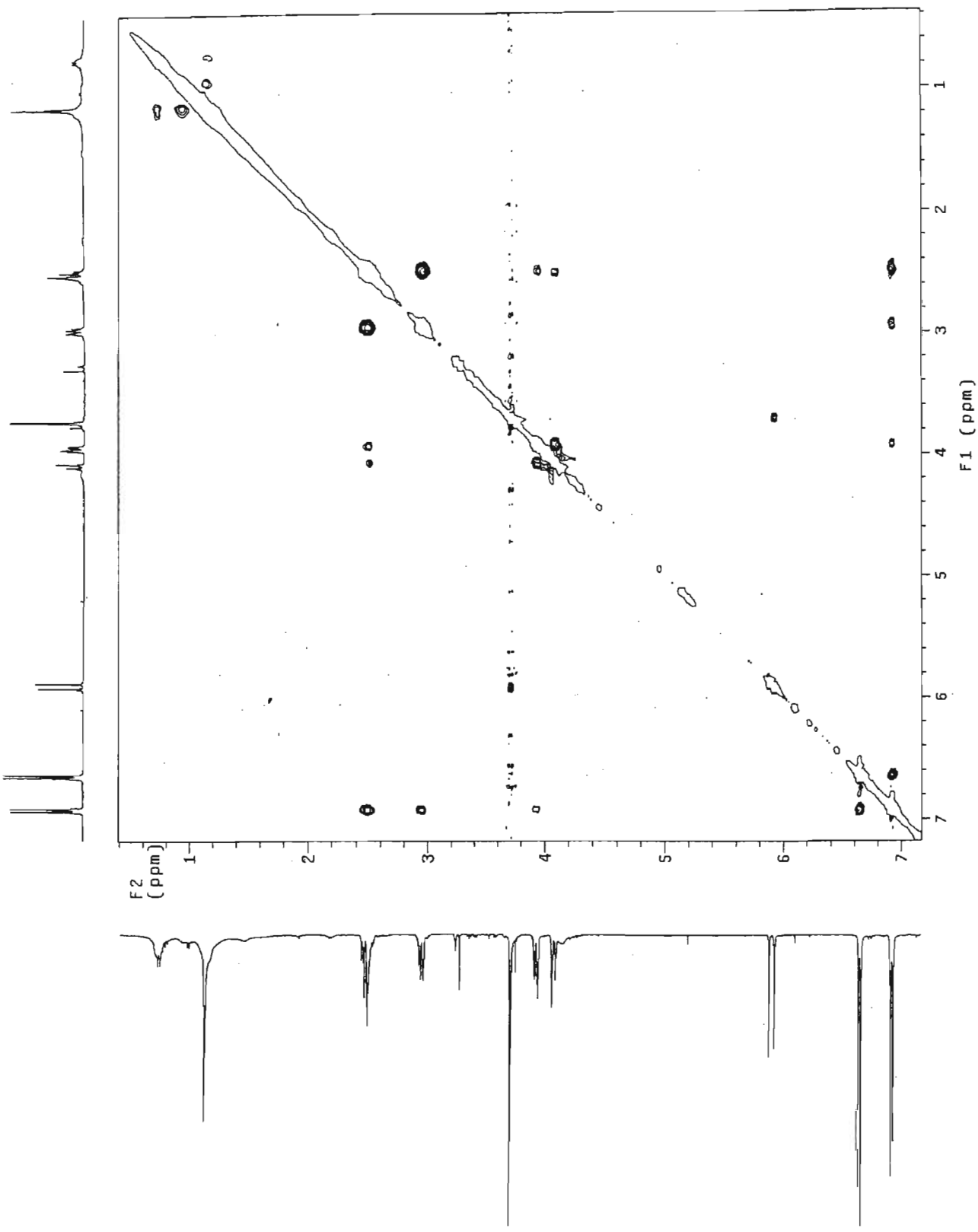

Spectrum 4f: NOESY spectrum of compound **4**

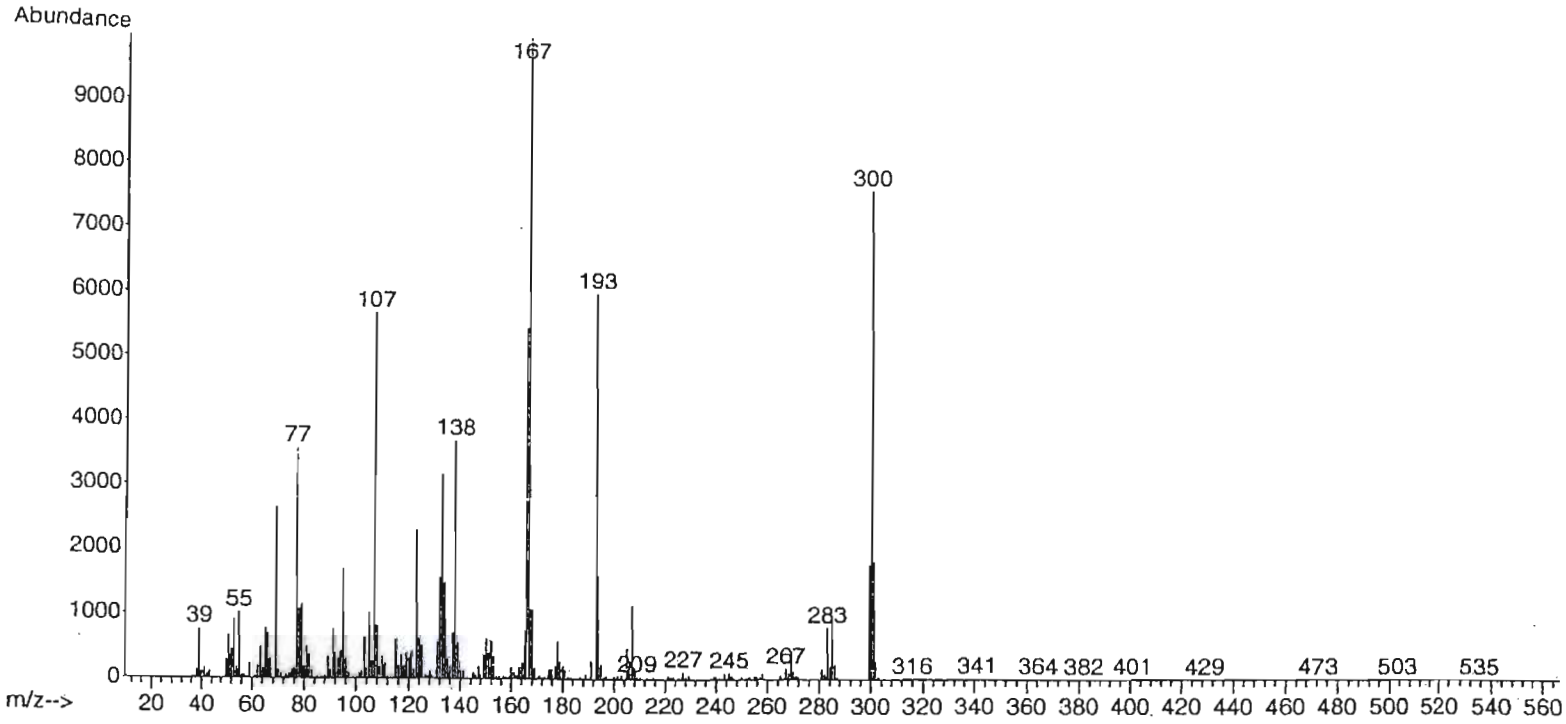

Spectrum 4g: Mass spectrum of compound **4**

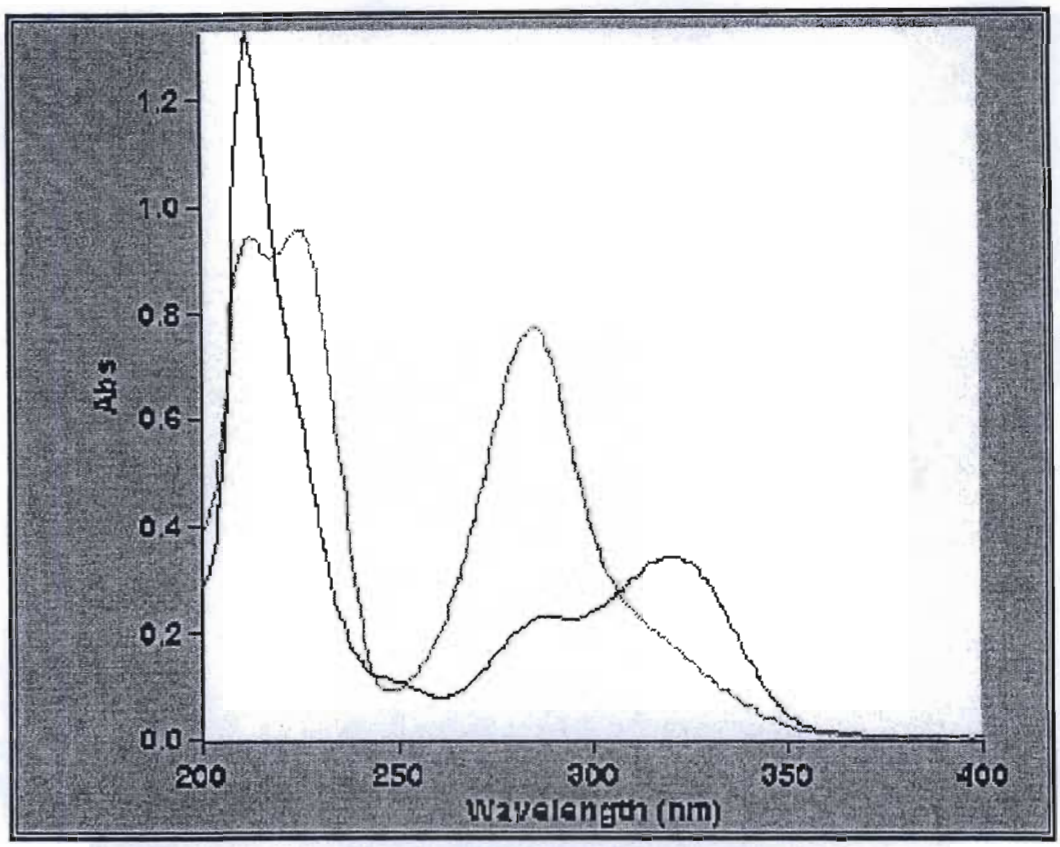

Spectrum 4h: UV spectrum + UV (NAOAc) spectrum of compound 4

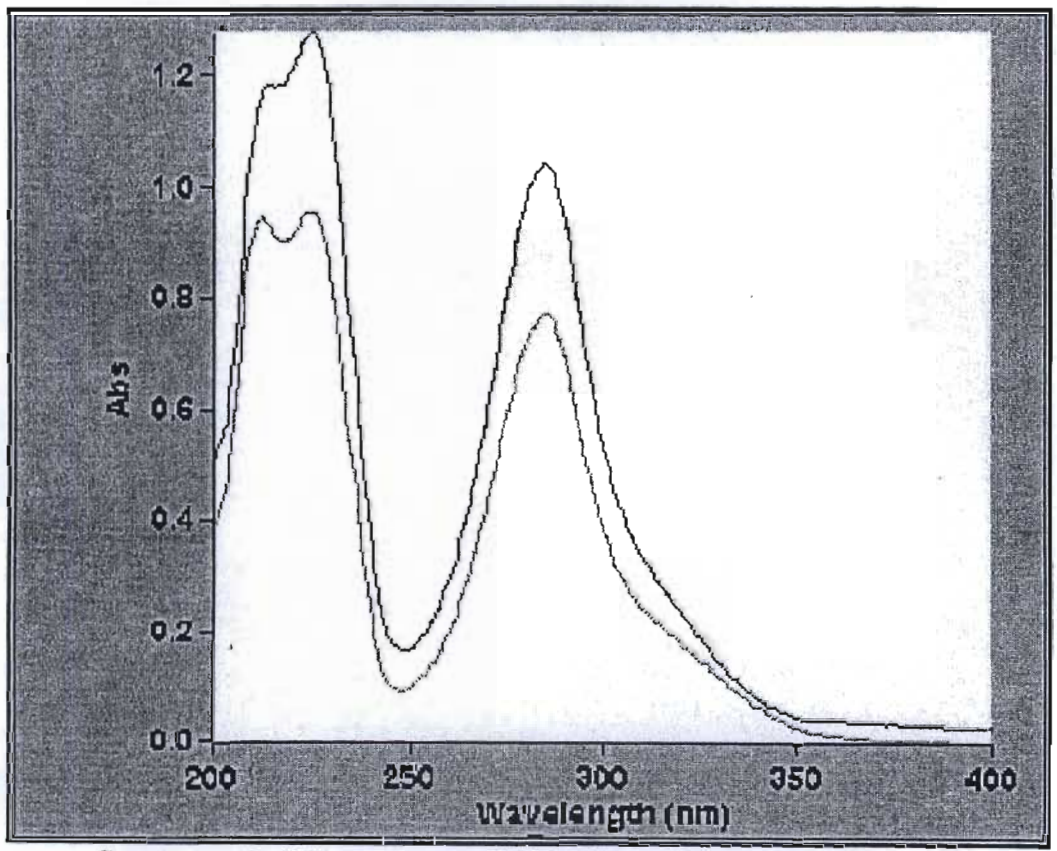

Spectrum 4h: UV spectrum + UV ($AlCl_3$) spectrum of compound 4

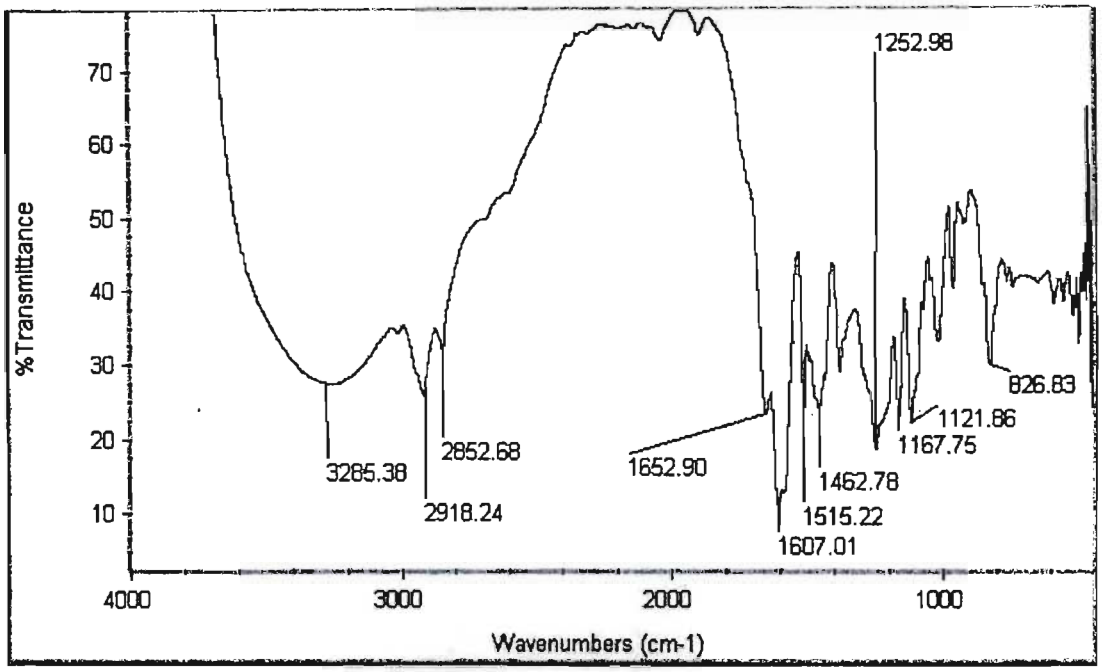

Spectrum 4j: IR spectrum of compound 4

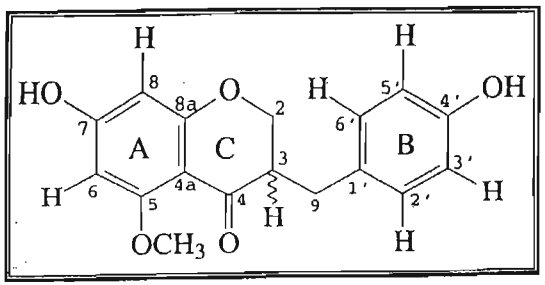

Spectrum 4k: ^{1}H NMR spectrum of compound **4** (CD_3OD)

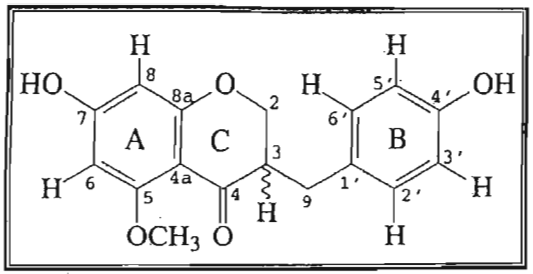

Spectrum 41: ^{13}C NMR spectrum of compound **4** (CD_3OD)

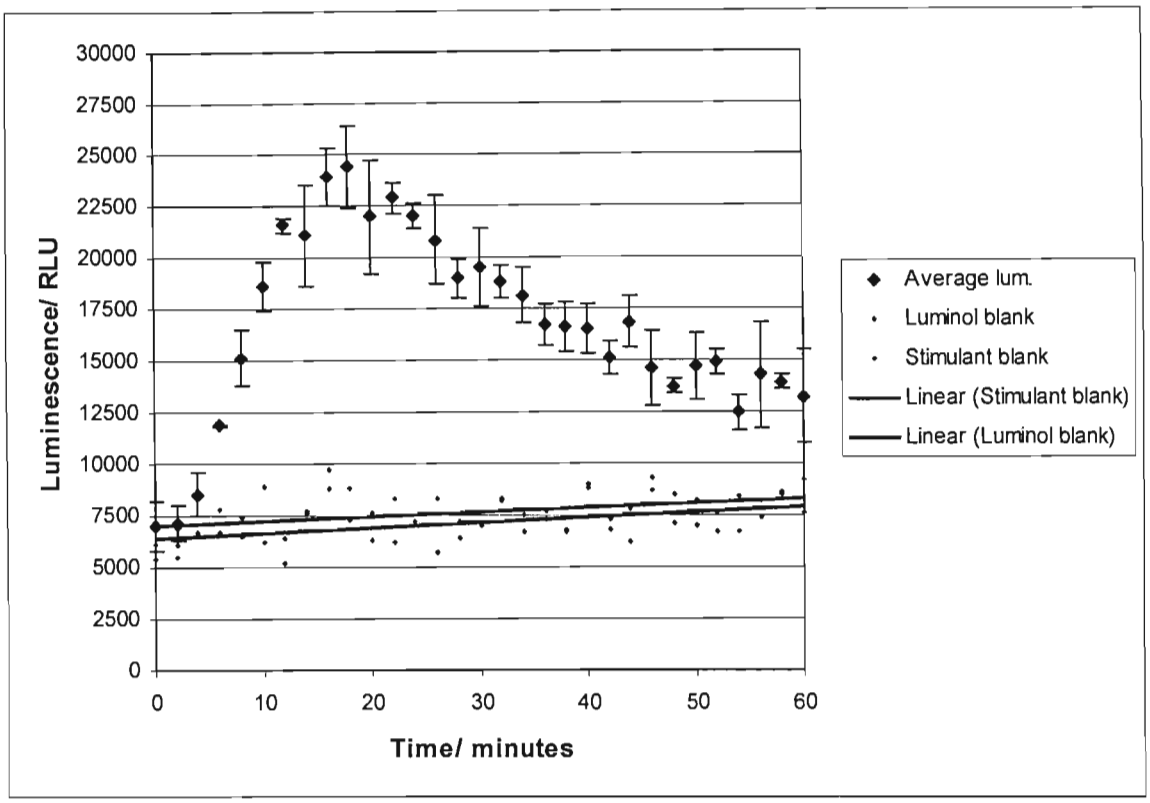

Graph 1: Graph of varying concentrations of luminol solution. Volume of blood cells and opsonized zymosan stimulant were kept constant at 400uL and 100uL respectively, 1mM luminol solution.

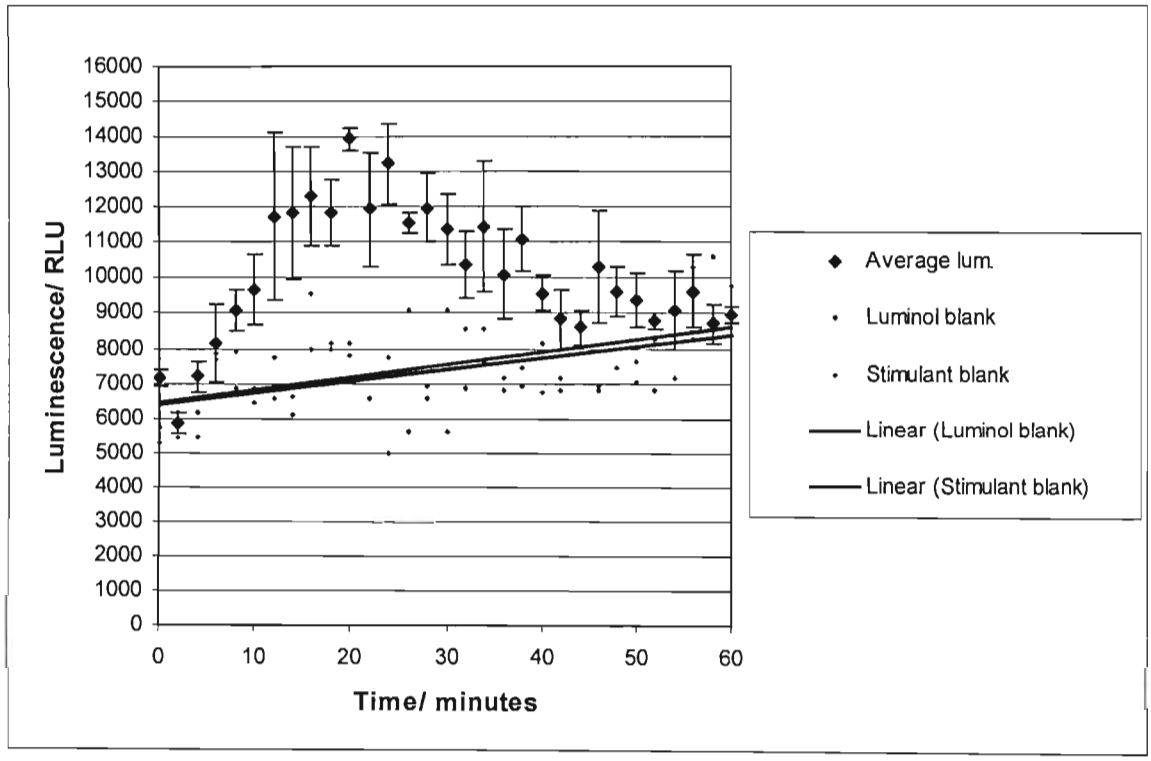

Graph 2: Graph of varying concentrations of luminol solution. Volume of blood cells and opsonized zymosan stimulant were kept constant at 400uL and 100uL respectively, 3mM luminol solution.

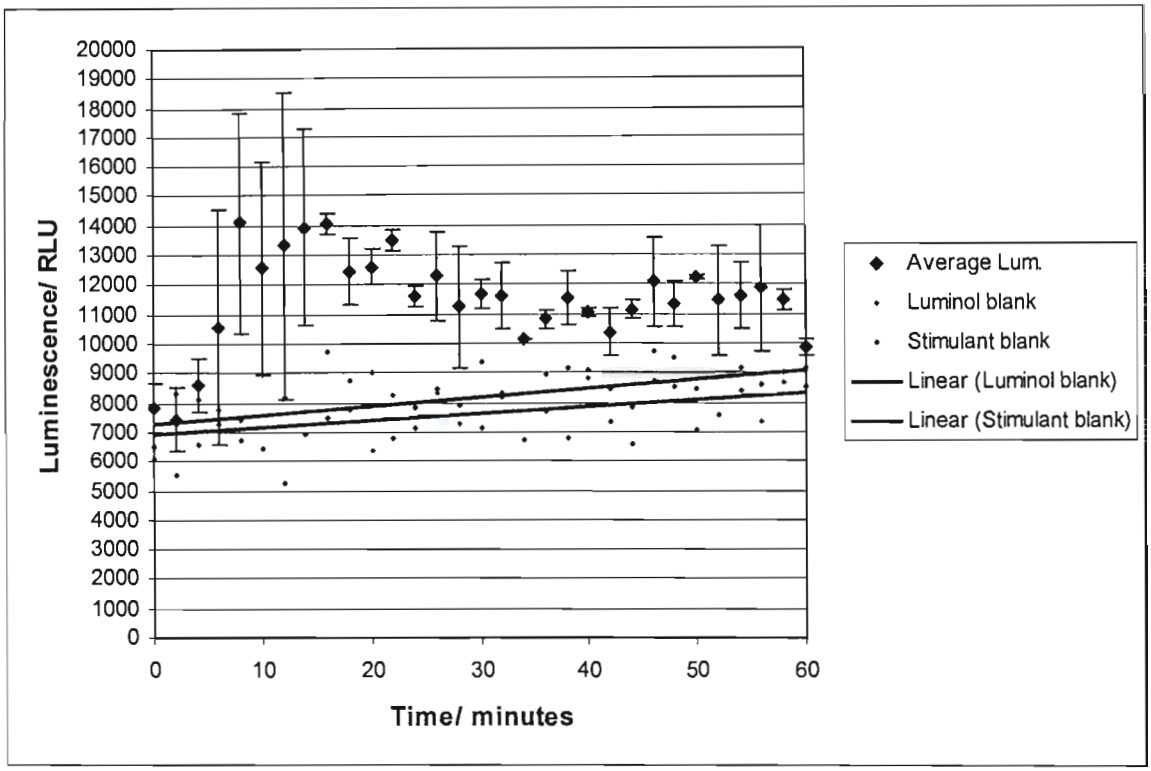

Graph 3: Graph of varying concentrations of luminol solution. Volume of blood cells and opsonized zymosan stimulant were kept constant at 400uL and 100uL respectively, 5mM luminol solution.

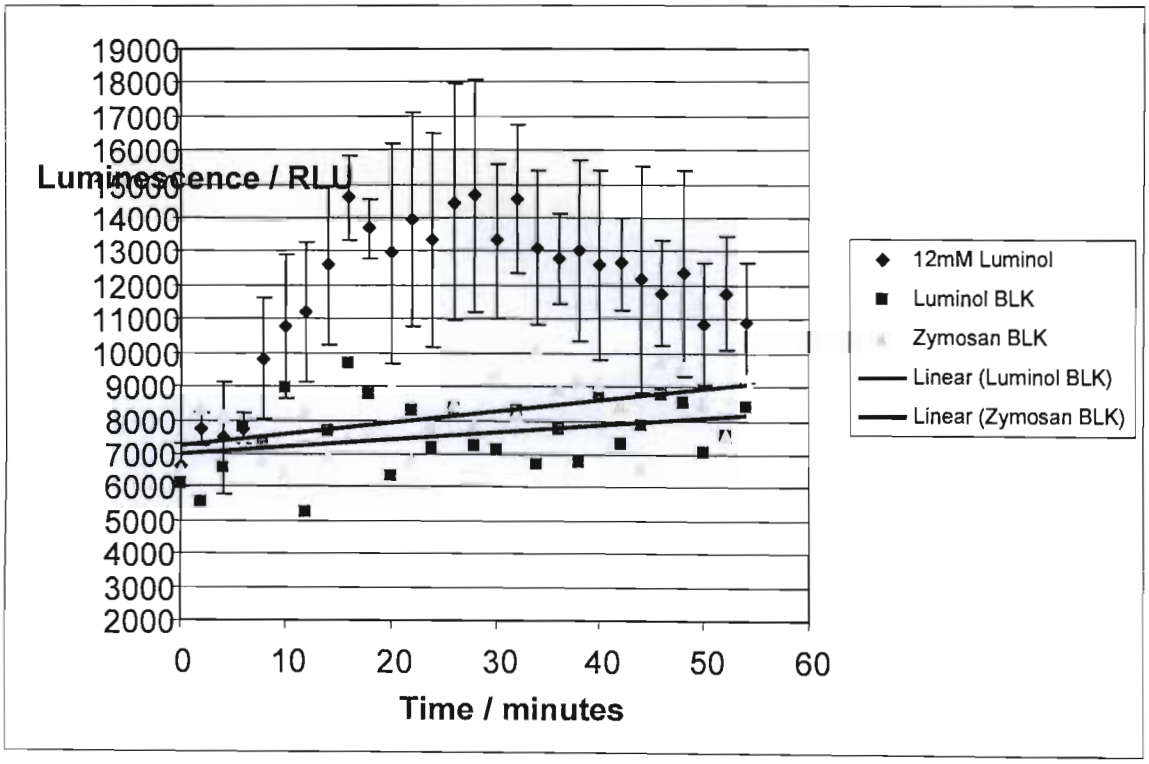

Graph 4: Graph of varying concentrations of luminol solution. Volume of blood cells and opsonized zymosan stimulant were kept constant at 400uL and 100uL respectively, 12mM luminol solution.

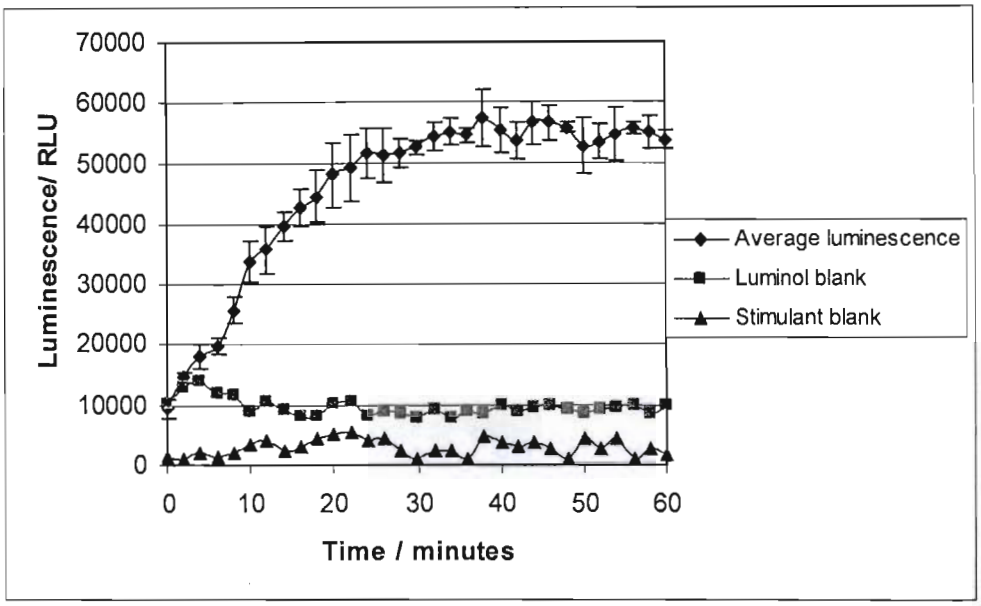

Graph 5: Graph of varying volumes of luminol solution, opsonized zymosan, and blood cells. 400µL blood cells, 50µL luminol, 50µL zymosan.

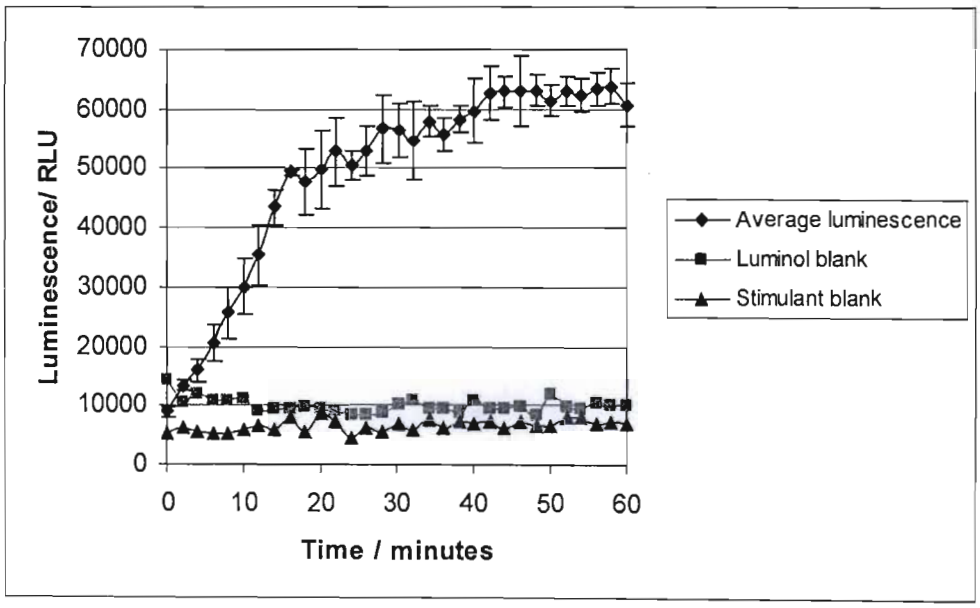

Graph 6: Graph of varying volumes of luminol solution, opsonized zymosan, and blood cells. 400µL blood cells, 100µL luminol, 50µL zymosan.

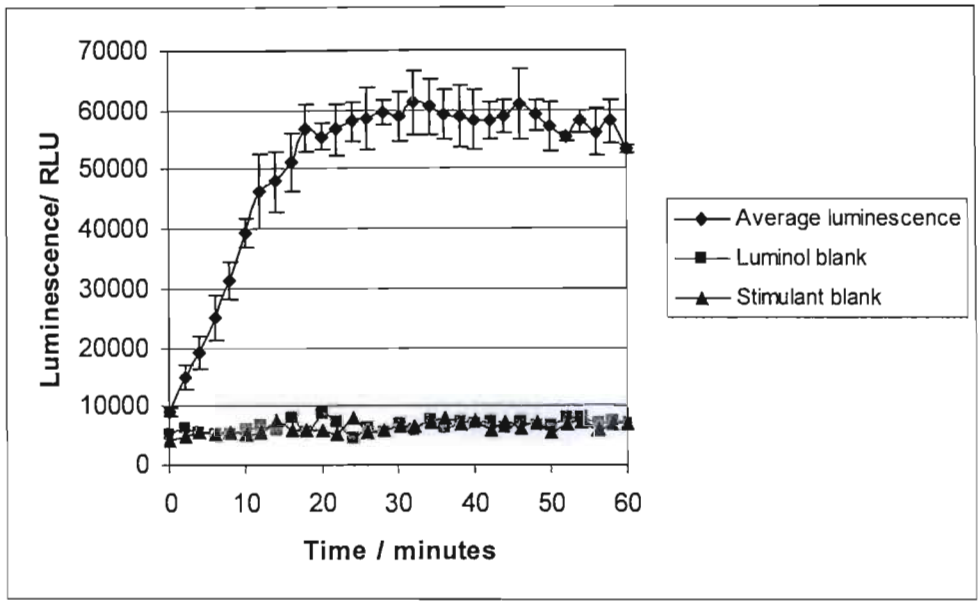

Graph 7: Graph of varying volumes of luminol solution, opsonized zymosan, and blood cells. 400µL blood cells, 100µL luminol, 100µL zymosan.

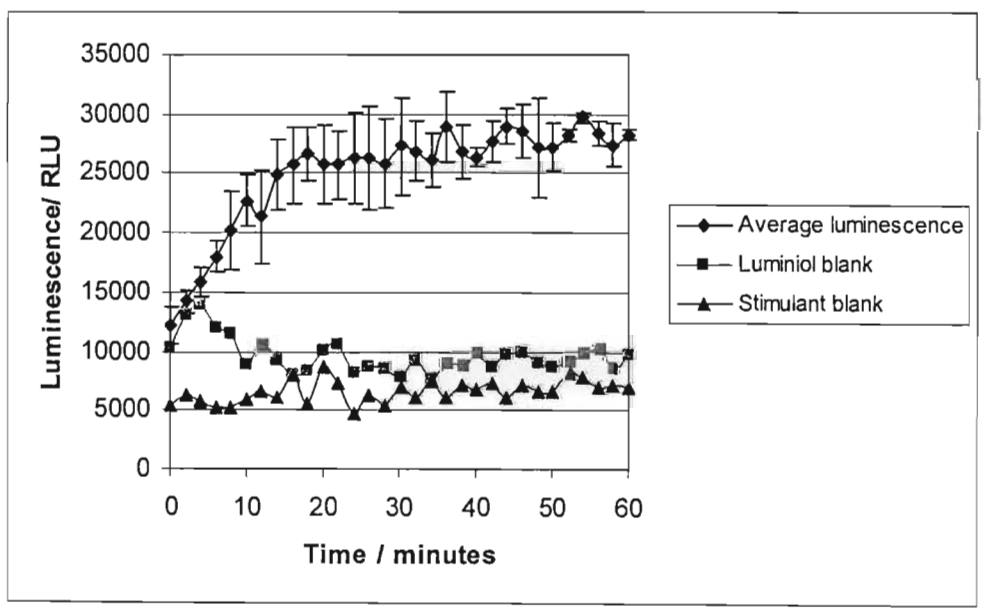

Graph 8: Graph of varying volumes of luminol solution, opsonized zymosan, and blood cells. 500µL blood cells, 50µL luminol, 50µL zymosan.

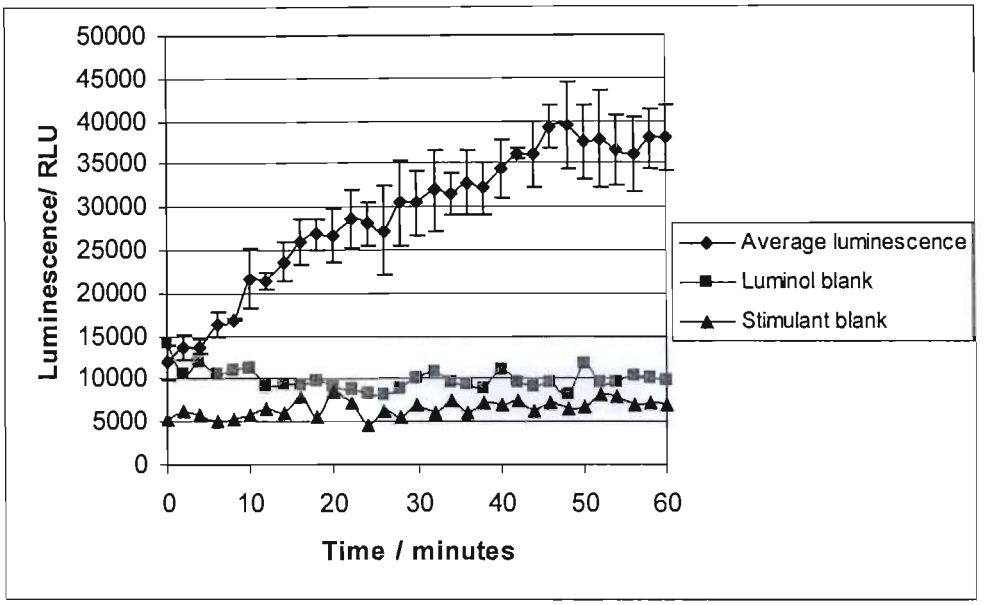

Graph 9: Graph of varying volumes of luminol solution, opsonized zymosan, and blood cells. 500μL blood cells, 100μL luminol, 50μL zymosan.

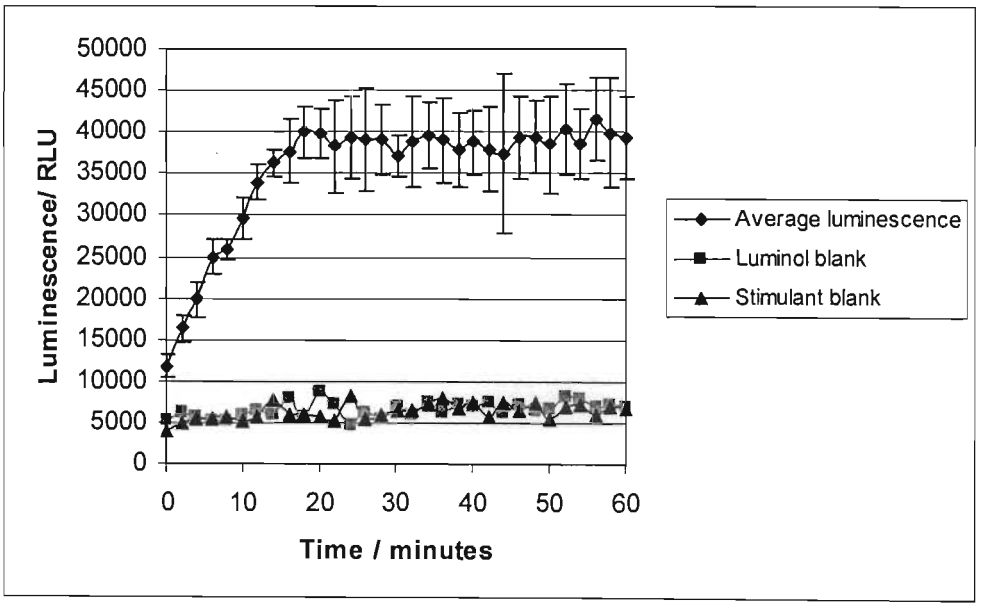

Graph 10: Graph of varying volumes of luminol solution, opsonized zymosan, and blood cells. 500μL blood cells, 100μL luminol, 100μL zymosan.

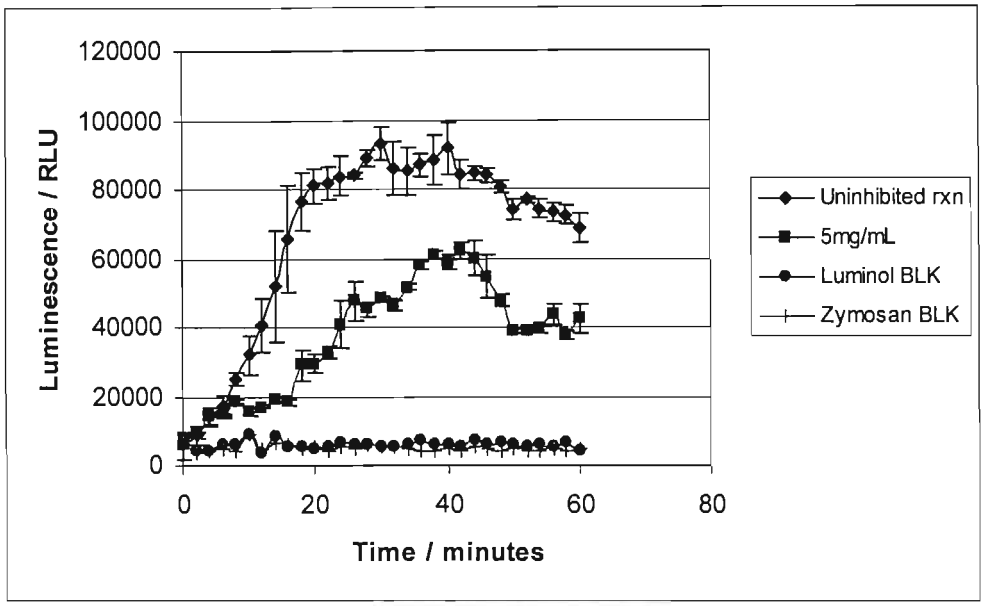

Graph 11: Graph of anti-inflammatory activity of compound 2. 50µL of compound 2 at 5mg/mL concentration was added.

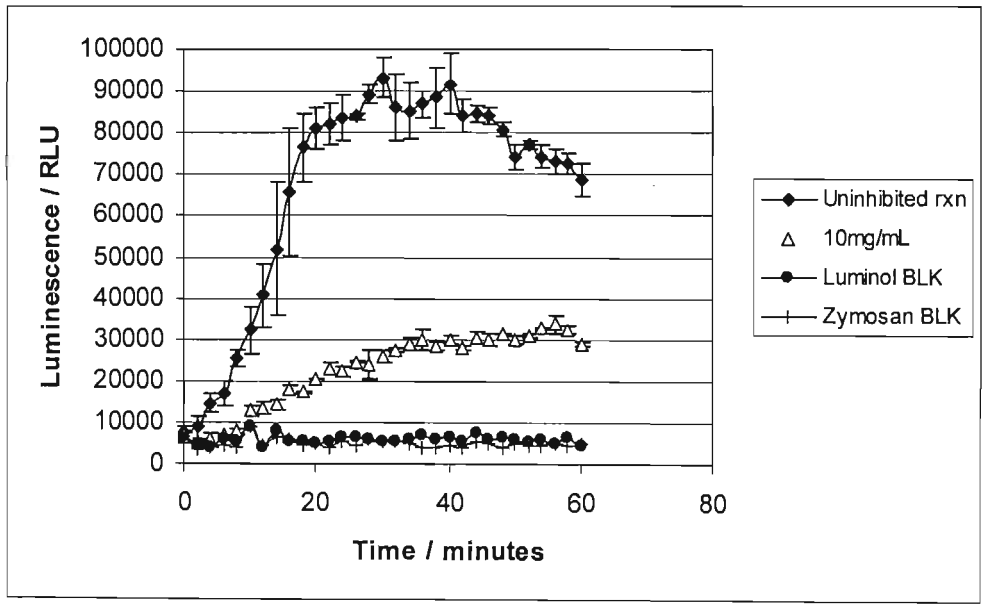

Graph 12: Graph of anti-inflammatory activity of compound 2. 50µL of compound 2 at 10mg/mL concentration was added.

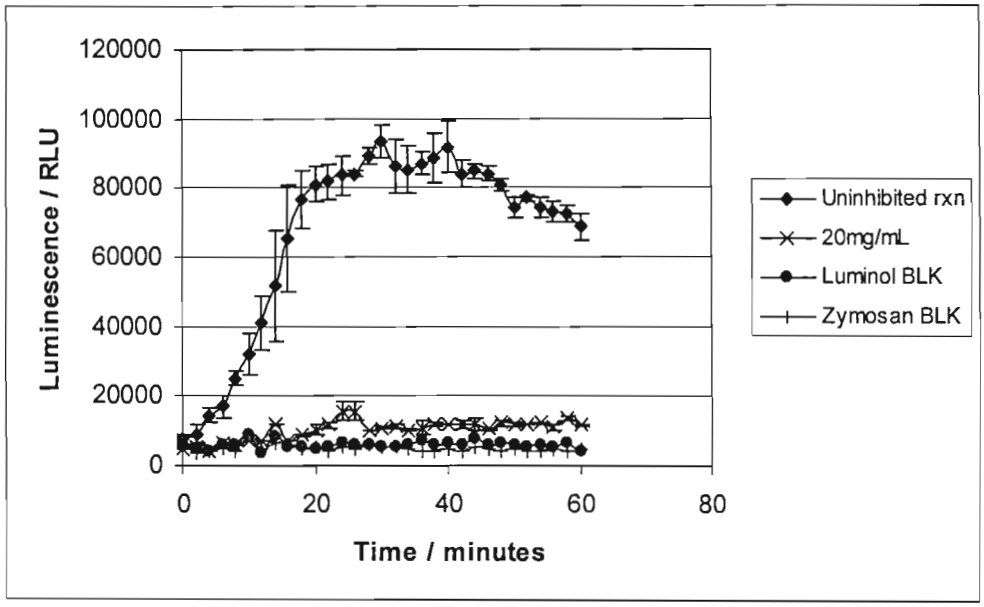

Graph 13: Graph of anti-inflammatory activity of compound 2. 50µL of compound 2 at 20mg/mL concentration was added.

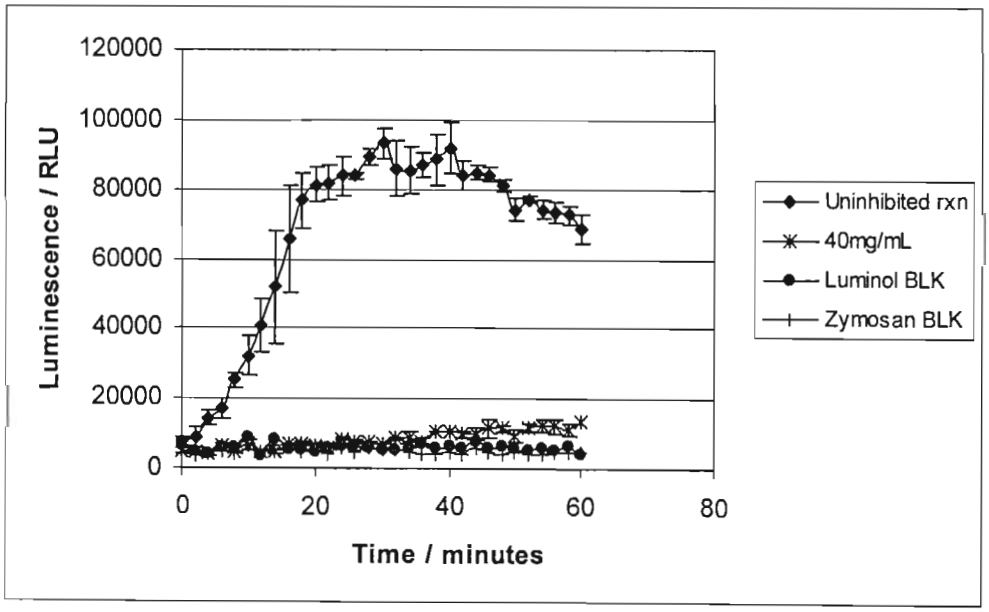

Graph 14: Graph of anti-inflammatory activity of compound 2. 50µL of compound 2 at 40mg/mL concentration was added.

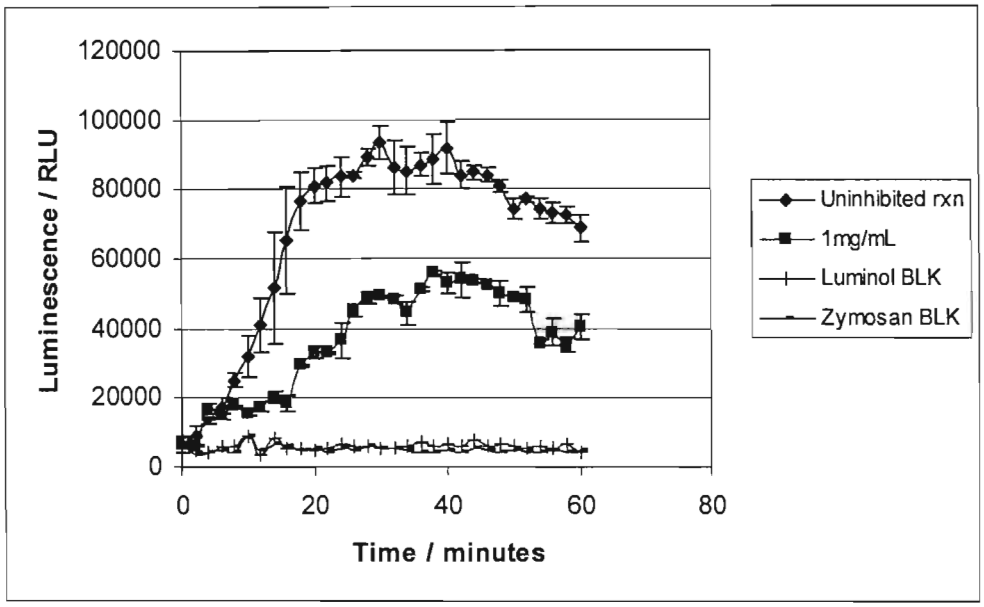

Graph 15: Graph of anti-inflammatory activity of compound 3. 50µL of compound 3at 1mg/mL concentration was added.

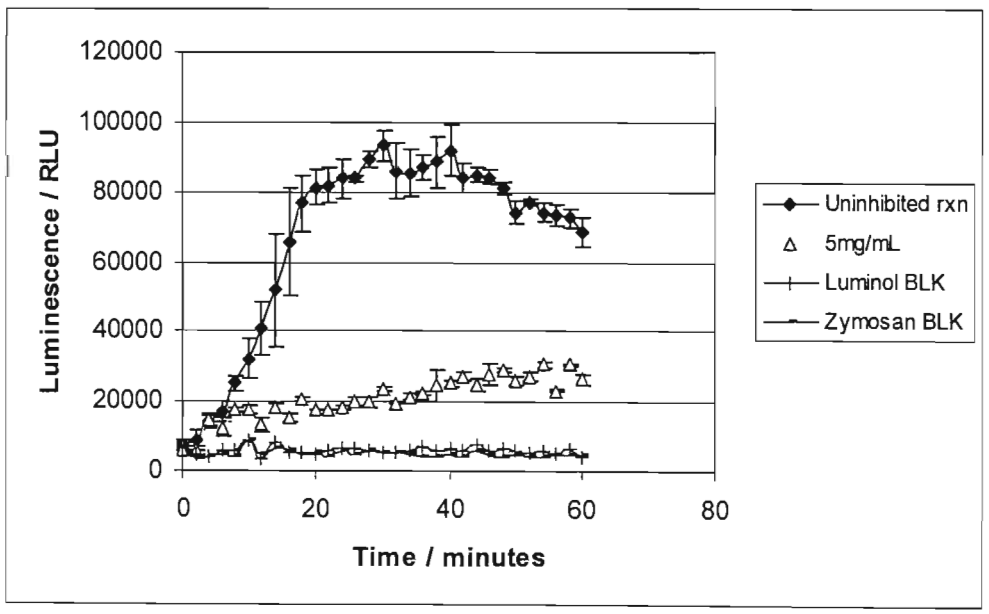

Graph 16: Graph of anti-inflammatory activity of compound 3. 50µL of compound 3at 5mg/mL concentration was added.

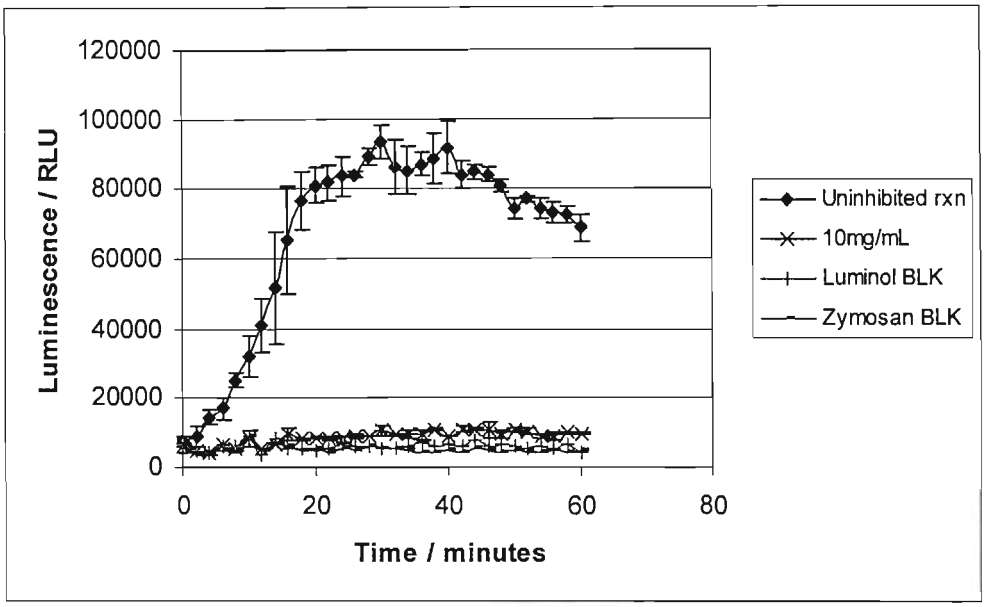

Graph 17: Graph of anti-inflammatory activity of compound 3. 50µL of compound 3at 10mg/mL concentration was added.

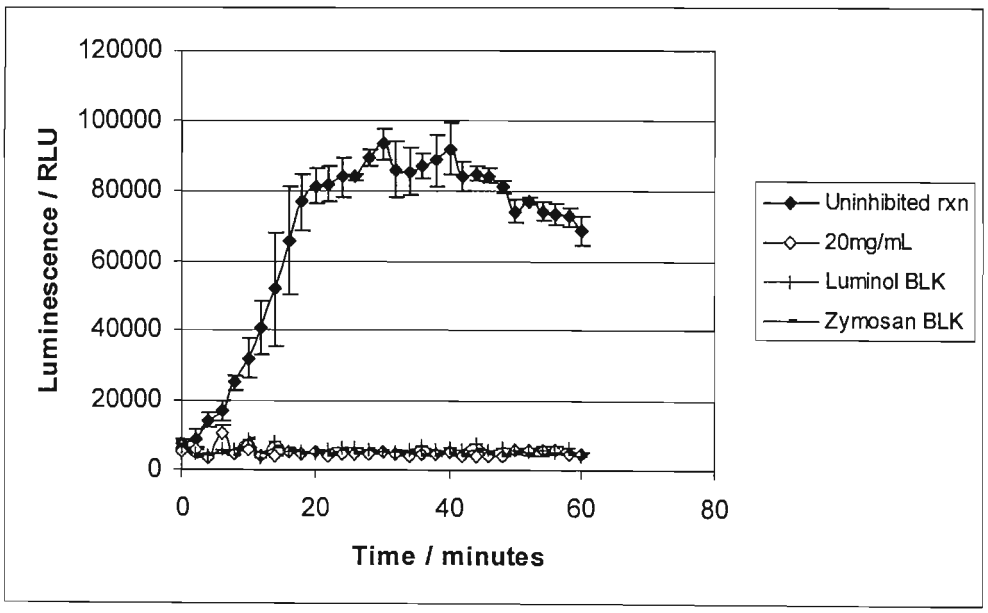

Graph 18: Graph of anti-inflammatory activity of compound 3. 50µL of compound 3at 20mg/mL concentration was added.

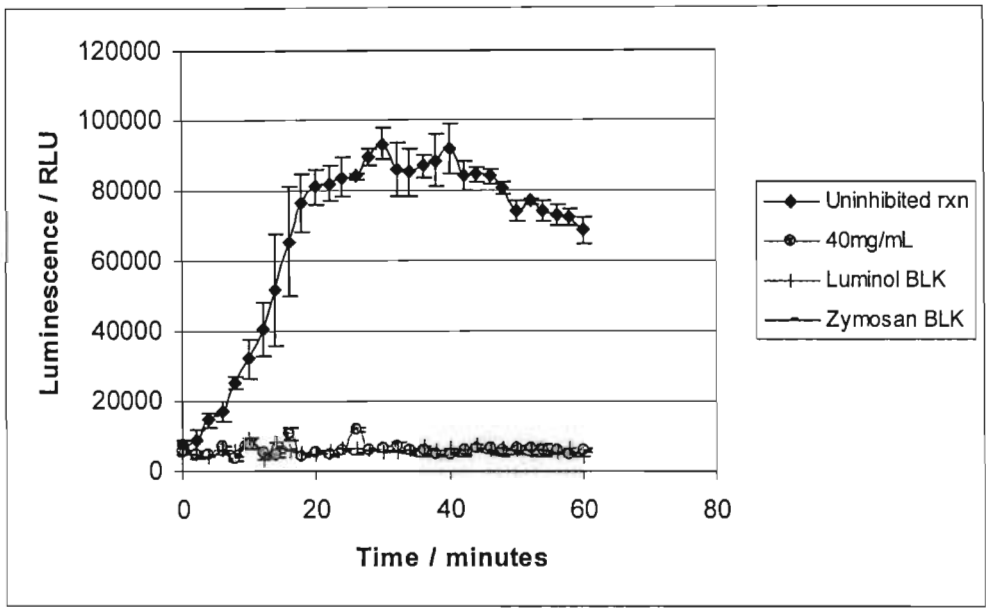

Graph 19: Graph of anti-inflammatory activity of compound 3. 50µL of compound 3at 40mg/mL concentration was added.

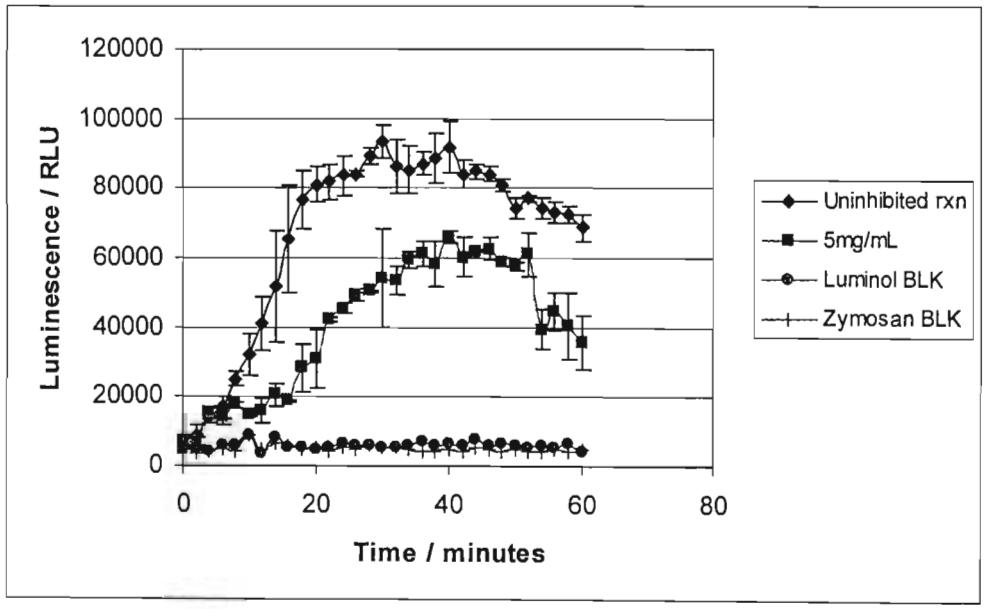

Graph 20: Graph of anti-inflammatory activity of compound 4. 50µL of compound 4at 5mg/mL concentration was added.

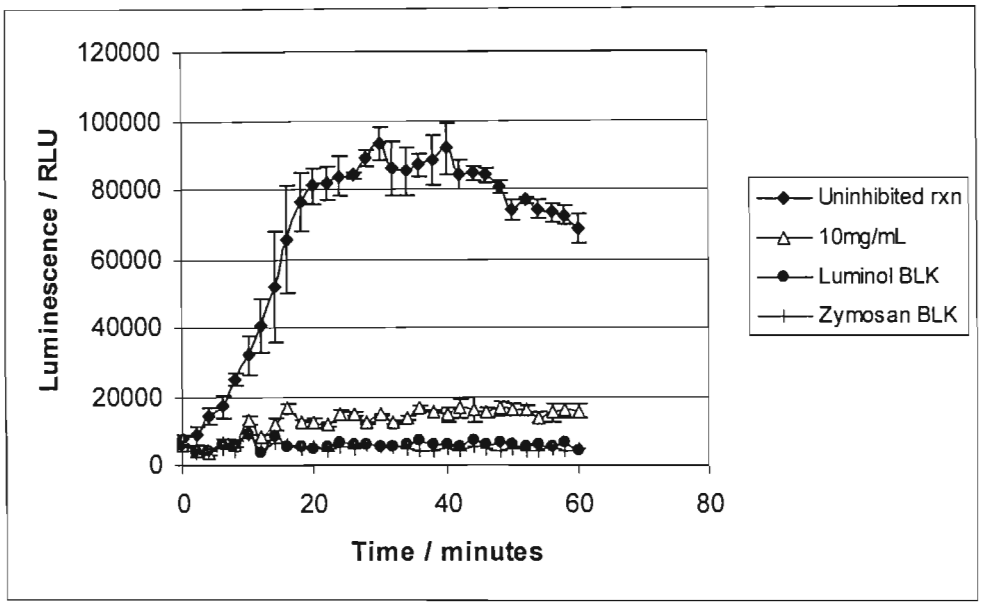

Graph 21: Graph of anti-inflammatory activity of compound 4. 50µL of compound 4at 10mg/mL concentration was added.

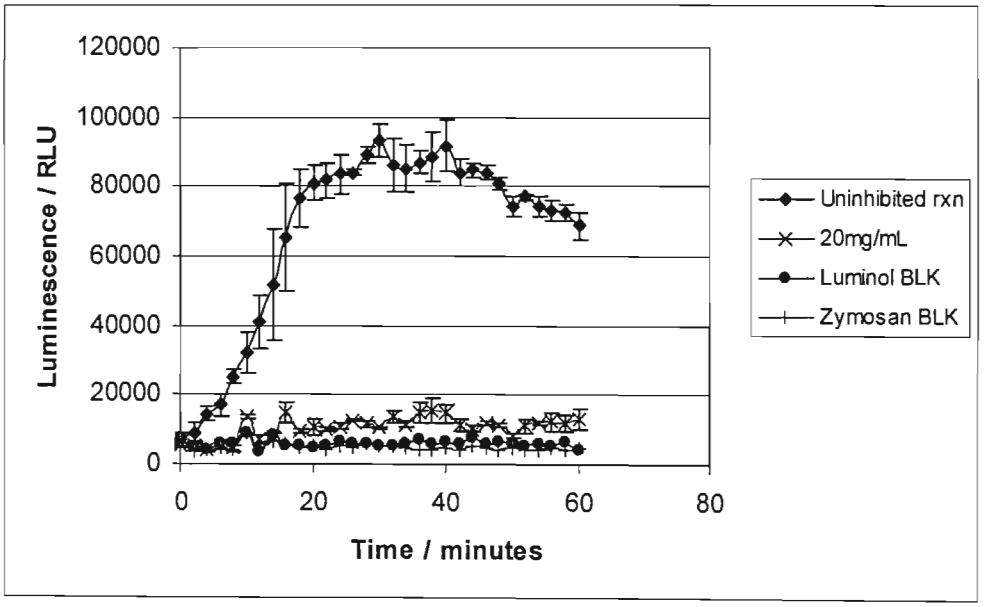

Graph 22: Graph of anti-inflammatory activity of compound 4. 50µL of compound 4at 20mg/mL concentration was added.

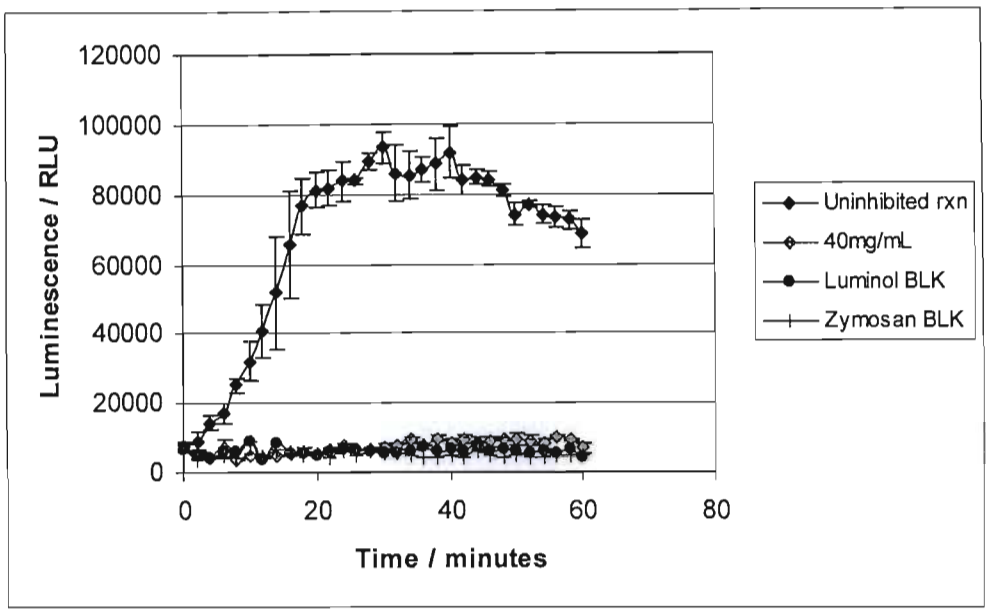

Graph 23: Graph of anti-inflammatory activity of compound 4. 50µL of compound 4at 40mg/mL concentration was added.

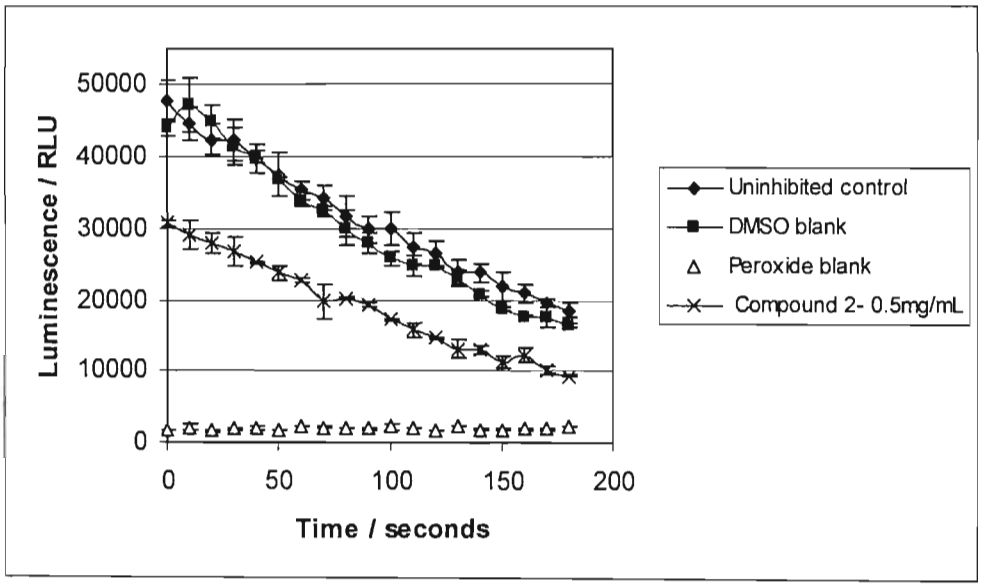

Graph 24: Results of Antioxidant/ free radical scavenging activity of compound 2, 0.5mg/mL concentration

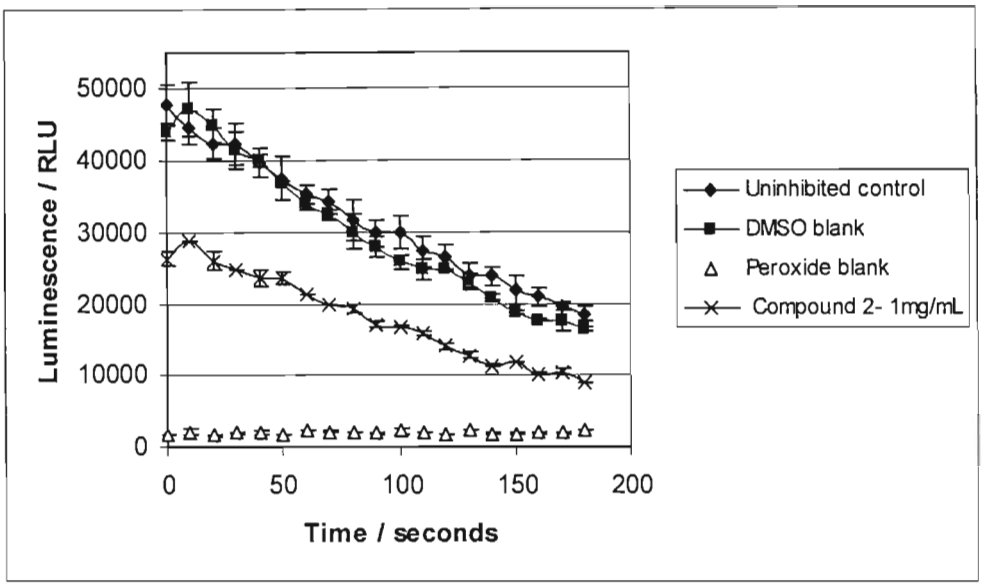

Graph 25: Results of Antioxidant/ free radical scavenging activity of compound 2, 1mg/mL concentration

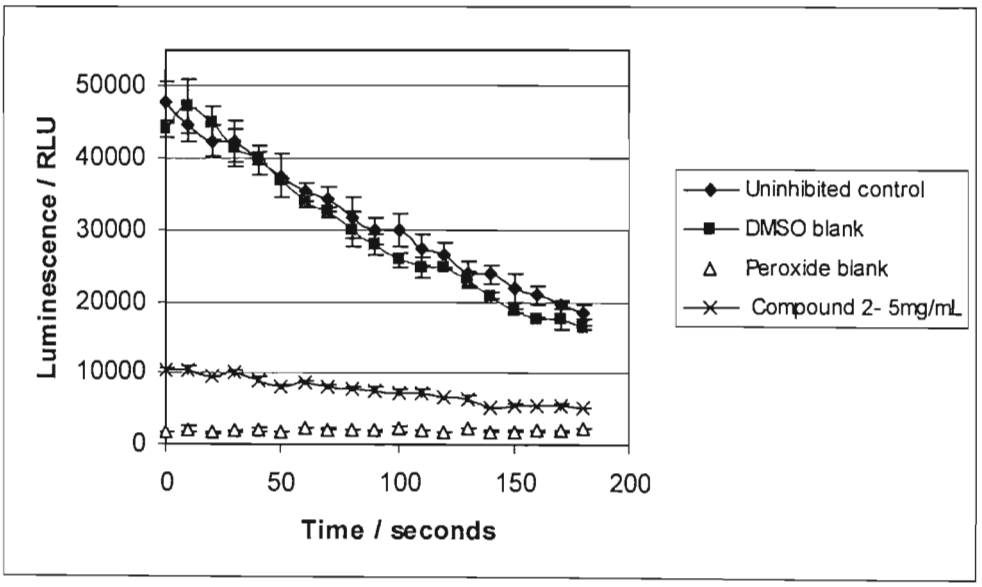

Graph 26: Results of Antioxidant/ free radical scavenging activity of compound 2, 5mg/mL concentration

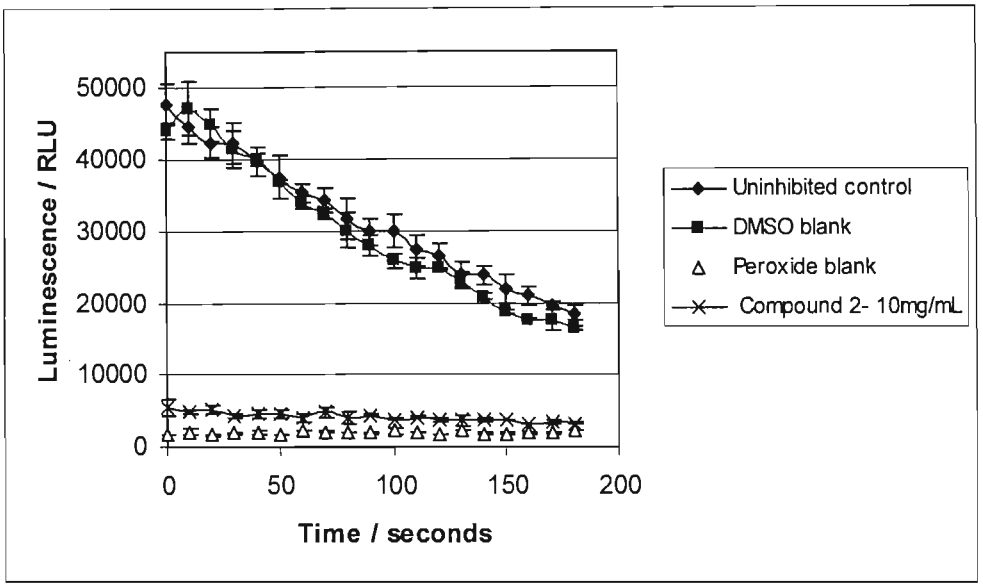

Graph 27: Results of Antioxidant/ free radical scavenging activity of compound 2, 10mg/mL concentration

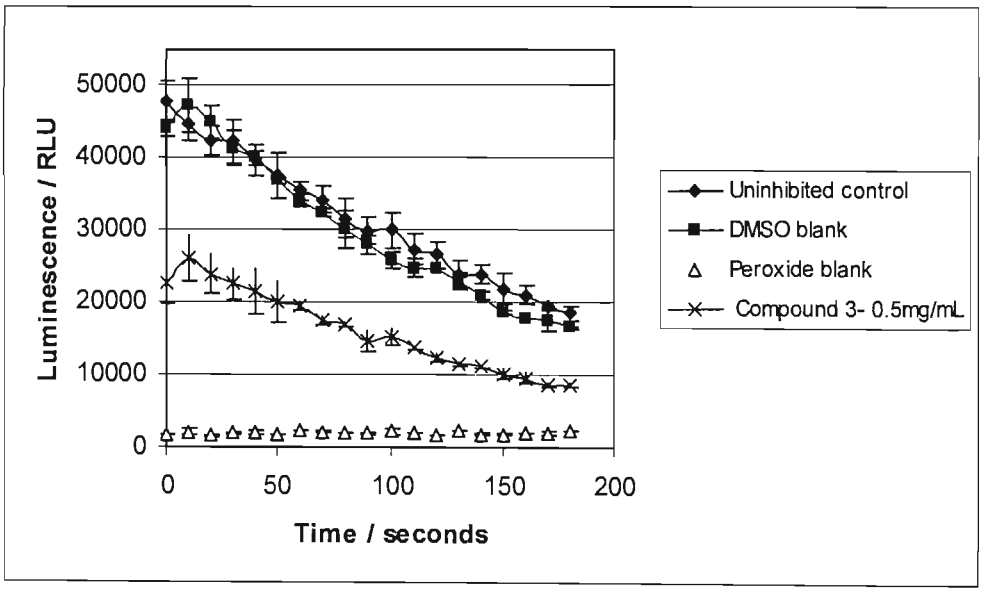

Graph 28: Results of Antioxidant/ free radical scavenging activity of compound 3, 0.5mg/mL concentration

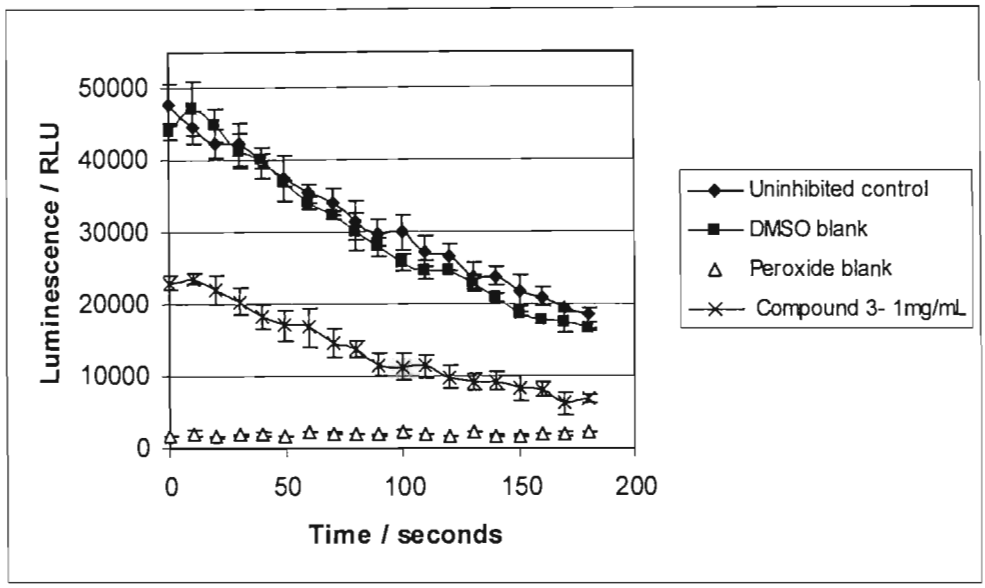

Graph 29: Results of Antioxidant/ free radical scavenging activity of compound 3, 1mg/mL concentration

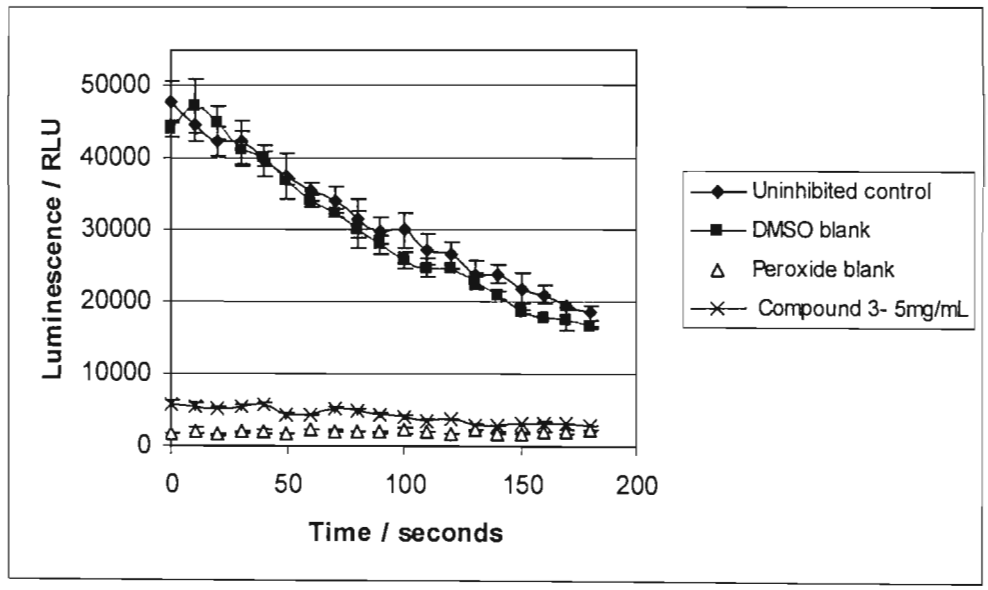

Graph 30: Results of Antioxidant/ free radical scavenging activity of compound 3, 5mg/mL concentration

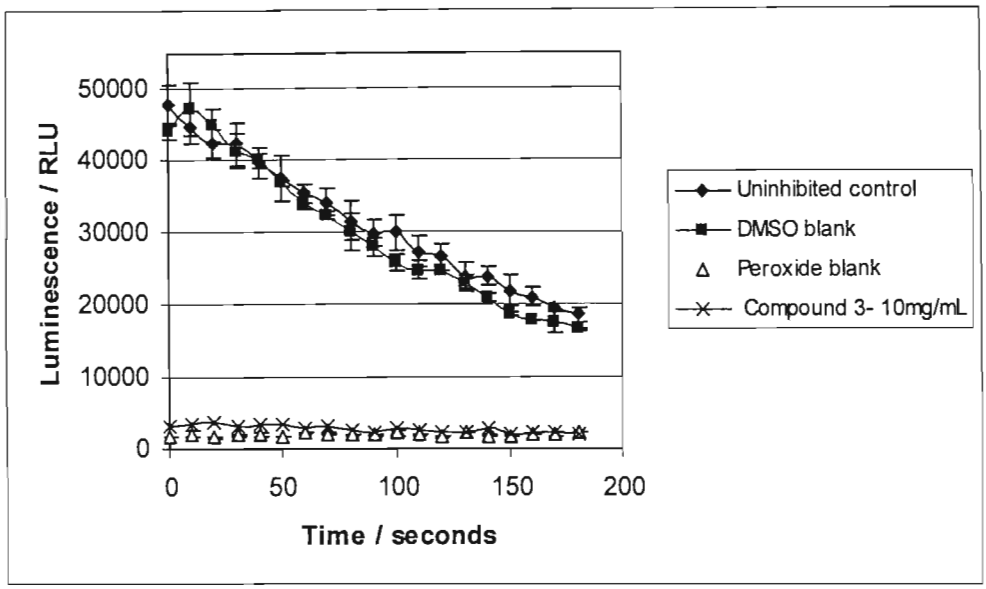

Graph 31: Results of Antioxidant/ free radical scavenging activity of compound 3, 10mg/mL concentration

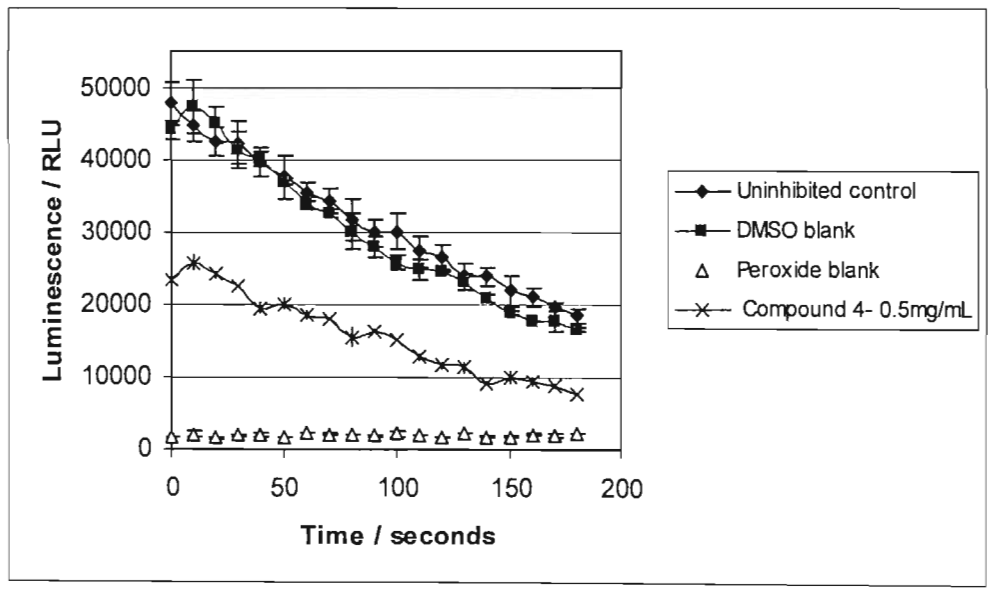

Graph 32: Results of Antioxidant/ free radical scavenging activity of compound 4, 0.5mg/mL concentration

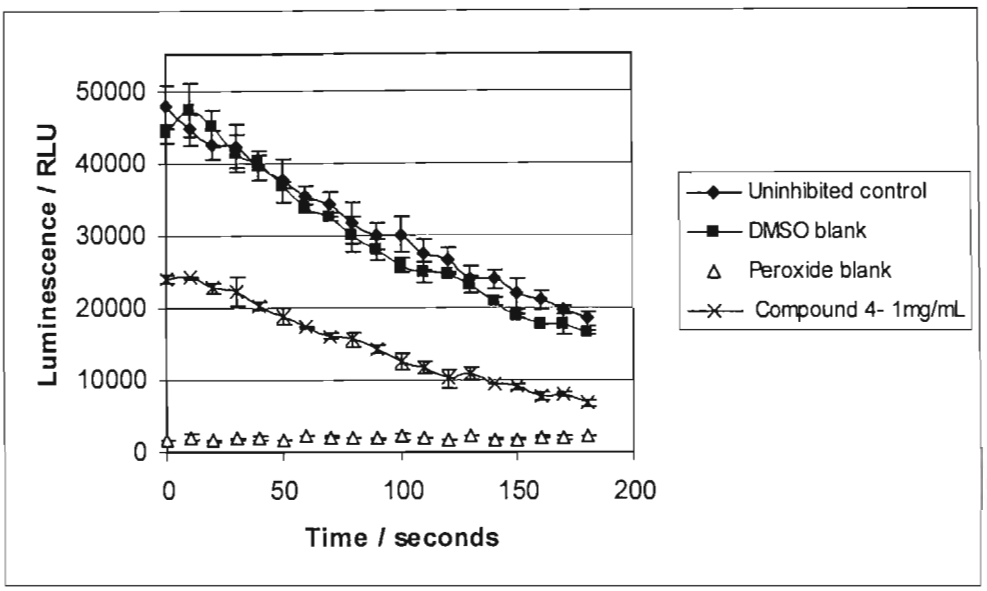

Graph 33: Results of Antioxidant/ free radical scavenging activity of compound 4, 1mg/mL concentration

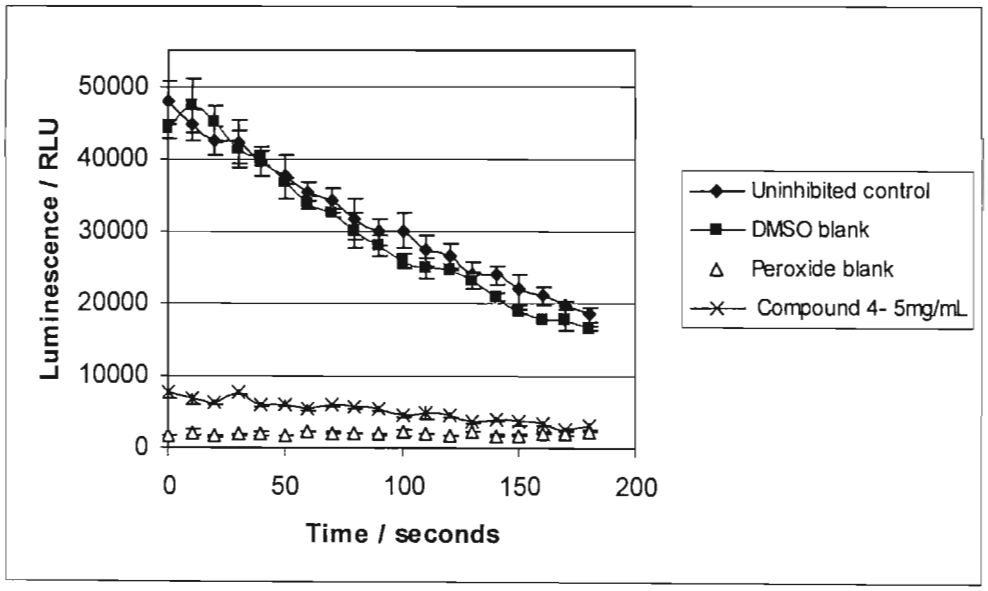

Graph 34: Results of Antioxidant/ free radical scavenging activity of compound 4, 5mg/mL concentration

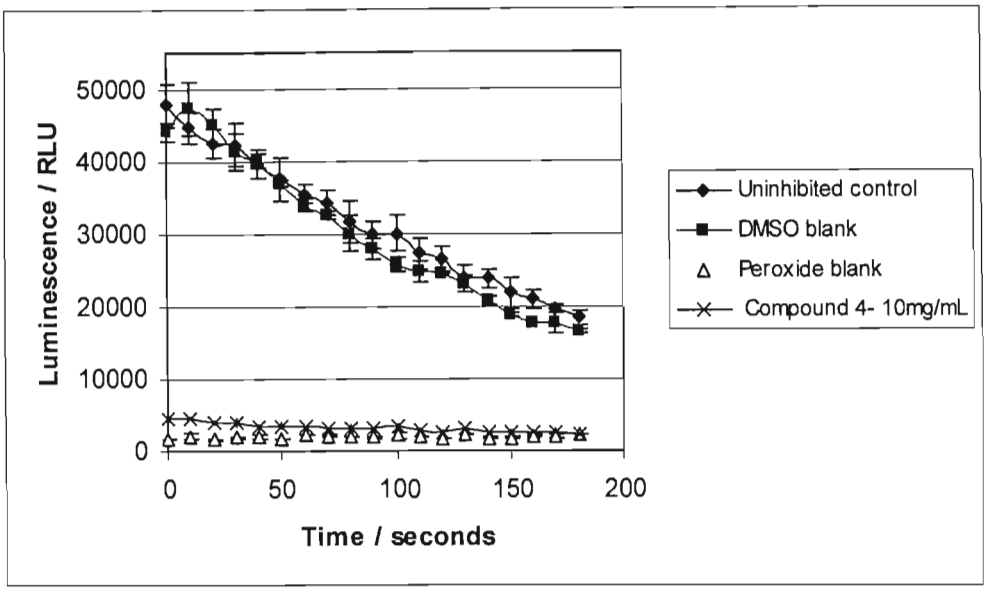

Graph 35: Results of Antioxidant/ free radical scavenging activity of compound 4, 10mg/mL concentration

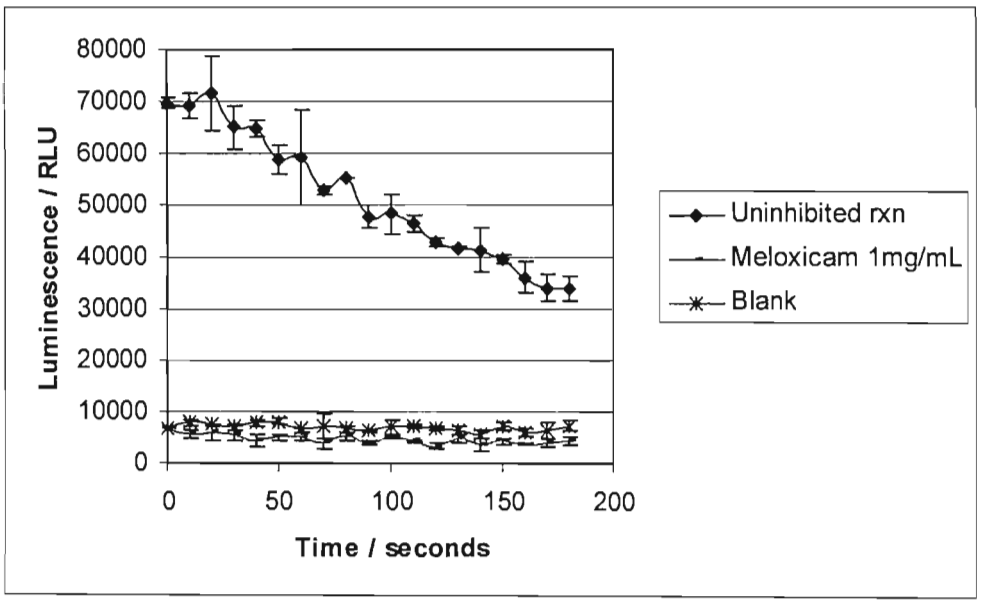

Graph 36: Results of Antioxidant/ free radical scavenging activity of meloxicam, 1mg/mL concentration

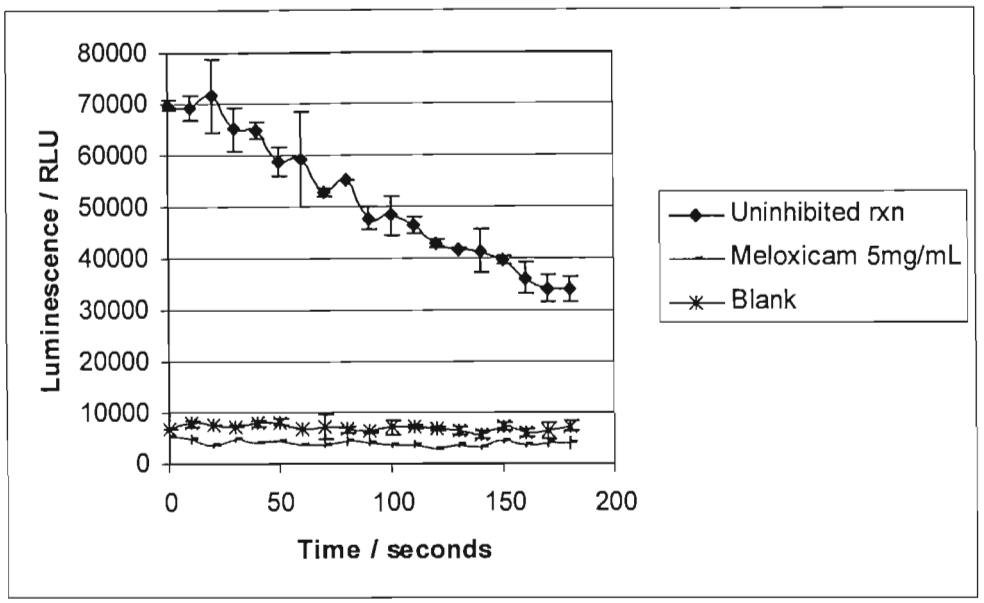

Graph 37: Results of Antioxidant/ free radical scavenging activity of meloxicam, 5mg/mL concentration

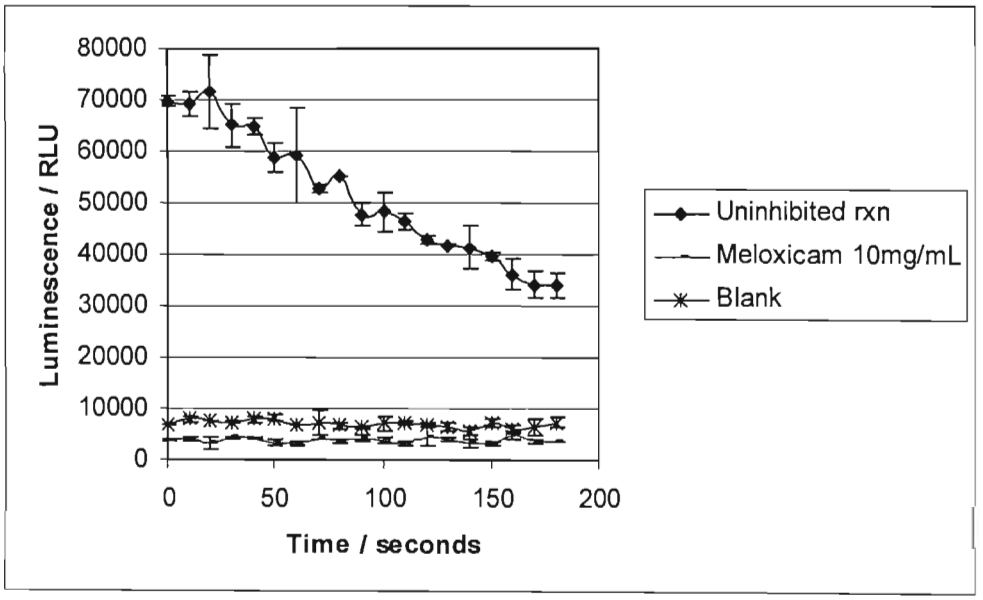

Graph 38: Results of Antioxidant/ free radical scavenging activity of meloxicam, 10mg/mL concentration

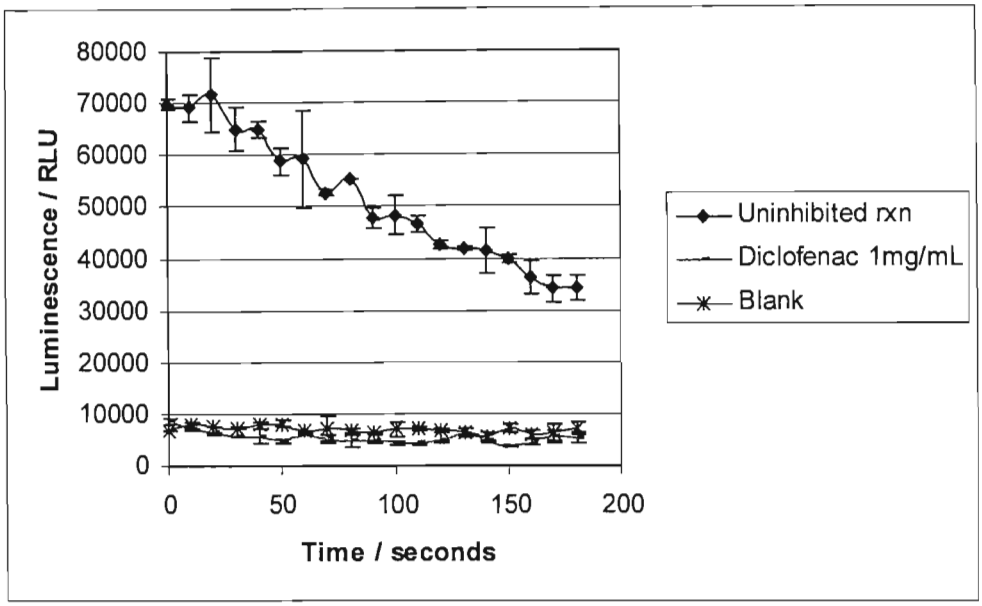

Graph 39: Results of Antioxidant/ free radical scavenging activity of diclofenac, 1mg/mL concentration

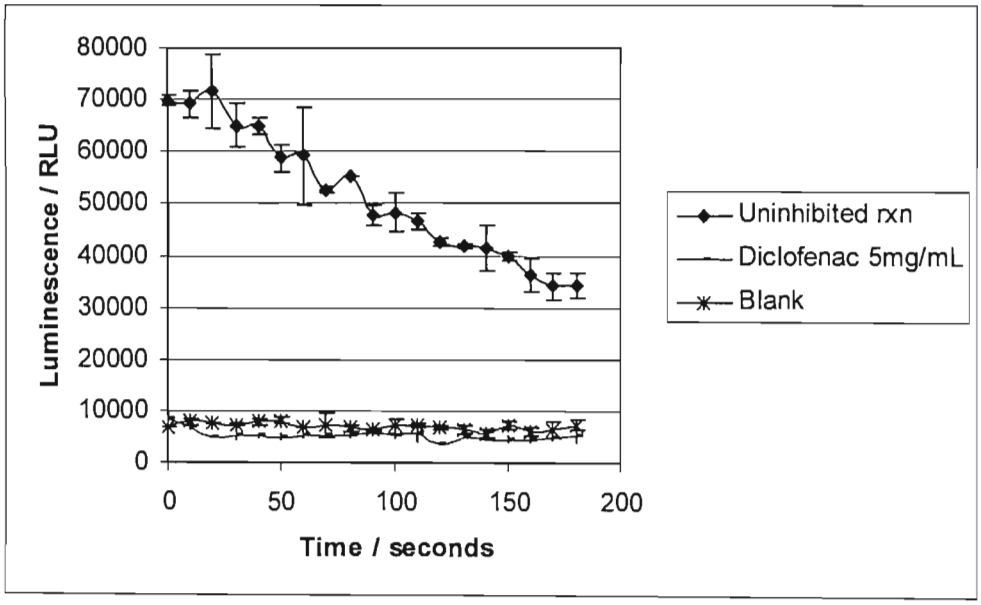

Graph 40: Results of Antioxidant/ free radical scavenging activity of diclofenac, 5mg/mL concentration

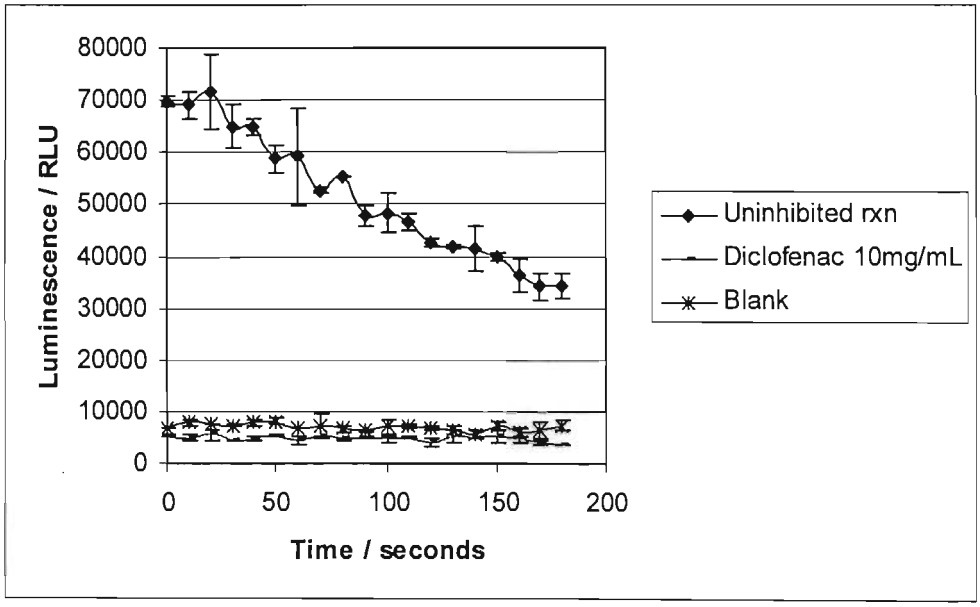

Graph 41: Results of Antioxidant/ free radical scavenging activity of diclofenac, 10mg/mL concentration